Canada

Québec

FIELD EVALUATION OF THE EFFECTIVENESS OF ENGINEERED SOIL COVERS FOR REACTIVE TAILINGS

Volume 1: Laboratory and Field Tests

MEND Project 2.21.2

This work was done on behalf of MEND and sponsored by Noranda Inc., as well as the Centre de recherches minérales (CRM) and the Canada Centre for Mineral and Energy Technology (CANMET)

October 1993

FIELD EVALUATION OF THE EFFECTIVENESS OF ENGINEERED SOIL COVERS FOR REACTIVE TAILINGS

Final Report, Volume 1:

LABORATORY AND FIELD TESTS

by

E.K. Yanful, M.R. Woyshner, B.C. Aubé

Noranda Technology Centre
240 Hymus Boulevard
Pointe-Claire, Québec, Canada
H9R 1G5

DSS Contract Number: 23440-0-9061/01-SQ

Submitted to the MEND (Mine Environment Neutral Drainage) Program

October 1993

EXECUTIVE SUMMARY

A project was initiated in July 1990 under the MEND (Mine Environment Neutral Drainage) program to assess the performance of engineered covers. The project was funded by Noranda Inc., Canada Centre for Mineral and Energy Technology (CANMET) and Centre de Recherches Minérales (CRM) of Minister de l'Énergie et des Ressources of Quebec.

The principal objective of the project was to design, construct and evaluate the effectiveness of soil covers and a plastic or geomembrane cover in reducing acid generation in reactive mine tailings. The evaluation consisted of performance monitoring of field test plots at the decommissioned Waite Amulet tailings site and laboratory experiments at Noranda Technology Centre (NTC), as well as studies by McGill University and École Polytechnique de Montréal. In particular, the McGill University Geotechnical Research Centre measured geotechnical properties of the tailings such as grain size, compaction and drainage parameters, and resistance of the soils and HDPE membrane to freeze-thaw. École Polytechnique de Montréal was mandated to measure the hydraulic properties of the tailings and to perform flow modelling to verify the hydraulic conditions in the covered and uncovered tailings. The department of geological sciences of McGill University investigated the possible effects of sulphide oxidation on the concentration of sulphide gases such as COS, CS_2 , and SO_2.

The soil cover consisted of a 60 cm thick compacted silty clay layer placed between two sand layers, each 30 cm thick. A final 10 cm gravel crust blanketed the cover system to minimize erosion. These thicknesses were selected to provide maximum reductions in the predicted oxygen flux and a sufficient safety factor to minimize the effects of adverse climatic conditions such as freezing and thawing. The design of the cover was based on the results of a previous laboratory study which concluded that this composite cover would be able to resist significant moisture losses for a long time. The uppermost layer consisted of a fine sand which minimized the evaporation of water from the underlying, nearly saturated clay. The coarser bottom sand drained to residual saturation (minimum water content at high suction) and prevented significant moisture drainage from the clay. At high suctions both fine and coarse sands have low hydraulic conductivities or permeabilities (even lower than the saturated hydraulic conductivity of the clay) which would minimize both upward and downward water fluxes. The upper fine sand also reduces run off, increases storage and allows more water to percolate into the clay.

The geomembrane cover consisted of an 80 mil (2 mm thick) high density polyethylene (HDPE) placed between the upper fine sand and the bottom coarse sand.

A total of four test plots, consisting of two composite soil covers, one geomembrane cover and a control (tailings without cover) were constructed at the Waite Amulet site. Each test plot was instrumented to measure gaseous oxygen concentrations, water content, suction, temperature and pore water quality at various depths. In addition, a collection basin

lysimeter, initially filled with unoxidized tailings, was installed below each cover to measure both the quantity and quality of percolated water.

Six columns were installed in the laboratory to simulate soil-covered and uncovered tailings. The soil cover consisted of a 30 cm thick clay layer placed between two sand layers, each 15 cm thick. The soils were similar to those used in the construction of the field test plots. Unoxidized tailings used in the laboratory experiments were collected from the deep saturated zone of the south end section of the Waite Amulet tailings impoundment. The covered and uncovered tailings were subjected to cyclic wetting and drying, at laboratory temperature. Gaseous oxygen concentration, water content, temperature and drainage water quality were monitored over time. The covered tailings did not produce any drainage water during normal wetting or rain application because of the low hydraulic conductivity of the compacted clay layer. Most of the added water reported as run off. The covered tailings were periodically flushed (by by-passing the soil cover) in order to obtain drainage water to assess the amount of acid produced from sulphide oxidation. The uncovered tailings were also flushed.

Results of the laboratory, field and modelling studies indicated that the oxygen flux into is reduced by 91 to 99% by the soil cover. Acid fluxes, obtained from covered and uncovered tailings, indicated the same degree of cover effectiveness. Monitoring of acid fluxes over time suggested that the rate of acid production decreases with time. This may be explained by the reduced diffusion of gaseous oxygen to active sulphide mineral sites due to the formation of inert solids.

Hydrologic modelling indicated that water percolation through the cover is about 4% of precipitation. Field lysimeter data gave 6% or 54 mm per year which indicates a reduction of 80% in the total annual infiltration into the uncovered tailings.

The effects of freeze-thaw on the integrity of the compacted clay layer in the composite cover was also investigated. The results showed that most of the negative effects occur during the first two freeze-thaw cycles. Laboratory hydraulic conductivities increased by one to two orders of magnitude after the first two freeze-thaw cycles and then remained steady afterwards. Field hydraulic conductivity was measured in 1991 and 1992 the results of which indicated a value of ~1.0 x 10^{-7} cm/s, similar to the initial design value. Based on these results and those of the laboratory freeze-thaw studies, it is concluded that freezing and thawing have not adversely affected the cover and that no future negative effects need be anticipated.

The stability of the geomembrane cover was evaluated with respect to acid leach, freeze-thaw and tensile stresses. A tensile resistance of ~1.5 kN was obtained for both untreated and acid leached (pH of 3) specimens of 80 mil HDPE. A similar tensile resistance was obtained for specimens subjected to three freeze-thaw cycles. From these results, it is inferred that the long-term stability of the HDPE cover is not a major concern except for the possible effects of equipment, burrow animals and sunlight.

It is recommended that the tailings in each test plot lysimeter be sampled and examined for signs and extent of oxidation. This would involve detailed pore water analysis and mineralogical investigation. The water balance of the two soil-covered test plot should be confirmed by further field monitoring through the fall of 1993. The results presented and discussed in this report and those of the recommended additional monitoring should be integrated into a set of design and construction protocols for soil covers for use by mining companies and consultants. A new project should be initiated to investigate the effects of root penetration on the soil covers.

SOMMAIRE

Un projet a été entrepris en juillet 1990 dans le cadre du programme NEDEM (Neutralisation des eaux de drainage dans l'environnement minier) pour évaluer le rendement de recouvrements pour les sites de résidus miniers. Ce projet était co-financé par Noranda Inc., le Centre canadien de technologie des minéraux et de l'énergie (CANMET) et le Centre des recherches minérales (CRM) du ministère de l'Énergie et des Ressources du Québec.

L'objectif principal du projet était de concevoir, d'aménager et d'évaluer un recouvrement géologique et un recouvrement d'une membrane de plastique (géomembrane) qui permettraient de réduire la production d'acide dans les amas de résidus miniers réactifs. L'évaluation a été effectuée à l'aide d'emplacements d'essai à la mine fermée de Waite Amulet et de colonnes d'essai en laboratoire au Centre de technologie Noranda (CTN), ainsi que d'études par l'université McGill et l'École Polytechnique de Montréal. En particulier, le Centre de Recherches Géotechniques de l'Université McGill a fait la caractérisation géotechnique des recouvrements et des résidus miniers tels que la granulométrie, les paramètres de compaction et de drainage ainsi que des études sur les effets des cycles de gel-dégel sur les recouvrements incluant la géomembrane HDPE. L'École Polytechnique de Montréal a été mandatée pour mesurer les propriétés hydrauliques des résidus et faire la modélisation des écoulements afin de confirmer l'équilibre hydraulique des résidus recouverts et non recouverts. Le département des sciences géologiques de l'Université McGill a étudié les effets possibles de l'oxydation des sulfures sur les gaz sulfureux tels que le COS, le CS_2 , et le SO_2.

Le recouvrement géologique était composée d'une couche d'argile silteuse compactée d'une épaisseur de 60 cm, placée entre deux couches de sable de 30 cm chacune. Une couche finale de 10 cm de gravier fut placée sur le dessus pour minimiser l'érosion. Ces épaisseurs ont été choisies afin de réduire au minimum le flux d'oxygène prévu et d'assurer un facteur de sécurité suffisant pour minimiser l'effet de conditions climatiques adverses comme le cycle de gel-dégel. Le recouvrement a été conçu en fonction des résultats d'une étude en laboratoire antérieure qui avait conclu que ce recouvrement composite réduirait considérablement le drainage acide pour une longue période de temps. La couche de sable supérieure était composée d'un sable fin pour minimiser l'évaporation de l'eau de la couche d'argile sous-jacente presque saturée. Le sable de la couche inférieure, plus grossier, a drainé l'eau à un niveau de saturation résiduelle (teneur en eau minimum sous une pression négative élevée) et ainsi prévenu un drainage important de l'eau renfermée l'argile. À une pression négative élevée, la conductivité hydraulique (ou perméabilité) du sable fin et du sable grossier sont faibles (même plus faibles que la conductivité hydraulique de l'argile saturée), ce qui minimise la migration de l'eau vers le haut et vers le bas. De plus, le sable fin de la couche supérieure réduit l'écoulement, augmente la rétention de l'eau et permet à une plus grande quantité d'eau de s'infiltrer dans l'argile.

La géomembrane était un recouvrement de polyéthylène haute densité de 80 mils (2 mm) placé entre une couche supérieure de sable fin et une couche inférieure de sable grossier.

Quatre emplacements d'essai ont été aménagés à Waite Amulet: deux avec un recouvrement composite, un avec géomembrane et un sans recouvrement (pour fins de contrôle). Des instruments ont été installés à chaque emplacement pour mesurer les concentrations d'oxygène gazeux, la teneur en eau, la pression négative, la température et la qualité de l'eau interstitielle à diverses profondeurs. De plus, un bassin collecteur (lysimètre) rempli de résidus non oxydés a été installé sous chaque recouvrement pour mesurer la quantité et la qualité de l'eau percolée.

Six colonnes ont été installées en laboratoire pour simuler le comportement de résidus recouverts et non recouverts. Le recouvrement était composé d'une couche d'argile de 30 cm d'épaisseur placée entre deux couches de sable de 15 cm d'épaisseur chacune. Les matériaux étaient semblables à ceux utilisés pour l'aménagement des emplacements d'essai de Waite Amulet. Les résidus non oxydés utilisés dans les essais en colonnes ont été obtenus dans la zone profonde et saturée de l'extrémité sud de l'amas de résidus de Waite Amulet. Les résidus recouverts et non recouverts ont été soumis à des cycles de mouillage et d'évaporation. La concentration d'oxygène gazeux, la teneur en eau, la température et la qualité de l'eau de drainage ont été mesurées périodiquement. Les résidus recouverts n'ont produit aucune eau de drainage pendant le mouillage normal à cause de la faible conductivité hydraulique de la couche d'argile compactée. La plus grande partie de l'eau ajoutée s'est écoulée. Les résidus recouverts ont été périodiquement inondés (en contournant le recouvrement) afin d'obtenir de l'eau de drainage pour évaluer la quantité d'acide produit par l'oxydation des minéraux sulfureux. Les résidus non oxydés ont également été inondés.

Les résultats des études en laboratoire, sur le terrain et par modélisation, ont indiqué que le recouvrement géologique réduisait le flux d'oxygène dans les résidus de 91 à 99%. Le même degré de réduction est obtenu pour l'eau de drainage acide produite dans les résidus recouverts par rapport aux résidus non recouverts. De plus, les mesures prises indiquent que la production d'acide diminue avec le temps. Ceci s'explique probablement par la formation de solides inertes qui réduisent la diffusion d'oxygène gazeux vers les minéraux sulfureux.

La modélisation hydrologique a indiqué que 4% environ de l'eau de pluie s'infiltre dans le recouvrement. Les lysimètres ont indiqué une pénétration de 6%, ou 54 mm par an, ce qui se traduit par une réduction de 80% de l'infiltration annuelle totale dans les résidus recouverts par rapport aux résidus non recouverts.

Les effets du cycle de gel-dégel sur l'intégrité de la couche d'argile compactée ont également été analysés. Les résultats révèlent que la plupart des effets négatifs se produisent au cours des deux premiers cycles de gel-dégel. En laboratoire, les conductivités hydrauliques ont augmenté de 10 à 100 fois après les deux premiers cycles de gel-dégel et sont restées stables par la suite. Sur le terrain, la conductivité hydraulique

a été mesurée en 1991 et 1992. Les résultats indiquent une valeur de ~1.0 x 10^{-7} cm/s, ce qui est près de la valeur calculée. Ainsi, les résultats obtenus sur le terrain et en laboratoire permettent de conclure que le cycle de gel-dégel n'a pas eu d'effet adverse sur les recouvrements et qu'il ne devrait y avoir aucun effet négatif futur.

La stabilité de la géomembrane a été évaluée en termes de drainage acide et de résistance à la tension et aux cycles de gel-dégel. Une résistance à la tension de ~1,5 kN a été obtenue pour des échantillons neufs et des échantillons acidifiés (pH 3) de polyéthylène haute densité de 80 mils d'épaisseur. Une résistance semblable a également été obtenue pour des échantillons soumis à des cycles de gel-dégel. Ces résultats indiquent que la géomembrane devrait rester stable à long terme et que les principaux risques de dommages possibles proviendraient de la machinerie, des animaux fouisseurs et de la lumière du soleil.

Nous recommandons d'échantillonner et d'analyser les résidus de chaque lysimètre pour déterminer la portée de l'oxydation. Cette étude comprendrait une analyse détaillée de l'eau interstitielle ainsi qu'un examen minéralogique. Les bilans hydrologiques des deux emplacements recouverts devraient être confirmés par de nouvelles mesures à l'automne 1993. Les résultats présentés et discutés dans ce rapport et ceux des mesures supplémentaires recommandées devraient être intégrés aux protocoles de conception et d'aménagement de recouvrements géologiques qui seront utilisés par des entreprises minières et des consultants. Un nouveau projet devrait être entrepris pour analyser l'effet de la pénétration de racines dans les recouvrements.

ACKNOWLEDGEMENTS

This project is a contribution to the MEND (Mine Environment Neutral Drainage) program. Funding was provided by Noranda Minerals Inc., Canada Centre for Mineral and Energy Technology (CANMET) and Centre de recherches minérales (CRM) of Ministère de l'Énergie et des Ressources of Quebec.

A number of people have made substantial contributions to the project. K. Wheeland, L. St-Arnaud, K. Shikatani and S. Payant of Noranda Technology Centre were project participants. N. Davé of CANMET (Elliot Lake Laboratories) was the DSS Scientific Authority and G. Tremblay was the MEND Coordinator for the project. P. Friedrich, L. Marcoux and L. Bienvenu of CRM managed the CRM-University contracts. C. Alpers (formerly of McGill University), A.M.O. Mohamed of McGill Geotechnical Research Centre and R. Chapuis of École Polytechnique contributed to the technical objectives of the projects. Recognition is also given to the several co-op students from the University of Waterloo and École Polytechnique who provided excellent technical support. M. Tardif of D'Alembert, Quebec, provided occasional field support. E.K. Yanful also provided overall project coordination and management. K.M. Howard-Vincent of NTC assembled the report.

Table of Contents

Appendices

List of Figures

1.0 INTRODUCTION

1.1 Mine Tailings and the Environment

A large number of Canadian metal and uranium orebodies contain sulphide minerals in either the ore or the surrounding waste rock. Milling of the sulphide-rich ores results in the production of tailings which are generally deposited in exposed environments. When iron-bearing sulphide minerals (particularly, pyrite and pyrrhotite) contained in the tailings are exposed to oxygen and water, they oxidize and turn receiving surface waters acidic if sufficient alkaline minerals are not present. The solution resulting from this oxidation is characterized by low pH and high concentrations of ferrous iron and sulphate. The process of oxidation, using pyrite (FeS_2) as the sulphide mineral, can be summarized by the equation:

$$FeS_2(s) + \frac{7}{2}O_2 + H_2O \rightarrow Fe^{2+} + 2SO_4^{2-} + 2H^+ \qquad [1.1]$$

The ferrous iron [Fe^{2+}] can further oxidize to ferric iron [Fe^{3+}] when the pH of the system is low (1.5-3.5) and oxygen is readily available. Naturally occurring bacteria, notably the genus *Thiobacillus ferrooxidans*, catalyze the oxidation reaction (Nordstrom, 1982). The ferric iron generated may either be hydrolysed and precipitated as ferric hydroxide [$Fe(OH)_3$] or oxidize other heavy metal sulphides present such as galena [PbS], sphalerite [ZnS] and chalcopyrite [$CuFeS_2$]. The final acidic solution may therefore also contain high concentrations of heavy metals. This solution is generally referred to as acid mine drainage (AMD) or, in the case of seepage associated with mine waste rock, acid rock drainage (ARD). The overall process of sulphide oxidation, may be summarized by the equation:

$$FeS_2(s) + \frac{15}{4}O_2 + \frac{7}{2}H_2O \rightarrow Fe(OH)_3(s) + 2SO_4^{2-} + 4H^+ \qquad [1.2]$$

The formation of $Fe(OH)_3$ gives rise to the reddish brown coating often observed in mines and streams polluted with ARD. Rainfall and snow-melt flush the acidic solutions from the tailings sites into the downstream environment. If ARD is not collected and treated, it could contaminate groundwater and local water courses, damaging the health of plants, wildlife, fish and possibly humans.

1.2 The Extent of the Acid Drainage Problem

Acid drainage is the single largest environmental problem facing the Canadian mining industry. Studies conducted between 1984 and 1987 to determine the extent of the ARD problem indicated Canada has, in total, some 12,000 hectares of sulphidic tailings and 350 million tonnes of waste rock. These wastes are largely the accumulation of the last forty years of mining and milling. It is reasonable to assume that an equal quantity of mine wastes will be accumulated in the future, especially if lower grade ores are mined and

mineral production is increased. The cost of rehabilitation of the existing tailings sites alone is estimated to be $2.4 billion, using an average cost of $200,000 per hectare and applying existing, unproven technology. The cost of reclamation of waste rock sites is in the order of $3.5 billion, at an average cost of $10 per tonne (Wheeland and Feasby, 1991).

1.3 Management of Acid Drainage from Tailings

Current major tailings management practices for decommissioning are flooding, revegetation of the tailings dam and treatment of the acidic drainage from the tailings area. Flooding requires construction and long-term maintenance of engineering structures (dams and dykes). More than twenty years of research (started in the early 1970's) has shown that while revegetation controls dust and prevents erosion, it does not reduce acid generation. Treatment of acid drainage involves the addition of lime to neutralize the acidity and precipitate heavy metals and calcium as hydroxides and sulphates in the form of sludge. This sludge has to be disposed of in an environmentally acceptable manner. Lime treatment plants, when well-operated and maintained, are sufficient to prevent adverse, downstream, environmental impact. However, acid generation may occur for several hundreds of years following mine closure, necessitating the operation of these plants in perpetuity.

1.4 The MEND Program

With the recognition that none of the existing management techniques would result in cost-effective, permanent solutions, the Canadian mining industry and the Federal and Provincial Governments initiated a task force in 1986. The task force made recommendations for research which are currently being implemented under the MEND (Mine Environment Neutral Drainage) program. The program, which began in 1988, is a joint industry and government consortium aimed at developing and applying technologies for decommissioning of reactive mine wastes in a reliable, predictable, affordable, and environmentally acceptable manner. Detailed descriptions of the MEND program are presented by Filion and Ferguson (1989) and Wheeland and Feasby (1991).

1.5 Covers for Tailings Management

Dry or non-water covers can be used for controlling acid generation in sulphidic mine wastes. Such covers will generally be in the form of geomembranes, cementitious materials or natural soils. These covers have, however, not been extensively applied on tailings because of high cost and lack of reliable methods for predicting and evaluating their effectiveness. Longevity is also a major unknown.

In recent years, there has been a resurgence of interest in Canada to develop reliable methods for designing and constructing effective soil covers, as part of the MEND program. An initial research project to develop laboratory methodologies for evaluating the effectiveness of covers was undertaken by Noranda Technology Centre in

collaboration with the University of Waterloo (Yanful, 1991). The results of the study indicated that the flux of oxygen in nearly saturated geologic materials is low. The low flux results from the fact that oxygen dissolves only sparingly in water (11 mg/L at 11°C) and diffuses 10,000 times more slowly in water than in air. It was inferred from the study that, since the movement of gaseous oxygen through soil covers into underlying tailings deposits will be dominated by molecular diffusion, the low oxygen flux will result in reduced acid generation.

Following completion of most of the laboratory study, it was proposed that the findings be evaluated in the field, prior to full-scale implementation. A project was therefore initiated in 1990 by Noranda Technology Centre (NTC), Canada Centre for Mineral and Energy Technology (CANMET) and Centre de recherches minérales (CRM) to evaluate soil covers in the field. The project, which became known as the *Waite Amulet Covers Project,* was conducted under the auspices of the MEND Prevention and Control program.

1.6 Objectives and Scope of the Waite Amulet Covers Project

The principal objective of the project was to design and construct covers from locally available soil materials to minimize both water infiltration and oxygen diffusion into underlying sulphide-bearing tailings. The decommissioned Waite Amulet tailings site, located approximately 20 km west of Rouyn-Noranda, Québec, was selected for the following reasons:

i) the hydrogeochemistry of the tailings had been adequately defined in previous studies;

ii) site instrumentation (such as piezometers) had been installed and could be used to generate additional information;

iii) the site has typical acid-generating tailings with well-defined oxidized and unoxidized zones so that the effect of a cover on the oxidation front can be rapidly assessed; and

iv) the site is one of those being studied under the MEND program and its use would provide continuous information and enhance the overall program.

The evaluation was proposed to consist of a combined field and laboratory study. The advantages of a field program include the ability to realistically evaluate the effects of meteorological changes (freezing and thawing). In addition, controlling factors such as scale, hydrology and hydrogeology are difficult to adequately simulate in the laboratory. In spite of these advantages, it was felt that there was still some merit in combining field studies with well-designed experimental programs. For one thing, the laboratory provides a controlled environment which makes material placement (soil compaction), installation of instrumentation, and monitoring more convenient. Laboratory installations are also not

susceptible to disruptions (for example, vandalism). Such disruptions can adversely affect the database and, therefore, interpretation.

The project consisted of the design, construction and instrumentation of soil and plastic (geomembrane) covers on three tailings test plots at the Waite Amulet site. For comparison, a fourth test plot without a cover was installed as a control. Laboratory columns were installed to simulate the soil cover and the control test plots. The tests have been monitored since installation in September 1990. The official completion date of the contract is April 30, 1993. Monthly progress reports were issued by NTC (the principal contractors) in the course of the project. Technical papers on the projects were also prepared and published in conference proceedings and peer-reviewed journals. In addition, several subcontracts between CRM and university participants (McGill University and École Polytechnique) were initiated on major parts of the investigation, based on terms of reference and scopes of work defined by NTC. The results of these investigations were regularly reported in full and are only briefly summarized in this report.

The present report constitutes the final major report on the project. It documents the design philosophy and techniques, field construction and laboratory methods, results and interpretations and recommendations. All papers and reports produced during the life of the project are either summarized or cited in appropriate sections of this report.

2.0 WAITE AMULET TEST PLOTS

A project was initiated at the Waite Amulet site in July 1990 to evaluate the performance of pilot-scale, engineered soil covers on reactive mine tailings. The project involved the design and construction of test plots of two covers consisting of layered natural soils. A control plot without a cover and a plot with a geomembrane cover were also included in the study for comparison. The geomembrane consisted of an 80-mil (~2 mm thick) high density polyethylene (HDPE).

Instrumentation was installed *in situ* to monitor water quality, sample pore gas, measure moisture content and hydraulic heads, and to measure hydrometeorological parameters, rainfall and pan evaporation. The overall purpose of the design and the associated instrumentation was to assess the effectiveness of the covers in reducing sulphide oxidation and acid generation in sulphide-rich mill tailings.

2.1 Technical Design and Investigative Methods

2.1.1 Design Concepts

The Capillary Barrier Concept

The design of the two composite soil covers focused on the curtailment of oxygen and water to the tailings. To curtail oxygen and water, the covers must retain high water saturation and also have a low hydraulic conductivity, K. One method of achieving these two objectives above the water table is by incorporating a capillary barrier in the design of the cover. In a capillary barrier, a saturated, fine-grained soil layer with a low hydraulic conductivity is placed on top of a coarse-grained soil layer (Rasmuson and Eriksson, 1986; Nicholson *et al.*, 1989). The coarse layer, having larger pores, has a higher air entry pressure ψ_a and is the first to drain as the pressure head in the system becomes negative. Figure 2.1 illustrates this phenomenon with a graph of typical drainage curves of a fine sand, silt, and clay (Ho, 1979). The air entry pressure is the pressure required to initiate drainage and any soil initially saturated will not drain unless the applied suction exceeds ψ_a (Nicholson *et al.*, 1989). When the sand base is drained, capillary suction forces prevent drainage of the fine-grained soil cover. In order to reduce evaporation from the fine-grained cover, a coarse-grained cover overlying the fine-grained soil cover may be included in the design of the capillary barrier system. This sand cover also reduces run-off and provides a storage of water following infiltration, thereby allowing more water to reach the fine-grained cover to ameliorate antecedent moisture losses.

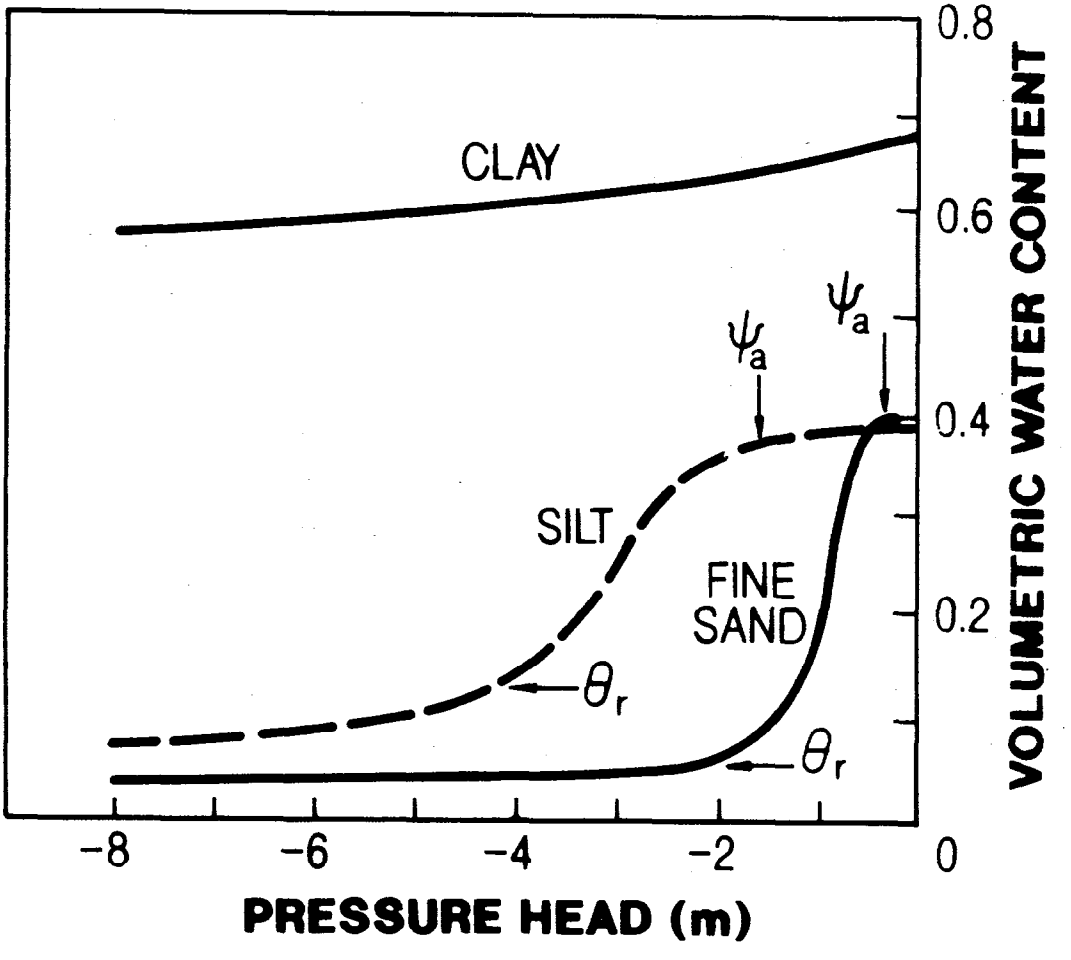

Figure 2.1: Typical Moisture Storage Curves for Soils (Adapted from Ho, 1979)

Cover Design Requirements

In order to obtain maximum reductions in oxygen fluxes, the design aimed at placing the fine-grained covers at high water contents (as close to full saturation as practicable). The near-saturation requirement ensures that the diffusive flux of gaseous oxygen through the cover is very low since the diffusion coefficient of gaseous oxygen decreases with moisture content (Yanful, 1993).

Results of oxygen flux modelling (Figure 2.2), conducted prior to the construction of the test plots, indicated that, for the expected diffusion coefficients, a 1 m thick cover is adequate in reducing oxygen fluxes to very low values. Based on these results, the cover design was developed, calling for a 60 cm thick compacted fine-grained layer sandwiched between two sand layers, each 30 cm thick. Thus the total design thickness of cover was 1.2 m.

The cover design was facilitated by the fact that the desired soil types were all readily available within 1 to 6 km of the site. A gravelly sand layer was selected for the sand base, a compacted varved clay for the fine-grained soil cover, and a fine to medium sand for the sand cover. Figure 2.3 shows the grain size distributions of these soils obtained by ASTM D 420. A 10 cm thick gravel crust was placed on the sand cover to reduce erosion.

Since the compacted clay layer in the composite cover is required to function as both an infiltration and oxygen barrier, it should have a low hydraulic conductivity and also be nearly fully saturated. In order to meet these two requirements, it was stipulated in the design that the clay be compacted and placed at a water content slightly (2 percent) higher than the optimum moisture content (OMC). Placement at a water content slightly higher than the OMC ensures a high degree of water saturation (> 95%) and a low hydraulic conductivity, K, provided a good placement protocol (for example, destruction of soil clods and adequate interlift bonding) is followed. The low K value minimizes water percolation to the tailings following infiltration. Several authors (Lambe, 1958; Daniel *et al.*, 1985; Daniel and Benson, 1990; Elsbury *et al.*, 1990) have shown that the hydraulic conductivities of compacted fine-grained soils decreases with moulding water content and attains minimum values at water contents slightly higher than optimum. In addition, compacting at a water content slightly wet of optimum minimizes drying and cracking. The design of the composite cover, therefore, called for a relative compaction of 93% to 96% of the maximum modified Proctor density (MDD) and a placement gravimetric water content of 24% to 26%. A modified Proctor compaction curve for the varved clay, obtained from two laboratory tests using ASTM D 1557, is shown in Figure 2.4 along with the various saturation lines. The design specifications were intended to provide a clay cover close to saturation (90% to 96%), as shown in Figure 2.4.

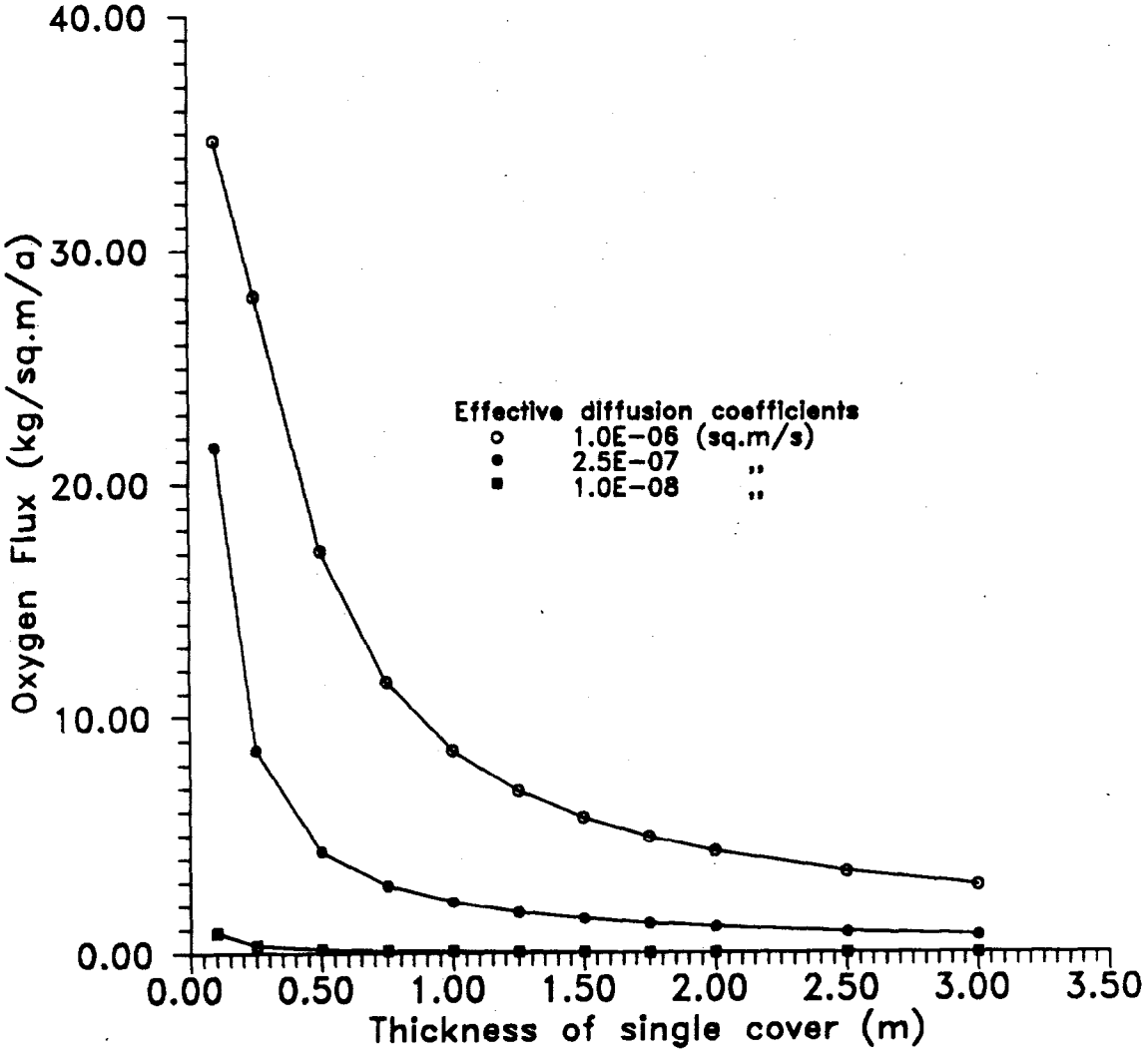

Figure 2.2: Results of Oxygen Flux Modelling

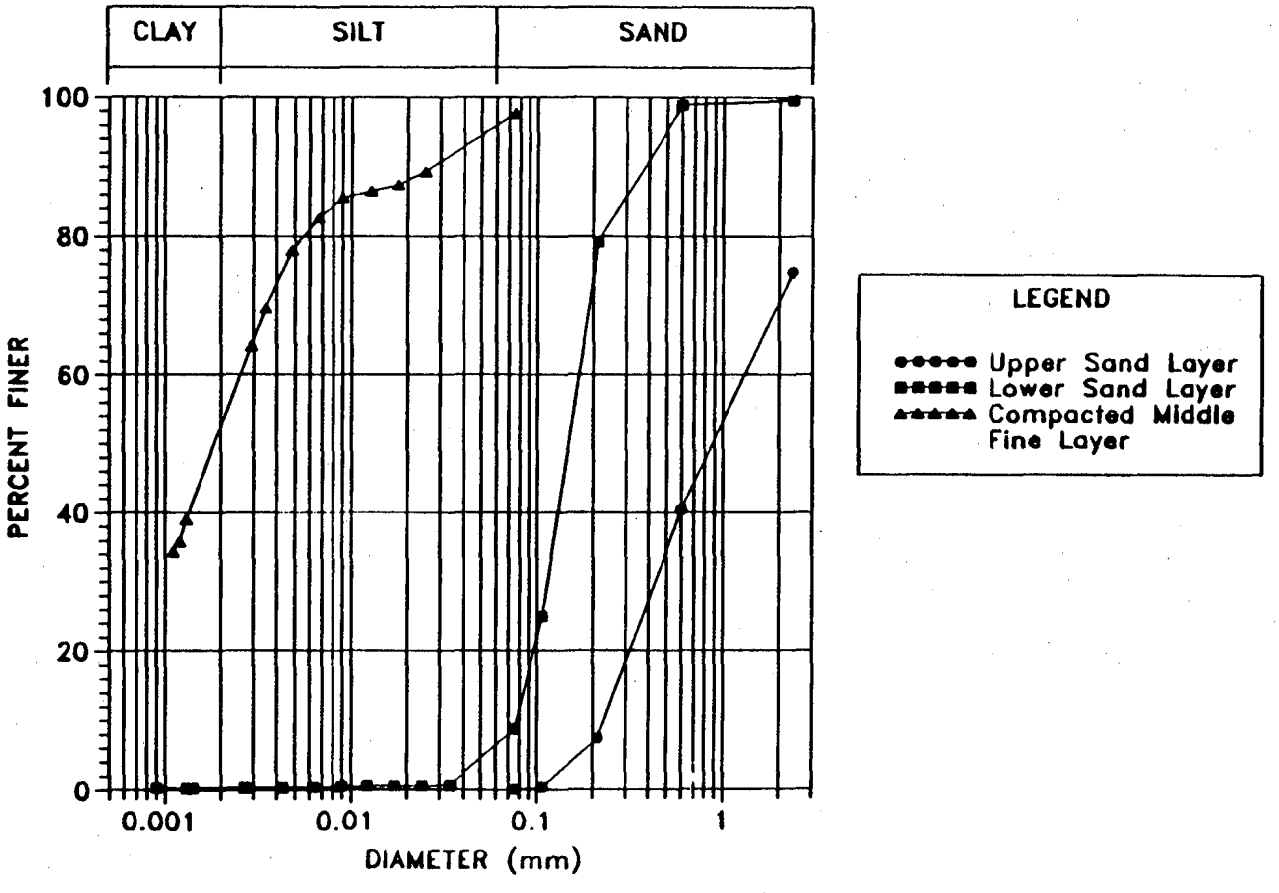

Figure 2.3: Grain Size Distribution of Cover Materials

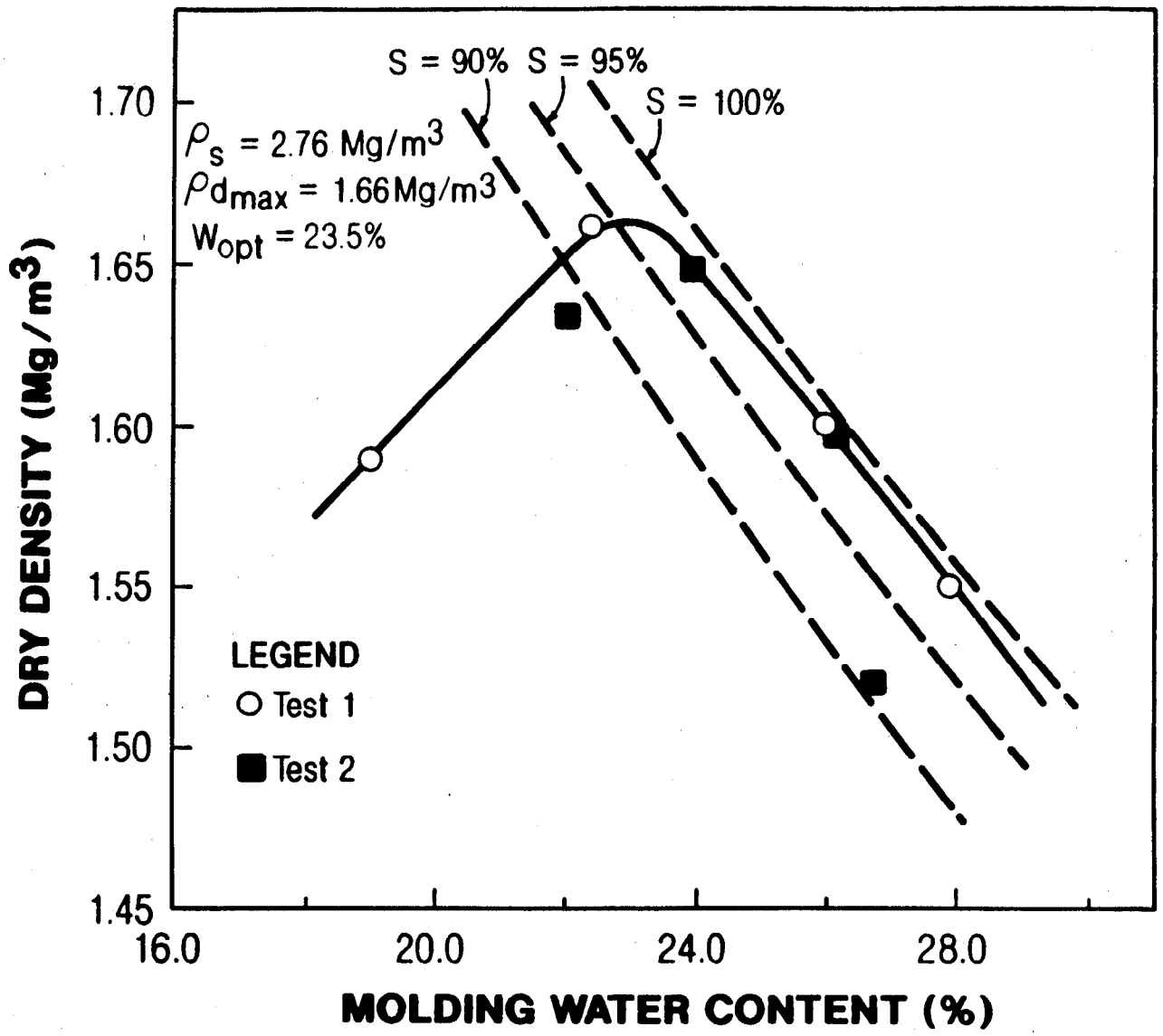

Figure 2.4: Modified Proctor Curve for Clay Layer

A composite geomembrane/soil cover was also designed in which an 80 mil (2 mm) HDPE sheet served as the middle infiltration and oxygen barrier. In this system, the lower sand layer provided a uniform base for the placement of the HDPE sheet. This design also enabled a direct comparison to be made between the performances of the clay and HDPE layers.

2.1.2 Design of Test Plots

Four 20 m x 20 m test plots were designed as follows: (1) control plot without a cover, (2) composite plot consisting of upper and lower sand layers and a middle varved clay layer compacted at 93% modified Proctor and a water content of 25%, (3) composite plot consisting of upper and lower sand layers and a middle varved clay layer compacted at 91% modified Proctor and a water content of 26%, and (4) composite plot consisting of upper and lower sand layers and a middle 80 mil (2 mm thick) HDPE geomembrane. Figure 2.5 shows the plan view of the test plots. Each test plot was designed with 3:1 (H:V) end slopes and perimeter drainage ditches to conduct surface run-off away from the plots. The design specified that the slopes be lined with 40 mil HDPE sheets at the clay-upper sand contact in order to prevent lateral transfer of gaseous oxygen into the covers. For the same reason, a similar lining was specified for all the perimeter ditches. Longitudinal and transverse sections through a clay composite plot are presented in Figures 2.6 and 2.7, respectively.

2.1.3 Construction of Test Plots

Surveying and Drilling

Prior to the construction of the test plots, the site was surveyed and exact dimensions were mapped out by stakes. The exact location of the test plots was selected on the basis of the ease of surface drainage, and accessibility of construction equipment without damage to existing piezometers and trees. The plots were also located on the crest of the groundwater divide where lateral subsurface drainage was expected to be minimal (Yanful *et al.*, 1990). The location of the test plots is shown in Figure 2.8.

The initial phase of the construction involved the drilling of piezometer holes with a hollow stem auger attached to a track mounted drill rig. After completion of the holes, the PVC piezometers with the attached gas samplers and thermocouples were installed at appropriate depths and a layer of sand placed around each sampling point. The space between the hole and the piezometer was backfilled with tailings. Piezometer tips were completed in the tailings saturated zone at depths of 2 and 4 m from the ground surface. The upper ends of the tygon gas samplers were fitted with non-collapsible neoprene rubber and clamped at all times other than during sampling.

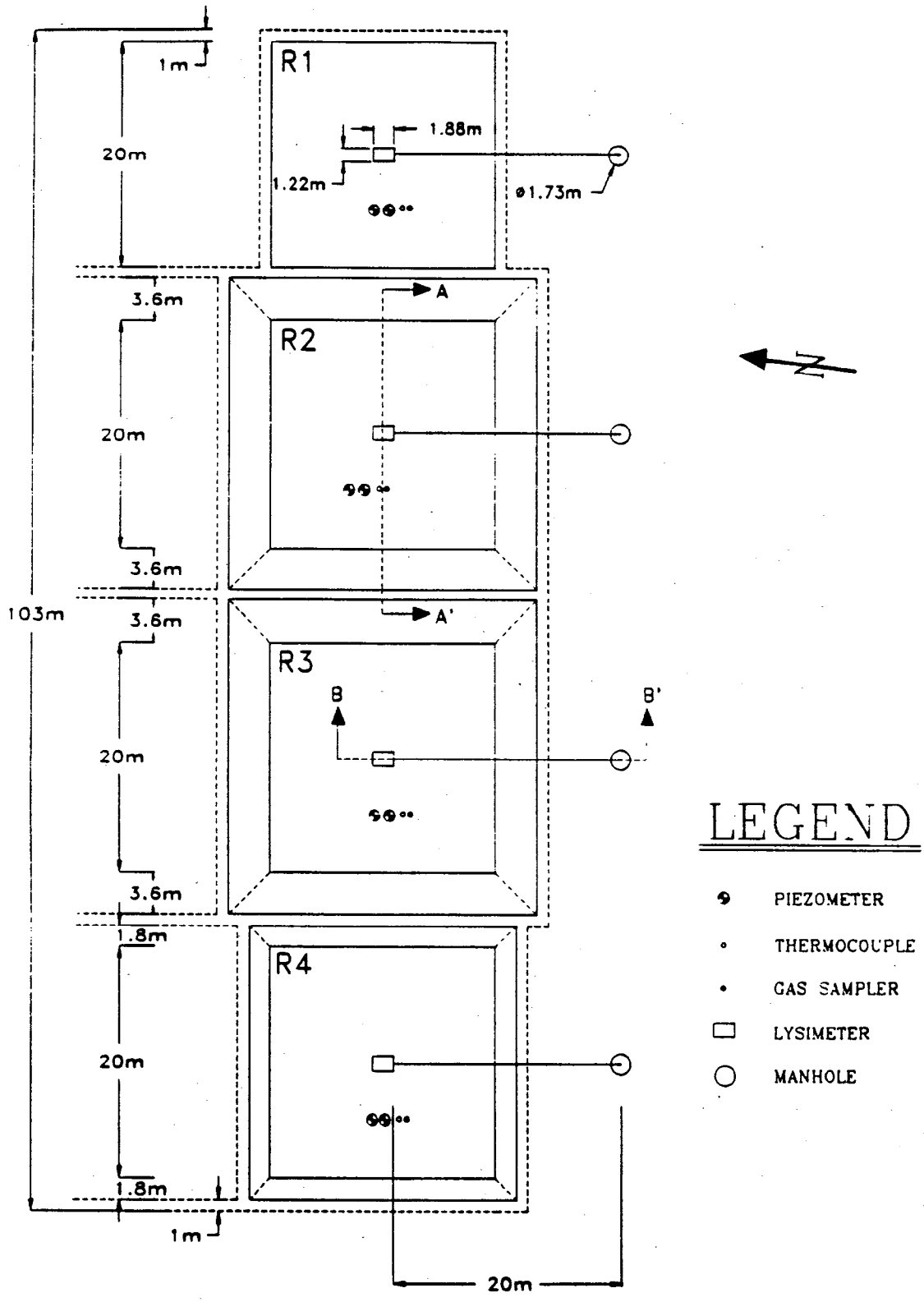

Figure 2.5: Plan View of Test Plots

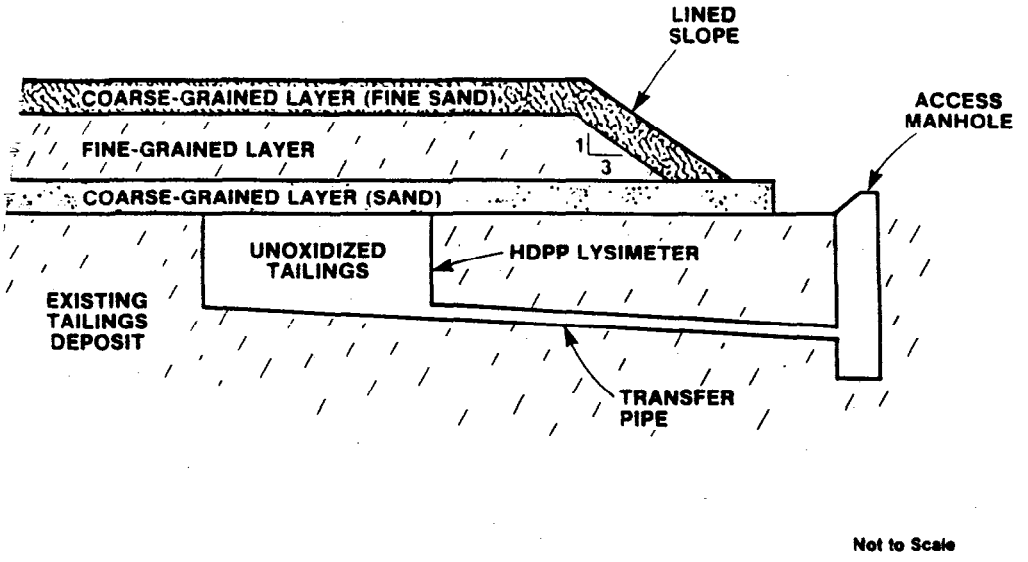

Figure 2.6: Longitudinal Section B-B' through Composite Soil Cover

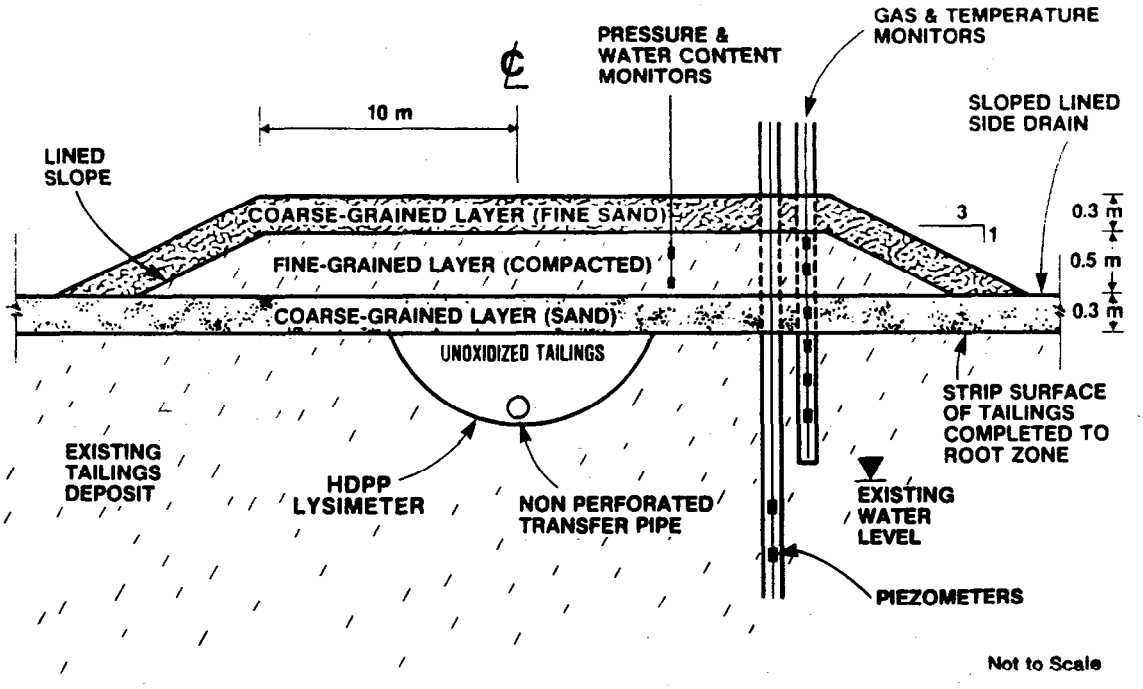

Figure 2.7: Transverse Section A-A' through Composite Soil Cover

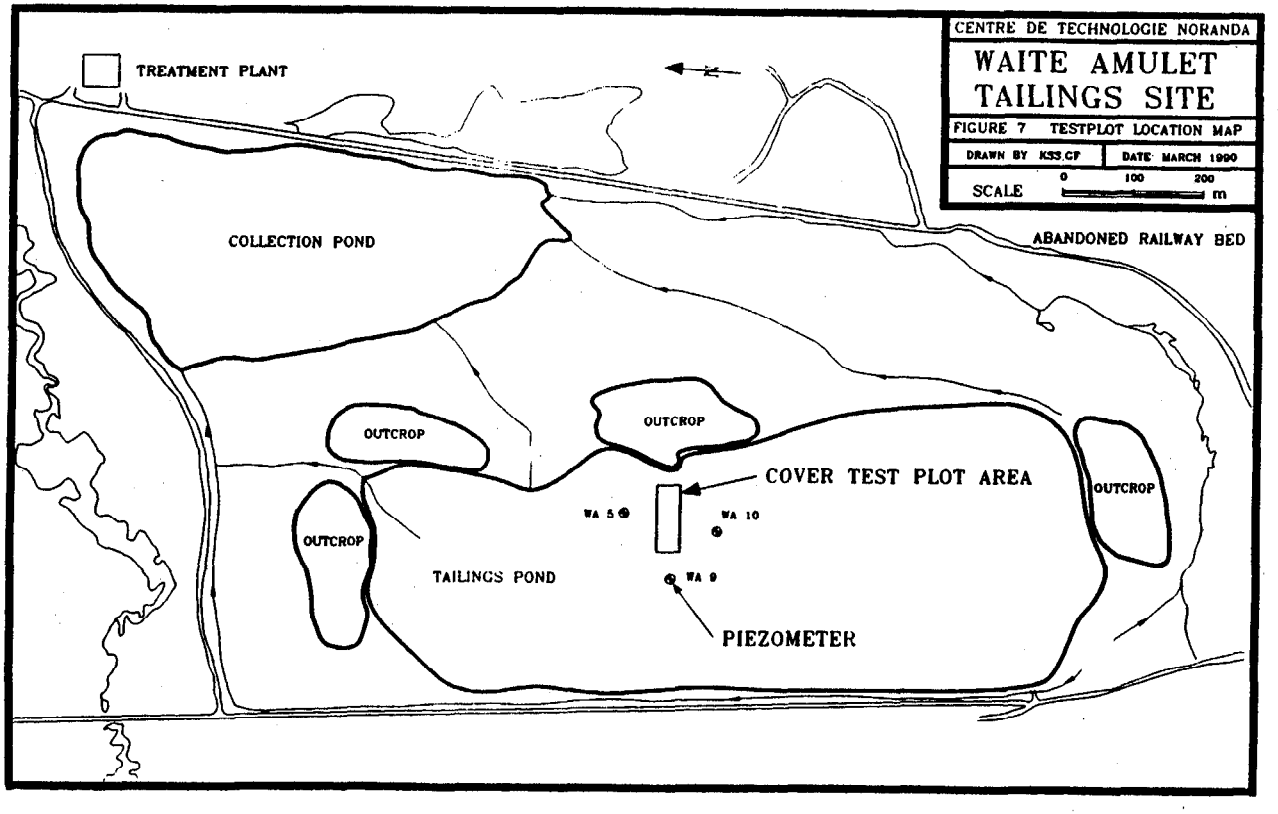

Figure 2.8: Test Plot Location Map

Installation of Manholes and Lysimeters

After the installation of the piezometers, the vegetated surface of the existing tailings at the location of the test plots was cleared. Excavations were made into the tailings for the installation of the manholes. In order to counteract high pore water pressures encountered in the bottom of the excavations, the manholes were anchored into the tailings with steel cables. Concrete was next poured into the floor of the manholes and allowed to set. This strengthened and stabilized the manholes and prevented further uplift.

Shallow excavations were then made in the existing tailings at selected locations for the installation of the collection basin lysimeters. The lysimeters were subsequently connected to the manholes via transfer pipes. These installations essentially completed the construction of the control (no cover) test plot.

Placement of Covers

Placement of the lower sand layer for the remaining test plots proceeded in sub-layers. This gravelly sand was excavated from a nearby pit at a water content close to residual saturation. Each sub-layer was compacted with a smooth drum (wheel) roller.

The clay soil required for the middle layer was obtained from the extensive varved clay deposit located about 0.5 km away from the test plots. The clay was excavated and allowed to dry from its natural water content of 44% to the design water content of 24% to 27%. Moisture content measurements were made for the calibration of a nuclear density apparatus that was subsequently used for monitoring the efficiency of compaction.

After drying to the desired water content, the clay was hauled to the location of the test plot and compacted in 3 lifts of 20 cm each. Density and moisture content measurements were made at 5 to 7 locations during the compaction of each lift. Placement of the next lift proceeded only if the specified relative compaction and range of moisture contents were attained. During placement of the soils, tree roots and large stones were manually removed by site personnel prior to compaction. Figure 2.9 presents the results of *in situ* density tests conducted at various locations on the compacted clay layers during the construction of test plots R2 and R3. The data indicate that the average water saturation achieved in R2 and R3 was 95% and 90%, respectively. The clay cover in plot R2 was placed at 93% modified Proctor and an average water content of 26%. A slightly lower compaction density of 91% modified Proctor and an average water content of 26% was achieved in plot R3.

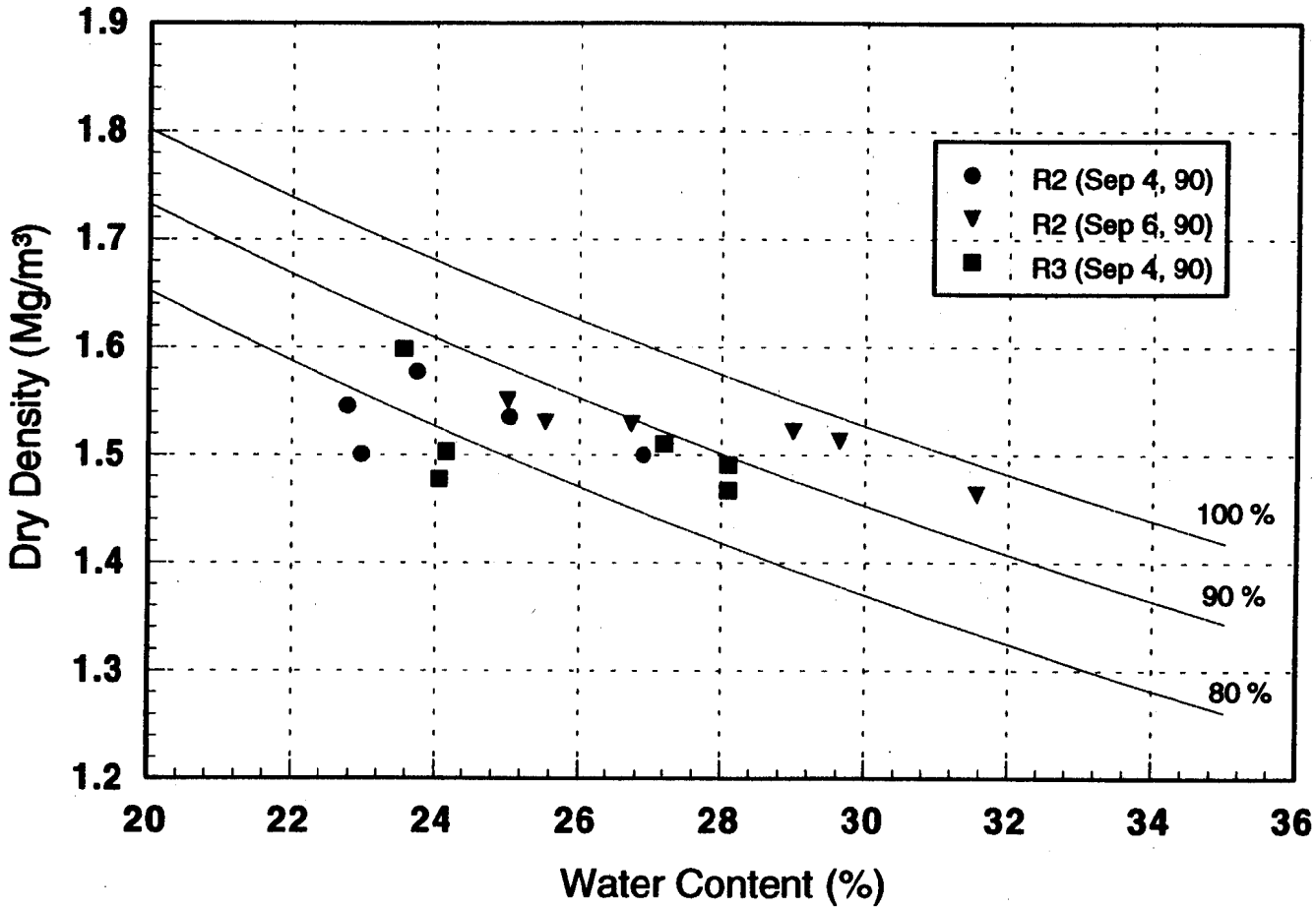

Figure 2.9: *In situ* Density Tests

In the construction of the test plot with HDPE cover, R4, the bottom gravelly sand was placed with 3:1 (H:V) end slopes, as described for the clay composites. HDPE sheets were carefully welded to provide the required dimensions of 20 m x 20 m and then placed on the sand pad. The slopes were then welded to the main sheet before the placement of the upper sand layer.

The HDPE sheets lining the end slopes in all 3 covered test plots were keyed to the perimeter ditches. The installation work described here was completed in mid-September, 1990. As a result of time constraints, placement of a final gravel layer for erosion control was deferred until spring, 1991.

2.1.4 Sampling and Monitoring Methods

An integral component of the test plot design was the installation of instrumentation to assess the performance of the covers. The critical parameters for this assessment were identified to be (1) the moisture content of the cover, particularly that of the clay layer and the sand base, (2) the hydraulic heads in the cover/tailings soil column, (3) the concentration of gaseous oxygen in the cover and in the tailings directly below the cover, (4) the water quality of the tailings pore water, and (5) the temperature of the cover and tailings.

Moisture Content

The moisture content of each layer of the composite cover was measured with time-domain reflectometry (TDR). TDR is a radar technique in which a fast rise-time voltage pulse is propagated through the soil and its reflection measured. The pulse is guided through the soil by stainless-steel rods of known length. The measurement of travel time (Δt) yields an estimate of "apparent" dielectric constant (K_a) of the soil. The volumetric soil-moisture content (θ_v) is then calculated using a relation developed by Topp *et al.* (1980), or other soil-specific relations. A good review of the method can be found in Topp and Davis (1985).

A three-rod TDR probe system was adapted from Zegelin and White (1989). Stainless steel rods, 30 cm in length, 6 mm in diameter and spaced 3 cm apart, were used in the probe design. The probes were horizontally placed in the sand base and the two lifts of the clay, as the cover was constructed. Probes of 30 cm in length and 60 cm in length were also placed in the tailings of the control plot and below each composite cover, prior to construction. In all, a vertical profile in each test plot was developed. The TDR measurements were not automated and were therefore conducted during site visits. TDR probes were not established in the sand cover since moisture content in the sand cover would vary with rainfall and infrequent measurements would simply be a snapshot of the moisture dynamics. Long-term or seasonal changes in the moisture content of the clay and sand base were considered more useful.

A Tektronix 1502B TDR metallic cable tester was used to define the voltage pulse reflections of the beginning and end of the TDR probe from which Δt was calculated. A computer program developed by the University of Waterloo was used to facilitate the analysis of the output trace from the cable tester.

Hydraulic Head

The piezometers consisted of 63.5 mm diameter PVC tubes with 75 cm slotted tips screened with geotextile fibre. The tips were installed at depths of 2 and 4 m in the tailings saturated zone for sampling pore water and for measuring water levels.

Thermal conductivity sensors (AGWA-II sensors, manufactured by Agwatronics Incorporated) were installed at the same depths as the TDR probes. These sensors indirectly measure the matric suction in a soil. Each thermal conductivity sensor consists of a porous ceramic block containing heating and temperature-sensing elements. Measurements are made by inserting the sensor in a drill hole and allowing the moisture contents of the ceramic block and the surrounding soil to equilibrate. The equilibrium moisture content of the block affects the rate of heat dissipation within the block. The quantity of heat dissipated increases with the moisture content of the block. The heat that is not dissipated causes a temperature rise in the block; thus, temperature rise in the block is inversely proportional to the moisture content of the block. The heat dissipated is measured by delivering a controlled amount of heat to the centre of the block and measuring the resulting rise in temperature, after a specified period of time (20 min). The measured temperature is calibrated to measure the matric suction in the soil. Detailed descriptions of the principles and applications of thermal conductivity sensors are provided by Sattler and Fredlund (1989) and Rahardjo *et al.* (1989).

Gaseous Oxygen

Two types of pore gas samplers were designed for the test plots: one type for the unsaturated zone of the tailings, and one type for the test plot cover. The initial samplers functioned for about a year, after which time leaks were detected. New samplers were designed and tested for leaks and subsequently installed in May, 1992. All gaseous oxygen concentrations were determined with a Teledyne model 340 FBS portable oxygen analyzer.

In the tailings unsaturated zone, sampling ports were installed during placement of the piezometers. Prior to the installation of each piezometer, a non-collapsible tygon tube was taped to the side of the piezometer stem. The piezometer was then lowered in the drilled hole and backfilled with tailings and sealed at the surface with a bentonite plug. A flexible rubber tube was attached to the exposed end of the tube and pinched to prevent atmospheric oxygen from entering the tube. At each test plot, sampling ports were established at 2 and 4 m depths. A small peristaltic pump was attached to the oxygen meter and used to sample the ports at periodic intervals.

The initial design of the pore gas samplers for the covers consisted of a 6 mm diameter stainless steel tube (1/4" x .035") with a conical brass tip at one end. The end of the tube with the brass tip was driven to the required sampling depth and then pulled up from the surface by 2 mm, so as to leave a clearance between the end of the tubing and the collar of the brass tip for sampling of the pore gas. A flexible rubber tube was attached, as previously described, to prevent atmospheric oxygen from entering the tube. A small peristaltic pump which was attached to the oxygen meter was used to sample the ports. Each cover was instrumented with pore gas sampling tubes to the depth of every layer, establishing an oxygen-concentration vertical profile. In the case of the test plot with the geomembrane, small holes were made in the HDPE cover prior to installations. Gas sampling tubes were driven into the sand layer underlying the HDPE cover through the pre-installation holes. These holes were carefully sealed prior to the placement of the top sand layer.

Following the detection of leaks in the initial set of pore gas samplers, the sampling tube design was altered to accommodate the small pore gas volume of fine-grained soils. The new design called for the 6 mm stainless steel tube to be permanently placed and sealed from side tube leakage. The buried end of the tube was wrapped with geotextile, placed in sand at the bottom of an auger hole, and sealed to the surface with bentonite (Figure 2.10). The exposed end of the tube, from which to extract a gas sample, was sealed with a rubber septum. The meter was then equipped with a syringe needle with which to sample a small volume of gas.

Water Quality

As already mentioned, piezometers were installed in the existing tailings directly underneath the covers to provide information on potential changes in water quality resulting from the presence of the covers. Since the movement of oxidized products in the tailings is expected to be slow, changes in pH, acidity, sulphate and metal concentrations in the existing oxidized tailings will not be seen for a few years because of stored acidity. This stored acidity is released only slowly and the rate of release will be even slower in fine-grained tailings.

In order to provide information on changes in water quality in the short term, a collection basin lysimeter was installed in the existing tailings directly beneath the cover. The lysimeter was filled with unoxidized tailings recovered from the southern section of the existing impoundment where the tailings are known to be more coarse-grained (Yanful *et al.*, 1990). Each lysimeter was designed to have a collection surface area of 2.2 m^2 and an approximate volume of 2000 L. These dimensions were based on the annual water balance of the site and an assumption that half of the observed infiltration will percolate through the cover. A practical design requirement was that each sampling of the lysimeter provides enough sample volume (500 to 1000 ml) for chemical analysis. Each lysimeter was designed to be connected to a 122 cm diameter and 400 cm high manhole by means of a 25 mm diameter sloping transfer pipe. The manhole was fabricated from 25 mm thick polyethylene. The transfer pipe connects to the manhole at a lower elevation to promote

drainage by gravity. Each lysimeter was constructed from acid resistant, high density polypropylene (HDPP). The locations of the lysimeter and the transfer pipe are illustrated in Figures 2.5 and 2.6.

Temperature

Type K thermocouples for monitoring the tailings temperature were secured to piezometers prior to installation, as described above for the gas samplers. In the covers, thermocouples were installed directly from the surface by pushing to the required depth.

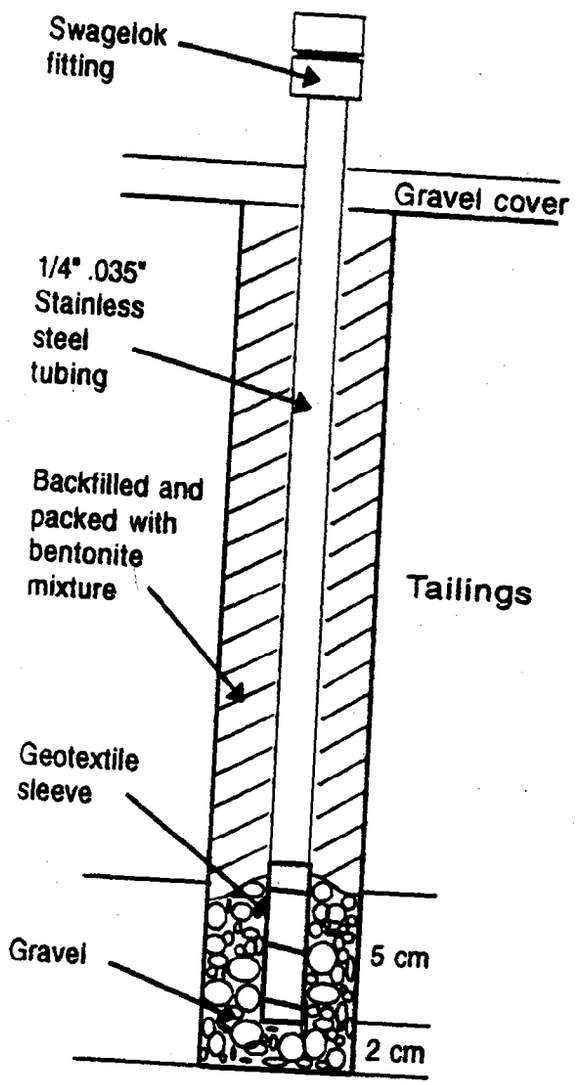

Figure 2.10: Pore Gas Sampling Probe

2.2 Results and Interpretation of the Field Study

Meteorological Conditions

Following the construction of the test plots in the fall of 1990, rainfall was measured on site with a tipping-bucket rain gauge. Unfortunately during 1992, power supply failures to the monitoring system resulted in an incomplete and non-discernible rainfall record. Rainfall during 1991, though, was collected from June through October and totalled for each month.

Station	June	July	Aug.	Sept.	Oct.	Total	% of WA
Waite Amulet 1991 (mm)	84.6	105.4	87.2	106.8	47.8	431.8	100
Amos 1991 (mm)	70.6	127.2	86.0	110.4	87.2	481.4	111
Duparquet 1991 (mm)	48.7	64.0	119.1	87.7	100.3	419.8	97

Amos and Duparquet are two regional meteorological stations. Amos is approximately 75 km ENE of Waite Amulet and Duparquet is approximately 25 km NNW. Meteorological summaries for both stations are located in Appendix A. As indicated, the total rainfall at Waite Amulet for June through October, 1991 agrees reasonably well with the totals from the regional stations. In addition, the database for the regional stations is quite extensive, consisting of 30 years of records. The 1992 total rainfall for the regional stations and other statistical parameters were, therefore, used to characterize rainfall and other meteorological conditions at the test plot site.

Table 2-I presents a qualitative description of the summer, winter and annual meteorological conditions for 1991 and 1992. Since the construction of the test plots, the winters have generally been normal in terms of both temperature and snowfall. Summer rainfall has been normal, with the exception of June, 1992 which was dry. The summer temperatures, though, have not been normal: 1991 was warm, which contributed to very high evaporation, and 1992 was cool while evaporation was normal.

TABLE 2-I - GENERALIZED METEOROLOGICAL CONDITIONS DURING THE FIELD STUDY

Season	Parameter	1991	1992
Summer (May - Sep)	Rainfall (mm)	normal	normal
	Evaporation (mm)	**very high**	normal
	Average Temperature (C)	warm	cool
Winter (Nov - Mar)	Snowfall (mm)	normal	normal
	Average Temperature (C)	normal	normal
Annual (Jan - Dec)	Precipitation (mm)	normal	normal
	Average Temperature (C)	warm	cool

normal = within one standard deviation of the mean

warm & cool temperature |
wet & dry precipitation | = between one and two standard deviations
high & low evaporation |

hot & cold temperature |
very wet & very dry precipitation | = between two and three standard deviations
very high & very low evaporation |

Soil Temperature

Soil temperature was measured with the thermocouples located in the heat dissipation sensors at each test plot. The sensors were located in the centre of each 30 cm lift of the soil cover and in the tailings at 25, 50 and 75 cm below the tailings surface. Figures 2-11 through 2-14 show the mean monthly temperature of each sensor during the study period for the four plots, R1 through R4, respectively.

Most significantly, the four figures show the depth of freezing at each test plot. At the control site (R1), freezing temperatures were encountered at the 25 cm depth but not at 50 and 75 cm depth. At the two clay cover sites (R2 and R3), the covers froze but the tailings did not. The soil cover with the geomembrane layer (R4) also froze but because the sensor located at 25 cm in the tailings malfunctioned in February, 1992 (before freezing temperatures were recorded), it is uncertain whether the tailings froze. The sensors located at 50 and 75 cm, though, did not indicate freezing conditions.

Table 2-II shows the values which are illustrated in the four figures. By placing a soil cover on the tailings, the tailings surface is insolated from the atmosphere and solar radiation. The outcome of this, as shown by the temperature data, results in three phenomena: (1) the average temperature of the surface tailings is reduced, as shown by the average of all the monthly values; (2) range in temperature is also reduced, particularly during the summer months which is depicted by the decreased deviation from the mean; and (3) the response to seasonal temperature changes is delayed, most evident in the delay of the maximum and minimum monthly mean temperature by about a month.

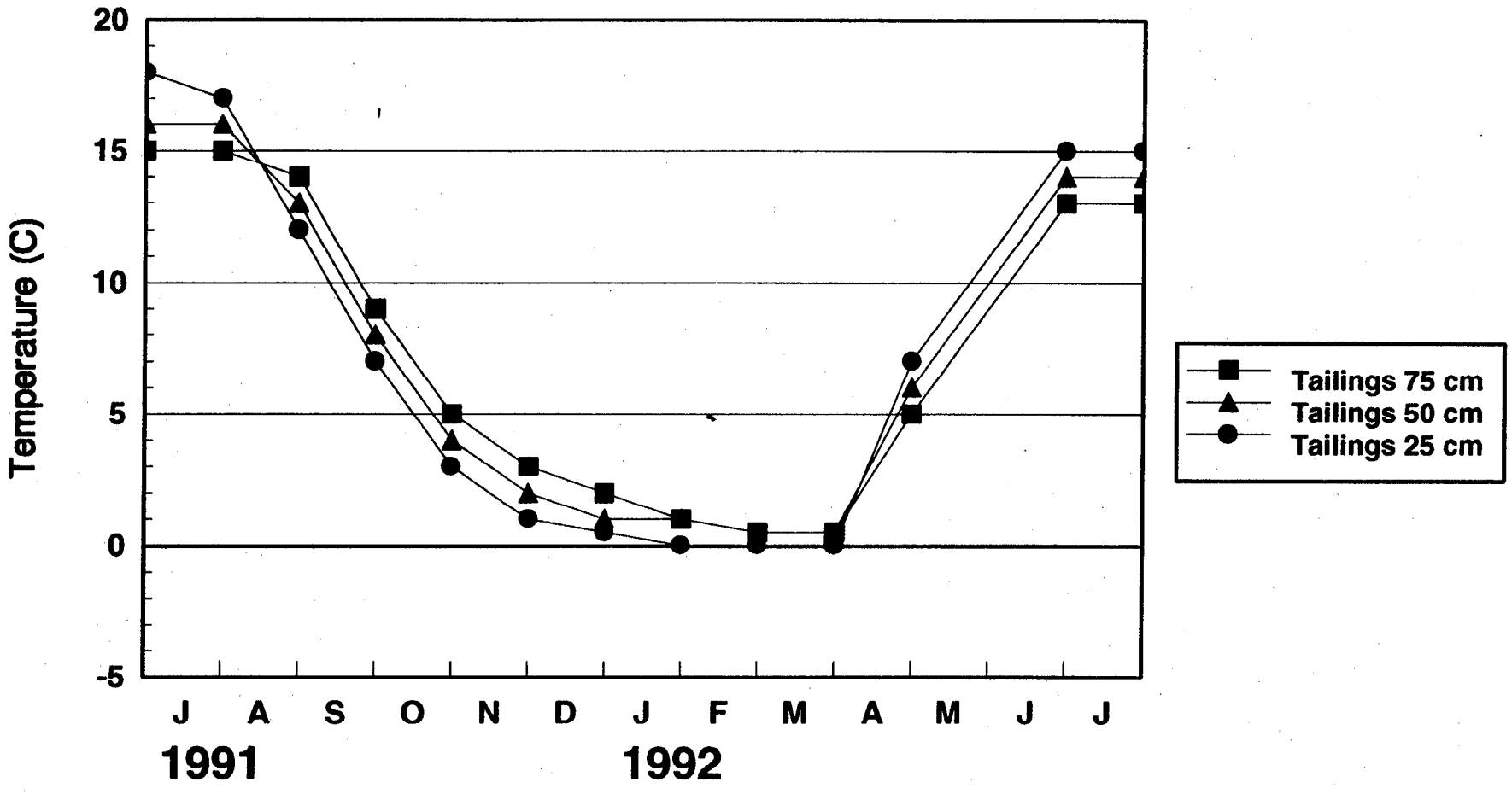

Figure 2.11: Average Monthly Temperatures at R1

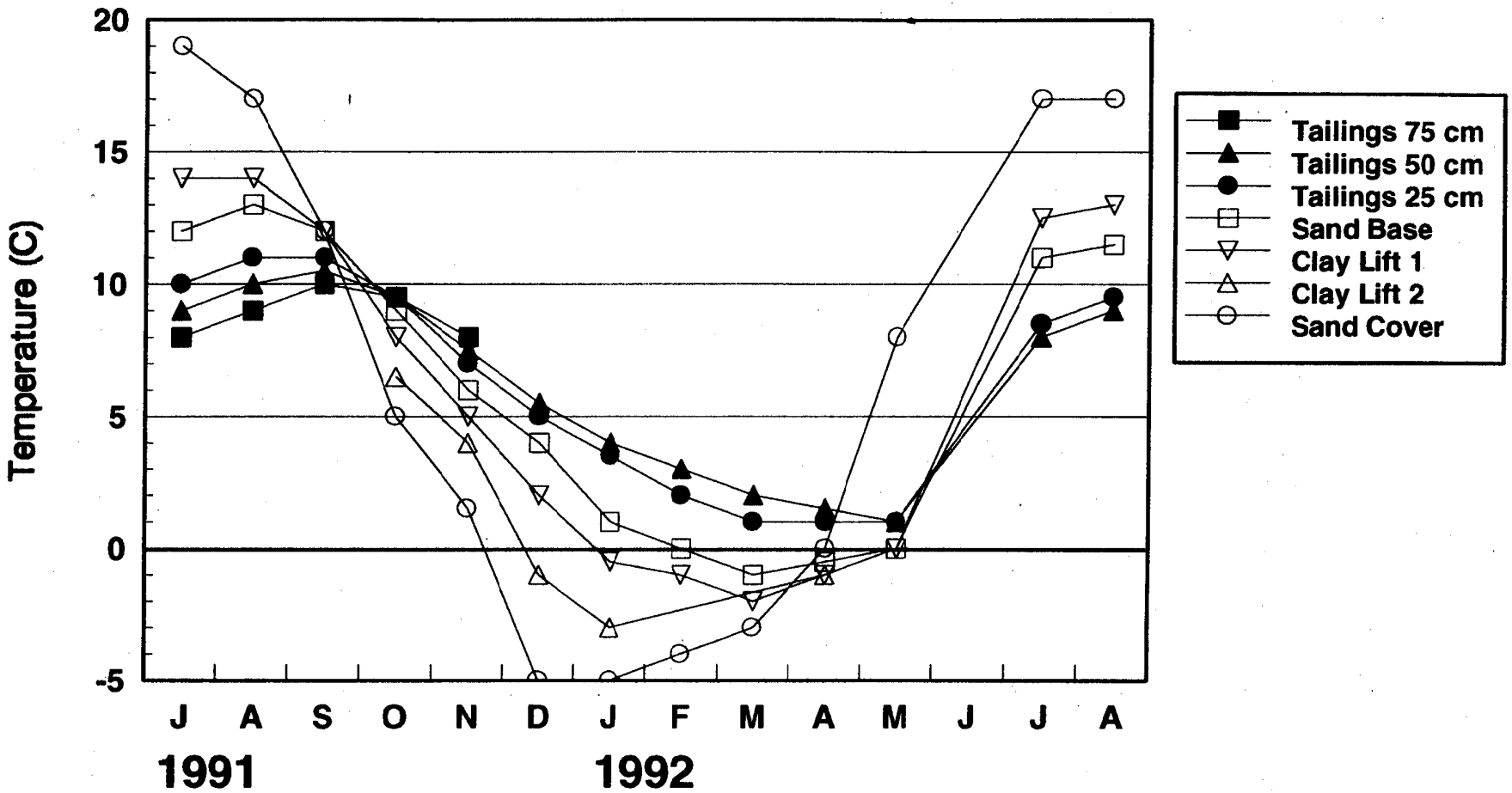

Figure 2.12: Average Monthly Temperatures at R2

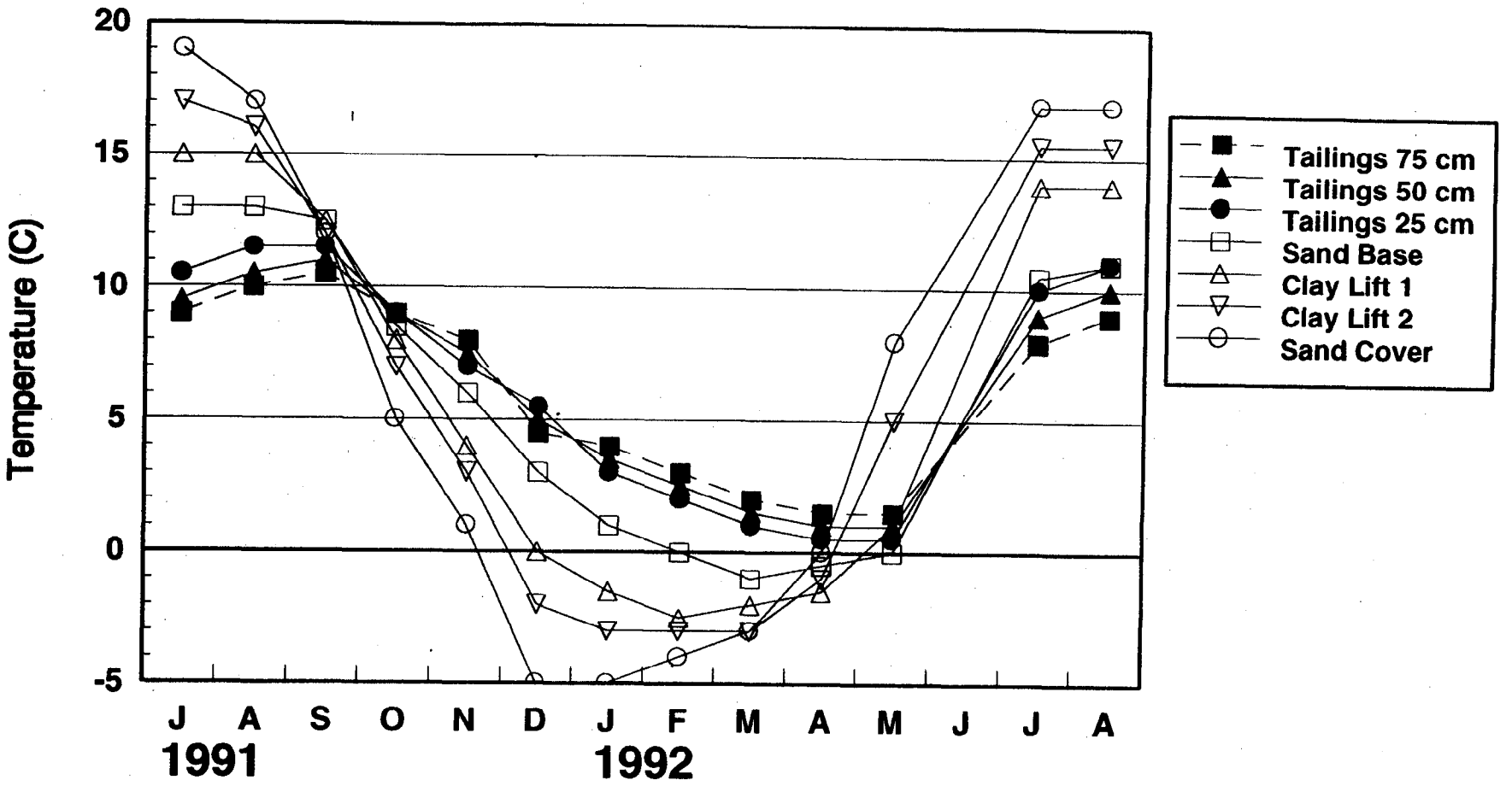

Figure 2.13: Average Monthly Temperatures at R3

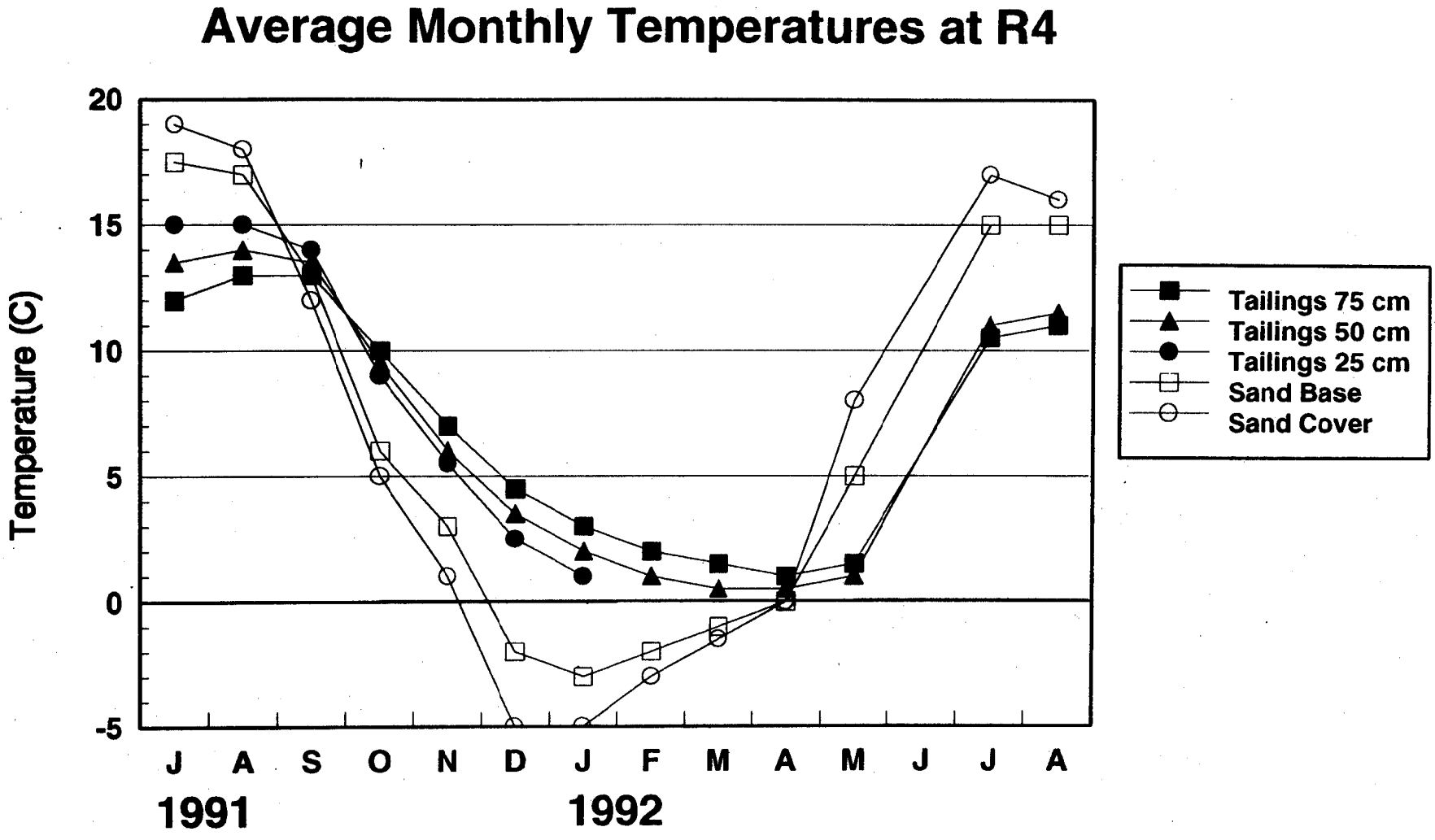

Figure 2.14: Average Monthly Temperatures at R4

Table 2-II - AVERAGE MONTHLY TEMPERATURES (C) 0F THE TEST PLOT COVERS.

Test Plot	Sensor Location	1991 Jul	Aug	Sep	Oct	Nov	Dec	1992 Jan	Feb	Mar	Apr	May	Jun	Jul	Aug	Max.	Min.	Avg.	Std. Dev.
R1	Tailings 25 cm depth	18.0	17.0	12.0	7.0	3.0	1.0	0.5	0.0	0.0	0.0	7.0	-	15.0	15.0	18.0	0.0	7.3	7.2
	Tailings 50 cm depth	16.0	16.0	13.0	8.0	4.0	2.0	1.0	1.0	0.5	0.5	6.0	-	14.0	14.0	16.0	0.0	7.4	6.4
	Tailings 75 cm depth	15.0	15.0	14.0	9.0	5.0	3.0	2.0	1.0	0.5	0.5	5.0	-	13.0	13.0	15.0	0.0	7.4	5.9
R2	Sand Cover	19.0	17.0	12.0	5.0	1.5	-5.0	-5.0	-4.0	-3.0	0.0	8.0	-	17.0	17.0	19.0	-5.0	6.1	9.4
	Clay Lift 2	-	-	-	6.5	4.0	-1.0	-3.0	-	-	-1.0		-	-	-	-	-	-	-
	Clay Lift 1	14.0	14.0	12.0	8.0	5.0	2.0	-0.5	-1.0	-2.0	-1.0	0.0	-	12.5	13.0	14.0	-2.0	5.8	6.6
	Sand Base	12.0	13.0	12.0	9.0	6.0	4.0	1.0	0.0	-1.0	-0.5	0.0	-	11.0	11.5	13.0	-1.0	6.0	5.6
	Tailings 25 cm depth	10.0	11.0	11.0	9.5	7.0	5.0	3.5	2.0	1.0	1.0	1.0	-	8.5	9.5	11.0	0.0	6.2	4.0
	Tailings 50 cm depth	9.0	10.0	10.5	9.5	7.5	5.5	4.0	3.0	2.0	1.5	1.0	-	8.0	9.0	10.5	0.0	6.2	3.5
	Tailings 75 cm depth	8.0	9.0	10.0	9.5	8.0	-	-	-	-	-	-	-	-	-	10.0	-	-	-
R3	Sand Cover	19.0	17.0	12.0	5.0	1.0	-5.0	-5.0	-4.0	-3.0	0.0	8.0	-	17.0	17.0	19.0	-5.0	6.1	9.4
	Clay Lift 2	17.0	16.0	12.0	7.0	3.0	-2.0	-3.0	-3.0	-3.0	-1.0	5.0	-	15.5	15.5	17.0	-3.0	6.1	8.2
	Clay Lift 1	15.0	15.0	12.5	8.0	4.0	0.0	-1.5	-2.5	-2.0	-1.5	1.0	-	14.0	14.0	15.0	-2.5	5.8	7.4
	Sand Base	13.0	13.0	12.5	8.5	6.0	3.0	1.0	0.0	-1.0	-0.5	0.0	-	10.5	11.0	13.0	-1.0	5.9	5.7
	Tailings 25 cm depth	10.5	11.5	11.5	9.0	7.0	5.5	3.0	2.0	1.0	0.5	0.5	-	10.0	11.0	11.5	0.0	6.4	4.5
	Tailings 50 cm depth	9.5	10.5	11.0	9.0	7.5	5.0	3.5	2.5	1.5	1.0	1.0	-	9.0	10.0	11.0	0.0	6.2	3.9
	Tailings 75 cm depth	9.0	10.0	10.5	9.0	8.0	4.5	4.0	3.0	2.0	1.5	1.5	-	8.0	9.0	10.5	0.0	6.2	3.4
R4	Sand Cover	19.0	18.0	12.0	5.0	-	-5.0	-5.0	-3.0	-1.5	0.0	8.0	-	17.0	16.0	19.0	-5.0	6.7	9.5
	Geomembrane	-	-	-	-	-	-	-	-	-	-	-	-	-	-	-	-	-	-
	Sand Base	17.5	17.0	13.0	6.0	-	-2.0	-3.0	-2.0	-1.0	0.0	5.0	-	15.0	15.0	17.5	-3.0	6.7	8.3
	Tailings 25 cm depth	15.0	15.0	14.0	9.0	-	2.5	1.0	-	-	-	-	-	-	-	15.0	-	-	-
	Tailings 50 cm depth	13.5	14.0	13.5	9.5	-	3.5	2.0	1.0	0.5	0.5	1.0	-	11.0	11.5	14.0	0.0	6.8	5.8
	Tailings 75 cm depth	12.0	13.0	13.0	10.0	-	4.5	3.0	2.0	1.5	1.0	1.5	-	10.5	11.0	13.0	0.0	6.9	5.0

Comparing the soil-covered plots (R2 and R3) with the control (R1), the change in temperature due to the placement of the composite soil cover is illustrated in the adjacent figure. A negative value for the change in temperature indicates cooler temperatures under the cover, while a positive value shows warming. In general, although there are warmer temperatures in the surface tailings during the winter and cooler temperatures during the summer, cooling predominates. Indeed, the overall (annual) change in temperature due to the presence of the cover is -1.2°C in the upper 1 m of the tailings: -1.1°C at 25 cm depth, -1.2°C at 50 cm, and -1.3°C at 75 cm. Thus, cooler temperatures occur under the cover in winter than in summer, as expected. The geomembrane-covered tailings (R4) showed similar results but to a lesser extent, with the overall change in temperature being -0.75°C in the upper 1 m of tailings.

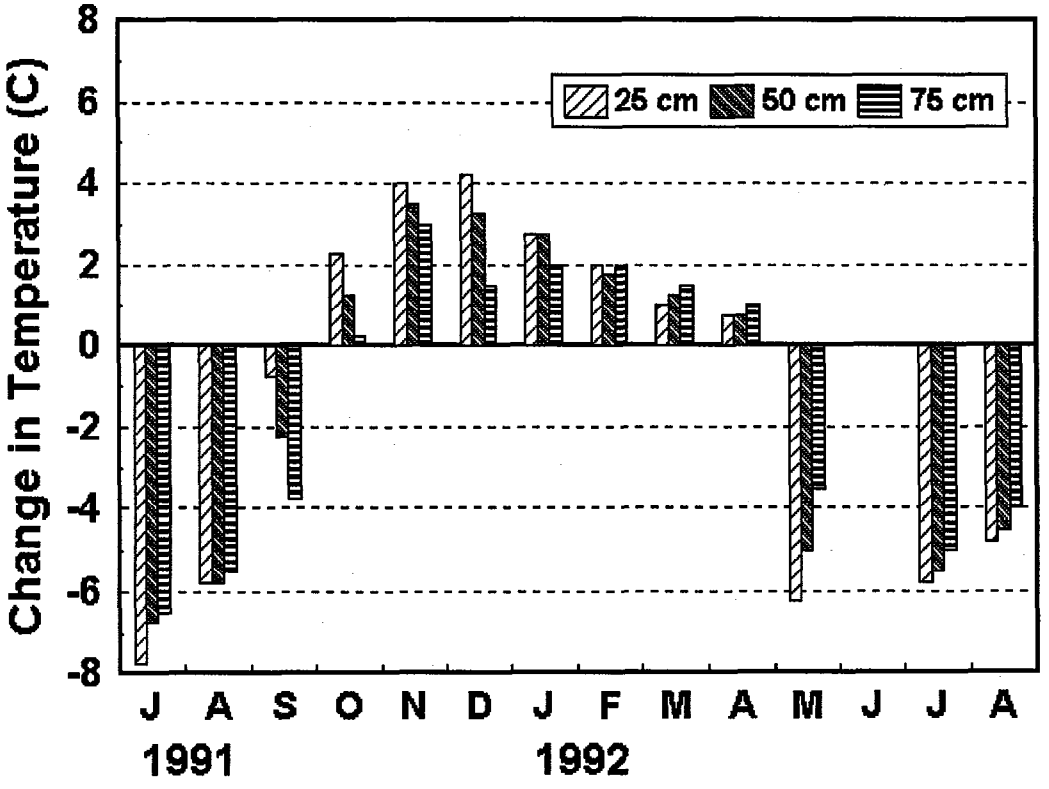

Figure 2.15: Change in Temperature

Water Content

Water content of the cover was periodically measured with time-domain reflectometry (TDR). In general, TDR is weakly dependent on soil type, density, temperature and electrical conductivity (Topp *et al.*, 1980). However, TDR measurements made on actively oxidizing tailings with high ionic strength gave poorly-defined waves which were difficult to interpret. The absolute values of the reported water contents of the tailings may, therefore, not be entirely correct. In fact, some of the water contents were too high, compared to the porosity. These high water contents were generally found to be associated with pore waters containing high dissolved total iron. The TDR data are, however, useful as an indication of the degree of water saturation and as a comparison when soil properties are similar. TDR measurements in the composite soil cover are accurate and were validated against gravimetric measurements made in October of 1992 and during construction of the cover.

Figures 2.16 through 2.19 show the TDR measurements at R1 through R4, respectively. During construction of the test plots, it was observed that the tailings were very wet and close to saturation. In general, the tailings remain close to saturation under the covers (R2, R3, and R4) while the control, uncovered tailings (R1), underwent periods of wetting and drying. The tailings also appear to be progressively wetter from R1 to R4. Figures 2.17 and 2.18 clearly show that the clay layer at both R2 and R3 has remained at the original high saturation of at least 93%. The sand base has remained at residual water content, thus providing a capillary barrier and restricting drainage of the clay.

Since TDR measures only unfrozen water, it can be used to indicate when soils are frozen. The TDR data indicate the tailings under the soil covers do not freeze while the uncovered tailings freeze during the winter. The clay cover also shows freezing during winter. These data agree with the temperature data.

Water Table

The water table is an equilibrium surface at which the fluid pressure in the voids equals atmospheric pressure. At the water table the pressure head (Ψ) equals zero. In general, the water table indicates the division between saturated and unsaturated soils, although, a saturated capillary fringe typically extends above the water table. The extent of the capillary fringe is inversely proportional to the size of the soil void and hence the particle size. The water table was located at each piezometer nest by extrapolating pressure heads to zero. These figures appear in Appendix B.

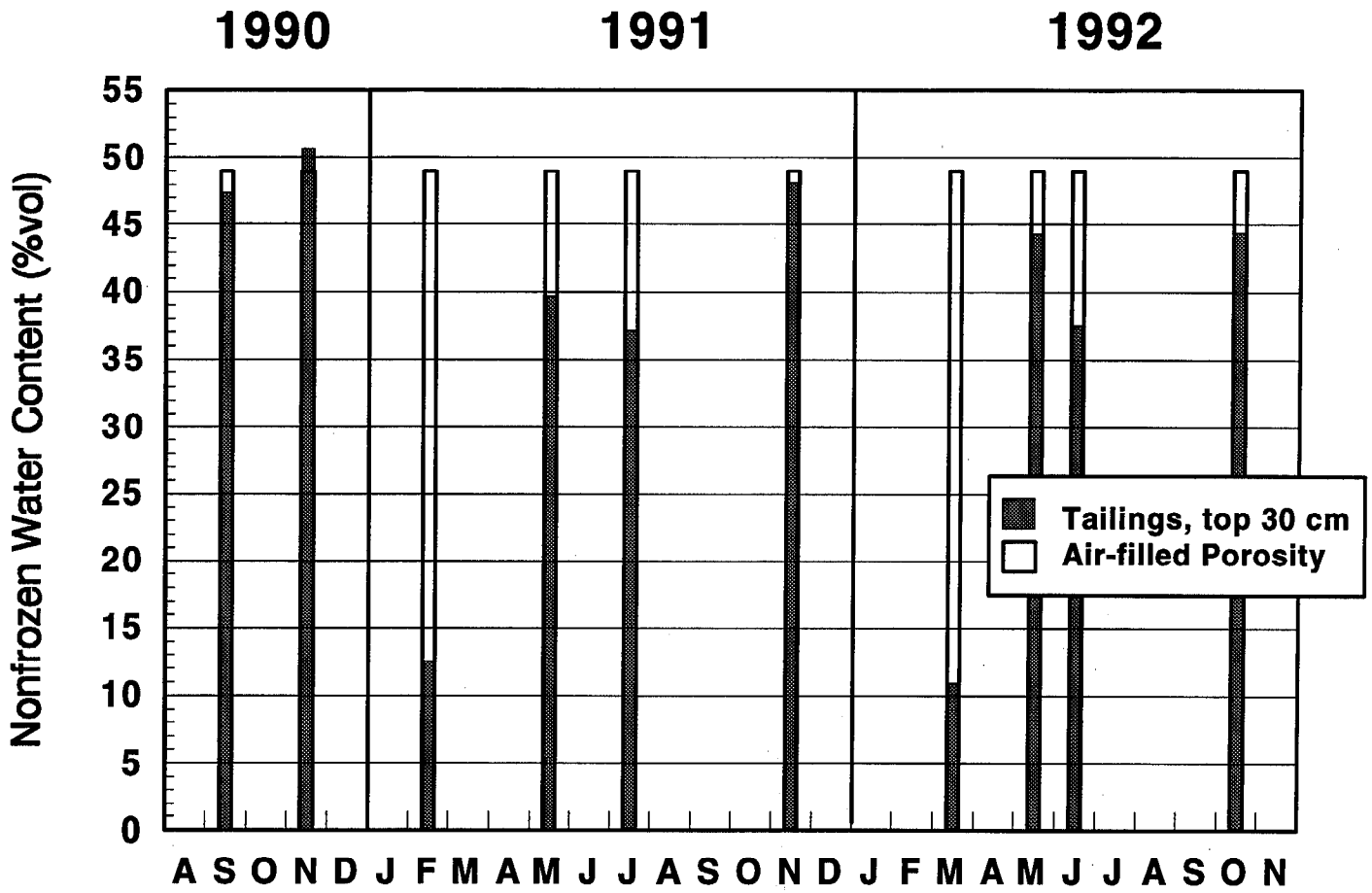

Figure 2.16: Water content at R1, the control test plot.

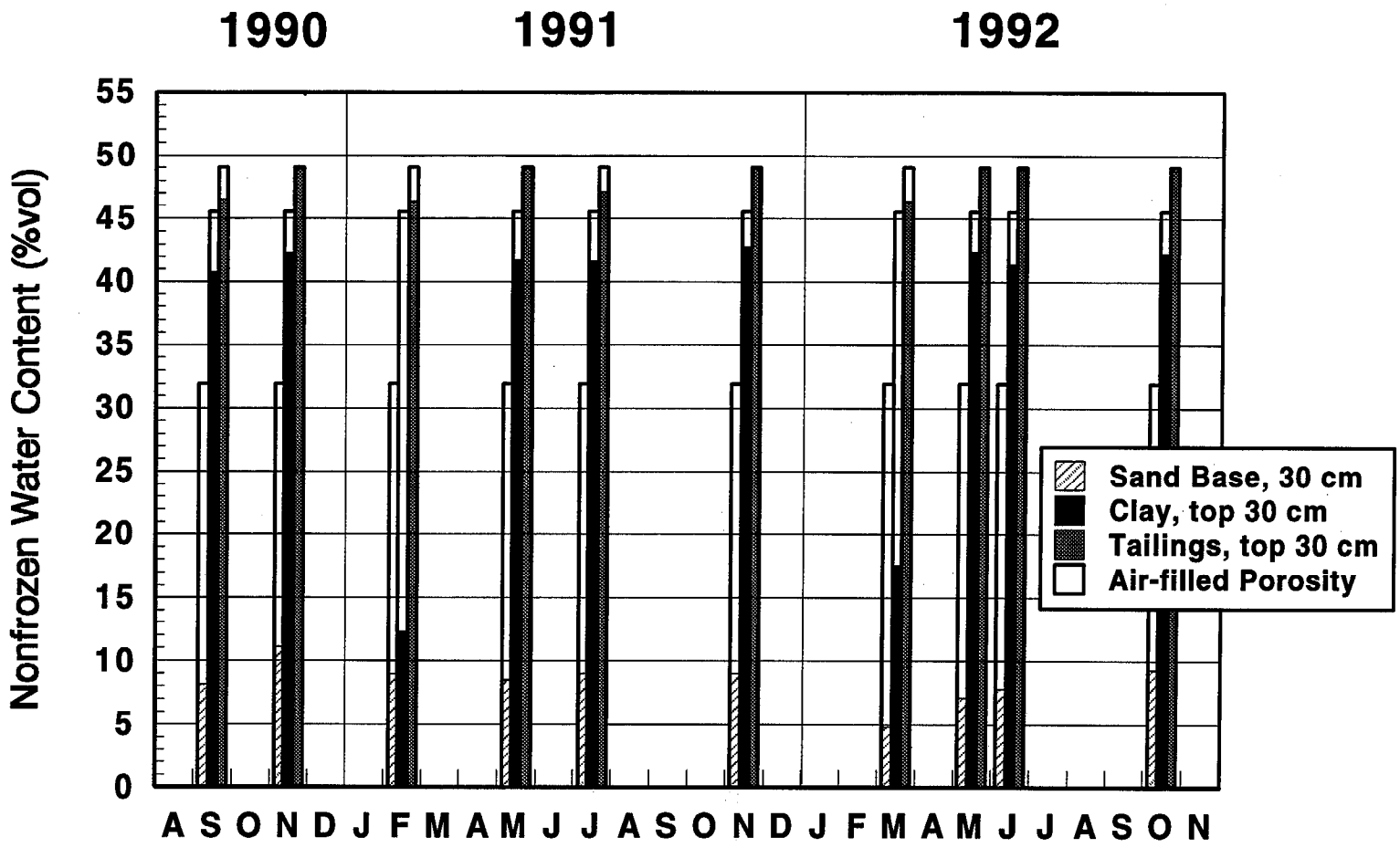

Figure 2.17: Water content at R2, clay cover test plot.

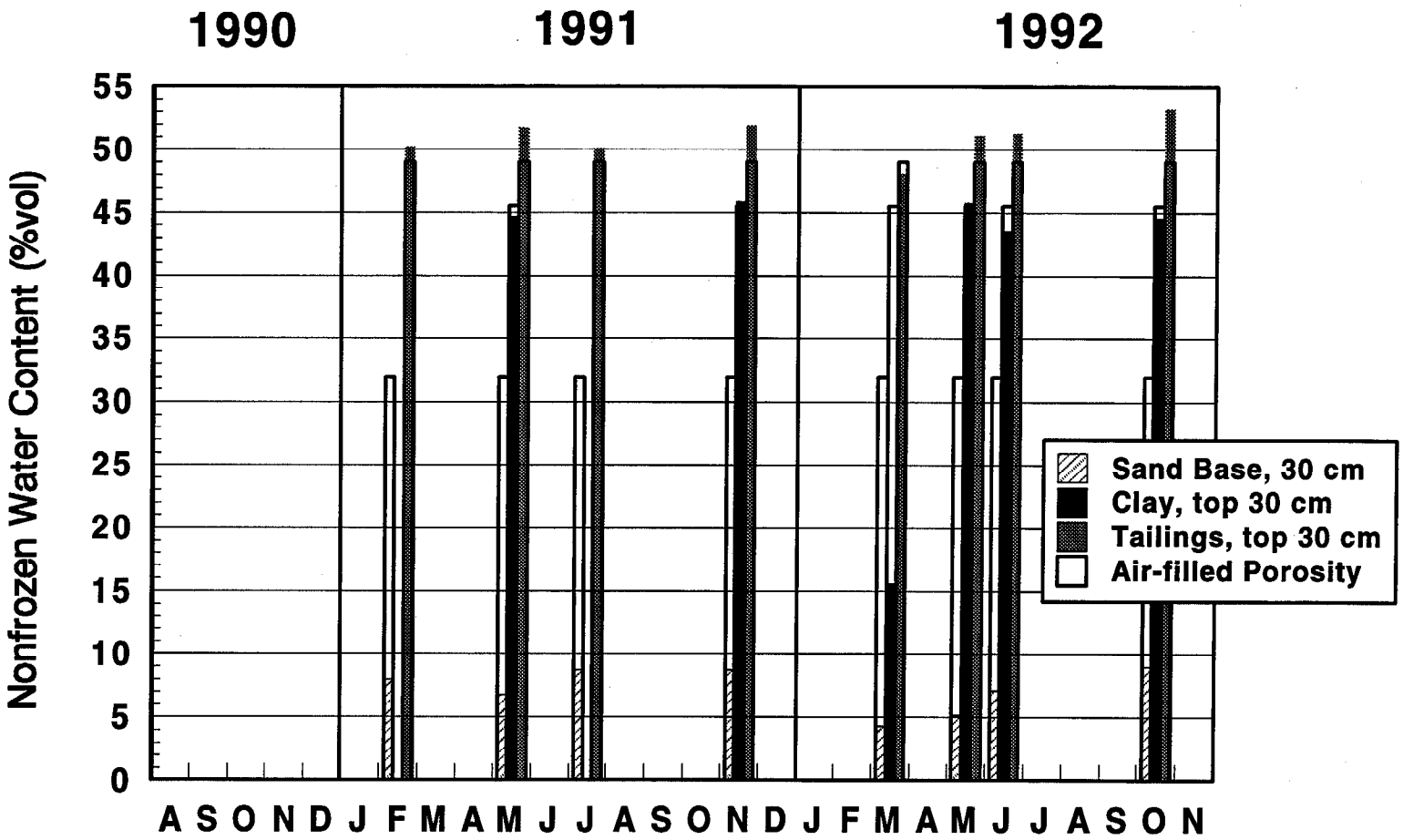

Figure 2.18: Water content at R3, clay cover test plot.

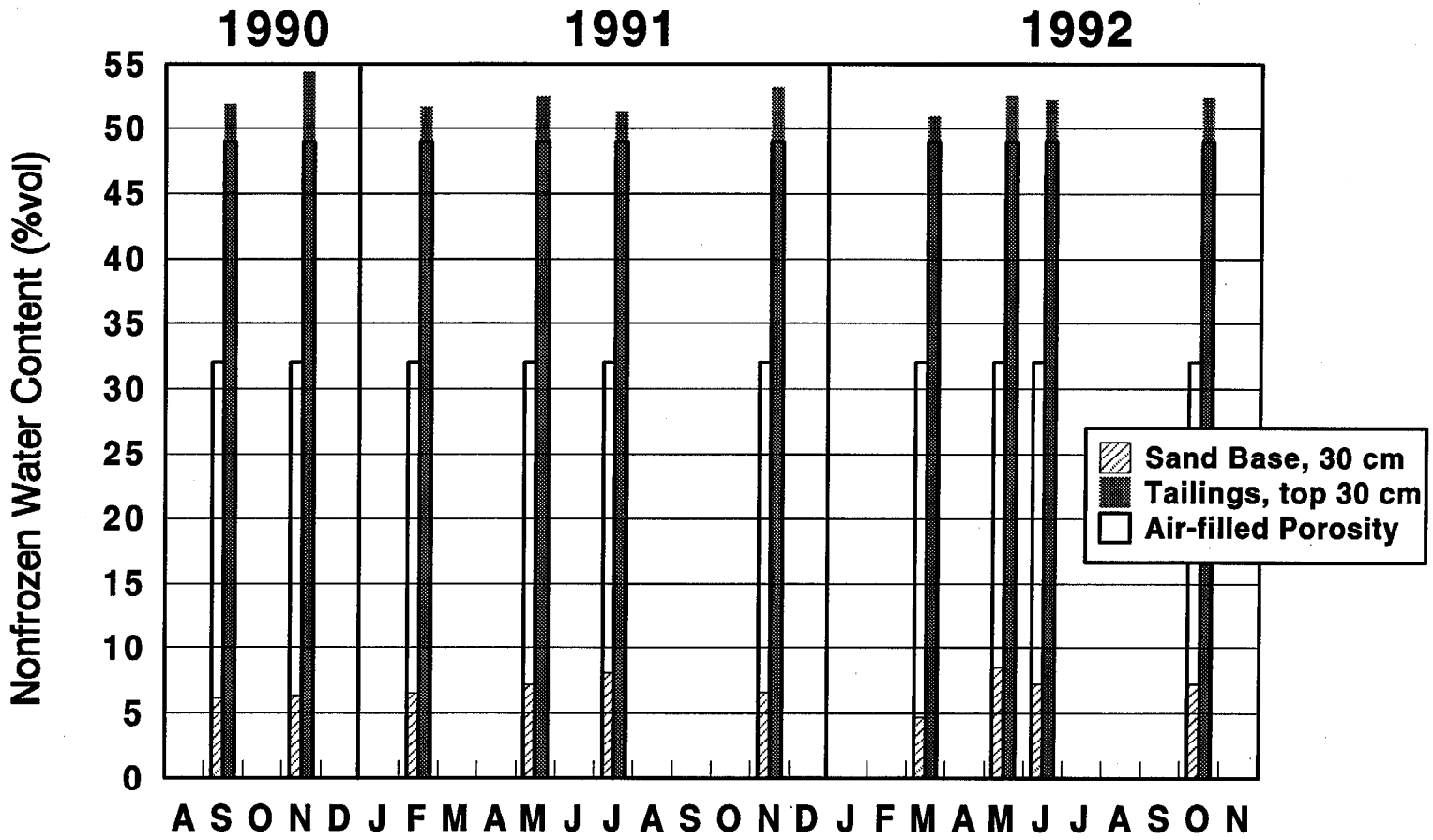

Figure 2.19: Water content at R4, geomembrane cover test plot.

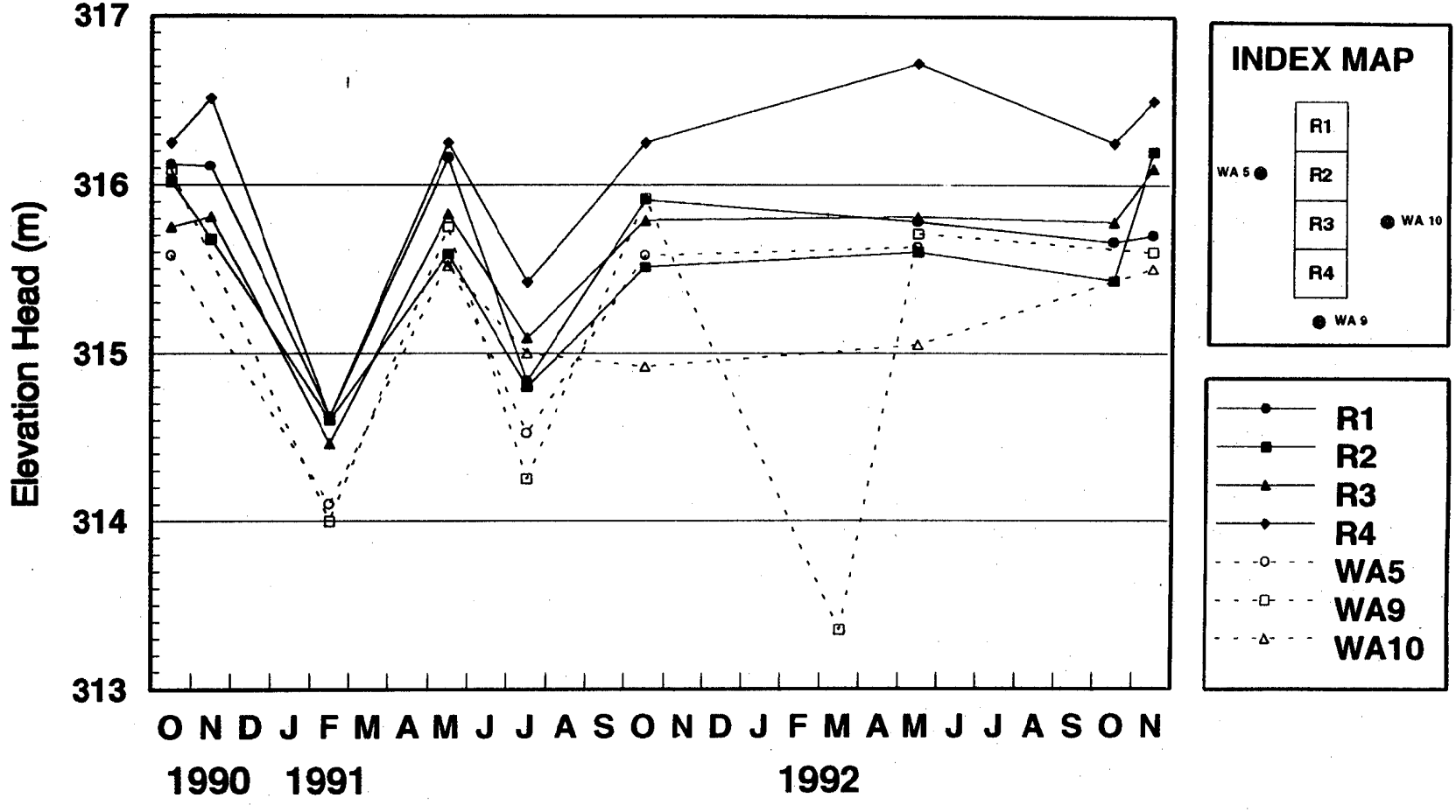

Figure 2.20: Water Table Elevation Hydrograph

Figure 2.20 shows the water table elevation at each piezometer nest. The water table was highest during spring and fall and lowest during winter and summer. During the winter, much of the precipitation is held at the surface as snow which reduces recharge to the water table. As the tailings continue to drain, the water table also falls. During the summer, evaporation can drive the water table down during dry periods.

The test plot site location was selected near the groundwater divide where horizontal movement of the tailings pore water and off-site impacts are minimal. At the groundwater divide, though, the water table is higher than surrounding (down gradient) areas. The off-site, generally northward and westward regional flow is evident in Figure 2.21 at times when the water table is low and recharge is minimal. During periods of elevated recharge, localized ponding raises the water table and enhances the local flow patterns. Figure 2.22 shows, in plain view, the water table elevation contours in the summer (July 1991) when the water table was low.

At the test plot site, the water table is often higher at R4 (and R1) than at R2 (and R3). The observed (bow shape) dimple in the water table profile is presumably caused by the reduced vertical flow of water through the soil covers at R2 and R3. In addition, upward gradients are commonly observed at R2 (Appendix B), indicating local flow from the surrounding uncovered tailings. The water table is consistently highest at R4 and at times above the tailings surface. This suggests tailings pore water has likely contaminated the lysimeter at R4 and, possibly, the lysimeters at R3 and R2 by flowing through the sand base.

Soil Suction

Below the water table the pressure head (Ψ) is positive and above the water table it is negative. Negative pressure head is commonly expressed as a positive number and called soil suction. The soil suction was measured in the covers and surface tailings with electrical resistance sensors (gypsum blocks). These sensors, though principally dependent on soil suction, are also dependent on pore water chemistry (i.e., high levels of electrical conductivity). Therefore, as a measure of soil suction, they are more accurate in the cover than in the actively oxidizing tailings.

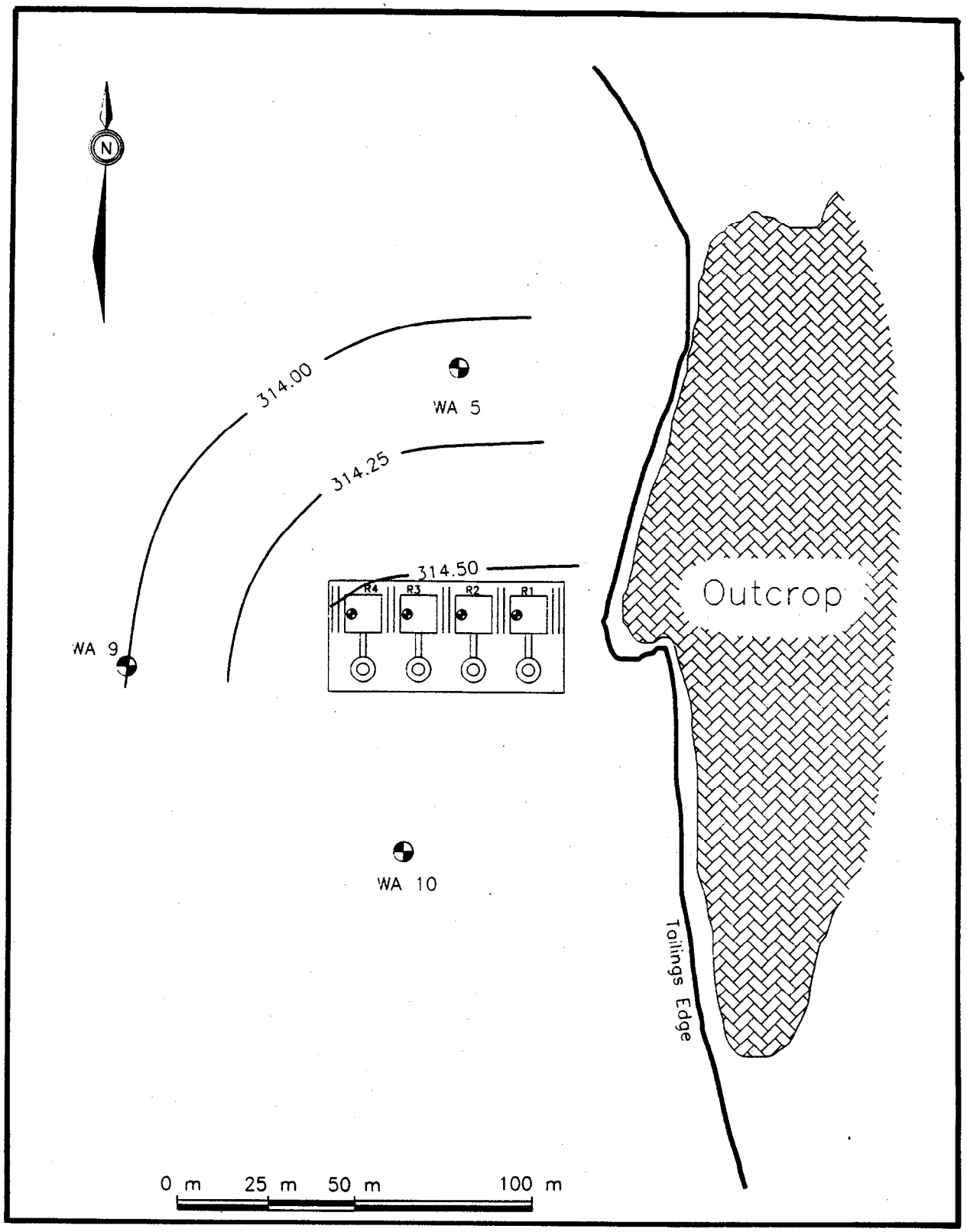

Figure 2.21: Water Table Elevations at Waite Amulet, Quebec February, 1992

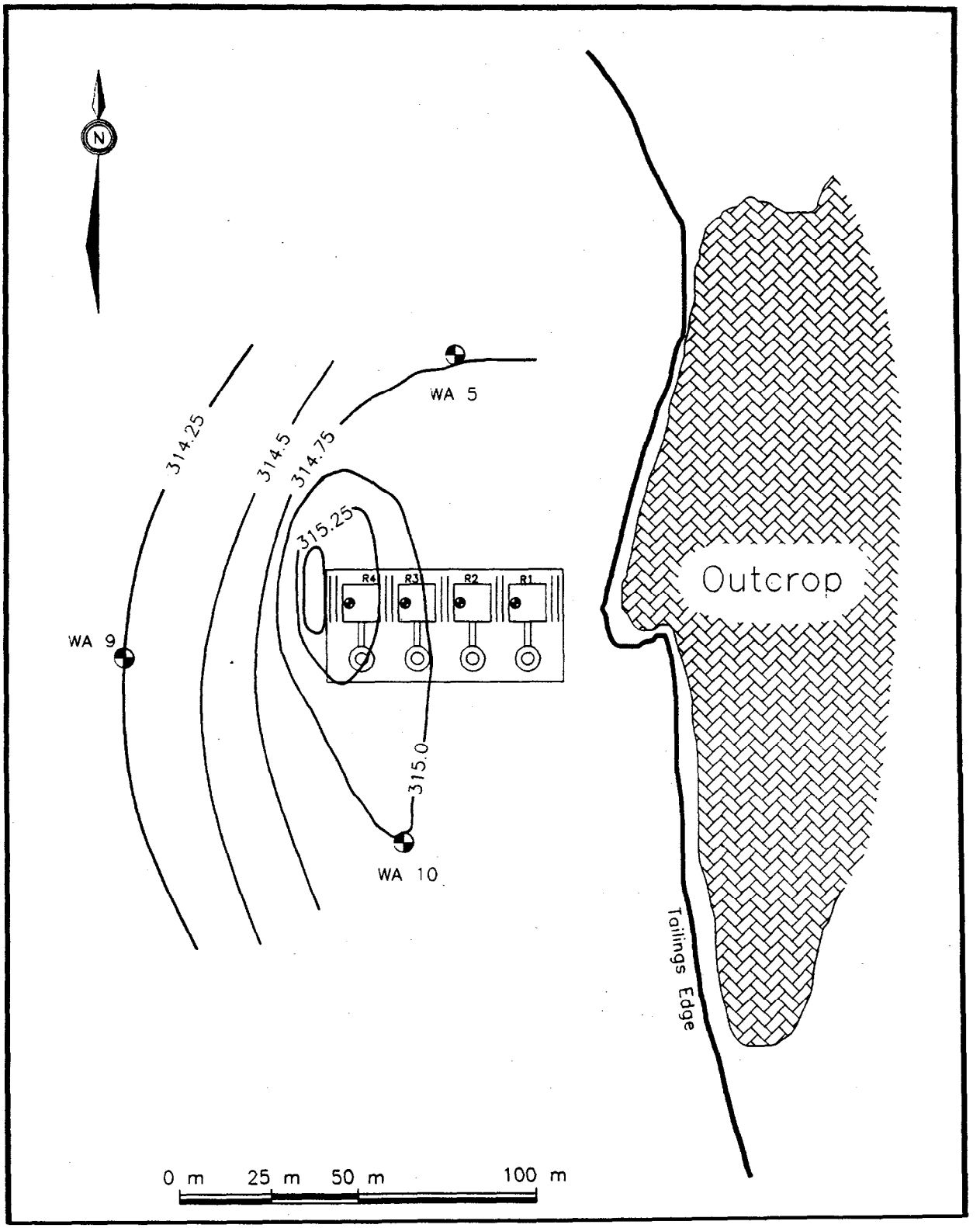

Figure 2.22: Water Table Elevations at Waite Amulet, Quebec July, 1991

A generalized calibration is provided by the manufacturer to convert the gypsum block output (ohms) to pressure (kPa, bars, or m of water). The calibration, though, is not applicable when the suction is low, i.e., when the sensors are saturated. Prior to installation, 42 sensors were saturated with deionized water and the sensor outputs measured. The mean was 83 Ω and the standard deviation was 21 Ω. These results indicate that at about 83 Ω, Ψ=0 and there is no suction. The manufacturer's calibration defines no suction as 0 Ω (no resistance), 1 m water as 20 Ω, and 2 m suction as 72 Ω. The calibration was, therefore, adjusted by eye to fit zero suction to 83 Ω.

Gypsum blocks were successfully measured during July and August 1993, during a time of high evaporation. The results generally indicate low suctions, between -3 and -1 m water, and a slight gradient of 0.5 from the sand base upward, and downward to the tailings. Table 2-III shows the hydraulic heads measured with the gypsum blocks.

TABLE 2-III - MEAN HYDRAULIC HEADS IN THE COVER AND UNSATURATED TAILINGS

Test Plot	Layer	July 1993 (m water)	August 1993 (m water)
R1	Tailings, 15 cm below tailings surface	-3.0	-3.0
	Tailings, 45 cm below tailings surface	-3.0	-3.0
	Tailings, 75 cm below tailings surface	-3.0	-3.0
R2	Sand Cover, 105 cm above tailings	-1.8	-1.8
	Clay, 75 cm above tailings	-	-
	Clay, 45 cm above tailings	-1.8	-1.8
	Sand base, 15 cm above tailings	-1.2	-1.2
	Tailings, 15 cm below tailings surface	-	-
	Tailings, 45 cm below tailings surface	-1.8	-1.8
	Tailings, 75 cm below tailings surface	-2.0	-2.0
R3	Sand Cover, 105 cm above tailings	-1.8	-1.8
	Clay, 75 cm above tailings	-1.8	-1.8
	Clay, 45 cm above tailings	-1.8	-1.8
	Sand base, 15 cm above tailings	-1.2	-1.2
	Tailings, 15 cm below tailings surface	-2.0	-
	Tailings, 45 cm below tailings surface	-	-2.3
	Tailings, 75 cm below tailings surface	-	-
R4	Sand Cover, 45 cm above tailings	-3.2	-3.2
	Sand base, 15 cm above tailings	-2.5	-2.2
	Tailings, 15 cm below tailings surface	-3.3	-3.3
	Tailings, 45 cm below tailings surface	-	-
	Tailings, 75 cm below tailings surface	-	-

Note: Tailings surface is the elevation reference (z=0).

2.3 Modelling of Percolation through the Soil Cover

2.3.1 HELP Model Background

The Hydrological Evaluation of Landfill Performance (HELP) model is a deterministic water balance model which uses climatic, soil and design data to determine the water budget of a landfill (Schroeder *et al.*, 1984). This model is intended for use in assessing the effectiveness of soil covers on landfills containing hazardous or municipal solid waste. The objective in using a soil cover for solid waste is to minimize the infiltration of water and hence the formation of leachate. The composite soil covers at the Waite Amulet experimental site are similar in design to landfill covers. An additional design requirement for tailings covers, however, is to minimize the flux of oxygen. This is accomplished by maintaining a high saturation of the clay layer. The HELP model was therefore utilized in this project to evaluate the magnitude of percolation that is expected through the composite soil covers. A small amount of percolation is required to maintain a high saturation; however, a large amount of percolation will tend to drain the clay layer. The magnitude of the other water balance components at the field site were also estimated by the model.

The initial step in the HELP modelling involved dividing the cover into layers and detailing the thickness, soil type and slope of each layer. There are four types of layers which are defined by the HELP model: (1) a vertical percolation layer which allows only vertical flow, (2) a lateral drainage layer which allows both vertical and horizontal flow, (3) a barrier soil layer which restricts vertical flow, and (4) a waste layer. Once the thickness and type of layer is selected, the soil data (such as porosity and hydraulic conductivity) are input. Where actual soil data are not available, the model has 18 default soil types.

Climatic data needed to run the HELP model consist of daily precipitation, temperature, and solar radiation. The daily precipitation data may be synthetically generated[1] for 139 US cities and corrected with mean monthly data for the study site. There is also a data base of 5-year data sets for 102 US cities which can be site corrected. Daily temperature and radiation is synthetically generated for the selected city and corrected for the site latitude and mean monthly temperature and precipitation data. Daily precipitation, temperature, and solar radiation may also be directly input.

The HELP model simulates 4 hydrologic processes on a daily account: (1) run-off, and hence infiltration, is computed using the US Soil Conservation Service (SCS) Curve

---

[1]The synthetic generation of data is a method with which a record of daily values is formulated using the monthly average value and several statistical coefficients describing the distribution. The coefficients are constant for a given month but vary from month to month. The HELP model has default statistical coefficients and mean monthly values for 184 U.S. cities. A synthetic data record, however, can be corrected to the study site with mean monthly values from the site or a regional meteorological station.

Number method; (2) percolation (i.e., saturated and unsaturated vertical flow) is modeled using Darcy's law; (3) lateral drainage is computed using Boussinesq equation; and (4) evaporation is estimated with a modified Penman method. Other components of the water budget are deduced from these results.

The impact of vegetation on the hydrologic system is considered with a leaf area index (LAI). The LAI is a dimensionless ratio of the leaf area of active transpiration vegetation to the normal surface area of land on which the vegetation is growing. The LAI is used to model evaporation during the growing season. In addition to the LAI, the evaporative zone depth and SCS run-off curve number is also selected with regard to vegetative cover type.

Schroeder and Peyton (1987) performed a study to evaluate the sensitivity of the input parameters in order to determine which were the most influential in terms of evaluating the water budget. The parameters which were determined to have the greatest effect on the water budget were the hydraulic conductivity of the topsoil and lateral drainage layers, and the clay liners. These parameters are particularly important in estimating the percolation.

In addition to the sensitivity analysis of the input parameters, Schroeder and Peyton (1987) attempted a verification of the model with field data. The field data were obtained from seven sites for the purpose of comparison with model simulations. In general, the model agreed with field data, though, in some cases it was difficult to find agreement between observed surface run-off and that determined by HELP. In other cases, it was difficult to find agreement between evapotranspiration determined by HELP and that measured in the field. However, it was concluded that lack of adequate field data made it difficult to correlate the two sets of data.

2.3.2 Input Data to the HELP Model

Table 2-IV lists the input data used in the HELP modelling. Default soil parameters were initially selected to guide model set-up, but laboratory measured values replaced the default values where feasible. Twenty years of daily precipitation, temperature and solar radiation data were synthetically generated with the HELP model for Caribou, Maine, the most applicable site in the HELP data base. These values were corrected for the latitude of Waite Amulet (48.3°) and the mean monthly precipitation and temperature for Amos, Quebec (1961-90).

TABLE 2-IV - HELP MODEL INPUT DATA

Soil and Design Specifications			
Layer	Sand Cover	Clay	Sand Base
Layer Type	Lateral Drainage	Barrier	Vertical Percolation
Layer Thickness	30 cm	60 cm	30 cm
Porosity [a]	0.33	0.445	0.39
Field Capacity [a]	0.08	0.43	0.05
Wilting Point	0.03	0.35	0.025
Initial Water Content [a]	0.08	0.44	0.05
Saturated Hydraulic [a] Conductivity	2.6×10^{-3} cm/s	8.4×10^{-3} cm/s	1.0×10^{-7} cm/s
Slope	0 %		
Maximum Drainage Length	14 m		
Cover Area	400 m^2		
Synthetic Climatic Formulation and General Simulation Data			
SCS Run-off Curve Number	81; MIR=10 mm/min, bare ground		
Evaporative Zone Depth	30 cm		
Maximum Leaf Area Index	0; bare ground		
Synthetic Climatic Formulation	Caribou, Maine		
Study Site Latitude	48.3°		
Temp. and Precip. Normals	Amos, PQ		
Initial Snow Water Content	50.8 mm (2 inch)		
Growing Season	June - September; not applicable to bare ground		

[a] Laboratory measured soil parameters

The synthetic generation of data is a method by which a daily climatic record is formulated using the monthly averages and several statistical coefficients describing the distribution. The statistical coefficients are constant for a given month but vary from month to month. The Caribou site therefore provided only the statistical parameters with which to generate, for each month, the occurrence of wet or dry days, the associated distribution of maximum and minimum temperature values and mean solar radiation values. The SCS run-off curve number was chosen using a correlation based on the minimum infiltration rate (MIR) and vegetative cover. The saturated hydraulic conductivity of the sand cover was used as the MIR. Since there is no vegetation on the test plots, its impact is negligible and "bare ground" input values were used where applicable.

The amount of annual infiltration predicted with the HELP model was used as the soil surface boundary condition in SEEP/W, a finite-element flow model used to solve the two-dimensional equation for steady-state saturated and unsaturated flows at the site.

2.3.3 HELP Modelling Results

The HELP model was run with 20 years of synthetically generated climatic data. As explained above, these data were corrected to the Waite Amulet study site with the site latitude and the mean monthly precipitation and temperature records. The results are presented for each month in Table 2-V.

Figure 2.23 compares the inflows and outflows of the monthly results where the total inflows equal the precipitation and the total outflows equal evaporation, run-off, drainage off the clay surface (i.e., lateral flow from the sand cover), and percolation through the cover. The difference in the inflows and outflows depicts two hydrologic processes: (1) the accumulation and melting of snowfall; and (2) the change in soil moisture storage from month to month, principally in the sand cover. On the raised and exposed plots at Waite Amulet, wind would reduce the accumulation of snow during winter. Wind erosion is, therefore, a third process contributing to the difference in inflows and outflows. In general though, the snow pack that accumulates over winter melts in April and contributes heavily to run-off. During the summer months, run-off diminishes to a negligible amount and lateral flow off the surface of the clay stabilizes around 13 mm per month. The soil moisture losses during the summer months are replenished during Aug, Sep, and Oct with an increase in run-off and lateral drainage. Although most components vary throughout the year, percolation remains relatively steady, averaging 3.25 mm per month. The covers at Waite Amulet, however, freeze during the winter, thereby reducing percolation. The HELP model does not accommodate frozen soil.

TABLE 2-V - HELP MODELLING RESULTS AS APPLIED TO THE EXPERIMENTAL COMPOSIT SOIL COVERS AT WAITE AMULET.

DATA BASE:	20 Years Synthetic Record (site corrected)		Jan	Feb	Mar	Apr	May	Jun	Jul	Aug	Sep	Oct	Nov	Dec	Annual
INFLOWS:	Precipitation	Mean (mm)	58.7	40.9	47.5	49.8	77.5	101.1	92.5	124.7	110.0	87.9	64.3	49.0	903.7
		Sta. Dev.	23.4	15.7	20.8	28.7	40.9	31.8	26.2	52.3	56.6	34.8	23.9	20.1	89.3
OUTFLOWS:	Runoff	Mean (mm)	0.0	0.0	8.3	79.5	5.2	0.8	0.7	10.9	19.0	6.9	11.0	0.1	142.3
		Sta. Dev.	0.0	0.0	22.4	45.5	12.5	1.6	1.6	20.3	33.5	10.8	17.0	0.6	58.6
		% of inflows	0.0	0.0	17.4	159.7	6.7	0.8	0.7	8.7	17.3	7.8	17.1	0.3	15.7
	Evaporation	Mean (mm)	4.4	8.0	22.3	54.2	61.6	86.2	77.4	84.5	62.7	38.0	16.2	5.6	521.2
		Sta. Dev.	0.6	1.1	2.5	10.1	24.8	22.1	16.8	23.5	13.7	8.3	3.5	1.2	43.0
		% of inflows	7.5	19.6	46.9	108.8	79.6	85.3	83.8	67.7	57.0	43.3	25.3	11.4	57.7
	Drainage off clay	Mean (mm)	7.7	3.7	6.6	30.7	16.8	13.5	12.3	15.9	19.5	22.1	30.6	18.6	197.8
		Sta. Dev.	2.8	1.2	5.4	5.5	7.5	6.7	5.4	7.8	7.7	7.8	10.0	6.9	31.5
		% of inflows	13.0	9.0	13.9	61.6	21.6	13.3	13.3	12.8	17.7	25.1	47.6	38.0	21.9
	Percolation through cover	Mean (mm)	3.2	2.8	3.0	3.1	3.3	3.2	3.3	3.3	3.3	3.4	3.5	3.6	38.7
		Sta. Dev.	0.8	0.7	0.7	0.7	0.7	0.6	0.4	0.2	0.2	0.1	0.1	0.1	4.8
		% of inflows	5.5	6.8	6.2	6.2	4.3	3.1	3.5	2.6	3.0	3.9	5.4	7.3	4.3
	Total Outflows	Mean (mm)	15.3	14.5	40.1	167.4	86.9	103.7	93.7	114.6	104.4	70.4	61.3	27.9	900.0
		% of inflows	26.1	35.4	84.4	336.3	112.1	102.6	101.3	91.9	94.9	80.1	95.3	56.9	99.6
CHANGE IN:	Snow pack and Soil moisture	Mean (mm)	43.4	26.4	7.4	-117.7	-9.4	-2.6	-1.2	10.2	5.6	17.5	3.0	21.1	3.7

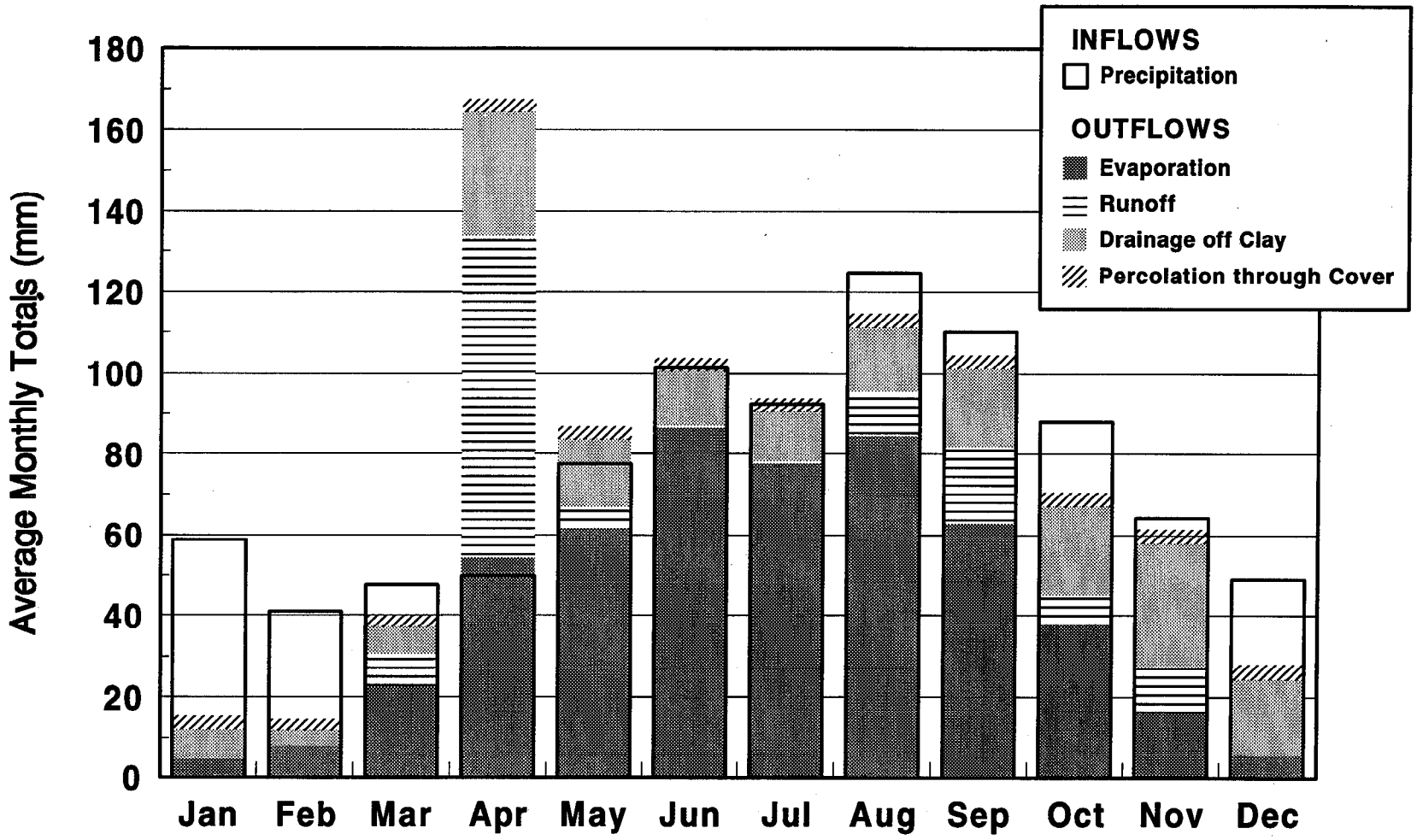

Figure 2.23: HELP Modelling Results, Average Monthly Totals

The average annual total of each water budget component is presented in Figure 2.24. The fact that 4% of the precipitation percolates through the cover implies the clay receives water for saturation. In addition, percolation (39 mm/y) is slightly greater than the hydraulic conductivity of 1 x 10^{-7}cm/s or 32 mm/y for the clay . This is possible only when free water is available (ponded) at the surface of the clay. The monthly results indicate these conditions exist for all months of the year, therefore, from the HELP modelling, it may be concluded that the clay will not desaturate. Indeed, the predicted soil water content at the end of the 20-year modelling period is similar to the initial value of 44%.

Since the hydraulic conductivity of the clay layer is the principal control on the flow of water through the cover, a sensitivity analysis was conducted to determine the percolation through the clay with varying values of hydraulic conductivity, K_s (Figure 2.25). When K_s is less than 5 x 10^{-7} cm/s, the hydraulic gradient is greater than 1, which indicates free water is available at the surface of the clay. The percolation for this K_s is 6.2 mm/y or 0.7% of mean annual precipitation. In general, though, percolation increases greatly at K_s values greater than 10^{-7} cm/s.

2.3.4 Flow Modelling

To validate the HELP modelling, the flow model SEEP/W (described in Section 3.1.2) was used to simulate flow through the composite soil cover at Waite Amulet. The test plot was modelled as a 2-dimensional system under steady-state conditions. The top boundary condition was specified as a constant flow of water equivalent to the precipitation minus the run-off and evaporation (240 mm/y).

Modelling the test plot as a steady-state system simulates the flow conditions as if infiltration and evaporation were constant throughout the year. Realistically, however, precipitation and run-off, and hence infiltration, would fluctuate throughout the year—wet periods and dry periods. Evaporation is highest during the summer and least during the winter. The cover would also freeze during the winter and limit percolation. The results of steady-state flow modelling is therefore only an indication of what one might expect as the average annual flow condition. The dynamics of the system are not depicted.

Figure 2.26 shows the results obtained with SEEP/W. Zero elevation is taken at sea level and the surface of the cover is at 317.45 m. The flow vectors, illustrated in the longitudinal view at the bottom of the page indicate that most of the flow travels off the top of the clay, laterally through the sand cover. This is due to the high hydraulic conductivity (K) of the material. As a rule of thumb, in a layered system a high K implies horizontal flow and a low K implies vertical flow.

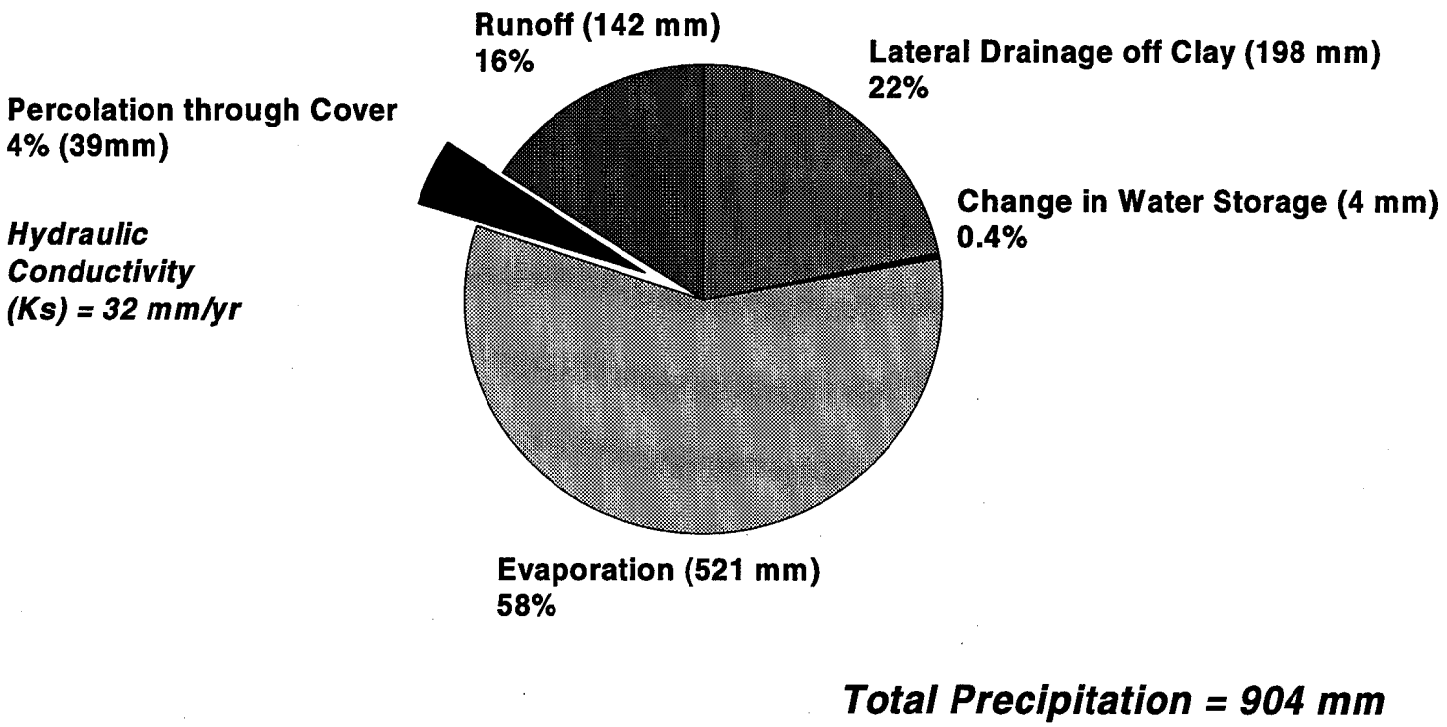

Figure 2.24: HELP Modelling Results, Average Annual Totals

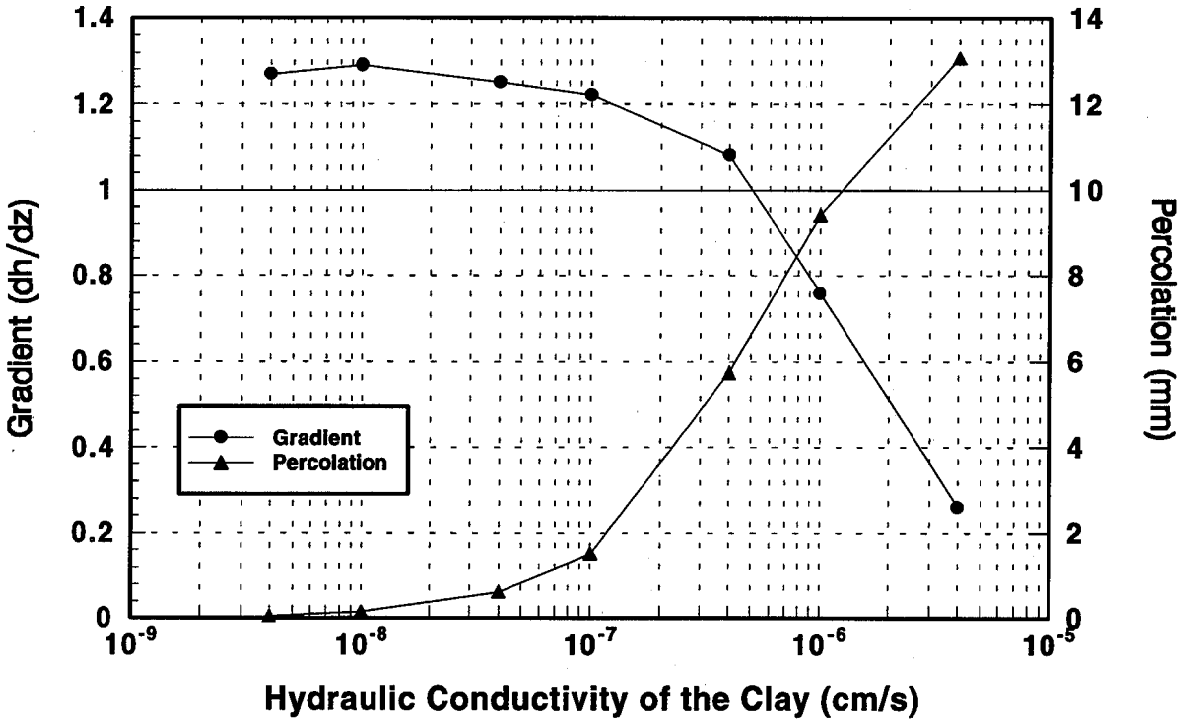

Figure 2.25: Sensitivity Analysis of HELP Modelling

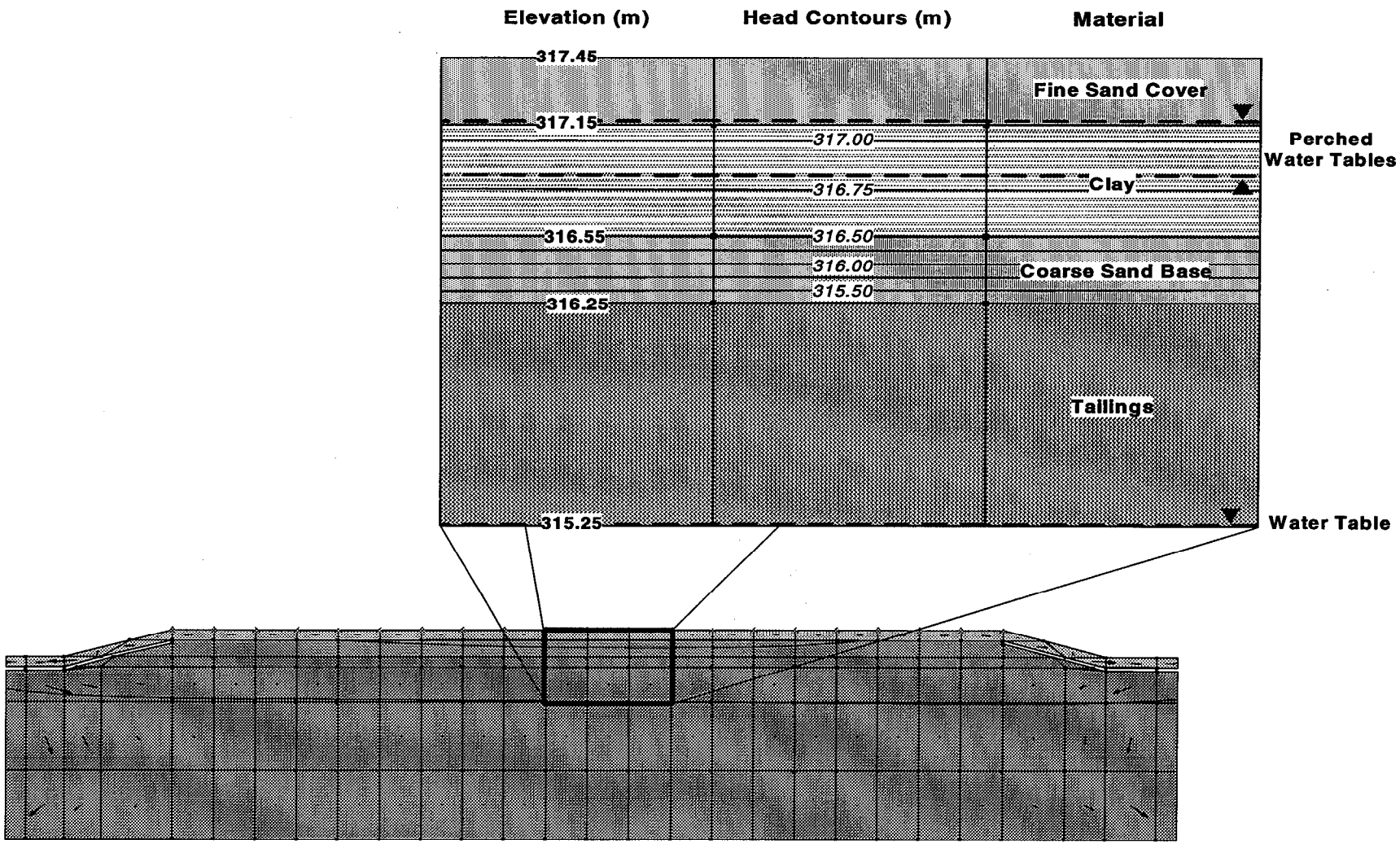

Figure 2.26: Results of SEEP/W steady-state flow modelling.

The water which enters the clay flows vertically as indicated by the hydraulic head contours; flow is perpendicular to the head contours. The flow continues vertically across the sand base, suggesting a low K. The head contours also concentrate across the sand base, illustrating the larger gradient needed to push the flow through the sand. Since the gradient across the sand base is greater than that across the clay, the K of the sand must be less than the K of the clay; flux is constant and K is inversely proportional to the gradient. And, since saturated hydraulic conductivity (K_s) of the sand is greater than the K_s of the clay, the sand must be unsaturated; the hydraulic conductivity of a porous material decreases with decreasing saturation. Therefore, the flow modelling indicates the sand base remains drained, providing a capillary barrier and restricting drainage of the clay. This result is consistent with HELP modelling.

The water table indicates where the pressure head equals zero (ψ=0); this is also called the free water surface. When ψ is less than zero, water is under tension (or suction), and when ψ is greater than zero, water is under pressure. Unsaturated soils contain water under tension. The water table occurs in the tailings at 1 m below the cover and in the clay (Figure 2.26). The water table in the clay, because it is above unsaturated soil, is a "perched" water table. The fact that the clay has a perched water table indicates that it is saturated, which is consistent with the HELP modelling. The extent of saturation or the size of the perched water table envelope is not actual, its presence is simply an indicator of saturation. Below the clay, the sand base is unsaturated.

The HELP modelling showed that approximately 84% of precipitation infiltrates the fine sand on the surface of the cover and 68% of this amount evaporates. The amount available for subsurface flow is therefore 240 mm per year. Using that value, SEEP/W flow modelling determined that 34.4 mm would percolate through the cover. HELP modelling determined that 39 mm would percolate through the cover. Both methods also indicate that the clay will remain saturated, theoretically implying a reduction in the flux of oxygen to the tailings. These converging results by the two modelling methods add to the confidence of these findings.

2.4 Oxygen Transport Into Tailings

Experimental observation and modelling results have shown that, if oxygen can be prevented from coming in contact with tailings, the oxidation of the constituent sulphide minerals and acid generation will be substantially reduced. The acid production rate could hypothetically be reduced to the extent that it is much lower than the rate of renewal of the tailings pore water. If this were achieved, water could flow through a tailings impoundment without a significant decrease in pH or increase in heavy metal concentrations. Such an improvement in the ensuing water quality could ultimately eliminate the need for collection and treatment thereby minimizing long-term operating costs. Oxygen diffusion into tailings can therefore be used as an indication of efficiency in the curtailment of acid production by comparing oxygen flux into covered tailings (test) to the flux into uncovered tailings (control).

As previously noted, oxygen dissolves in water but only to a very small extent. For example, at atmospheric conditions and 20°C, the equilibrium concentration of oxygen in water is only 9.17 mg/L. In addition, the diffusion of oxygen in water is also a very slow process, compared to its diffusion in air (2.5×10^{-9} m^2/s in water and 1.8×10^{-5} m^2/s in air). This implies that, if a stable column of water was placed above the tailings, the flux could be reduced by a factor of 10,000.

The transport of oxygen through fine-grained geologic materials is primarily by molecular diffusion. This process occurs in response to concentration gradients normally established between the atmosphere and the pore spaces in the materials, along with the constant movement and collisions of gaseous molecules. The diffusion of oxygen into a low oxygen concentration region of a fine-grained material is termed equimolar counter-diffusion. The air-filled soil pores which are low in oxygen are therefore high in nitrogen. As the oxygen diffuses into the soil, the nitrogen diffuses out into the atmosphere, at the soil surface. The natural forces in question tend to equilibrate the composition of the gases throughout the system which, in this case, can be considered to be the entire test plot and the air immediately above its surface.

Figure 2.27 presents gaseous oxygen profiles measured in July 1992 on both covered test plots as well as the uncovered control plot. These profiles show that the covers have a significant effect on the oxygen concentration at the surface of the tailings. When the tailings are not covered, the oxygen at the surface of the tailings is at atmospheric conditions (20.9% O_2). When the three-layer cover is placed over the tailings, the oxygen concentration is reduced to 2.0%. This represents a 90% efficiency in reducing oxygen availability. In the uncovered tailings, the surface layer would be expected to oxidize rather quickly due to the high concentration of oxygen. As this reaction proceeds, the oxygen would diffuse deeper to oxidize tailings at greater depths. In the covered test plots, the oxygen concentration at the surface of the tailings being much lower, the surface layer of the tailings would require considerably more time to oxidize. The diffusion of oxygen into the lower depths of tailings would therefore be restricted by the consumption of oxygen in the surface layer for an increased period of time.

Figure 2.28 presents gaseous oxygen profiles measured in the cover at different times in 1990 and 1991. The data indicate a rapid drop in oxygen concentrations in the clay layer from 12% to about 4%. During October and November 1990, there was heavy rainfall, which resulted in elevation of the water table and saturation of the entire tailings deposit. Thus, it was not possible to sample any pore gas. In July 1991, the oxygen profile penetrated the tailings with a concentration of about 2% near the surface.

The July 1991 field data were simulated with POLLUTE, using the November 1990 data as initial concentrations. Since the period from December to April was mostly characterized by frozen ground conditions, as well as rainfall and spring melting, it was assumed that the November data would persist until April 1991. Generally, significant lowering of the water table below the tailings surface after the spring thaw would have commenced from May to July 1991. The observed and simulated profiles for July 1991

are presented in Figure 2.29a. The diffusion coefficient of the clay layer in the field was determined from the simulations to be 8.57 cm_2/day (9.9 x 10^{-9} m^2/s). The corresponding data for the uncovered tailings are presented in Figure 2.29b from which an effective diffusion coefficient of 24 cm_2/day (2.8 x 10^{-8} m^2/s) was obtained for the tailings. The calculated flux of oxygen into the uncovered tailings is about 99% higher than the flux into the covered tailings (Yanful, 1993).

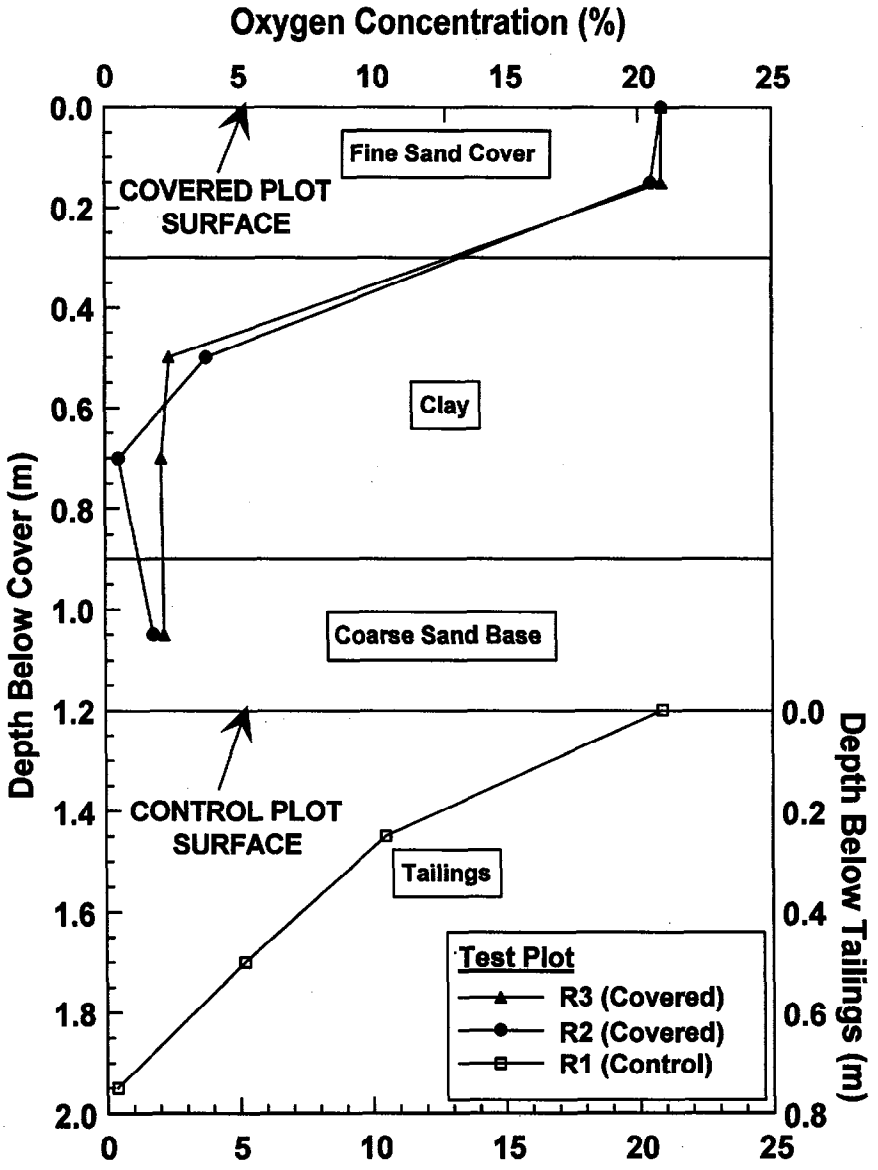

Figure 2.27: Field Oxygen Concentrations

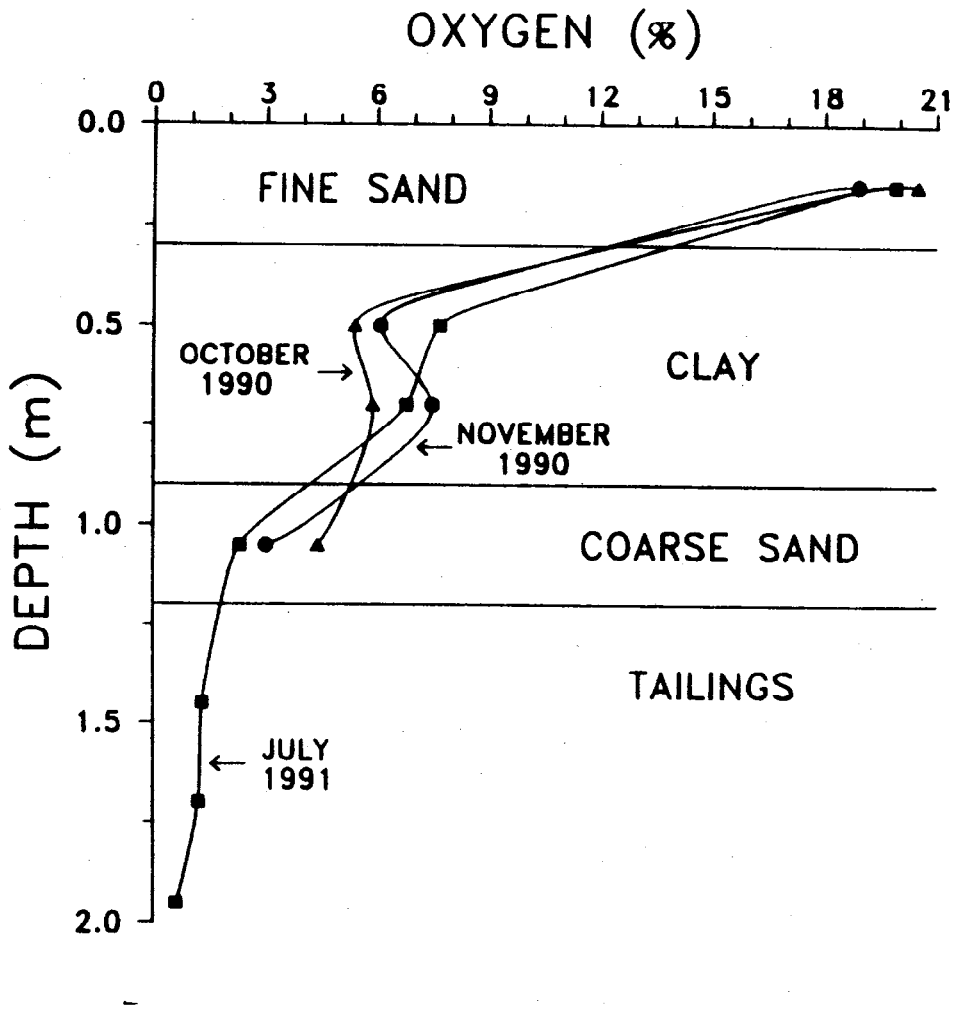

Figure 2.28: Field Gaseous Oxygen Profiles in Composite Soil Cover and Tailings

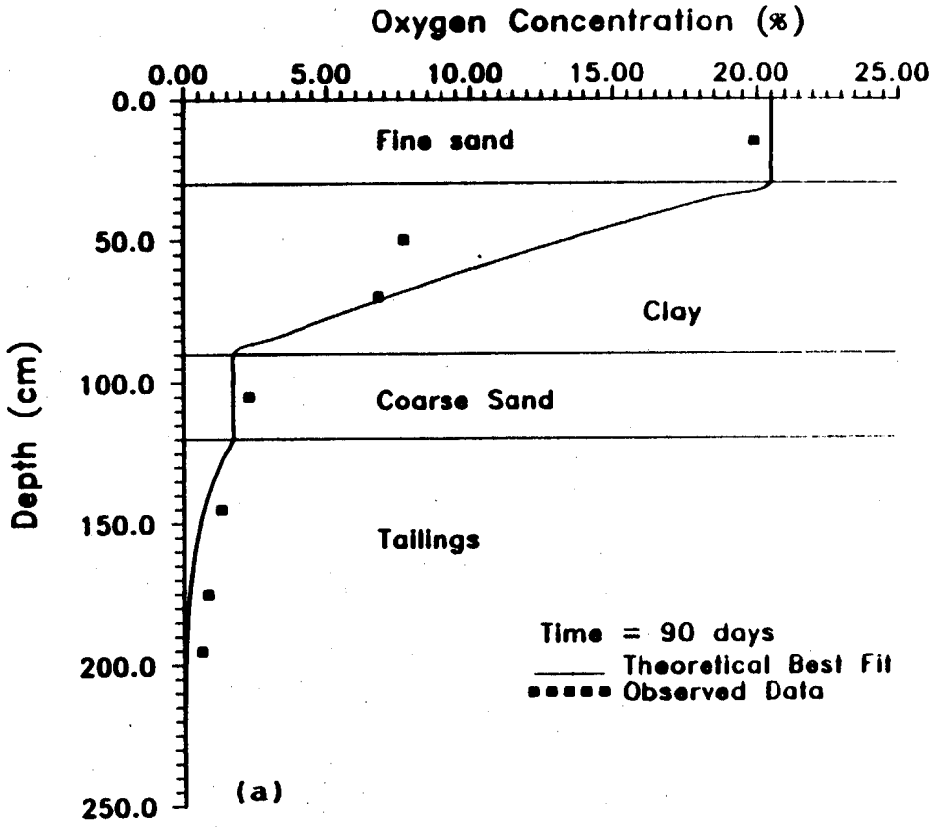

Figure 2.29a

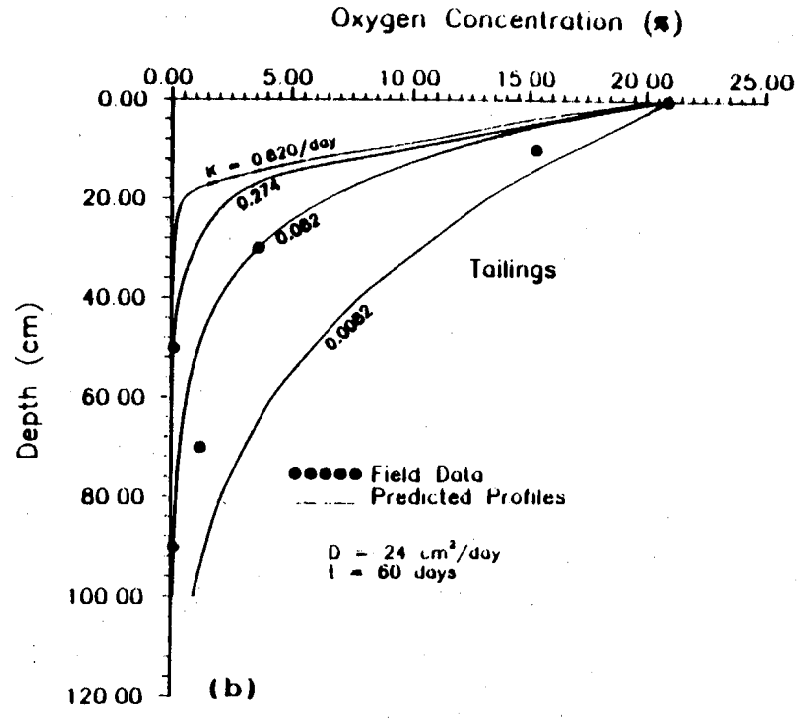

Figure 2.29b

Observed and Predicted Oxygen Profiles in Covered and Uncovered Tailings (field conditions).

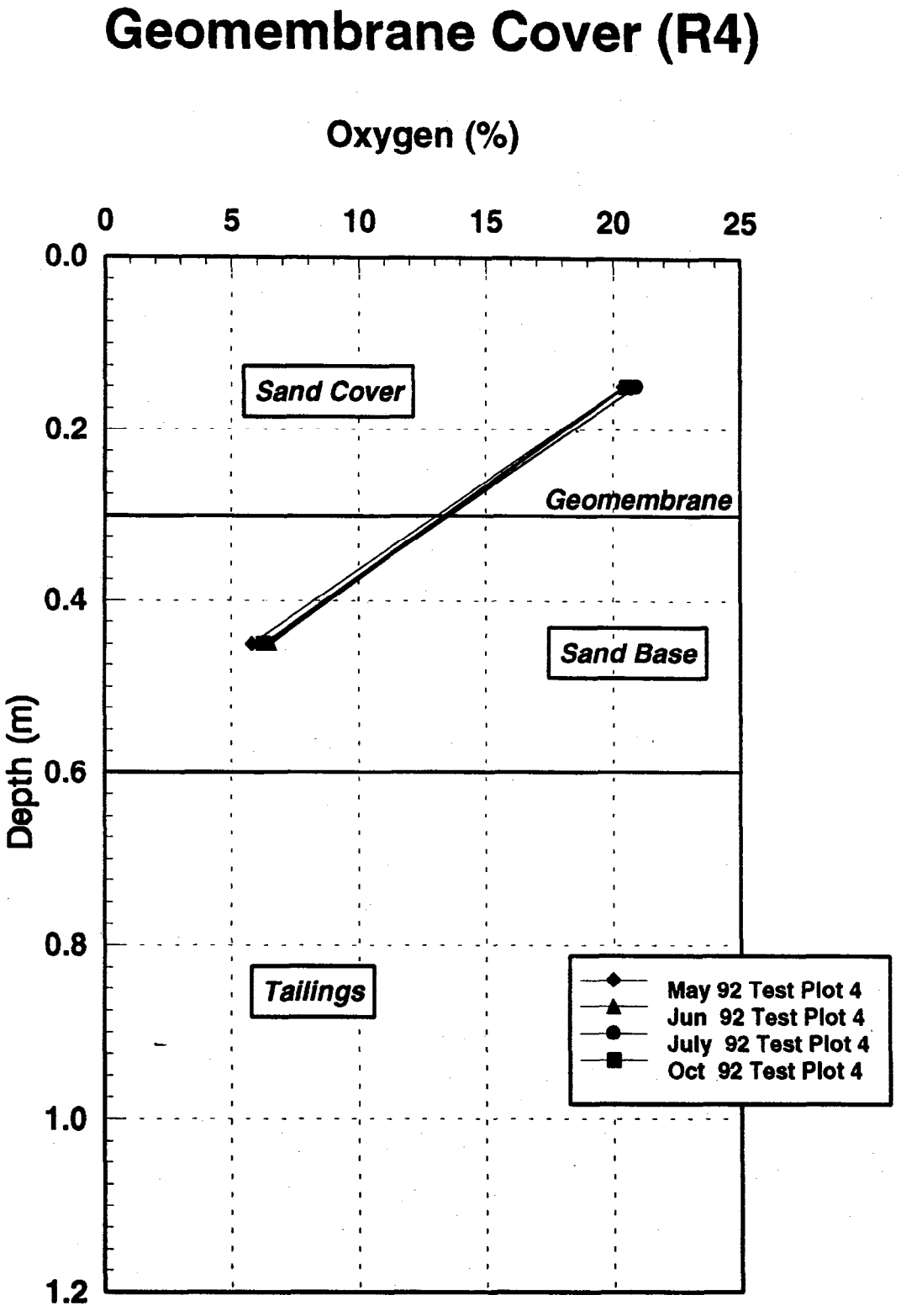

Figure 2.30: Field Oxygen Concentrations at R4 (geomembrane cover).

Figure 2.30 shows the gaseous oxygen concentrations in the geomembrane cover (R4). During 1992, measurements were consistently 21% above, and 6% below the geomembrane. The fact that the concentration is not lower than 6% below the geomembrane indicates a consistent supply of oxygen in the sand base layer. Great effort was taken, during installation and subsequent site visits, to seal the contact point between the sampling rod and the geomembrane to minimize vertical leakage of oxygen from the atmosphere. Horizontal inflow of oxygen from the edge of the cover is most likely responsible for the 6% oxygen observed in the sand base. In Figure 2.27, oxygen concentrations at R1 (the control) indicate 5% at ~ 0.5 m which suggests that the overlying tailings are depleted of reactive sulphides, thereby allowing oxygen ingress by vertical diffusion. The depletion of reactive sulphides in the shallow tailings in R4 would allow the oxygen concentration in the overlying sand base to be high.

Although tailings containing reactive sulphides (pyrrhotite and pyrite) are readily oxidized directly, *Thiobacillus ferrooxidans* is a genus of bacteria which is known to increase the rate of oxidation. The population of these bacteria has been found to be generally concentrated in the shallow depths where oxygen is readily available (Dave *et al.*, 1986; Nicholson *et al.*, 1989). As the oxygen concentration in the covered tailings is low, the predominantly aerobic *Thiobacillus ferrooxidans* may not be capable of survival. The ultimate effect would be a greater decrease in oxidation rate than that due to the reduction in oxygen concentration, since biological oxidation is eliminated. This would suggest that the 90% decrease in oxygen availability, conceivably, could imply a 98% decrease in tailings oxidation rate.

A simplified view of the overall process can be taken by examining one of the components involved in the oxidation process. In this case, oxygen can be isolated, and its concentration alone be used to determine the rate of diffusion. It will be assumed here that the transport of oxygen through the cover is Fickian in behaviour so that the flux can be predicted from Fick's first law as follows:

$$F(t) = -\theta_a D_e \frac{\delta C\ (t)}{\delta z} \qquad [2.1]$$

where:

F(t)	=	mass flux [M/L^2T]
θ_a	=	air-filled porosity [L^3/L^3]
D_e	=	effective diffusion coefficient [L^2/T]
C(t)	=	concentration at time t [M/L^3]
z	=	depth within material [L]

The air-filled porosity can be determined from knowledge of the total porosity and water content of the cover. The diffusion coefficient may be determined either from empirical equations or experimentally, as described by Yanful (1993).

Fick's second law, modified to include the consumption of oxygen, can be presented as follows:

$$\frac{\delta C}{\delta t} = D \frac{\delta^2 C}{\delta z^2} - KC \qquad [2.2]$$

where K is the first order reaction rate constant representing tailings oxidation.

Equations 2.1 and 2.2 are valid for single layer systems. In determining the flux, these equations would need to be altered to include all layers in the covered system and heterogeneities in the tailings. These heterogeneities include differences in water content and tailings oxidation rate as depth increases. A change in water content will affect the air-filled porosity of a layer which affects both the diffusion coefficient and the reaction rate constant. The tailings oxidation rate may vary with depth since the sulphide minerals have been exposed to oxygen for a long period of time and the surface of the tailings may be nearly completely oxidized.

Semi-analytic solutions to Equation 2.2, with appropriate boundary conditions, are implemented in the computer program POLLUTE (Rowe and Booker, 1990) which was adapted for this study. POLLUTE was used to determine the flux of oxygen into the covered and uncovered tailings. In determining the flux into the uncovered tailings, a value for the diffusion coefficient was estimated using an empirical equation developed by Millington and Shearer (1971). For better accuracy, the tailings were represented by three layers, each with a different water content and a separately calculated diffusion coefficient. The same oxygen consumption rate was used for each layer. Modelling results showed that, in July 1992, the flux of oxygen into the uncovered tailings was 2.76 g $O_2/(m^2 \cdot day)$, compared to 4.96×10^{-4} g $O_2/(m^2 \cdot day)$ for the covered tailings. This represents a cover effectiveness of at least 99.9%.

2.5 Geochemistry of Tailings Pore Water

As previously mentioned, collection basin lysimeters filled with fresh, unoxidized tailings and piezometers were installed in each test plot to permit an evaluation of changes in water quality with time. The water quality data obtained from piezometers installed in the test plots are summarized in Figures 2.31 to 2.46 for pH, sulphate, total dissolved iron and zinc. The results of the full analytical scans are presented in Tables 2-VI, 2-VII and 2-VIII.

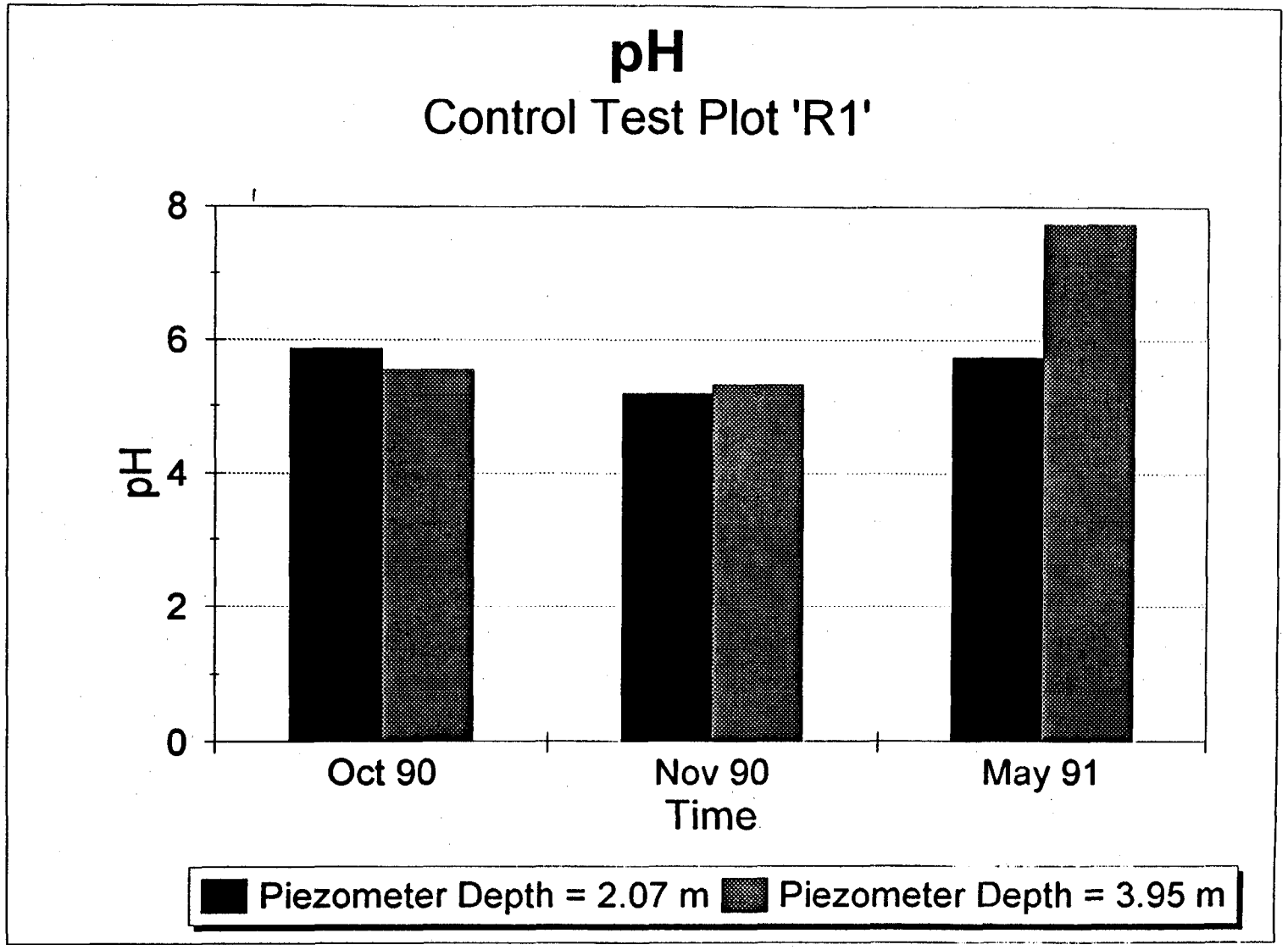

Figure 2.31: pH, Control Test Plot 'R1'

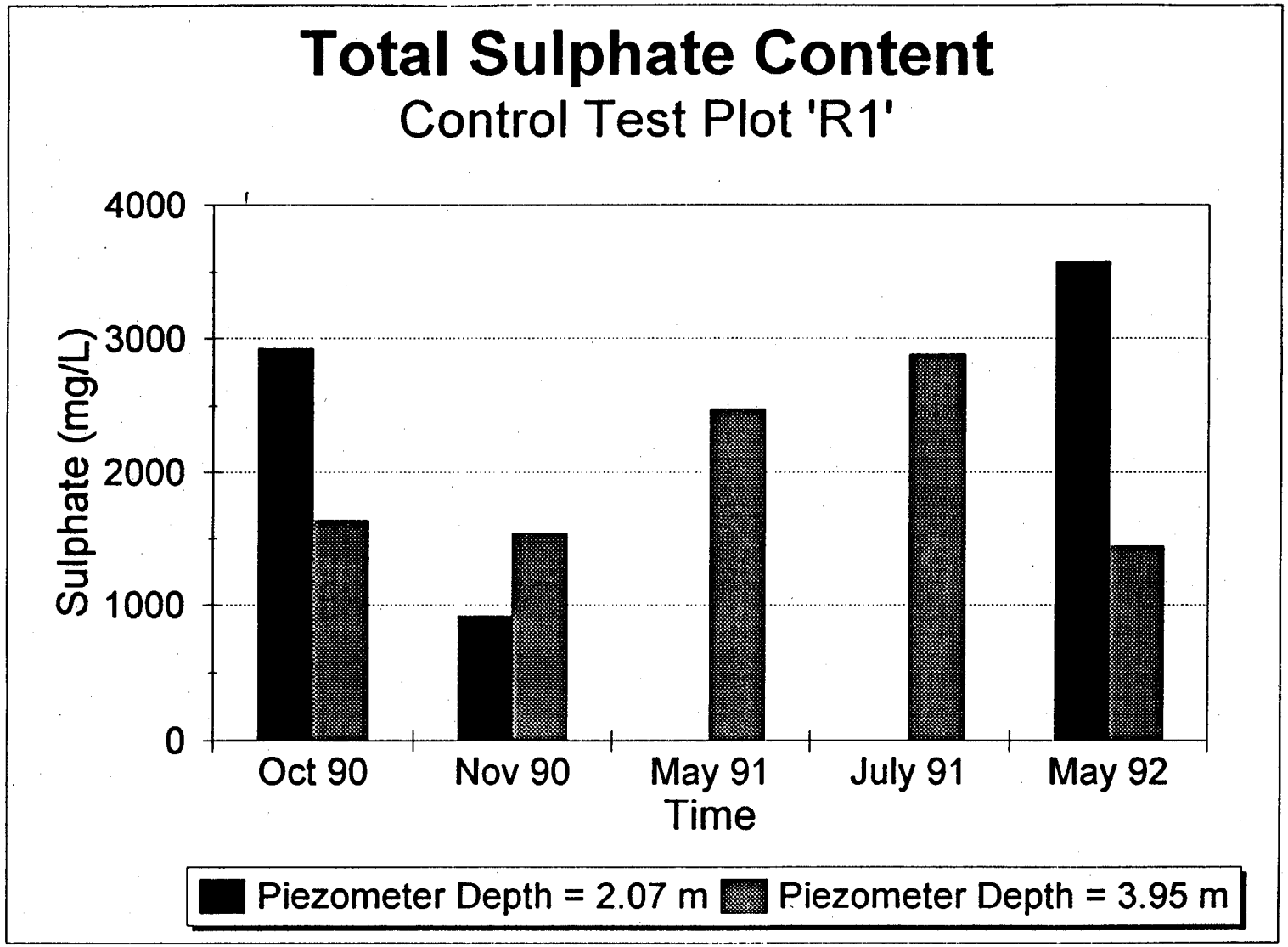

Figure 2.32: Total Sulphate Content, Control Test Plot 'R1'

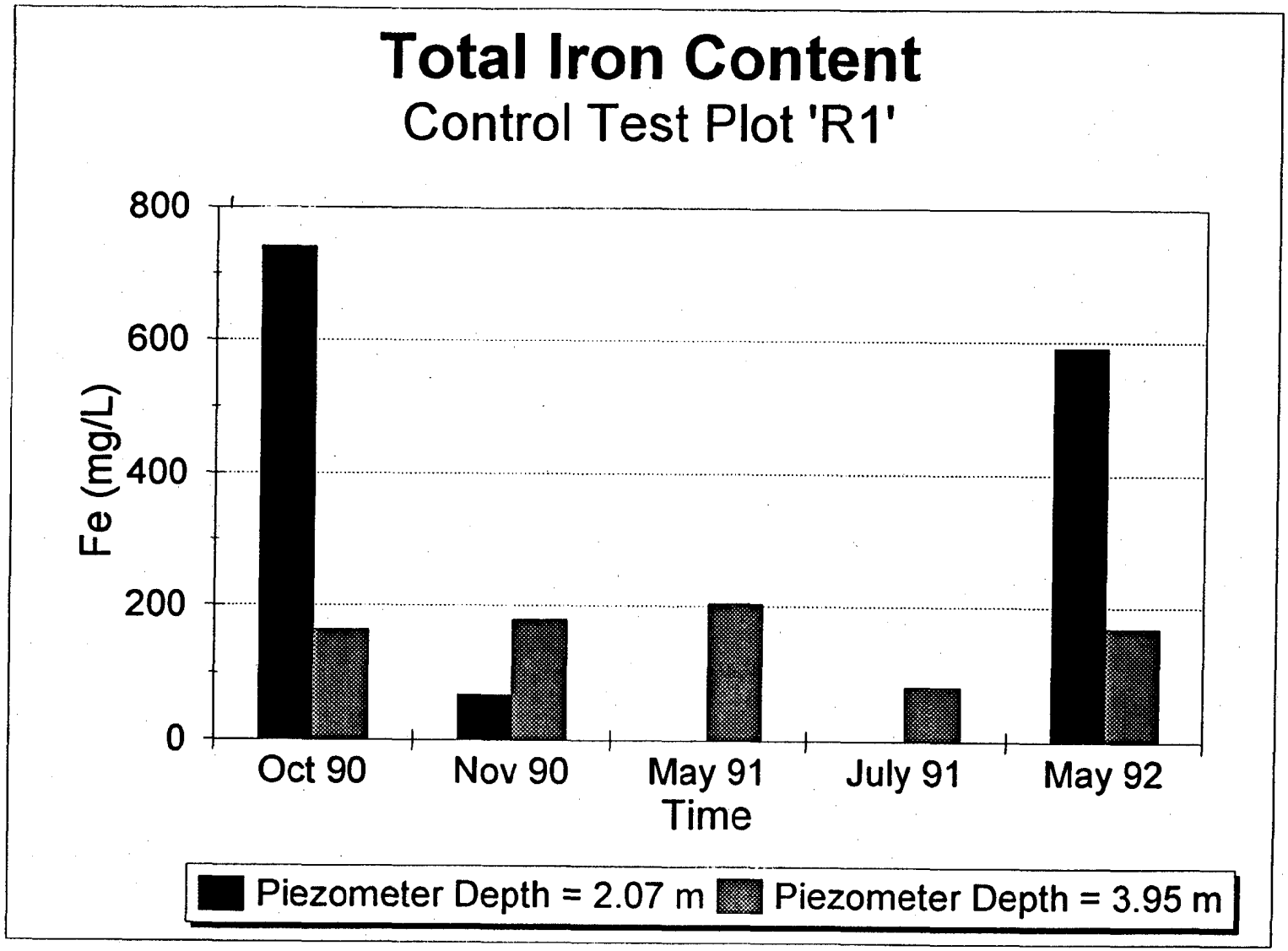

Figure 2.33: Total Iron Content, Control Test Plot 'R1'

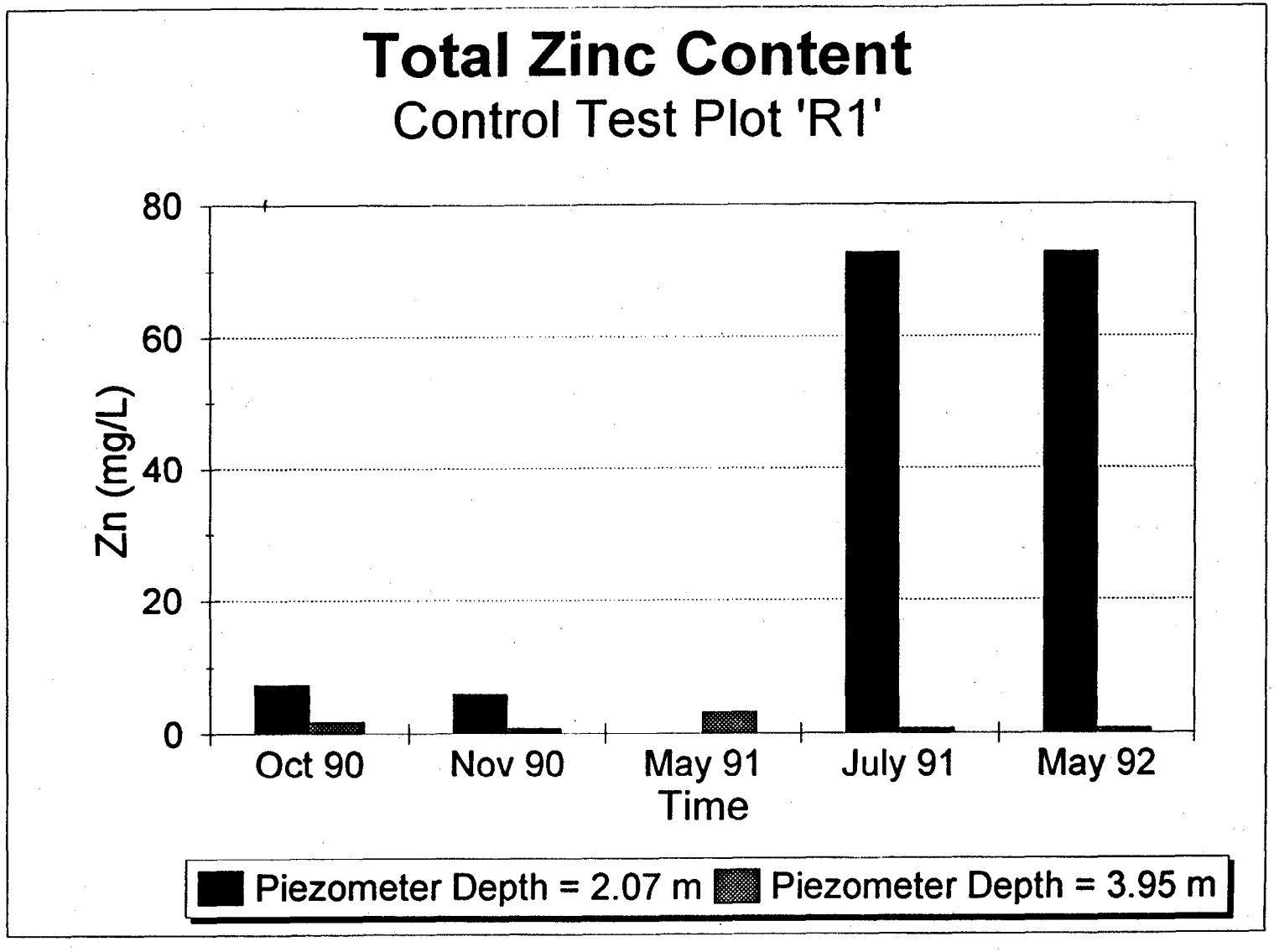

Figure 2.34: Total Zinc Content, Control Test Plot 'R1'

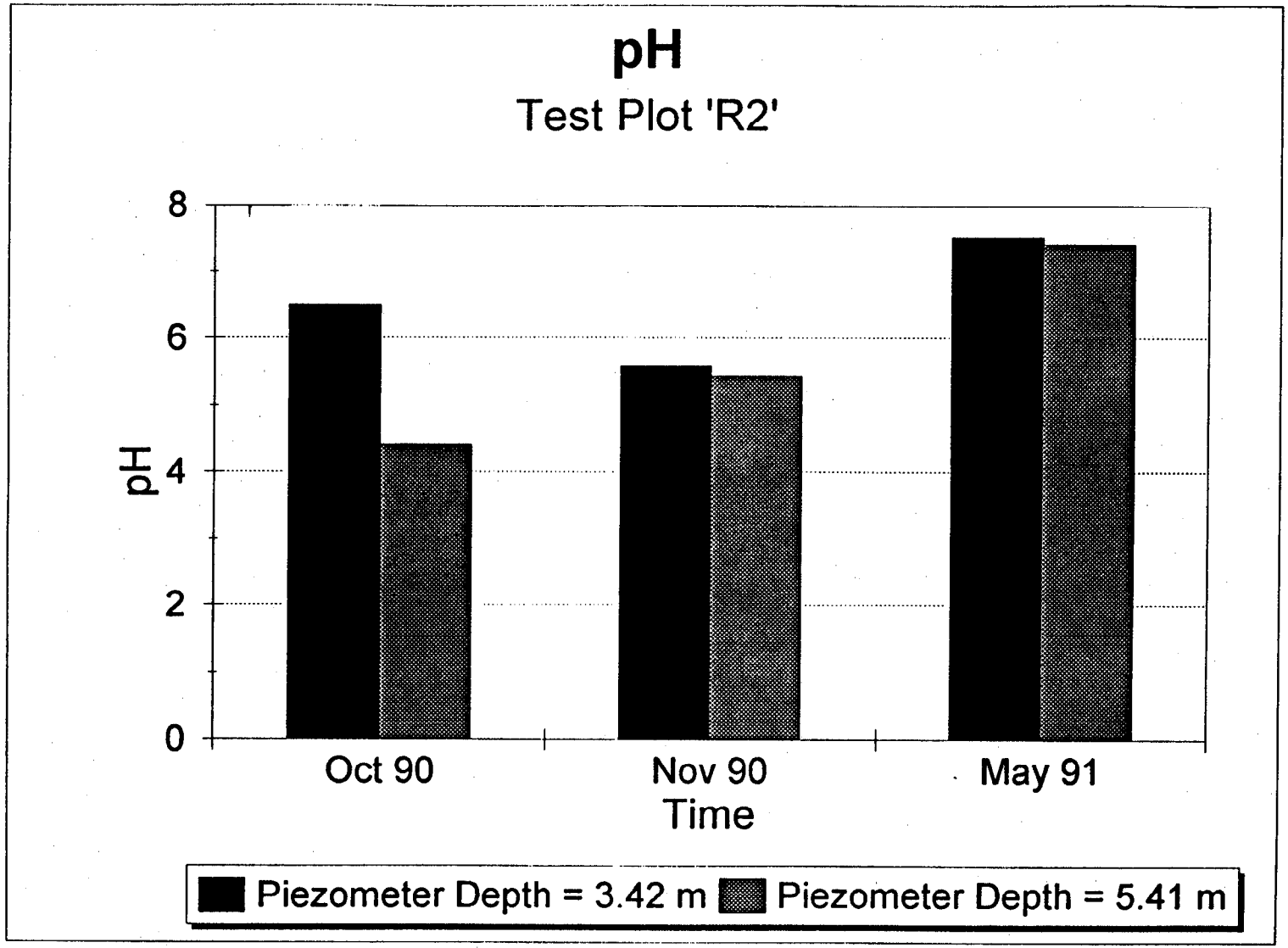

Figure 2.35: pH, Test Plot 'R2'

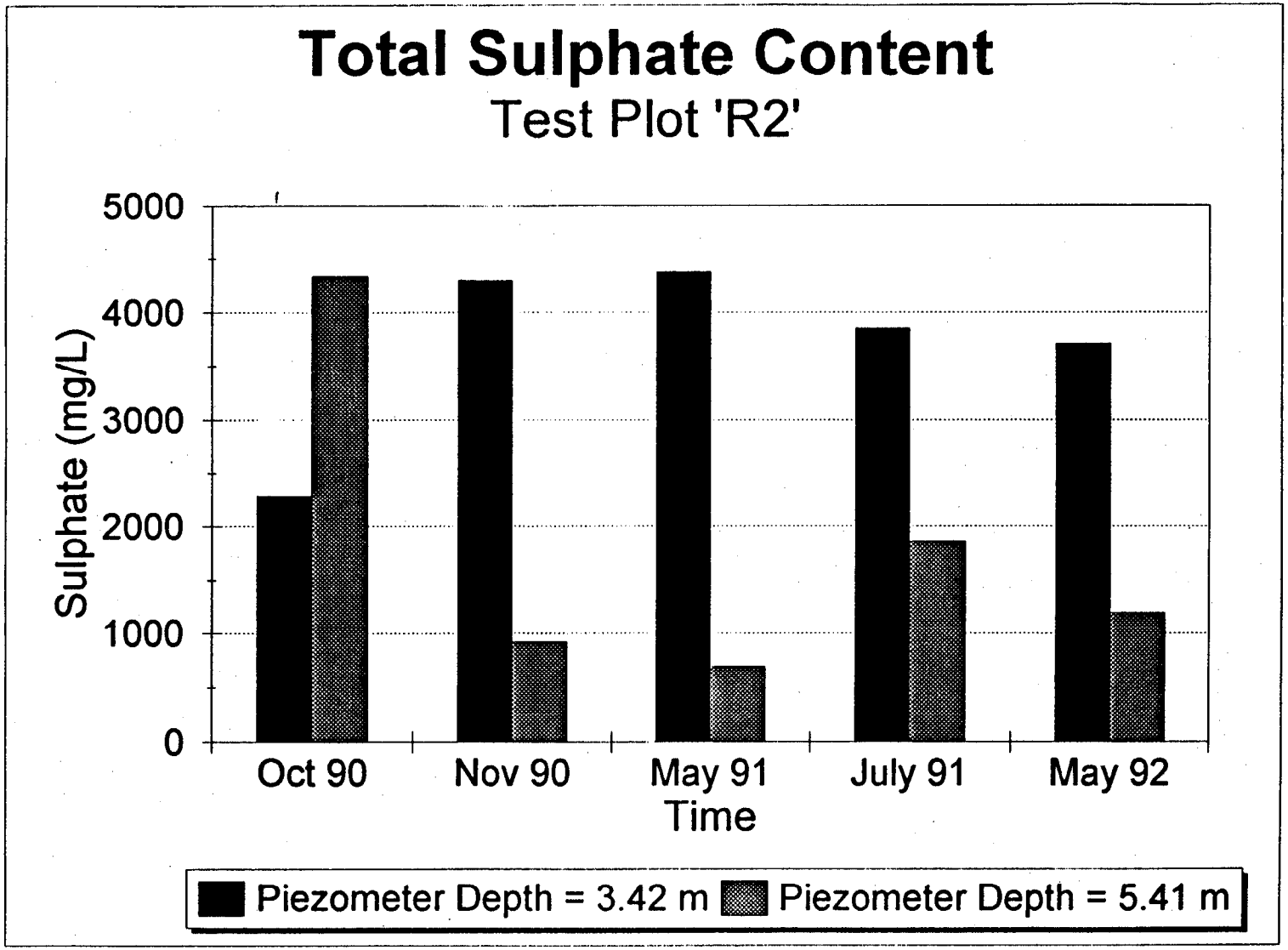

Figure 2.36: Total Sulphate Content, Test Plot 'R2'

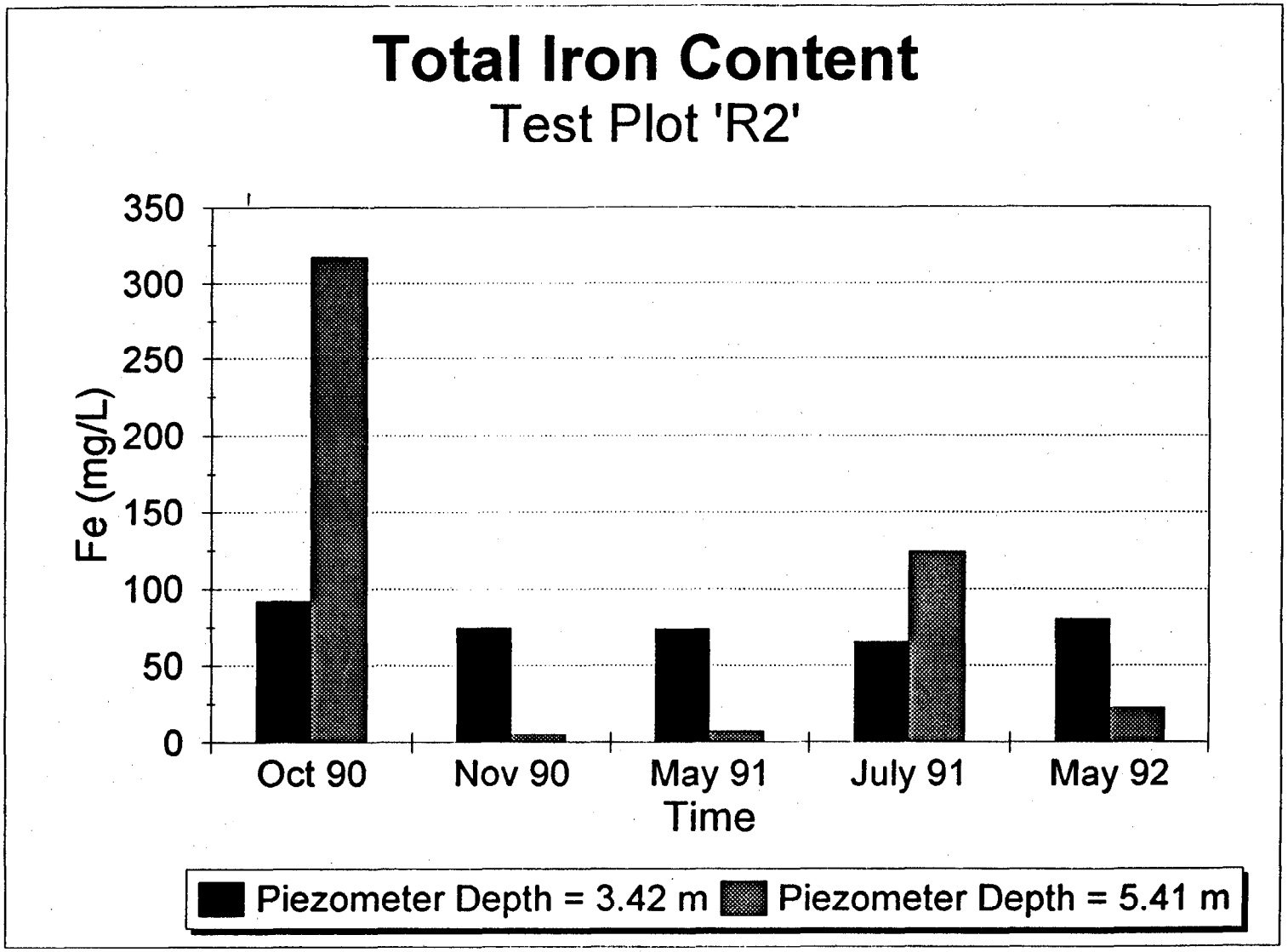

Figure 2.37: Total Iron Content, Test Plot 'R2'

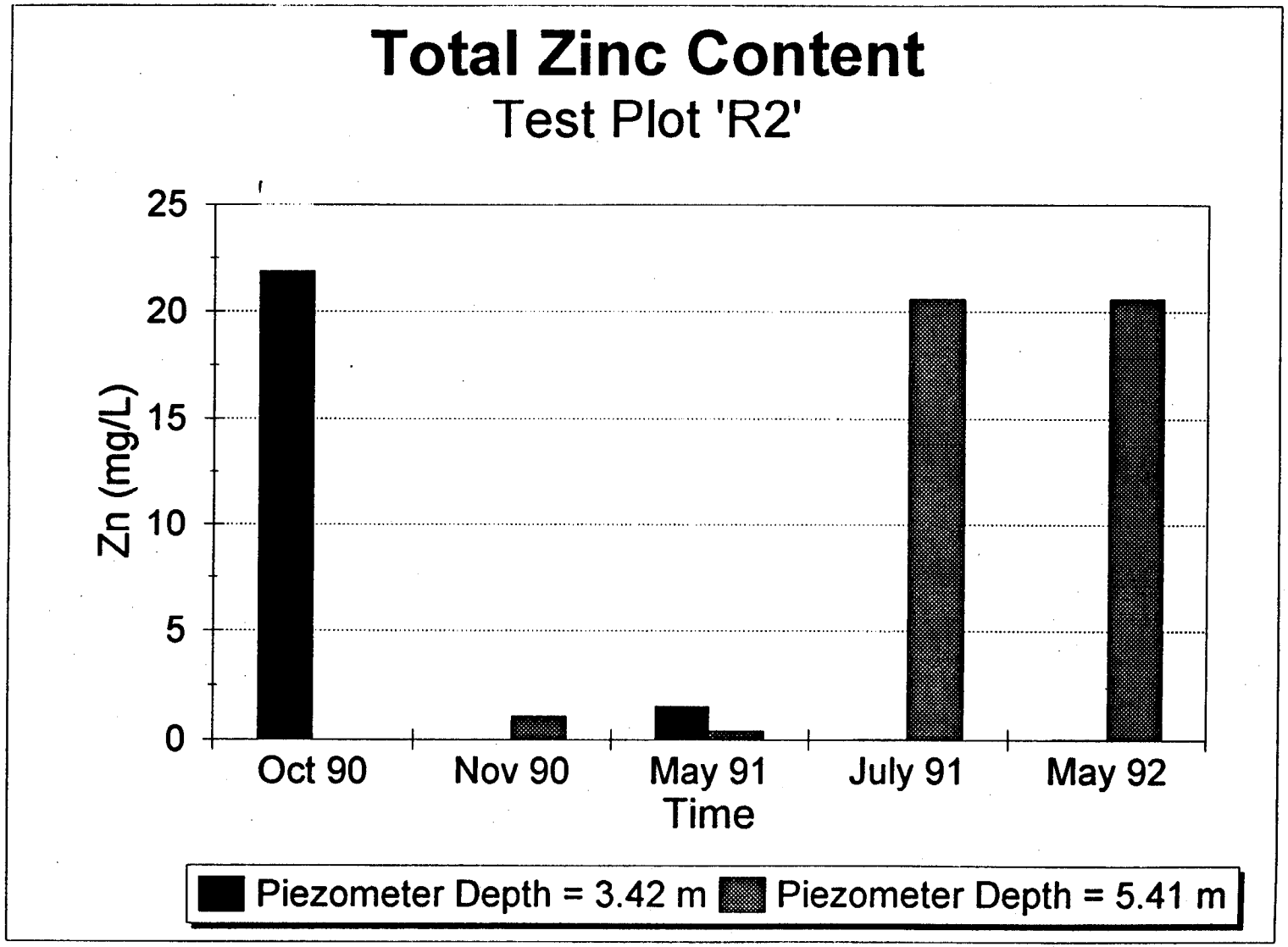

Figure 2.38: Total Zinc Content, Test Plot 'R2'

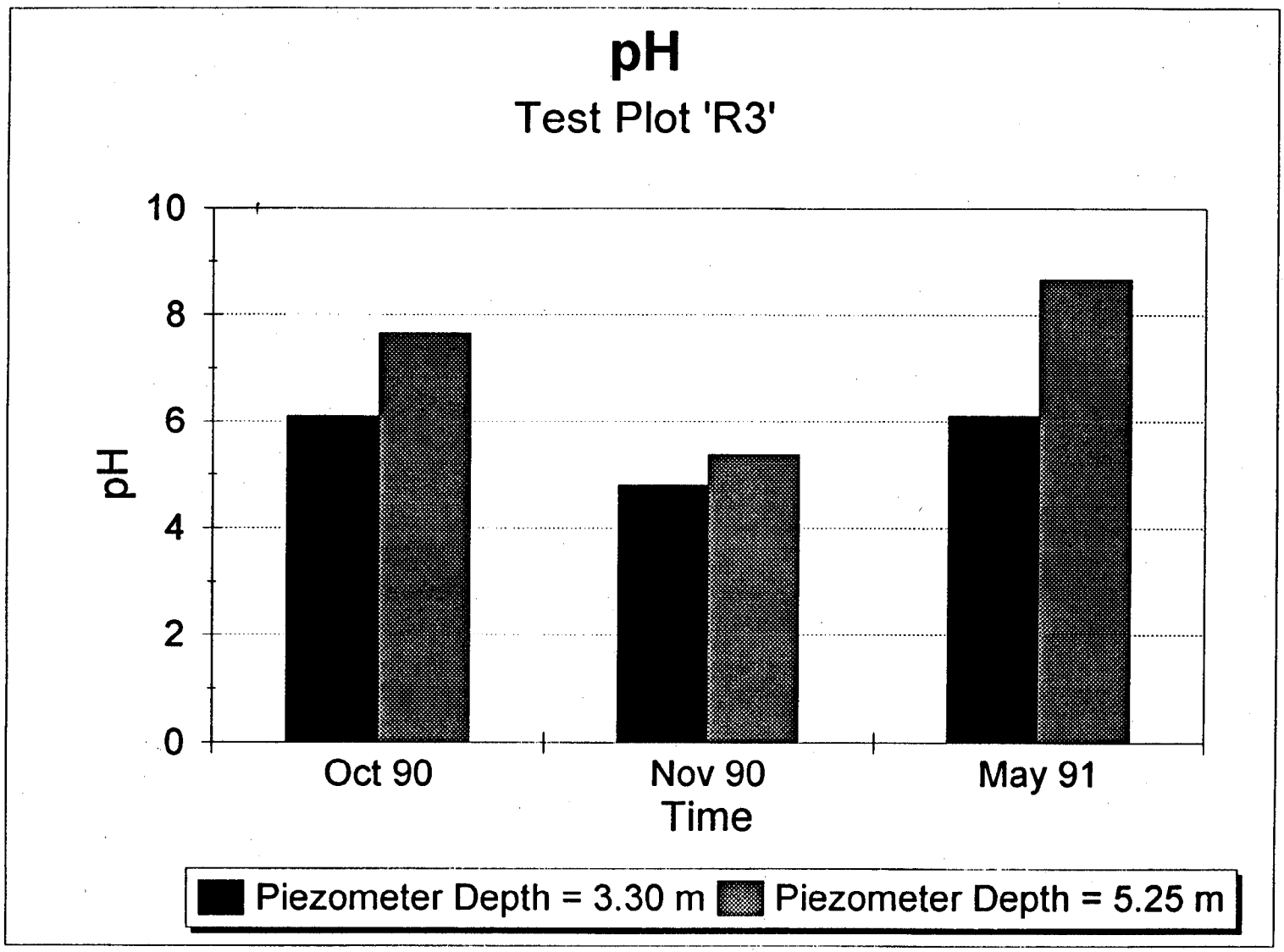

Figure 2.39: pH, Test Plot 'R3'

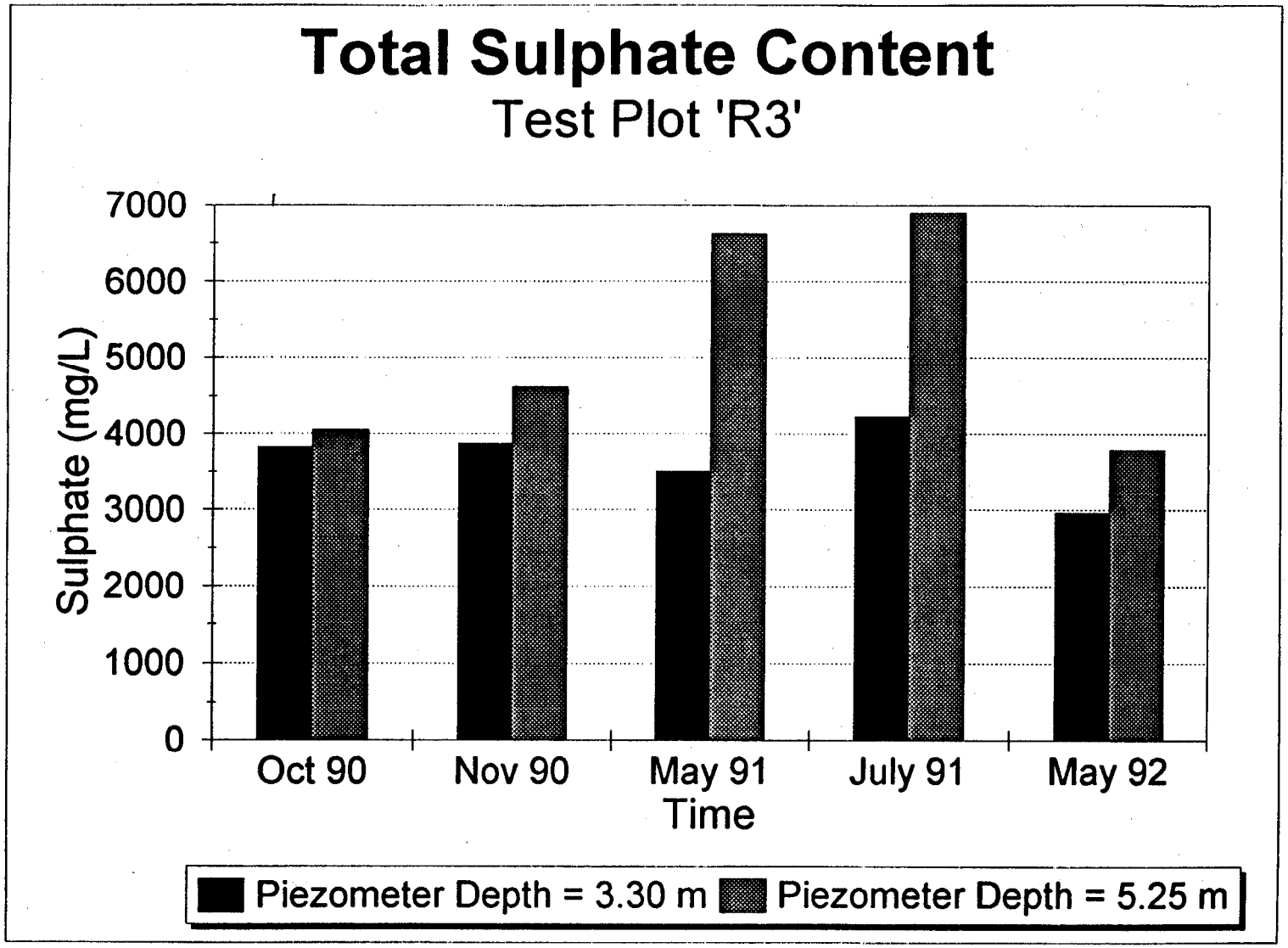

Figure 2.40: Total Sulphate Content, Test Plot 'R3'

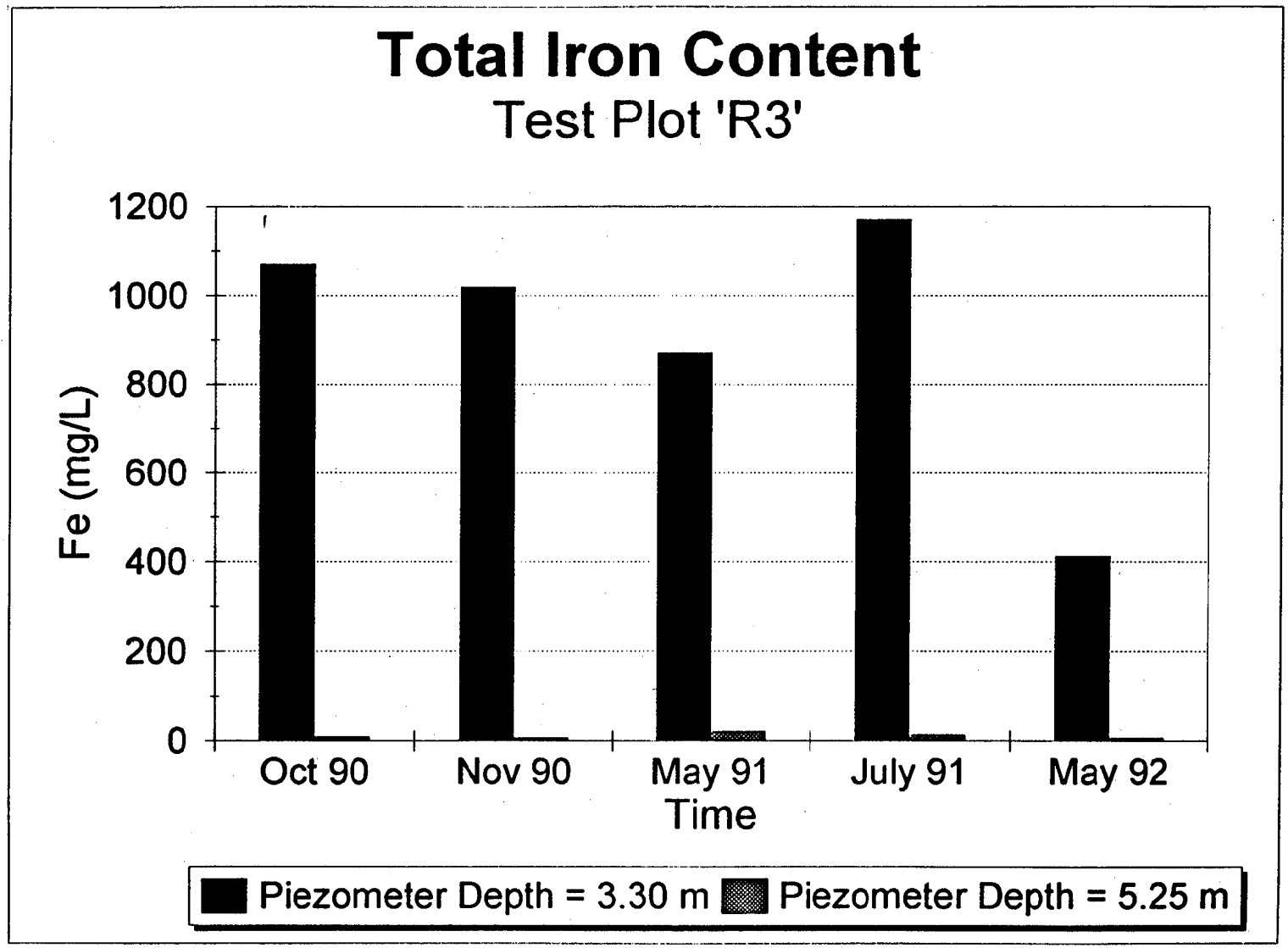

Figure 2.41: Total Iron Content, Test Plot 'R3'

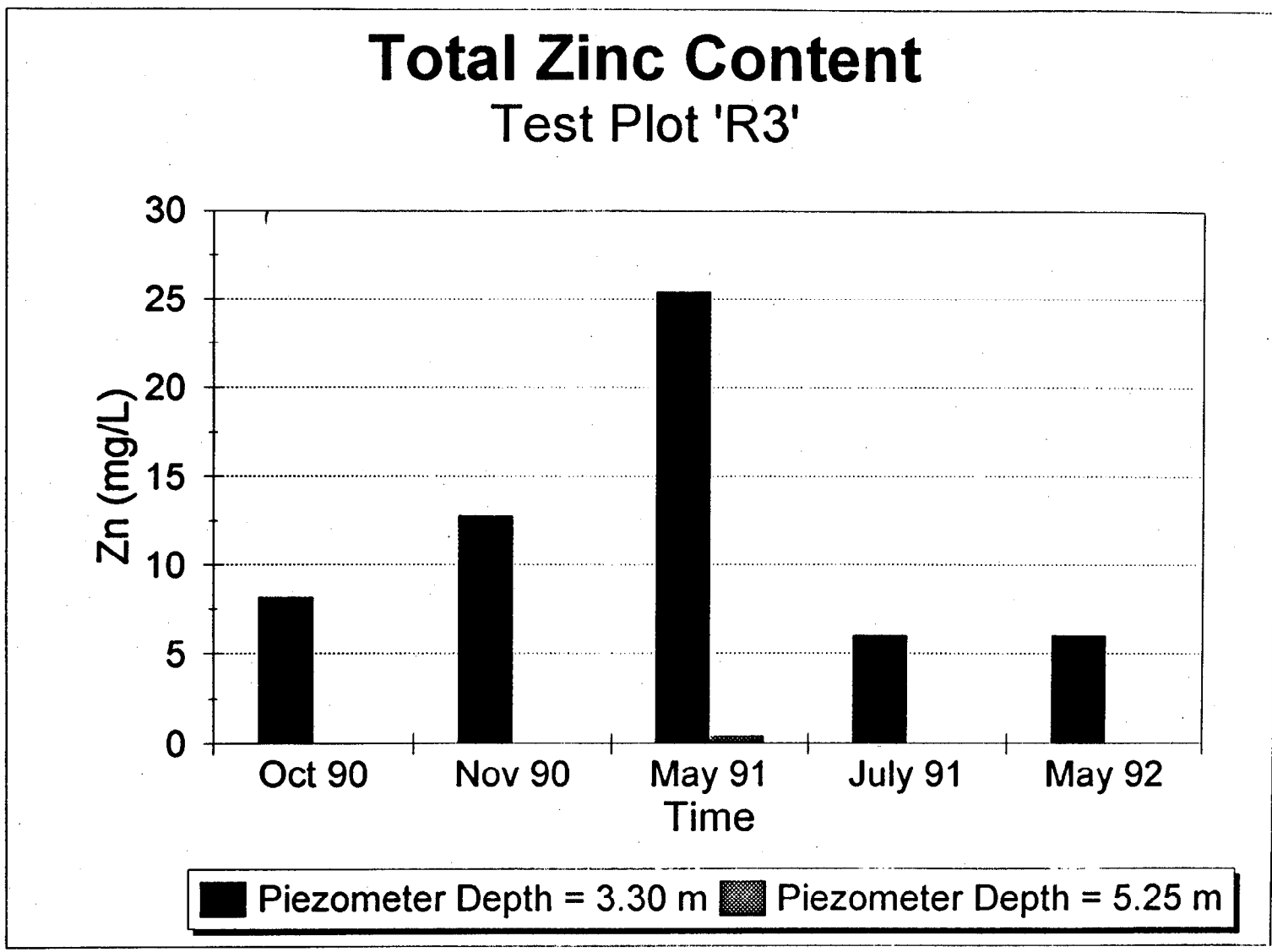

Figure 2.42: Total Zinc Content, Test Plot 'R3'

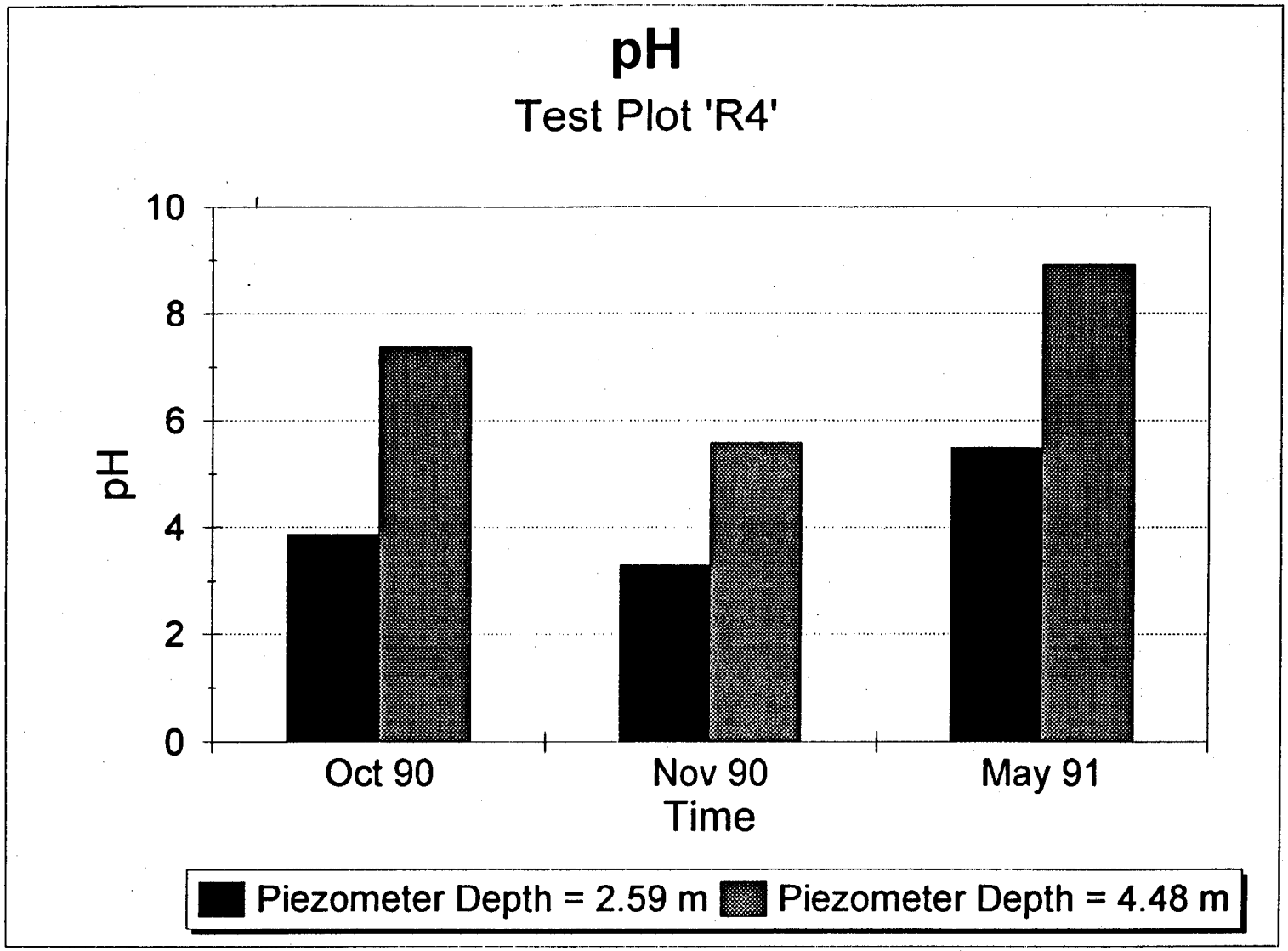

Figure 2.43: pH, Test Plot 'R4'

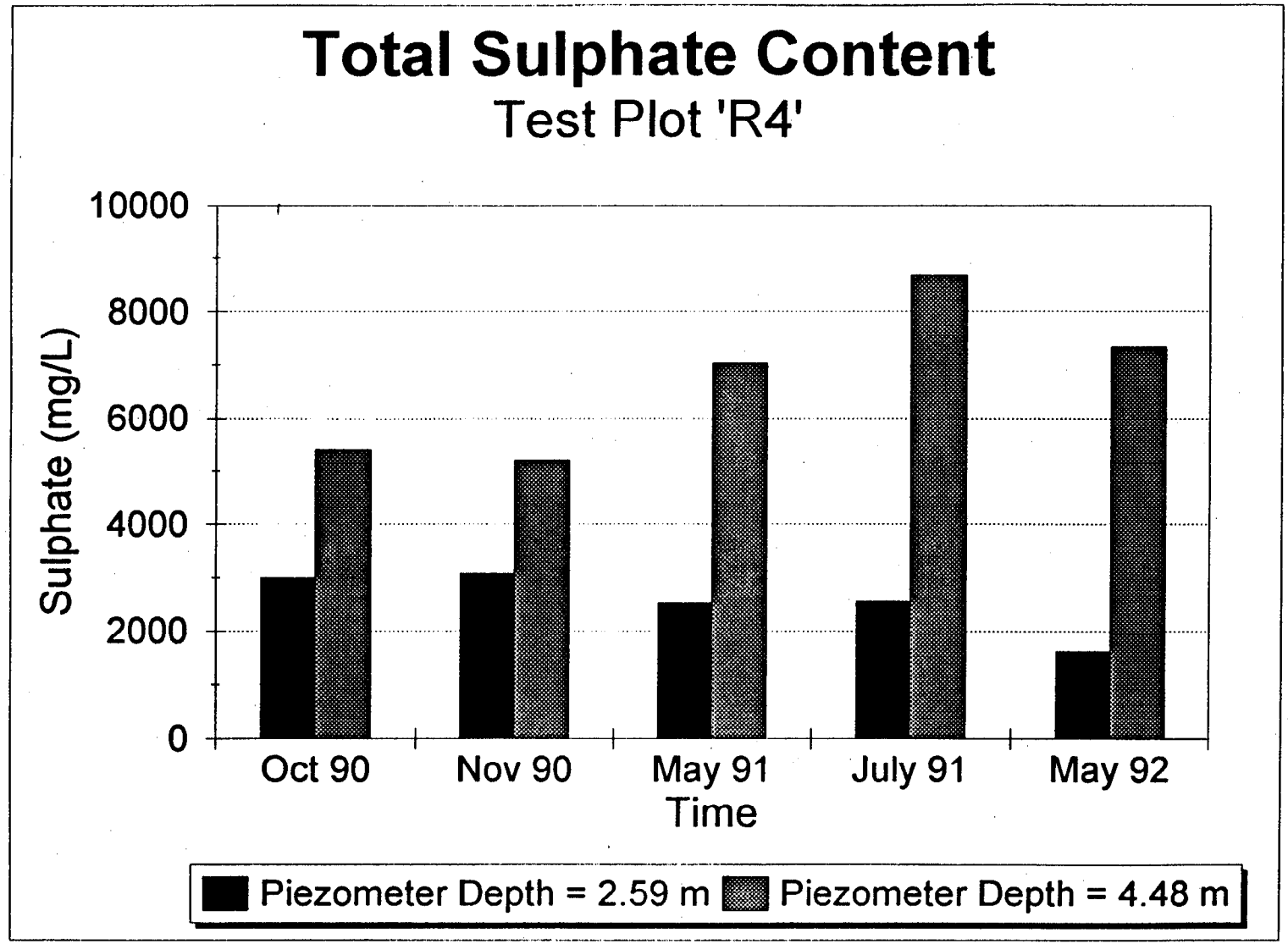

Figure 2.44: Total Sulphate Content, Test Plot 'R4'

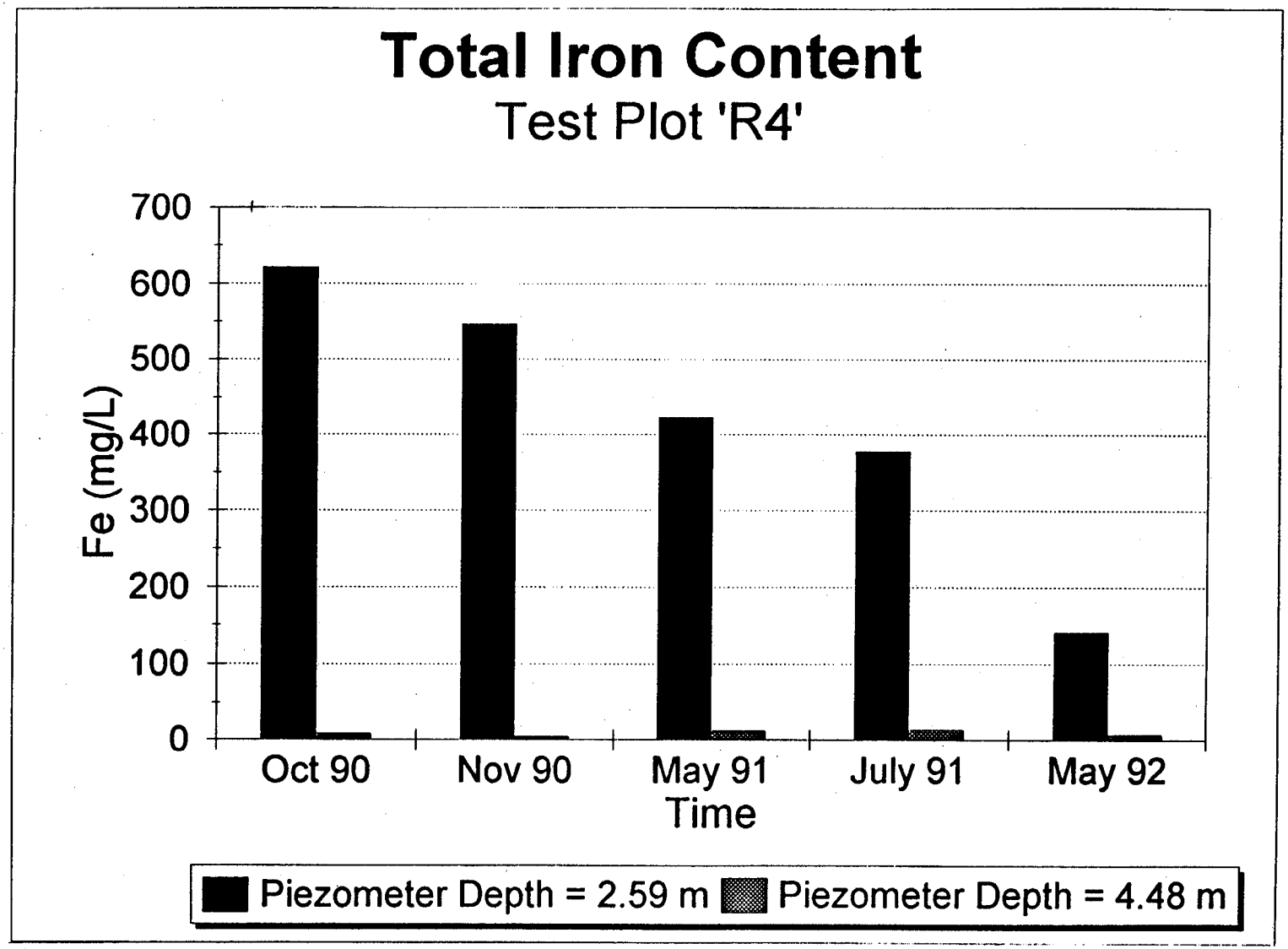

Figure 2.45: Total Iron Content, Test Plot 'R4'

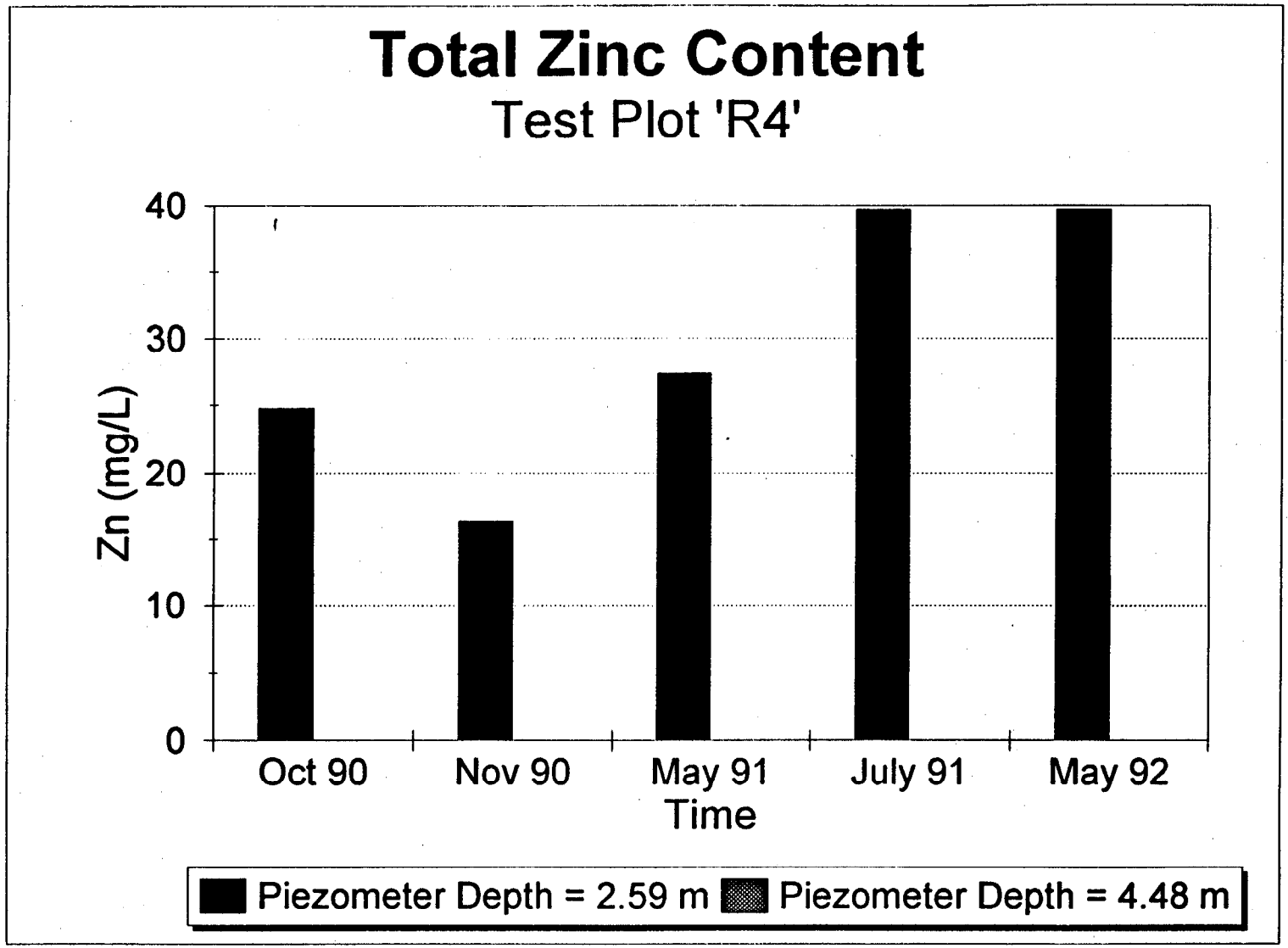

Figure 2.46: Total Zinc Content, Test Plot 'R4'

TABLE 2-VI - RESULTS OF PIEZOMETER WATER ANALYSIS, OCTOBER 1990

Results of Waite Amulet Water Analysis
October, 1990
Temperature Range = 6°C - 11°C

Piez #	Depth (m)	pH	Acidity (mg/L $CaCO_3$)	Alkalinity (mg/L $CaCO_3$)	Eh (mV)	Fe(T)	Fe2+	Al	Cu	Pb	Zn	Cd	Mg	Mn	K	Ca	Na	SO4	Cl-
R1-2	2.07	5.87	1200.00	<50	225.00	740.00	758.00	1.40	<0.01	0.07	7.37	<0.01	130.00	17.50	8.87	462.00	16.20	2930.00	1.44
R1-1	3.95	5.55	450.00	100.00	199.00	164.00	171.00	1.86	<0.01	<0.04	1.82	<0.01	144.00	29.50	2.55	288.00	48.90	1640.00	4.09
R2-2	3.42	6.50	200.00	1400.00	195.00		305.00	9.79	0.07	<0.04	21.90	<0.01	109.00	18.40	7.98	558.00	13.00	2290.00	1.23
R2-1	5.41	4.41	800.00	<50	187.00	317.00	85.90	0.21	<0.01	<0.04	<0.01	<0.01	889.00	1.87	41.10	457.00	23.60	4340.00	17.50
R3-2	3.30	6.10	1500.00	<50	157.00	1070.00	1100.00	1.84	<0.01	0.14	8.23	<0.01	227.00	24.20	17.60	574.00	21.90	3830.00	3.66
R3-1	5.25	7.66	<50	200.00	154.00	8.04	8.00	<0.1	<0.01	0.05	<0.01	<0.01	576.00	0.90	67.30	216.00	896.00	4050.00	21.30
R4-2	2.59	3.87	4300.00	<50	166.00	622.00	553.00	22.80	0.54	<0.04	24.80	0.05	159.00	22.90	7.27	595.00	21.40	3000.00	2.09
R4-1	4.48	7.37	<50	100.00	169.00	7.70	6.00	<0.1	<0.01	<0.04	<0.01	<0.01	874.00	1.26	77.30	308.00	875.00	5410.00	27.00
5-2	1.72	7.66	50.00	200.00	171.00	21.70	18.80	<0.01	<0.01	0.05	<0.01	<0.01	2430.00	1.52	62.30	455.00	63.80	10500.00	19.50
5-1	4.40	6.61	300.00	600.00	175.00	107.00	101.00	<0.01	<0.01	0.04	<0.01	<0.01	280.00	7.60	17.30	386.00	244.00	1940.00	7.93
9-2	1.63	6.92	<50	100.00	196.00	26.30	20.10	<0.1	<0.01	<0.04	<0.01	<0.01	201.00	1.94	28.30	601.00	15.40	2080.00	3.13
9-5	2.40	7.66	<50	<50	207.00	10.00	10.00	<0.1	<0.01	<0.04	<0.01	<0.01	232.00	1.35	33.50	593.00	21.30	2120.00	6.39
9-4	3.52	7.59	<50	200.00	192.00	7.00	6.20	<0.1	<0.01	<0.04	<0.01	<0.01	1520.00	2.02	53.70	447.00	158.00	6360.00	23.60
9-3	5.19	8.20	<50	<50	176.00	0.89	0.70	0.10	<0.01	0.08	<0.01	<0.01	170.00	0.38	65.60	144.00	1110.00	3230.00	17.80
9-1	6.67	7.12	50.00	600.00	176.00	13.90	11.90	0.13	<0.01	<0.04	<0.01	<0.01	51.10	0.60	17.30	75.90	423.00	690.00	6.16
9-6	8.61	6.96	100.00	300.00	245.00	20.00	17.60	0.15	<0.01	<0.04	<0.01	<0.01	172.00	8.58	43.90	113.30	1130.00	3026.70	9.98
9-7	10.39	6.81	100.00	250.00	218.00	11.10	9.40	0.12	<0.01	<0.04	<0.01	<0.01	156.00	24.50	16.50	202.00	1230.00	3310.00	9.28
10-2	1.58	/	/	/	/	/	/	/	/	/	/	/	/	/	/	/	/	/	/
10-1	7.30	6.84	100.00	800.00	149.00	1.05	1.20	<0.1	<0.01	<0.04	<0.01	<0.01	32.50	0.46	11.10	52.40	254.00	41.00	3.08

Note: All concentrations in mg/L.

TABLE 2-VII - RESULTS OF PIEZOMETER WATER ANALYSIS, NOVEMBER 1990, AND MAY 1991

Results of Waite Amulet Water Analysis
November 1990
Temperature Range = 5°C - 6°C

Piez #	Depth (m)	pH	Eh (mV)	Fe(T)	Fe2+	Al	Cu	Pb	Zn	Cd	Mg	Mn	K	Ca	Na	SO4	Cl-
R1-2	2.07	5.20	369.00	67.70	72.00	2.16	0.79	<0.04	5.83	<0.01	22.80	3.83	5.99	310.00	5.14	920.00	4.66
R1-1	3.95	5.33	389.00	179.00	211.00	1.33	0.01	<0.04	0.79	<0.01	134.00	29.30	2.83	260.00	45.30	1540.00	2.85
R2-2	3.42	5.59	352.00	74.30	103.00	0.44	< 0.01	<0.04	<0.01	<0.01	867.00	1.33	62.10	350.00	22.60	4300.00	13.50
R2-1	5.41	5.44	364.00	5.23	0.17	0.08	0.03	0.03	1.07	0.02	51.10	0.96	4.41	470.00	16.60	920.00	0.38
R3-2	3.30	4.80	375.00	1020.00	1020.00	2.94	0.02	<0.04	12.80	<0.01	204.00	18.60	28.70	500.00	19.50	3880.00	4.04
R3-1	5.25	5.37	404.00	6.74	6.00	0.03	<0.01	0.01	<0.01	<0.01	528.00	0.67	92.40	170.00	984.00	4620.00	25.40
R4-2	2.59	3.31	439.00	546.00	525.00	14.50	0.30	<0.04	16.40	<0.01	161.00	15.90	16.10	500.00	73.30	3080.00	1.77
R4-1	4.48	5.58	444.00	4.36	1.48	0.06	<0.01	0.03	<0.01	<0.01	667.00	0.85	96.80	220.00	936.00	5210.00	29.40

Results of Waite Amulet Water Analysis
May 1991
Temperature Range = N\A

Piez #	Depth (m)	Fe(T)	Fe2+	Al	Cu	Pb	Zn	Cd	Mg	Mn	K	Ca	Na	SO4	Cl-
R1-2	2.07	/	/	/	/	/	/	/	/	/	/	/	/	/	/
R1-1	3.95	204.740	209.000	1.690	0.100	<0.3	3.140	0.110	244.650	5.950	24.280	487.750	32.980	2475.150	9.100
R2-2	3.42	73.840	72.400	1.620	0.020	<0.3	1.520	<0.02	772.980	1.270	55.840	396.490	28.670	4380.000	19.400
R2-1	5.41	7.280	4.400	0.330	<0.01	<0.3	0.420	<0.02	39.610	0.480	<5	389.920	17.240	699.810	0.440
R3-2	3.30	871.620	898.000	6.160	0.160	<0.3	25.410	<0.02	161.070	20.100	18.200	421.580	25.570	3510.000	3.520
R3-1	5.25	20.950	18.800	0.460	<0.01	<0.3	0.390	<0.02	967.530	1.290	93.290	249.360	870.810	6630.000	100.000
R4-2	2.59	422.730	405.000	17.120	0.110	<0.3	27.440	0.050	115.650	14.750	9.460	483.560	24.950	2529.150	2.050
R4-1	4.48	12.350	11.800	0.260	<0.01	<0.3	<0.02	<0.02	1110.000	1.350	93.600	269.170	769.420	7020.000	90.600
5-2	1.72	13.470	10.100	0.540	0.130	<0.3	0.290	0.110	2840.000	1.660	89.370	407.410	72.330	11670.00	33.800
5-1	4.40	114.690	121.000	0.630	0.190	<0.3	0.730	0.210	317.780	7.840	28.220	368.560	256.990	2140.650	7.350
9-2	1.63	40.290	36.800	0.270	0.020	<0.3	0.020	<0.02	192.970	2.370	40.980	464.680	31.620	2177.820	2.370
9-5	2.40	14.590	13.500	0.330	<0.01	<0.3	<0.02	<0.02	203.840	1.230	49.890	470.520	25.700	2171.220	/
9-4	3.52	2.140	1.400	0.330	0.020	<0.3	0.300	<0.02	1290.000	1.680	75.350	350.530	145.660	6570.000	100.000
9-3	5.19	4.870	3.200	0.500	0.040	<0.3	0.280	<0.02	201.160	0.600	96.110	170.960	1140.000	3600.000	22.100
9-1	6.67	29.280	20.900	0.580	0.040	<0.3	0.090	0.030	56.190	0.780	31.030	101.520	450.960	847.650	17.900
9-6	8.61	27.230	24.600	0.460	0.030	<0.3	<0.02	<0.02	167.130	8.430	50.490	145.280	872.830	2426.040	13.400
9-7	10.39	15.130	13.000	0.630	0.060	<0.3	0.080	0.050	114.250	25.700	28.040	166.140	1280.000	3330.000	12.400
10-2	1.58	155.260	102.000	0.620	0.060	<0.3	0.170	0.060	35.370	2.660	17.370	340.150	84.860	1179.120	/
10-1	7.30	13.540	11.300	0.670	0.120	<0.3	0.100	0.080	44.210	1.060	19.190	69.950	322.170	67.260	4.090

TABLE 2-VIII - RESULTS OF PIEZOMETER WATER ANALYSIS, JULY 1991 AND MAY 1992

Results of Waite Amulet Water Analysis
July 1991
Temperature Range = 11°C - 23°C

Piez #	Depth (m)	pH	Acidity (mg/L CaCO3)	Alkalinity (mg/L CaCO3)	Eh (mV)	Fe(T)	Fe2+	Al	Cu	Pb	Zn	Cd	Mg	Mn	K	Ca	Na	SO4	Cl-
R1-2	2.07	5.74	/	/	134.00	/	/	/	/	/	/	/	/	/	/	/	/	/	2.65
R1-1	3.95	7.75	/	/	167.00	80.86	77.1	0.25	<0.02	<0.25	<0.02	<0.02	326.23	2.1	29.47	498.13	24.07	2884.77	13.8
R2-2	3.42	7.52	/	/	120.00	65.8	60.4	<0.25	<0.02	<0.25	0.02	<0.02	681.98	0.61	52.62	463.31	26.13	3840	14.5
R2-1	5.41	7.41	/	/	161.00	124.1	119	<0.25	<0.02	<0.25	5.9	<0.02	70.4	3.4	9.33	599.81	19.98	1862.73	0.91
R3-2	3.30	6.11	/	/	93.00	1170	1360	2.42	<0.02	<0.25	0.02	<0.02	220.48	23.3	34.46	469.89	25.28	4230	5.34
R3-1	5.25	8.67	/	/	94.00	13.69	12.1	<0.25	<0.02	<0.25	<0.02	<0.02	993.5	0.75	94.96	256.01	897.76	6900	27.9
R4-2	2.59	5.50	/	/	115.00	377.07	355	4.91	0.16	<0.25	0.35	<0.02	164.75	12.16	18.62	547.81	25.71	2556.21	4.84
R4-1	4.48	8.91	/	/	103.00	13.37	12.9	<0.25	<0.02	<0.25	<0.02	<0.02	1480	1.22	106.05	313	602.44	8670	40
5-2	1.72	7.10	/	/	148.00	/	/	/	/	/	/	/	/	/	/	/	/	/	29.7
5-1	4.40	6.47	600.00	600.00	232.00	132.68	101	<0.25	<0.02	<0.25	<0.02	<0.02	283.24	8.92	27.22	367.58	255.57	1863.57	7.25
9-2	1.63	/	/	/	/	/	/	/	/	/	/	/	/	/	/	/	/	/	/
9-5	2.40	7.75	<50	100.00	152.00	12.58	11.1	<0.25	<0.02	<0.25	<0.02	<0.02	217.28	1.2	53.48	511.84	25.33	1993.62	/
9-4	3.52	7.96	100.00	200.00	163.00	8.61	7.23	<0.25	<0.02	<0.25	<0.02	<0.02	1250	1.51	74.56	360.12	129.99	5280	25.6
9-3	5.19	7.80	/	/	177.00	0.87	0.06	<0.25	<0.02	<0.25	<0.02	<0.02	213.74	0.13	91.96	174.13	1.11	4110	/
9-1	6.67	7.22	100.00	1100.00	204.00	17.09	11.6	<0.25	<0.02	<0.25	<0.02	<0.02	58.04	0.48	31.59	86.82	501.53	799.68	13.2
9-6	8.61	7.08	/	/	237.00	6.43	4.96	<0.25	<0.02	<0.25	<0.02	<0.02	87.46	5.35	16.58	190.44	425.31	1254.87	10.8
9-7	10.39	7.56	/	/	200.00	11.68	8.41	<0.25	<0.02	<0.25	<0.02	<0.02	112.53	25.28	24.58	183.02	1260	3420	33.9
10-2	1.58	/	/	/	/	/	/	/	/	/	/	/	/	/	/	/	/	/	/
10-1	7.30	7.15	/	/	241.00	/	/	/	/	/	/	/	/	/	/	/	/	/	3.15

Results of Waite Amulet Water Analysis
May 1992
Temperature Range = NA

Piez #	Depth (m)	Fe(T)	Fe2+	Al	Cu	Pb	Zn	Cd	Mg	Mn	K	Ca	Na	SO4	Cl-
R1-2	2.07	591.29	557.59	30.42	0.66	<0.25	72.79	0.13	268.95	30.74	<5	675.49	28.24	3580.00	34.70
R1-1	3.95	168.49	166.16	1.93	<0.02	<0.25	0.72	<0.02	130.2	23.39	5.49	301.07	49.75	1440	39.5
R2-2	3.42	80.19	68.09	1.14	<0.02	<0.25	0.03	<0.02	718.2	1.09	51.55	400.12	32.12	3700	47.3
R2-1	5.41	22.34	12.84	1.49	0.24	<0.25	20.58	0.05	47.8	2.87	<5	491.8	26.29	1190	30.5
R3-2	3.30	412.18	376.68	3.05	1.3	<0.25	6.07	<0.02	272.58	8.2	26.32	504.39	33.35	2970	36.5
R3-1	5.25	6.84	2.74	0.9	<0.02	<0.25	<0.02	<0.02	775.5	0.86	88.18	253.88	912.25	3790	44.1
R4-2	2.59	141.04	134.96	8.84	0.11	<0.25	39.69	0.15	70.71	5.61	<5	497.01	25.75	1620	31.7
R4-1	4.48	6.88	4.86	0.56	<0.02	<0.25	<0.02	<0.02	1570	1.46	99.18	331.43	576.16	7320	74.3
5-2	1.72	7.23	0.9	0.84	<0.02	<0.25	0.43	<0.02	2800	2.32	86.89	422.7	68.7	/	/
5-1	4.40	126.25	123.76	0.76	<0.02	<0.25	0.03	<0.02	413.51	8.84	31.81	430.08	241.51	2450	41.5
9-2	1.63	/	/	/	/	/	/	/	/	/	/	/	/	/	/
9-5	2.40	20.92	20.65	0.88	<0.02	<0.25	0.05	<0.02	178.36	1.28	46.32	525.81	27.22	1960	41
9-4	3.52	5.11	4.67	0.78	<0.02	<0.25	<0.02	<0.02	1050	1.35	69.04	332.12	106.87	5020	29.9
9-3	5.19	0.9	0.825	0.59	<0.02	<0.25	0.05	<0.02	410.27	0.77	108.43	319.39	1040	3070	48.7
9-1	6.67	15.35	12.95	1.19	0.05	<0.25	0.1	0.03	64.67	0.56	35.64	97.01	567.47	1110	47.9
9-6	8.61	19.67	18.57	0.64	<0.02	<0.25	<0.02	<0.02	287.14	8.65	65.14	159.07	910.14	3450	48.6
9-7	10.39	/	/	/	/	/	/	/	/	/	/	/	/	/	/
10-2	1.58	/	/	/	/	/	/	/	/	/	/	/	/	/	/
10-1	7.30	5.46	5.30	0.90	<0.02	<0.25	<0.02	<0.02	40.40	1.12	16.58	68.12	302.16	60.00	34.40

2.5.1 Saturated Zone Pore Water

Control Test Plot

The pH of the pore water in the control (uncovered) test plot has remained essentially constant at about 5.6 in the shallow saturated zone since installation in October 1990. The deeper saturated zone was characterized by similar pH values, except during May 1991 when a value close to 8.0 was observed. Changes in the concentrations of SO_4^{2-}, Fe and Zn, observed during October 1990 to May 1992, reflect climatic variations. During the summer months evaporation is high and results in less flushing of the tailings and hence slightly higher concentrations (Figures 3.32 to 2.47). The pH levels and chemical data are similar to values reported by Yanful and St-Arnaud (1992) and reflect slight buffering of oxidation-derived pore water moving into the saturated zone.

Covered Test Plots

The presence of the clay composite cover (Test Plots R2 and R3) and the HDPE cover (Test Plot R3) does not seem to have had any effect, so far, on the quality of the pore water in the underlying tailings. Values of pH, SO_4^{2-} and Zn are generally similar to those observed in the control (uncovered) test plot. The Fe concentrations in the shallow saturated zone pore water in R4 (Figure 2.46) decreased steadily following cover installation. The Fe level in the pore water from the deeper saturated tailings, which is probably less flushed, has not changed with time. With the exception of the July 1991 data, a similar trend is observed for R4. Since the decrease in Fe concentration, following cover installation, is not corroborated by pH, SO_4^{2-} and Zn data, it does not indicate definite evidence of improvement in pore water quality.

The chemical data confirm the earlier inference that the presence of previously stored acidity in the tailings will preclude any observable improvements in the pore water quality in the short term (that is, over the three-year life span of this project).

2.5.2 Lysimeter Drainage Water

The collection basin lysimeters installed below the soil-covered test plots did not produce any water until autumn, 1992. Estimates had indicated that the time required for any percolated water to initially saturate the tailings before reporting to the manholes was about two years from the date of installation. In the absence of cracks, no water percolation, and hence drainage, was expected from the HDPE-covered lysimeter.

The chemistry of the drainage water from the control lysimeter (LYS-R1) is presented in Table 2-IX. The data indicate rapid oxidation of the exposed tailings in the uncovered lysimeter, immediately following installation in October 1990. The pH of drainage water was 3.78 in October and decreased to 3.33 within a month. SO_4^{2-} concentrations were in the range of 40 g/L to 50 g/L during October-November 1990. Concentrations of Fe and other heavy metals (Zn, Cu and Cd) were higher than those observed in the saturated

zone tailings. This rapid oxidation reflects the presence of reactive, iron-bearing sulphide minerals in the tailings (15% pyrite and 6% pyrrhotite). After the initial flushing of the tailings, the concentrations of sulphate and metals apparently decreased in 1991. Further oxidation during the summer produced more acid, which would explain the high concentrations of sulphate and metals observed in November 1992.

The lysimeters from the covered plots started reporting water in October 1992. Analysis of the water indicated an average pH value of 3.6 and acidities in the range of 200 for the drainage from Plot R4. These are similar to pH and acidity values obtained in the shallow saturated zone pore water in May 1992. Total dissolved iron, copper and zinc concentrations were also similar. This would seem to confirm the water table data previously presented, which suggested that the water table overtopped and contaminated the lysimeters. During a site visit in November 1992, the lysimeters were again inspected and sampled. The lysimeter from R4 did not produce any water suggesting that water from the previous overtopping had completely drained.

Drainage water from plots R2 and R3 showed slightly lower pH values (~3.1) and much higher acidities (20,000 mg/L $CaCO_3$). These acidities are much higher than those obtained in the saturated zone pore water and do suggest some oxidation, or leaching of tailings contained in the lysimeters, was occurring. The oxidation can result from the diffusion of oxygen through the overlying soil or the deposition of ferric iron during overtopping of the lysimeters. Gaseous oxygen concentrations obtained in the cover, however, indicate that the flux of oxygen is low (Figure 2.27).

The tailings in the lysimeters were obtained from the deep saturated zone of the south end section of the impoundment and were probably not unaffected by oxidation-derived pore water from the unsaturated zone. However, the original mill process-waters discharged with tailings contained high concentrations of Na, Ca, and SO_4^{2-} (Blowes and Jambor, 1990). Thus, the sulphate levels of 15-30 g/L, presented in Table 2-IX, could not all be attributed to oxidation. Continual leaching of the tailings by water percolating through the cover would release any original SO_4^{2-} present. Further monitoring of the lysimeters and coring and characterization of the constituent tailings would provide information on the extent of oxidation.

TABLE 2-IX - RESULTS OF LYSIMETER WATER ANALYSIS, PLOT R1, OCTOBER 1990 TO MAY 1992.

Results of Waite Amulet Water Analysis

Date	Julian Day	Piez #	Temp °C	pH	Acidity (mg/L CaCO3)	Alkalinity (mg/L CaCO3)	Eh (mV)	Fe(T)	Fe2+	Al	Cu	Pb	Zn	Cd	Mg	Mn	K	Ca	Na	SO4	Cl-
Oct-90	0	LYS-R1	6 - 11	3.78	52600.00	<50	172.00	2010.00	1220.00	6830.00	123.00	<0.04	840.00	17.60	325.00	38.20	3.64	348.00	13.70	51300.00	0.86
Dec-90	61	LYS-R1	/	/	/	/	/	1590.00	995.000	5090.000	73.000	<0.04	8570.000	9.940	171.000	20.300	5.930	490.000	8.440	43100.00	2.050
May-91	212	LYS-R1	/	/	/	/	/	384.83	316.000	1160.000	45.090	<0.3	1190.000	3.110	45.790	4.970	<5	211.710	10.180	9840.00	0.600
Jul-91	273	LYS-R1	11 - 23	3.15	22500.00	/	241.00	1950	1790	3180	119.56	<0.25	2430	7.06	156.52	13.98	11.41	486.79	12.57	22710	1
May-92	578	LYS-R1	/	/	/	/	/	1910	1585	921.2	42.79	<0.25	444.59	1.04	110.24	5.11	<5	303.33	13.3	9500	34.3

Note: All concentrations in mg/L.

2.5.3 Aqueous Speciation Modelling

2.5.3.1 MINTEQ Model

Aqueous geochemical modelling was conducted on drainage water from the lysimeters and pore water from the saturated zone, using the equilibrium speciation model MINTEQ (Felmy *et al.*, 1984). The model applies the fundamental principles of thermodynamics to simulate equilibrium aqueous reactions and phase exchanges. MINTEQ can model ion speciation and solubility, adsorption, oxidation-reduction, gas phase equilibria, and precipitation and dissolution of solid phases. The MINTEQ database is based on that of the computer code WATEQ2 (Ball *et al.*, 1979).

2.5.3.2 Modelling Objectives

The objectives of the modelling were: (1) to evaluate the quality of the analytical data by checking the charge balance; and (2) to determine if some of the tailings pore water and drainage water samples are saturated, supersaturated, or undersaturated with respect to commonly formed mineral phases. Objective (2) is essential to understanding the role of mineral precipitation and dissolution in controlling water geochemistry. The degree of saturation of a water sample with respect to a mineral phase is presented as the saturation index (SI). SI is the logarithm of the ion activity product or the product of the aqueous activities of the ions in the mineral components (log IAP) minus the logarithm of the mineral solubility product (log K_{sp}). Saturation indices (SI) give information on minerals that could potentially precipitate out of solution and therefore control the chemical composition of the water. A positive SI value indicates supersaturation, a negative value undersaturation, and a value of zero suggests saturation. Geochemical equilibrium calculations performed using MINTEQ and other similar computer codes do not conclusively prove the presence or absence of primary or secondary solid phases, but rather give an indication of the tendency or potential for a reaction to occur.

2.5.3.3 Charge Balance and Error Analysis

Results of charge balance calculations performed on the drainage waters from the control lysimeter (LYS-R1), using MINTEQ, are presented in Table 2-X. A high discrepancy was observed for the October 1990 data with a reported SO_4^{2-} concentration of 51.3 g/L. In theory, all solutions must be perfectly charge-balanced (that is, 0.0% discrepancy) for electrical neutrality. In practice, however, discrepancies of less than 10% can be attributed to reasonable analytical errors, plus uncertainties in the thermodynamic constants used in the speciation calculations. The charge balance of -30.4% indicates a problem with the chemical analyses. Experience with the analysis of acid mine waters suggests that sulphate, the dominant anion, is often the source of such a discrepancy. The sulphate concentration was therefore adjusted to 45 g/L to obtain an acceptable charge balance of -9.5%. An adjustment was made in the sulphate concentration for July 1991 to give a charge balance close to 10%.

As shown in Table 2-IX, a zinc concentration of 8,570 mg/L was reported for LYS-R1 in December 1990. This value is quite high when compared to the 840 mg/L observed October 1990. Consideration of typical Fe/Zn and Cd/Zn ratios in mine waters would seem to suggest that the Zn value for December 1990 should have been 850 mg/L. A greater discrepancy in the charge balance (-35.5%) was, however, obtained when the lower value of Zn was used in the MINTEQ run, as shown in Table 2-X. The charge balance of +5.9% obtained with the original Zn concentration is quite acceptable. Charge balances obtained from modelling of the chemical data for piezometers in and around the test plots were all less than 10%.

TABLE 2-X - RESULTS OF CHARGE BALANCE AND SATURATION INDEX CALCULATIONS

Date	Julian Day	Lysim #	Redox	Charge Balance	SO4 (mg/L)	Zinc (mg/L)	SI Al(OH)3	SI Alunite	SI Boehmite	SI Gibbsite	SI Gypsum	SI Melanterite	SI Lepidocrocite	SI Ferrihydrite	SI Goethite	SI Diaspore	SI Haematite	pQ
Oct-90	0	LYS-RI	Eh (meas.)	- 30.4%	51,300	840	-2.944	+ 8.683	-1.180	-1.158	+ 0.378	-1.454	-	-	-	-	-	-
			Eh (meas.)	- 9.5%	45,000	840	- 2.792	+ 8.932	- 1.029	- 1.006	+ 0.327	- 1.511	-	-	-	-	-	-
Oct-90	0	LYS-RI	Fe2+/Fe3+ Couple	- 4.6%	45,000	840	- 2.811	+ 8.976	- 1.049	- 1.018	+ 0.327	- 1.508	+ 5.13	+ 1.603	+ 5.379	+ 0.806	+ 15.691	37.2
Nov-90	31	LYS-R1	Fe2+/Fe3+ Couple	+ 5.9%	43,100	8,570	- 4.348	+ 8.363	- 2.594	- 2.526	+ 0.447	- 1.611	-	+ 0.616	+ 4.291	- 0.714	+ 13.502	38.5
Nov-90	31	LYS-R1	Fe2+/Fe3+ Couple	- 35.5%	43,100	857	- 4.667	+ 5.905	- 2.915	- 2.839	+ 0.533	- 1.497	+ 3.924	+ 0.398	+ 4.052	- 1.030	+ 13.021	38.8
May-91	212	LYS-R1	Fe2+/Fe3+ Couple	- 4.1%	9,840	1,190	- 3.396	-	- 1.620	- 1.678	- 0.072	- 2.322	+3.998	+0.476	+ 4.50	+ 0.174	+13.962	37.6
Jul-91	273	LYS-R1	Fe2+/Fe3+ Couple	+ 16.6%	22,710	2,430	- 4.233	+ 4.749	- 2.450	- 2.538	+ 0.321	-1.564	+ 3.090	- 0.433	+ 3.668	- 0.674	+ 12.310	38.3
				+ 10.3%	24,000	2,430	- 4.268	+ 4.708	- 2.484	- 2.572	+ 0.341	- 1.543	+ 3.056	- 0.467	+ 3.635	- 0.709	+ 12.243	38.4

2.5.3.4 Mineral Saturation

Lysimeter Drainage Water

Results of mineral saturation index calculations conducted on the drainage waters from the control lysimeters are presented in Table 2-VIII. Attention is focused on Fe-, Al- and SO_4^{2-}-bearing minerals which are known to form in acid mine environments. With the exception of May 1991, the drainage water from the control lysimeter was slightly supersaturated with respect to gypsum [$CaSO_4.2H_2O$] at most times. This is a common property of waters to which a large amount of sulphate has been added. The drainage water was close to saturation (SI= -0.07) in May 1991 and suggests flushing of sulphate and other oxidation products during spring melt. It should be noted that a reasonable charge balance (-4.1%) was obtained on the May 1991 data; thus, the SO_4^{2-} concentration and the rest of the analytical data were, most likely, correct.

Others minerals apparently supersaturated include: ferrihydrite (taken as $Fe[OH]_3$ in MINTEQ), lepidocrocite [γ-FeOOH], goethite [α-FeOOH], and alunite [$KAl_3(SO_4)_2(OH)_6$]. Alunite and potassium jarosite (SI values were positive and high ~ +11.0) are commonly supersaturated in actively weathering, sulphide-bearing systems; the phases do form over geologic time frames (in the case of alunite) and over several years' time (for jarosite). There are, however, kinetic barriers which prevent instantaneous formation at low temperatures.

Goethite is a stable phase but its formation is kinetically inhibited and forms slowly from the aging of amorphous ferric hydroxide. It also precipitates by the relatively slow oxidation and hydrolysis of aqueous or solid ferrous iron species. Lepidocrocite can precipitate in the laboratory at pH values between 4 and 7, by the oxidation of aqueous or solid ferrous iron species.

Ferrihydrite or amorphous ferric hydroxide is a very likely phase to control the solubility of aqueous ferric iron (Fe^{3+}). An indication of the state of the ferric hydroxide was inferred from a calculation of pQ values (negative logarithm of the products of the ions present), based on the work of Langmuir and Whittemore (1971):

$$pQ = -\log [Fe^{3+}][OH^-]^3 \qquad [2.3]$$

where the activity of water is taken as close to unity.

The pQ values of ~37 and 38 (Table 2-VIII) suggest the ferric hydroxide was a fresh, rapidly precipitated amorphous material. More crystalline oxyhydroxides such as goethite and haematite would have pQ values of 44.

Although high SI values (~ +12.0) were calculated for haematite, this mineral is not stable under the temperature-pressure conditions of the tests and cannot be considered as

potential solid phases. Haematite rarely precipitates directly out of solution but slowly crystallizes from amorphous material by dehydration or long-term aging out of solution (Langmuir and Whittemore, 1971).

Saturated Zone Pore Water

The data presented in Table 2-VI suggest that the dissolved iron in the saturated zone pore water, in and around the test plots, is present mainly in the reduced state, or as ferrous iron, Fe^{2+}. Thus, where there is no alkalinity, very few iron-bearing minerals are likely to have SI values greater than zero. Supersaturation with respect to the aluminium oxyhydroxides—boehmite, diaspore [AlO.OH] and gibbsite [$Al(OH)_3$]—occurs in the shallow saturated zone where the pH is slightly acidic.

The tailings pore water is close to saturation with respect to gypsum (SI values range from -0.03 to +0.40). In the deeper saturated zone, where some alkalinity is present to provide buffering, it appears that Ca, Mg, and Fe concentrations in the pore water are controlled by carbonate minerals such as calcite [$CaCO_3$], dolomite [$CaMgn(CO_3)_2$] and siderite [$FeCO_3$]. The water is, however, slightly undersaturated with respect to other metal carbonates.

3.0 LABORATORY EVALUATION

3.1 Drainage Columns

3.1.1 Column Assembly and Experimental Methods

The water retaining capabilities of the three-layer cover system were investigated in a laboratory apparatus. The apparatus consisted of a 1 m tall plexiglass column with a 10.8 cm inside diameter. The column was instrumented with specially-designed tensiometer and pressure-transducer systems and stainless steel rods for a TDR (time domain reflectometry) unit. The tensiometers measured the suction developed in the column as the soils drained while the TDR unit was used to measure the corresponding water content without disturbing the soils. Each tensiometer consisted of a 0.5 bar (5 m of water pressure) porous ceramic tip. It was designed as a compromise between the amount of porous ceramic surface area making contact with the soil and impeding drainage.

The procedure for measuring the moisture content consisted of recording the travel time (t) of a step-voltage pulse in the form of an electromagnetic wave along two 2 mm diameter stainless steel transmission rods inserted horizontally in the soil. The spacing between each pair of rods was 20 mm. From the length of the rod in the soil (l), the apparent dielectric constant (K_a) for the soil is calculated as follows:

$$K_a = (ct/l)^2 \qquad [3.1]$$

where c is the velocity of the wave in free space (30 cm/ns).

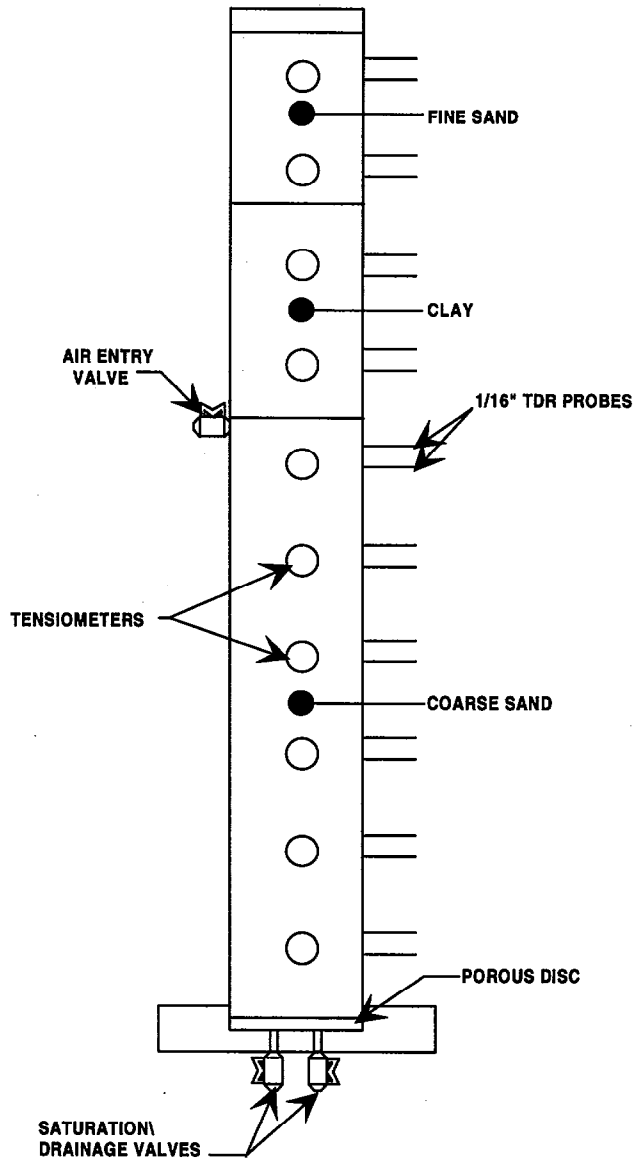

Figure 3.1: Drainage Column

The dielectric constant of the soil is wholly attributed to the presence of moisture. The volumetric water content of the soil (θ_v), is determined from an empirical equation between K_a and θ_v, derived by Topp *et al.* (1980):

$$K_a = 3.03 + 9.3\theta_v + 146.0\theta_v^2 - 76.7\theta_v^3 \qquad [3.2]$$

The voltage pulse was applied with a Tektronix Model 1502B Time Domain Reflectometer (TDR) Cable Tester and the travel time calculated from the TDR wave by means of a data acquisition system. The TDR data was compared with moisture contents determined by gravimetry. Agreement between the two methods was found to be within ±5%.

An air vent was installed just below the clay layer to permit drainage of the coarse sand. A 0.5 bar porous ceramic plate was installed at the base of the column to permit water drainage but prevent air flow. A tygon tubing line was connected from the base of the column to an Erlenmeyer flask. The flask was used to establish the water table and to collect water draining from the column.

The column was then placed inside a wooden box insulated with styrofoam. A thermostat and heating bulb were installed in the box to provide a reasonably constant temperature. The thermostat was set just slightly above room temperature (~25° C) to allow for acceptable temperature control within daily variations.

The column was packed with 62 cm of coarse sand (Ansil S-2), 27 cm of varved clay and 13 cm of fine sand (Ansil S-1). These soils were similar to those used in the construction of the field test plots described in Chapter 2. The top of the porous stone was taken as the zero elevation point. The soils were initially saturated and then allowed to drain while the water table was kept at 20 cm below the base of the column (h_w=-20 cm). This was done to simulate the lowering of the water table in a covered tailings deposit under dry conditions. The water content and pressure head were monitored at different times. The pressure head was then converted to total head by adding it to the elevation head. Figure 3.2 shows these profiles at various times for the test which was conducted while permitting evaporation. The data points represent the results obtained experimentally whereas the lines show the results obtained from saturated-unsaturated flow modelling.

To permit accurate modelling of the drainage, it was necessary that the evaporative flux be determined. To do this, an evaporation column was placed in immediate proximity to the drainage column. The evaporation column had a 10 cm diameter and was filled with the same fine sand as was used in the top layer of the drainage column. The sand was then saturated and left to evaporate at the same time and under the same conditions as the drainage column. The evaporation column was weighed periodically and the quantity of evaporated water determined. From this data, a profile was then plotted showing the evaporation rate vs. time.

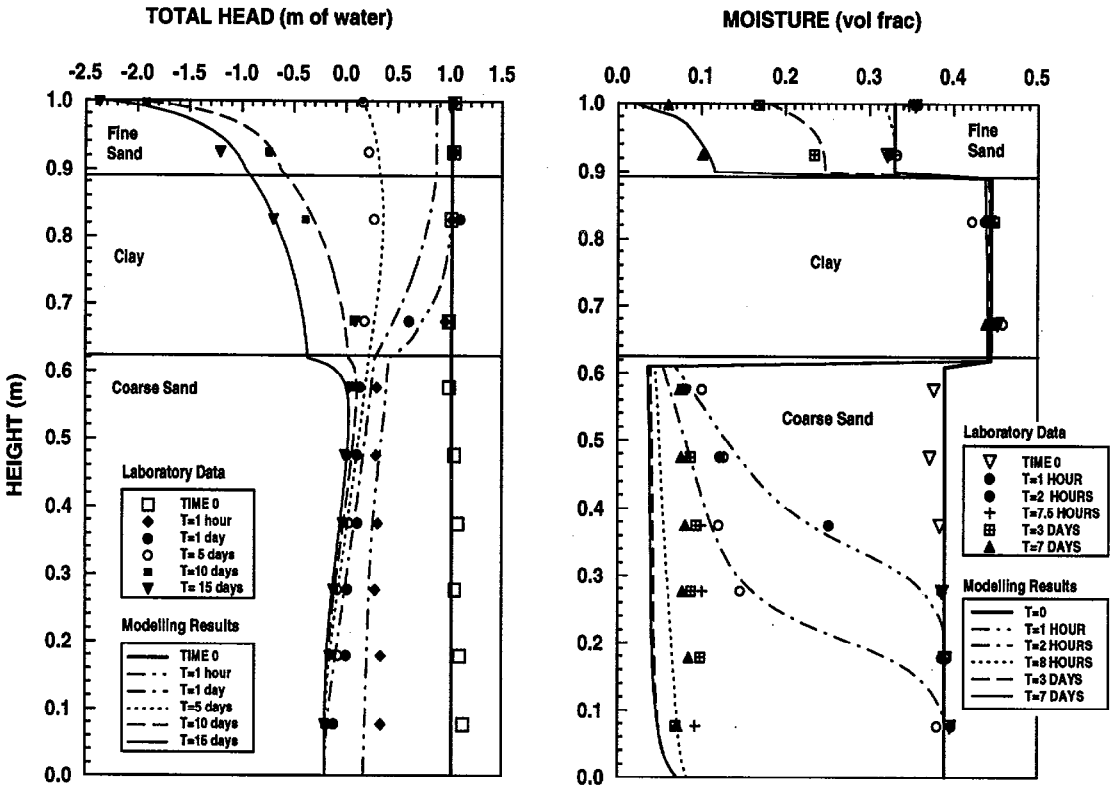

Figure 3.2: Column Pressure and Water Content Profiles

This profile was expected to be somewhat different from the actual drainage column evaporation profile for two reasons. Firstly, depth of the fine sand in the evaporation column was 8.6 cm (4.4 cm less than the drainage column), which meant that there was less water available and that the quick drop in the evaporation rate would therefore occur earlier than it would in the drainage column. Secondly, following depletion of the fine sand pore water, the clay in the drainage column could supply some water to the fine sand layer whereas the evaporation column fine sand would simply dry up. Ultimately, this would cause the evaporation column rate to go to zero quickly, whereas the drainage column evaporation could slowly drain the clay to a pseudo-steady state. For these reasons, the profile obtained from the evaporation column was used only as a starting point in determining the true evaporative function of the drainage column. In Figure 3.3, both the original evaporation column profile and the fitted drainage column profile are displayed. In the modelling process, the boundary conditions entered were the negative of the values shown, since evaporation represents a loss of water from the soil.

The second test was conducted while preventing evaporation from occurring by installing a plastic membrane over the top of the column. This membrane had a small perforation to ensure atmospheric pressure. The results of this test are displayed in Figure 3.4. Although not realistic, this test permits closer examination of the gravitational drainage by focusing on the effects of the porous stone, coarse sand and, to a limited extent, the clay.

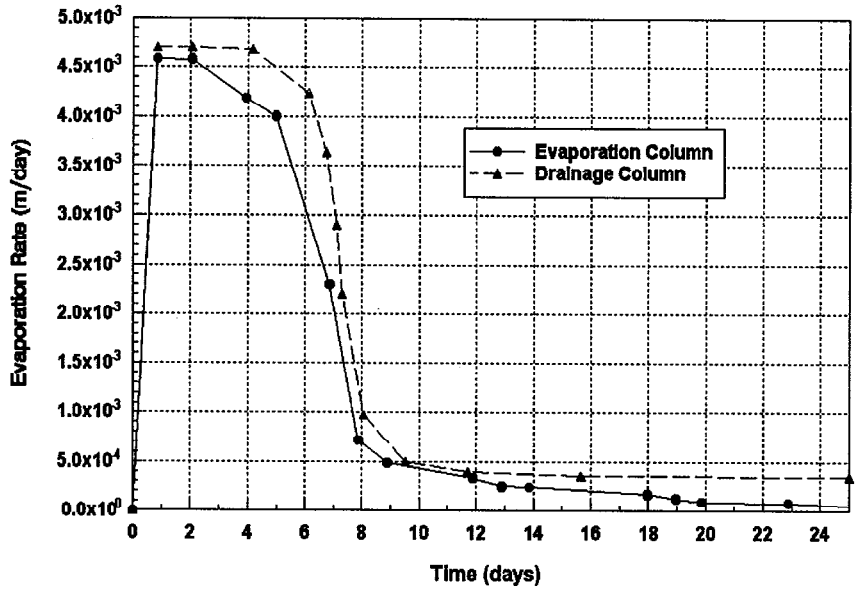

Figure 3.3: Evaporation Rates

Results

The profiles in Figure 3.2 show that the clay layer did not drain even though both the coarse sand on the bottom and the fine sand over top were dried nearly to residual saturation. On the bottom, the clay was prevented from drying by the capillary barrier effect, while on top, the presence of the fine sand considerably reduced evaporative losses from the clay. The high suction created by the evaporation of the fine sand pore water decreased the hydraulic conductivity of the sand significantly which, in turn, prevented the negative water flux from affecting the clay. These results are in complete agreement with what was observed in the field: the sands may dry, but the clay keeps a moisture content near saturation.

These test results suggest that, even in severe dry conditions, the clay would not lose its moisture and would continue to offer an effective barrier against oxygen diffusion. Although the tests were not run for extended periods, modelling could be used to extrapolate and determine the consequences of longer dry periods.

The test without evaporation permitted closer examination of the drainage profiles measured in the bottom layers (e.g. stone, coarse sand and clay). The resulting profiles show that very little suction is transferred by the clay to the fine sand on top. The water content profile confirms the water retention ability of the clay. These profiles could be modelled in the same way that the run with evaporation was modelled but some of the soil properties would differ because, in the run with evaporation, the soils were saturated then left to dry over a long period of time. The drying resulted in some soil consolidation and therefore affected the moisture retention capabilities of the materials. The drainage

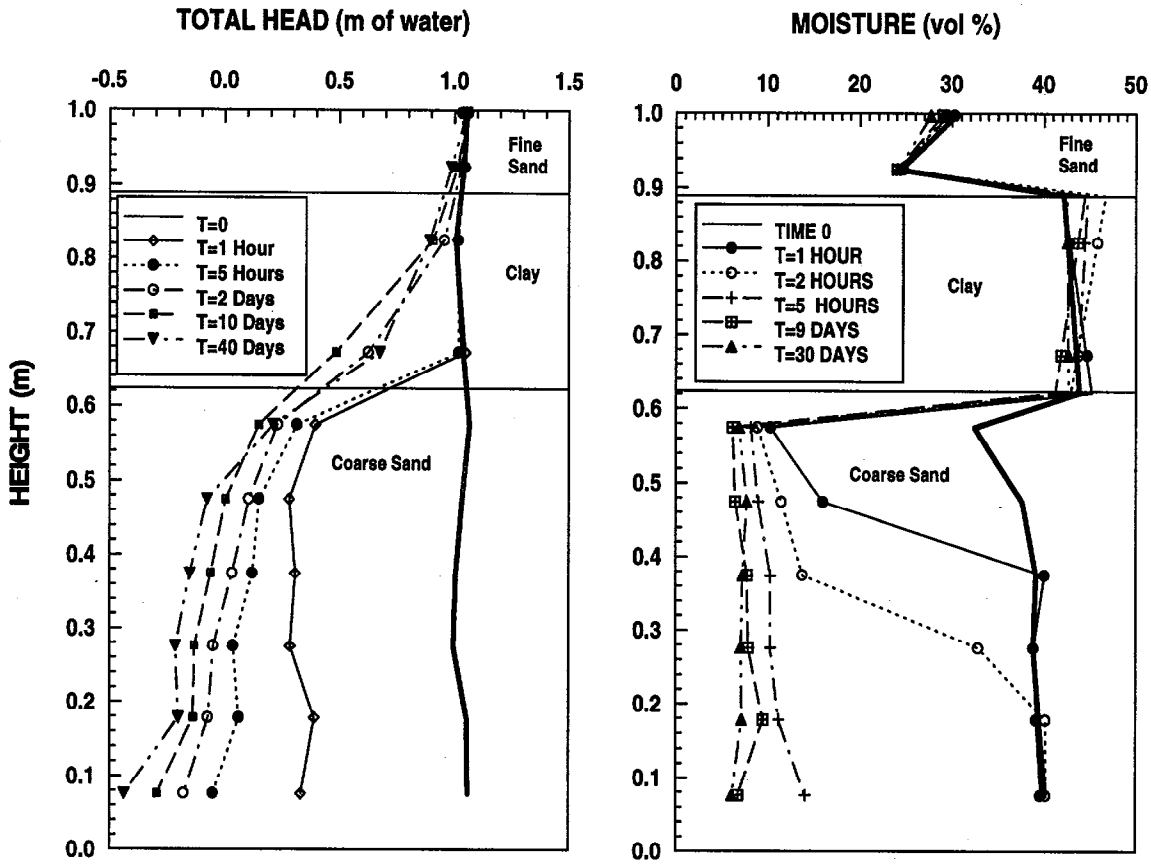

Figure 3.4: Results of Test Without Evaporation

profiles are very sensitive to factors such as the air entry value (AEV) of the soil which is defined as the suction where the water content of the soil begins to drop quickly. One noticeable example of consolidation is in the water content of the fine sand: at time zero, when the sand is saturated, there is approximately 5% (volumetric) less water in the second run than there was in the run with evaporation. This shows that, as the soil was saturated, left to dry and saturated again, the soil porosity decreased. The saturated water content of the clay decreased by 2% while changes in the coarse sand were insignificant.

3.1.2 Drainage Modelling

Saturated-Unsaturated Flow Model

The software used for modelling the drainage in the covers is a Windows version of PC-SEEP called SEEP/W (GEO-SLOPE International). SEEP/W is a finite element program that can be used to model water movement and pore water pressure distribution within porous materials such as soil and rock. The program is formulated to analyze both saturated and unsaturated flow. Flow in an unsaturated soil follows Darcy's law in a similar manner to flow in a saturated soil. The flow is proportional to the hydraulic

gradient and the hydraulic conductivity (coefficient of permeability). The major difference between saturated and unsaturated flow is that, in a saturated soil, the hydraulic conductivity is insensitive to pore water pressure, while in an unsaturated soil, the hydraulic conductivity varies greatly with changes in pore water pressure. To account for the hydraulic conductivity variation, a conductivity function (hydraulic conductivity vs. pore water pressure) must be defined for each soil type.

For the determination of the conductivity function, a program called KCAL is included in the SEEP/W software package. This program defines the conductivity function using pertinent soil properties, the moisture content-suction curve, and the Green and Corey equation:

$$k(\Theta)_i = \frac{k_s}{k_{sc}} * \frac{30T^2}{\mu g \eta} * \frac{\xi p}{n^2} * \sum_{j=i}^{m} [(2j+1-2i)h_i^{-2}] \qquad [3.3]$$

where:

$k(\Theta)_i$	=	the calculated conductivity for a specified water content or negative pore water pressure (cm/min)
k_s/k_{sc}	=	the matching factor (measured saturated conductivity/calculated saturated conductivity)
i	=	the last water content class on the wet end (e.g. i=1 identifies the pore class corresponding to the saturated water content, and i=m identifies the pore class corresponding to the lowest water content)
h_i	=	negative pore water pressure head for a given class of water-filled pores (cm of water)
n	=	total number of pore classes
Θ	=	water content
T	=	surface tension of water (Dyn/cm^3)
ξ	=	water-saturated porosity
η	=	viscosity of water (g/cm*s)
g	=	gravitational constant (cm/s)
μ	=	density of water (g/cm^3)
p	=	a parameter that accounts for interaction of pore classes

The variation of the hydraulic conductivity with pore water pressure makes the finite element equations non-linear, and an iterative process is required to solve the equations. Hydraulic head (or total head) is the primary unknown computed. Since hydraulic conductivity is related to hydraulic head, the appropriate conductivity is dependent on the computed results.

During a transient process, the amount of water entering an elemental volume may be larger than the amount of water exiting the volume, or vice versa. This results in a certain amount of water either being retained or released during a particular time increment. The

ability of each soil to store water must be defined by a storage curve (volumetric water content vs. pore water pressure) as water contents will change during a transient analysis.

SEEP/W is formulated on the basis that the flow of water through both saturated and unsaturated soil follows Darcy's law which states that:

$$q = ki \qquad [3.4]$$

where:

q	=	specific discharge
k	=	hydraulic conductivity
i	=	gradient of hydraulic head or potential

Darcy's law was originally derived for saturated soil, but later research has shown that it can also be applied to the flow of water in unsaturated soil provided that the hydraulic conductivity is no longer a constant, but varies with changes in water content (and indirectly with pore water pressure).

SEEP/W uses the Darcian velocity which is computed from a modified form of Darcy's Law:

$$v = ki \qquad [3.5]$$

where v is known as the Darcian velocity. The actual velocity at which water moves through the soil is the Darcian velocity divided by the porosity of the soil.

The governing 2-dimensional equation used in the formulation of SEEP/W is:

$$\frac{\partial}{\partial x}[k_x \frac{\partial H}{\partial x}] + \frac{\partial}{\partial y}[k_y \frac{\partial H}{\partial y}] + Q = \frac{\partial \Theta}{\partial t} \qquad [3.6]$$

where:

H	=	total head (hydraulic head)
k_x	=	hydraulic conductivity in the x-direction
k_y	=	hydraulic conductivity in the y-direction
Q	=	applied boundary flux
Θ	=	volumetric water content
t	=	time

This equation states that the difference between the flow entering and leaving an elemental volume, at a point in time, is equal to the change in the volumetric water content. More fundamentally, it states that the sum of the rates of change of flows in the

x- and y-directions is equal to the rate of change of the volumetric water content with respect to time. Note that, in a steady-state analysis, the term on the right is equal to zero.

Changes in volumetric water content are dependent on changes in the stress state and the properties of the soil. The stress state for both saturated and unsaturated conditions can be described by two state variables: $(\sigma - u_a)$ and $(\sigma - u_w)$ where σ is the total stress, u_a is the pore air pressure and u_w is the pore water pressure.

SEEP/W is formulated for conditions of constant total stress; that is, there is no loading or unloading of soil mass. Another assumption is that the pore air pressure remains constant at atmospheric pressure during transient processes. This means that $(\sigma - u_a)$ remains constant and has no effect on the change in volumetric water content. Changes in volumetric water content are consequently only dependent on the $(u_a - u_w)$ stress state variable, and with u_a remaining constant, the change in volumetric water content is a function of only pore water pressure changes.

A change in volumetric water content can be related to a change in pore water pressure by the equation:

$$\partial\Theta = m_w \partial u_w \qquad [3.7]$$

where m_w is the slope of the storage curve at that point.

The total hydraulic head is defined by:

$$H = \frac{u_w}{\gamma_w} + y \qquad [3.8]$$

where:

y	=	elevation
γ_w	=	unit weight of water

Substituting Equation 3.8 into 3.7 and rearranging gives:

$$\partial\Theta = m_w \gamma_w \partial(H-y) \qquad [3.9]$$

Since the elevation is a constant, the derivative of y with respect to time disappears so that the partial derivative of the water content can be substituted into Equation 3.6, leaving the following governing equation:

$$\frac{\partial}{\partial x}[k_x \frac{\partial H}{\partial x}] + \frac{\partial}{\partial y}[k_y \frac{\partial H}{\partial y}] + Q = m_w \gamma_w \frac{\partial H}{\partial t} \qquad [3.10]$$

Modelling Procedure

The pressure head in the drainage columns was monitored periodically at ten different locations. A total head profile was then plotted by adding the pressure head to the specific tensiometer elevation (zero elevation taken at the top of the porous stone supporting the coarse sand). The moisture content was also monitored periodically and plotted on a depth vs. moisture content graph. These profiles were used as the basis for the modelling procedure.

The individual soil characteristics were defined in SEEP/W, as well as the physical dimensions of the column and the soil layers. The representation was two-dimensional with the diameter of the column entered as the width. The bottom boundary condition was entered as a constant head of -0.2 m of water as the water table was kept 20 cm below the designated zero point for the run with evaporation. In the run without evaporation, the water table was kept at 50 cm below zero.

The top boundary conditions were entered as a negative water flux vs. time. The flux was determined using the evaporation column previously described (Section 3.1.1). It was not certain that this evaporative flux would be representative of the drainage column evaporation for reasons previously mentioned. This function nevertheless provided us with a starting point for the evaporative function used (see Figure 3.3).

For the soil characteristics, two sets of moisture-drainage curves were available from analyses conducted by McGill University and Noranda Technology Centre. Since some major discrepancies were found, moisture content versus suction functions were developed with both sets of data and trial runs conducted. The functions were altered within experimental range until the predicted moisture content and pressure profiles agreed reasonably with those observed in the experimental column. The moisture-drainage curves used are displayed in Figure 3.5.

The program KCAL was used to derive the hydraulic conductivity-suction functions. Although KCAL can generally supply adequate estimates for the conductivity function, it was found that it did not predict the low conductivities expected for sands at or near the residual moisture content. This shortcoming therefore required an adjustment of the conductivity functions until the low heads recorded in the laboratory were reasonably simulated. A hydraulic conductivity of 3.1×10^{-5} cm/s supplied by the manufacturer was used for the porous stone supporting the bottom sand. These conductivity functions are plotted against pressure head in Figure 3.6.

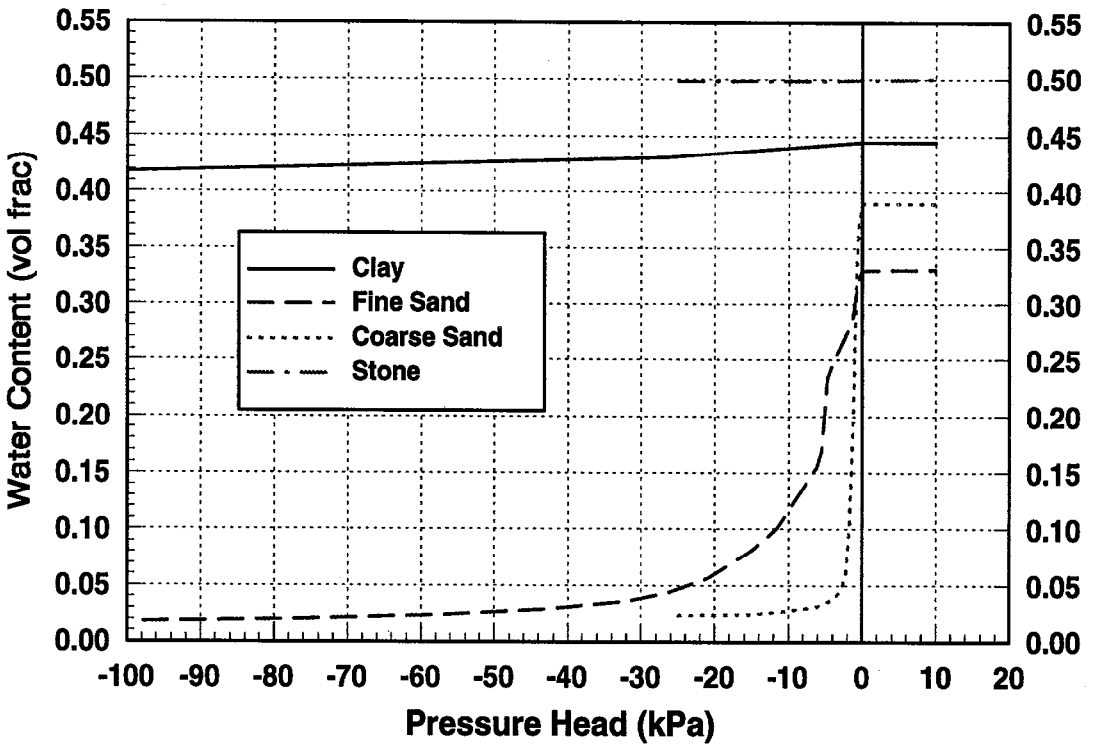

Figure 3.5: Column Materials Moisture

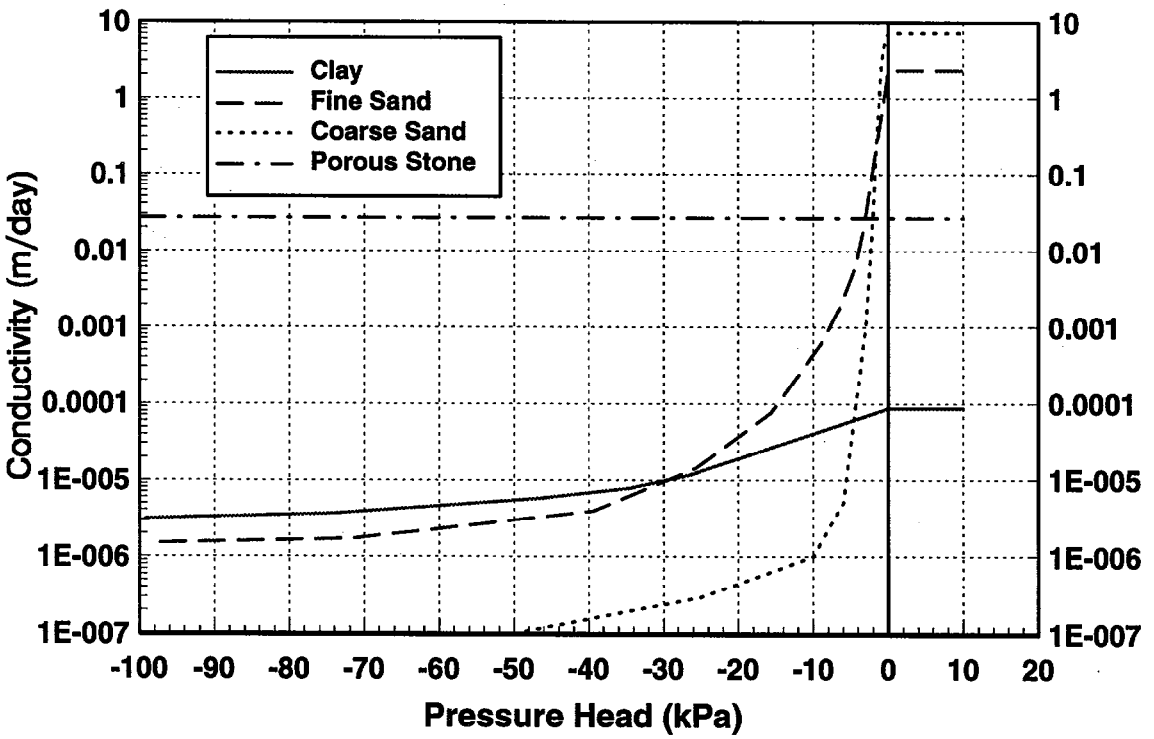

Figure 3.6: Column Materials Conductivities

Modelling Results

As was demonstrated by the results shown in Figure 3.2, the hydraulic head and moisture content profiles obtained in the laboratory can be successfully modelled using SEEP/W. After agreement between laboratory results and model simulations were obtained, the model was then used to predict the behaviour of the soils under dry periods that extend beyond 15 days. As shown in Figure 3.7, the clay stays near saturation even under extreme evaporative conditions. Another important point is the fact that the clay water content increases in response to simulated rain. This means that, even if long dry periods occur and the clay loses some moisture, the clay will return to saturation as rain is applied and continue to curtail oxygen diffusion.

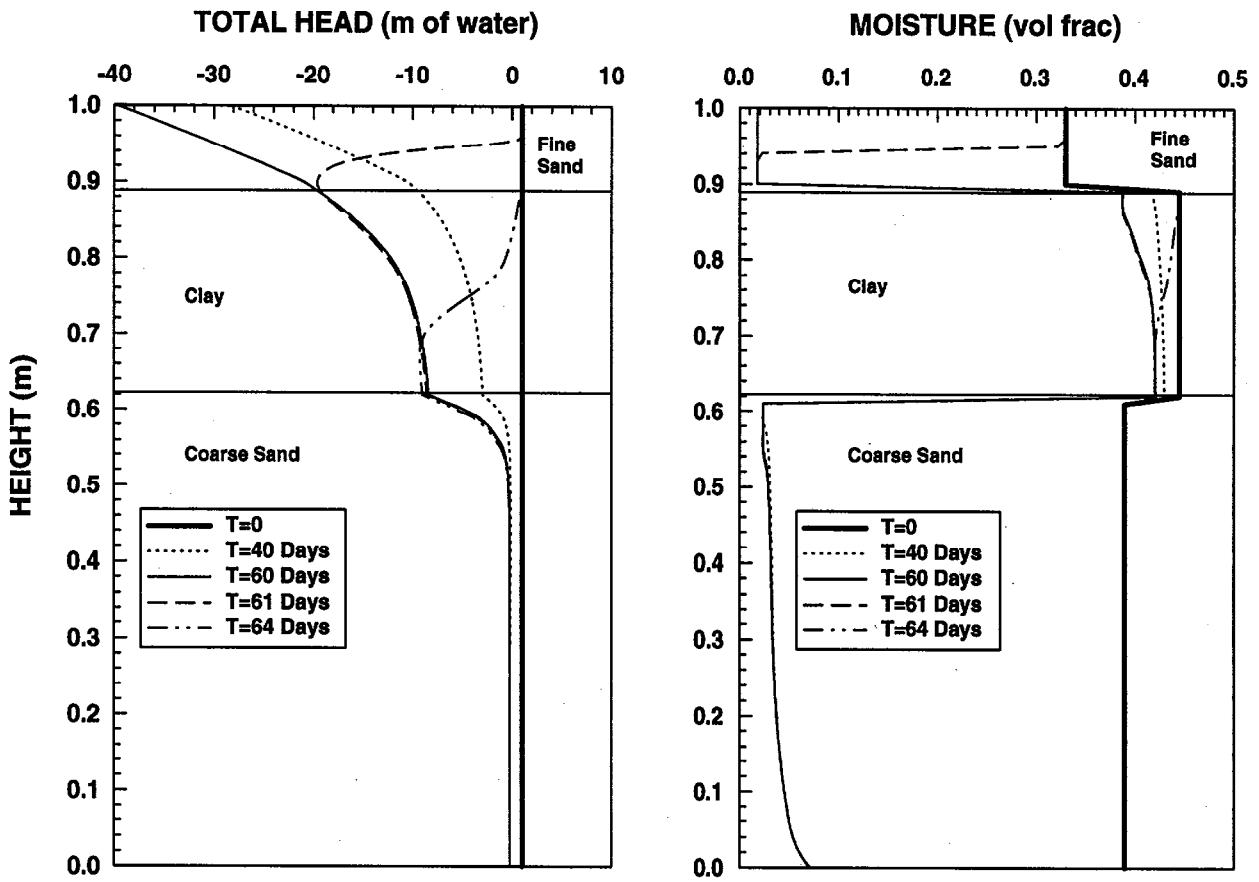

Figure 3.7: Extended Evaporation and Rain Simulation

To obtain these profiles, the evaporative rate that was calculated using the experimental data (i.e. approximately 0.3 mm/day) was continued until day 60, then 2 cm of rain per day for 3 days (60 to 63) was added. The 60-day drying time was chosen as a maximum foreseeable duration of null precipitation and the 2 cm of rain was chosen as a reasonably high rainfall. Any run-off that may occur in reality is taken into account by SEEP/W in the following way: if the positive flux is greater than the maximum conductivity of the soil, then the pressure head at the surface is set equal to its elevation. This sets the soil surface water content to saturation and the infiltration to the soil's maximum conductivity. Any rainfall above the maximum is assumed to run off and is subsequently ignored. Figure 3.8 shows the top boundary function used.

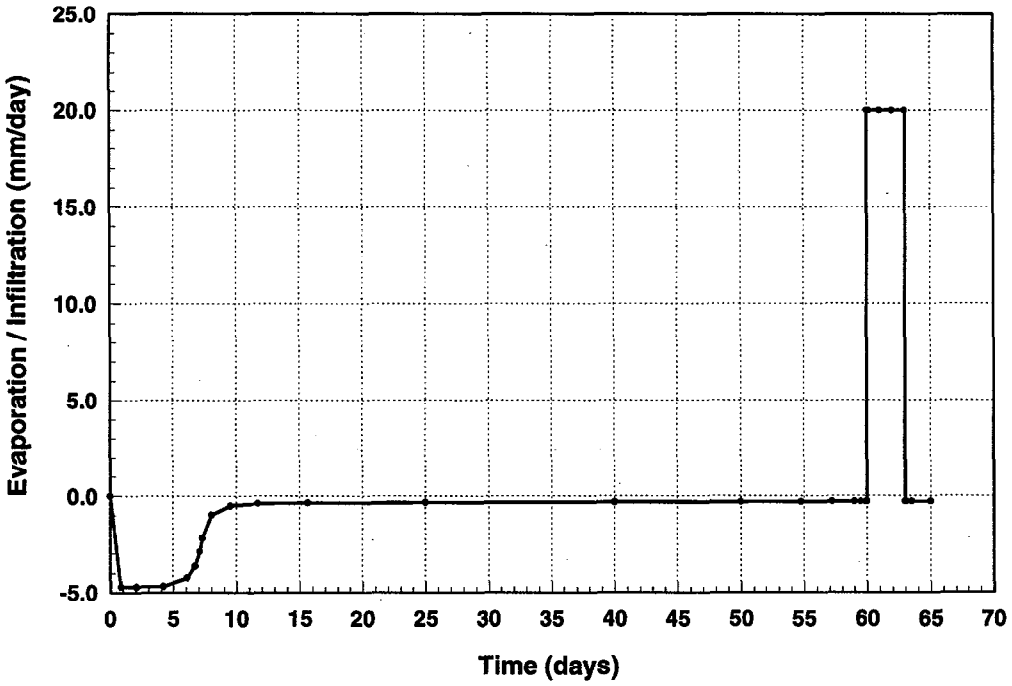

Figure 3.8: Extended Surface Boundary Function

As an oxygen barrier, the three-layer system performs adequately under the various simulated conditions. It is true that after 60 days the clay had lost nearly 5% of its water content and this would be sufficient to considerably increase the oxygen flux. But 60 days without significant precipitation in Canada could only happen very rarely and the clay would still offer a relatively effective barrier against oxygen at 90% saturation. The clay, if compacted and placed at a low hydraulic conductivity, could also be an effective infiltration barrier. In further testing, water could be added to the surface of the column and the infiltration rate over long periods could be measured.

The foregoing discussions indicate that, apart from the negative effects of freeze-thaw and root penetration, the three-layer soil cover system could certainly be an efficient long-term solution to acid mine drainage generation.

3.2 Cover Simulation Columns

3.2.1 Design and Construction

The effectiveness of the of the three-layer cover in reducing or preventing tailings oxidation was investigated by comparing covered tailings to uncovered tailings in laboratory columns. The cover design and soils used in the simulation columns were the same as those used in the field test plots and the drainage column: a coarse sand followed by a compacted clay layer and, finally, a fine sand layer on top. Tailings used in the evaluation were recovered from the unoxidized zone of the south end section of the Waite Amulet impoundment. These tailings are rich in sulphides, consisting predominantly of pyrite, pyrrhotite, chalcopyrite and marmite. The pyrite and pyrrhotite contents are 15% and 6%, respectively. The sulphur content is about 10% and the grain size distribution of the tailings indicate a sandy silt with some clay size materials.

The columns used in the evaluation consisted of square plexiglass columns (28 cm per side) of 105 cm length. The top 15 cm of each column had a larger area (39 cm per side) and were provided with holes along the perimeter. Four such columns were fabricated (Figure 3.9) and installed with soil and tailings materials as follows: (i) 2 identical columns packed with 45 cm of unoxidized tailings overlain sequentially with 15 cm coarse sand, 30 cm clay and 15 cm fine sand; and (ii) 2 identical columns packed with 90 cm thick unoxidized tailings. The upper fine sand filled the top 15 cm of the column with the larger area so that the fine sand/clay interface nearly coincided with the perimeter holes. A 4 mm thick woven geotextile underdrain was installed below the tailings in each of the columns.

The tailings and sands were packed to a bulk density of about 1.9 Mg/m^3. Both the coarse and fine sand were placed at residual saturation which corresponded to a volumetric water content of approximately 8%. The clay was compacted at 93% modified Proctor compaction and a water content 2% higher than optimum in a mould especially designed for this purpose. The compaction corresponded to a density of 1.53 Mg/m^3 and a water content of 26%. These compaction parameters were the same as those specified for the field covers. From these design parameters, it was estimated that the clay layer would have a degree of saturation of about 95% and a hydraulic conductivity of less than 1.0×10^{-7} cm/s, which would reduce the total infiltration by more than 50%.

Each column was instrumented to measure gaseous oxygen concentrations in the soil voids, soil moisture content, and temperature. For the installation of oxygen ports, holes of 6 mm diameter were drilled at specific points along the column prior to packing the materials. Each oxygen port consisted of a 3.2 mm diameter, 140 mm long polypropylene tube with a plastic connector which held a rubber septum for automatic sealing after sampling. The end of the tube inside the soil or tailings was slotted and wrapped with fine woven geotextile to prevent clogging. The oxygen ports were installed during the packing of the columns. The ports were sampled by means of a percent oxygen analyzer (Teledyne Model 340 FBS) with a hand-held sampling trigger and a syringe needle. The method for

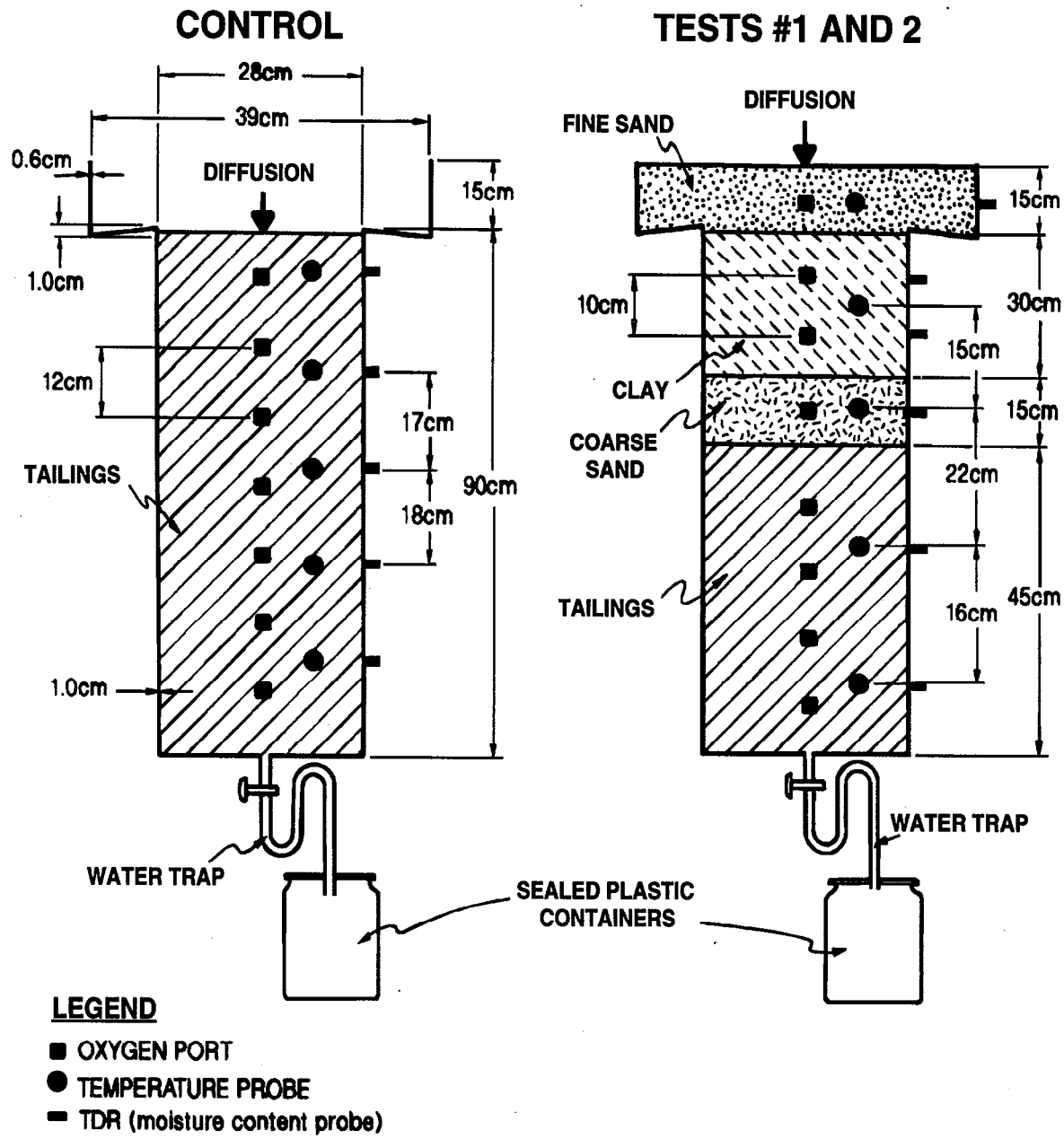

Figure 3.9: Cover Simulation Columns

measuring oxygen concentration consisted of pulling the trigger to empty the chamber, inserting the needle through the septum then releasing the trigger to fill the chamber and read the oxygen concentration directly from an attached analog display. The analyzer was calibrated to the atmosphere before each sampling and between various sampling points.

Moisture content was determined by time domain reflectometry (TDR) using the same method as was described in Section 3.1.1. Temperature was determined with two types of sensors: type J thermocouples and Resistance Temperature Device (RTD) sensors. Two columns were fitted with thermocouples (one Test and one Control Column) and the other two columns (also one Test and one Control) with RTD. This allowed a comparison of the two methods. Laboratory air temperature, relative humidity and the rate of evaporation from a water-filled container were monitored during the experiment.

Rainfall and snow-melt were simulated by means of square plastic containers (28 cm per side) with 1 mm diameter holes in the bottom. The containers were placed on top of the columns and water was added at a rate similar to that of the Waite Amulet tailings site. At the base of the columns, U-shaped flexible polyethylene tubes were installed and connected to plastic collection vessels. These vessels collected any water draining through the columns. Drainage water collected from the two Control Columns (without covers) was divided into two samples. The first sample was preserved with concentrated HCl for metal and major cation analysis by inductively-coupled plasma (ICP) techniques. The second sample was used for physico-chemical analysis and $[SO_4^{2-}]$ determination. The Test Columns (with covers) did not produce any drainage water because the clay layer essentially prevented infiltration.

To have a basis for comparison between the Control and Test Columns, it was essential that infiltration did occur and the drainage water be analyzed. It was also important to verify whether the clay would lose any moisture as the underlying sand and tailings drained to residual water content. For these reasons, holes were drilled into the columns beneath the clay layer, and water was poured through the tailings and preserved for analysis. This "flushing" of the tailings layer was done periodically and the acidity removed was measured.

One other comparison that could be made to measure the extent of oxidation was the colour of the tailings: dark grey tailings are fresh or unoxidized, whereas red or yellow tailings are oxidized. Thus the use of clear plexiglass columns allowed oxidizing spots to be seen through the walls. Soon after the columns had been installed, oxidation of tailings close to some of the sampling ports and in the corner of the columns for Tests #1 and #2 occurred. This was evident from the reddish yellow colorations observed at these locations. It was obvious that oxygen had entered the covered tailings in the columns by the sides of the sampling ports and through the corners. Two new Test Columns (Tests #3 and #4) were subsequently installed, approximately 200 days after the first set was constructed. These new columns were fabricated from one piece of clear plexiglass that minimized the number of glued corners. In addition, the number of sampling ports were reduced from 19 to 3 and packing was rigorously controlled to minimize pre-oxidation of

the tailings. The tailings were saturated immediately after placement in the columns and the coarse sand layer was purged with nitrogen to remove oxygen in the pores before the clay was placed over top.

As shown in Figure 3.10, an oxygen sampling port was placed in the coarse sand underlying the clay so that the oxygen flux through the clay could be determined. Two TDR probes were placed in the clay to monitor the water content and hence the state of saturation of the clay.

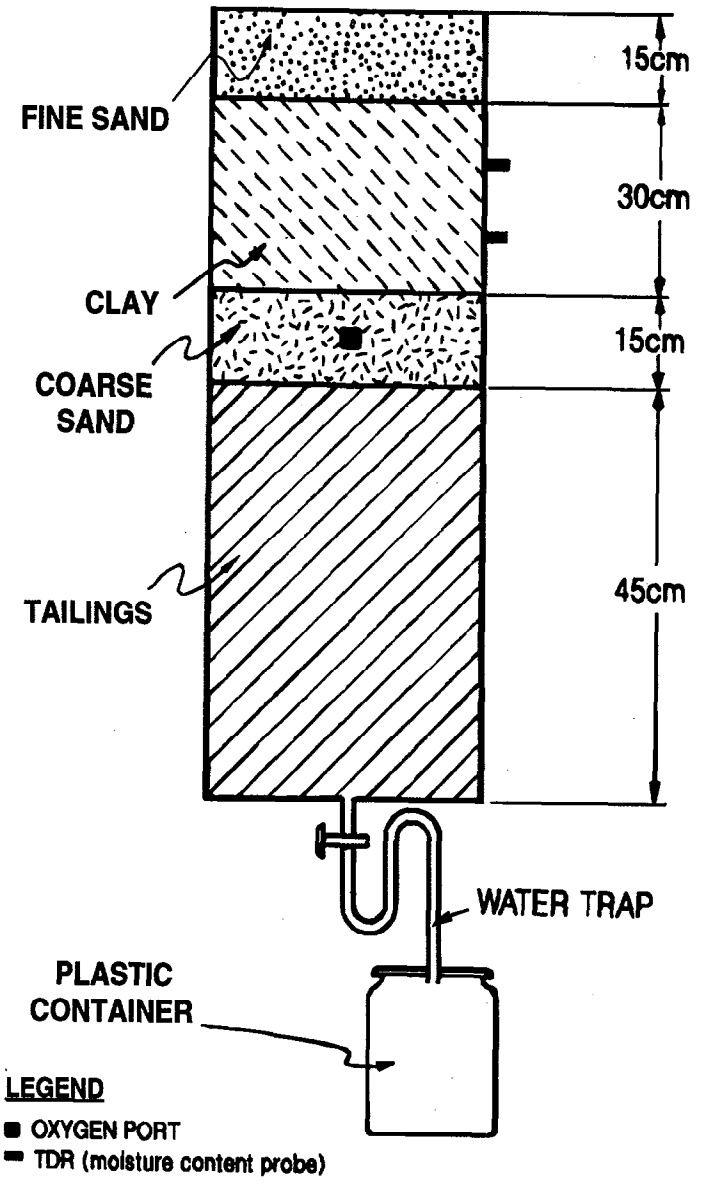

Figure 3.10: Test Columns 3 and 4

3.2.2 Simulation Columns Results

Oxygen

The resulting oxygen concentrations for the Control Columns are plotted against time in Figure 3.11. For the 7 cm depth, oxygen concentrations ranged from 19% to below 1%. The lower average concentration in the first 100 days can be attributed to oxygen consumption by tailings oxidation. After the 100th day, the dips in the graph would represent times where water was added and soil pores were saturated. Unfortunately, it was not possible to obtain accurate readings from the top port in Control #2 beyond 100 days, but there is otherwise very good agreement between the two columns. At 19 cm depth, high oxygen concentrations were measured during extended periods without water addition. Two such peaks were observed around day 440 and 600. At 31 cm depth, the oxygen concentrations remained essentially below 1% until approximately 550 to 590 days when the upper tailings layers were sufficiently oxidized to permit some oxygen to diffuse down to this level. Concentrations above 1% were never measured below the 42 cm depth, even when concentrations exceeding 12% were measured at a depth of 19 cm.

The gradual oxidation and the subsequent increase in oxygen transport is demonstrated by these profiles. In the first 300 days, the oxygen concentration at the 19 cm depth never reached 3%. Beyond that point, the oxygen concentration increases gradually to above 7.5% after an additional 140 days (near day 440). Water was added at that time and the oxygen concentration decreased considerably. Following this wetting, the columns were left to dry again and the increase in oxygen concentration was repeated. The interesting effect to point out here, is that the slope of the concentration-time graph is considerably steeper in the second dry period, therefore suggesting that less oxygen was being consumed in the upper layers of the tailings column during this drought. It is conceivable that the surface tailings were completely oxidized by the 600th day and that all oxygen entering the system diffuses into the lower layers (beyond 7 cm) to oxidize fresh or partly oxidized material. This hypothesis was supported by visual examination of the tailings in the columns. The tailings in the upper 30 cm were a yellowish colour, below this a colour gradient to red, and then a characteristic dark grey colour of fresh Waite Amulet tailings.

In the Test Columns, the oxygen concentration in the fine sand at the surface remained essentially constant near atmospheric value (20.9%). The profiles for the Test Columns (Figure 3.12) are similar to those of the controls but the decrease in oxygen concentration in the top layers is attributed to the low diffusion of oxygen through the clay as opposed to oxygen consumption. The rise and fall of the oxygen concentration in the clay coincide with the initiation of wetting and drying cycles. The steady increase in oxygen concentration in the clay, following the initiation of a drying cycle, could be interpreted to be the result of moisture loss in the clay and the consequent increase in the rate of oxygen diffusion. The moisture content data, presented previously, indicated, however, that the clay did not lose a significant amount of moisture. An alternate and correct interpretation is the time-dependent diffusion of gaseous oxygen in the clay layer. If the oxygen

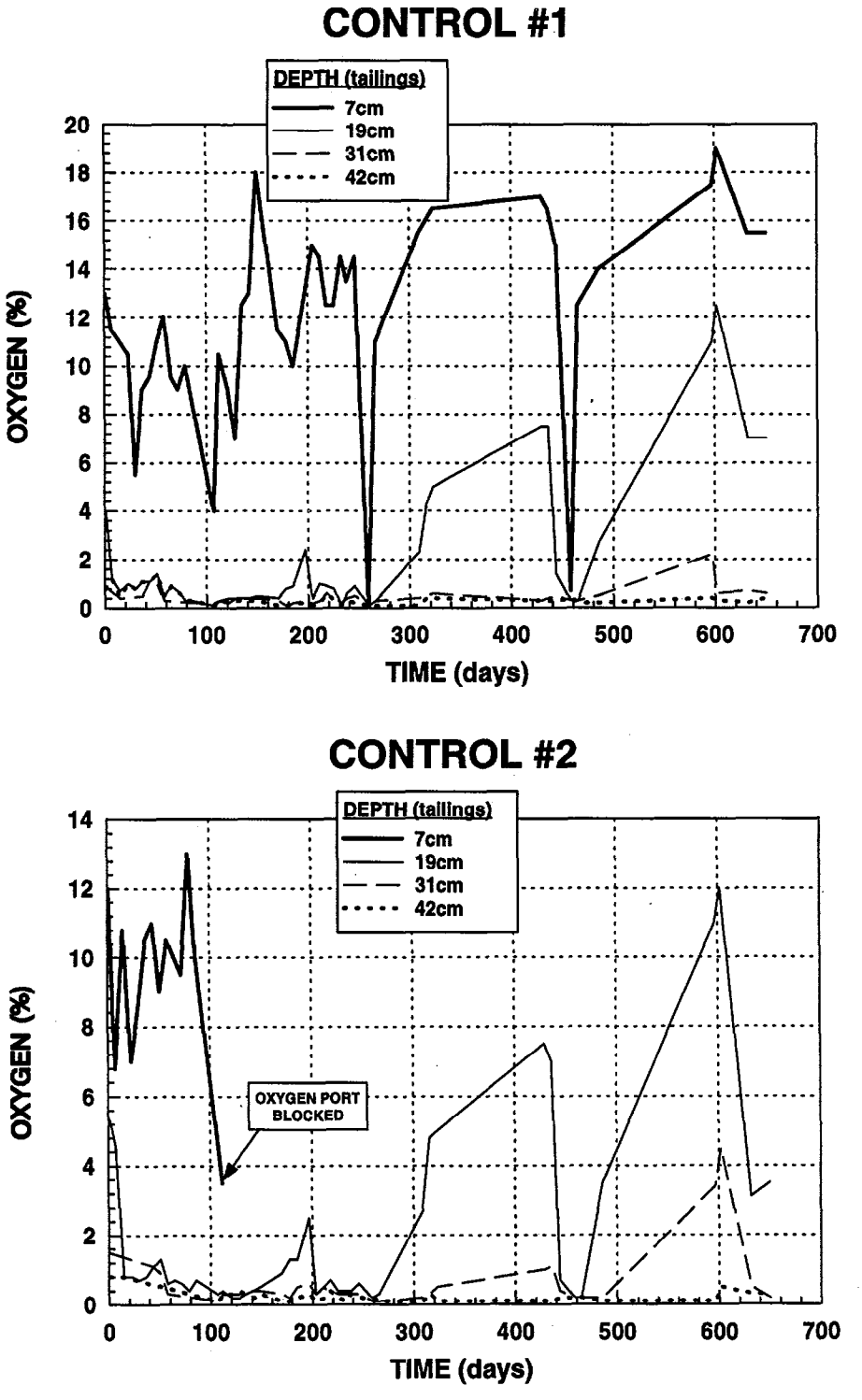

Figure 3.11: Oxygen Measurements from Control Columns

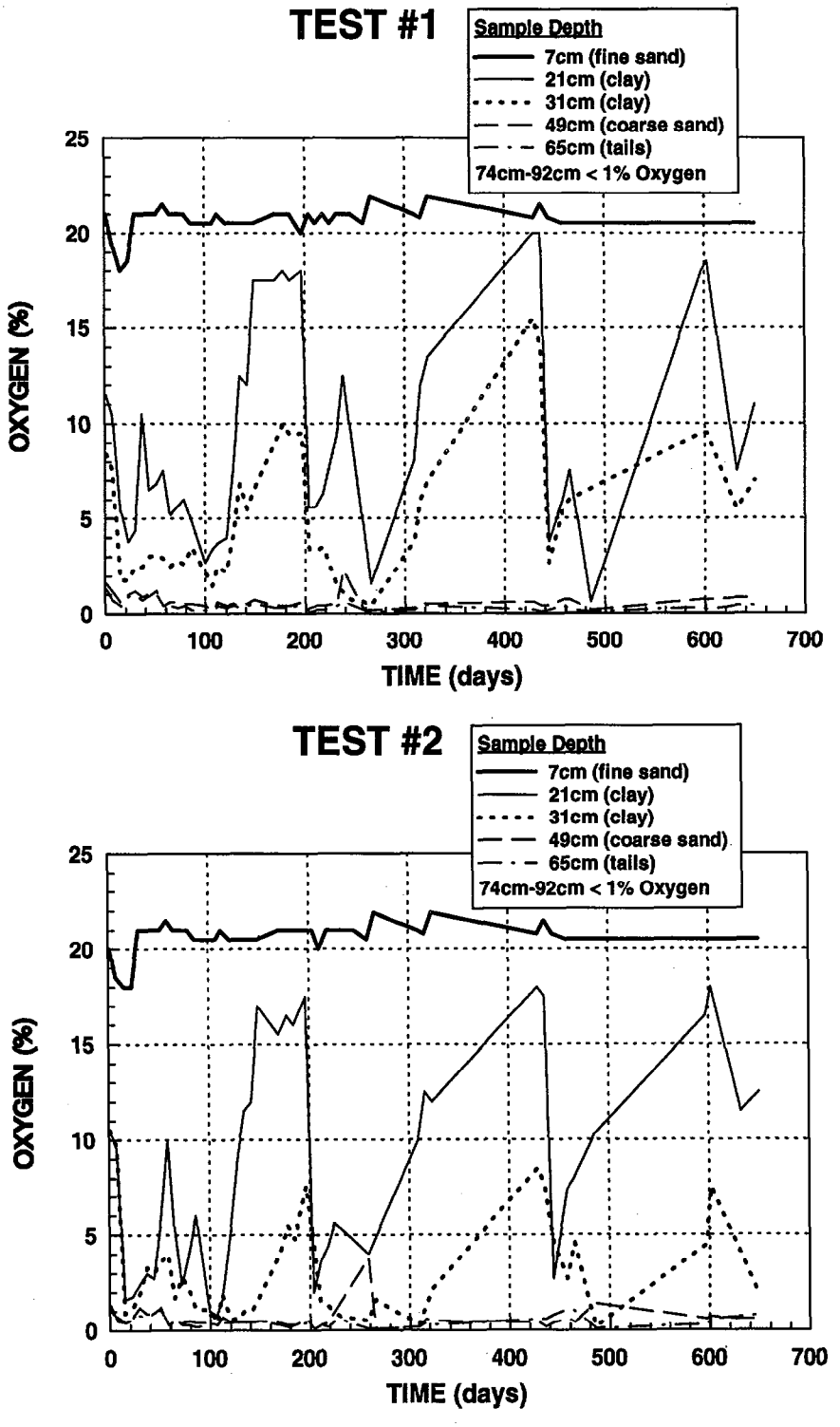

Figure 3.12: Oxygen Measurements from Test Columns

concentration directly above the clay is near atmospheric, a high concentration front is formed which gradually moves down into the clay by diffusion until steady state is attained. When water is added to the column (rain simulation), a thin layer of water may pond on top of the clay and cut off the oxygen supply. At this point, the oxygen left in the clay will diffuse toward the tailings where it will be depleted. This would then leave the oxygen concentrations in the clay to approach zero if the rain continued (or the ponding is sustained). As the water on the surface of the clay evaporates, the oxygen concentration on its surface rises again and the cycle repeats itself. Yanful (1993) modelled the oxygen concentrations in the clay during the dry period between 130 and 195 days to illustrate this phenomenon.

Figure 3.13 presents the oxygen concentrations measured in Test Columns #3 and #4. The results from Test Column #4 agree very well with Test Columns #1 and #2, where the oxygen concentration in the coarse sand is, on average, below 1%. As previously mentioned, the oxygen sampling port in the coarse sand is the only port in Columns #3 and #4. The rather high oxygen concentration (~ 6% to 15%) observed in Test #3 was probably a measurement error since no oxidation occurred in the tailings (based on the persistent dark grey colour). If the oxygen concentration in the coarse sand were actually as high as the measurements suggested, a considerable flux of oxygen would have resulted across the clay which would have initiated oxidation in the underlying tailings. Water quality data presented later in this report clearly confirm that the oxidation of the tailings was minimal and the acid generation insignificant. It was therefore concluded that the oxygen sampling port in Test Column #3 was defective. The defect could have been caused by a plugged tube inside the soil which, when sampled, would create a vacuum inside the tube and cause atmospheric gas to leak through the septum beside the needle.

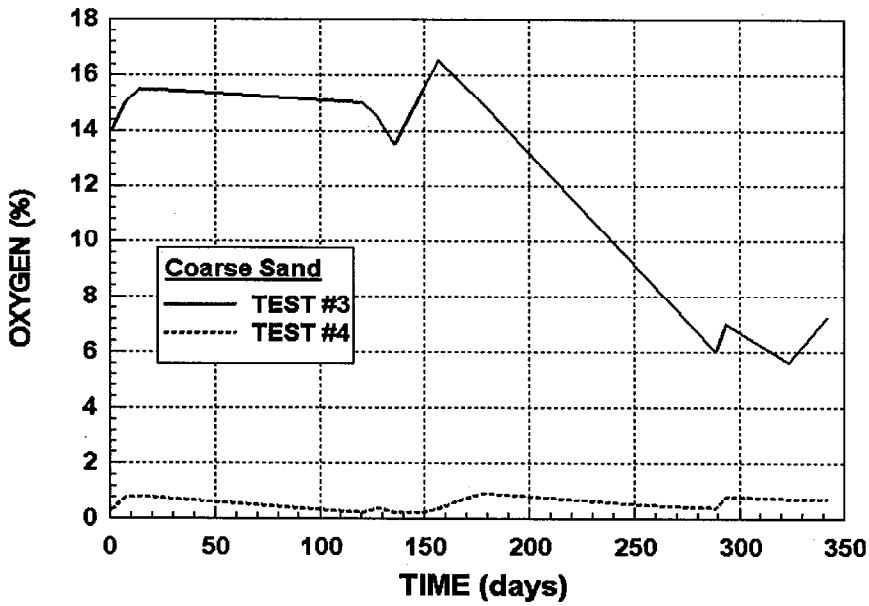

Figure 3.13: Oxygen Measurements from Test Columns 3 and 4

Water Contents

The water content data obtained in the control uncovered tailings are displayed in Figure 3.14. The saturated volumetric water content (total porosity) of the tailings is ~50%. The TDR readings often exceeded this value especially in the lower three probes. As mentioned previously, this discrepancy is believed to be the result of the high ionic strength of the pore water as the tailings oxidize. At high measured acidities, TDR waves were found to be poorly developed and difficult to interpret and may have resulted in unusually high water contents. The pore water near the top of the column, where the tailings were well-drained, was low in dissolved salts content. Much better TDR waves, and therefore more reliable water contents, were obtained at these depths.

The water content profiles in the Control Column indicate that the water content of the surface tailings was highly dependent on rainfall and that the deeper tailings were essentially saturated throughout the experiment.

The water contents for Test Columns #1 and #2 are displayed in Figure 3.15. As indicated, the water content of the fine sand layer is highly dependent on rainfall event while that of the clay remains constant at near-saturation ($\geq$ 95%). The coarse sand below the clay stays essentially dry except when the columns were flushed to measure acidity (peaks near 90, 110 and 240 days). The tailings below the coarse sand layer remained at a constant water content of 30% to 35% until the first column flush (90 days) when it became saturated and remained so to the end of the experiment. These data confirm the effectiveness of the upper sand as an evaporation barrier that prevents the clay from losing moisture by evaporation. The bottom sand attains residual water content and prevents the clay from draining by gravity, illustrating its efficiency as a capillary barrier (Nicholson *et al.*, 1989). The water content data in the two Test Columns are very similar and therefore confirm the reliability of these results. The water contents of the clay observed in Test Columns #3 and #4 (Figure 3.16a) indicate near-saturation conditions, as was observed in Test Columns #1 and #2.

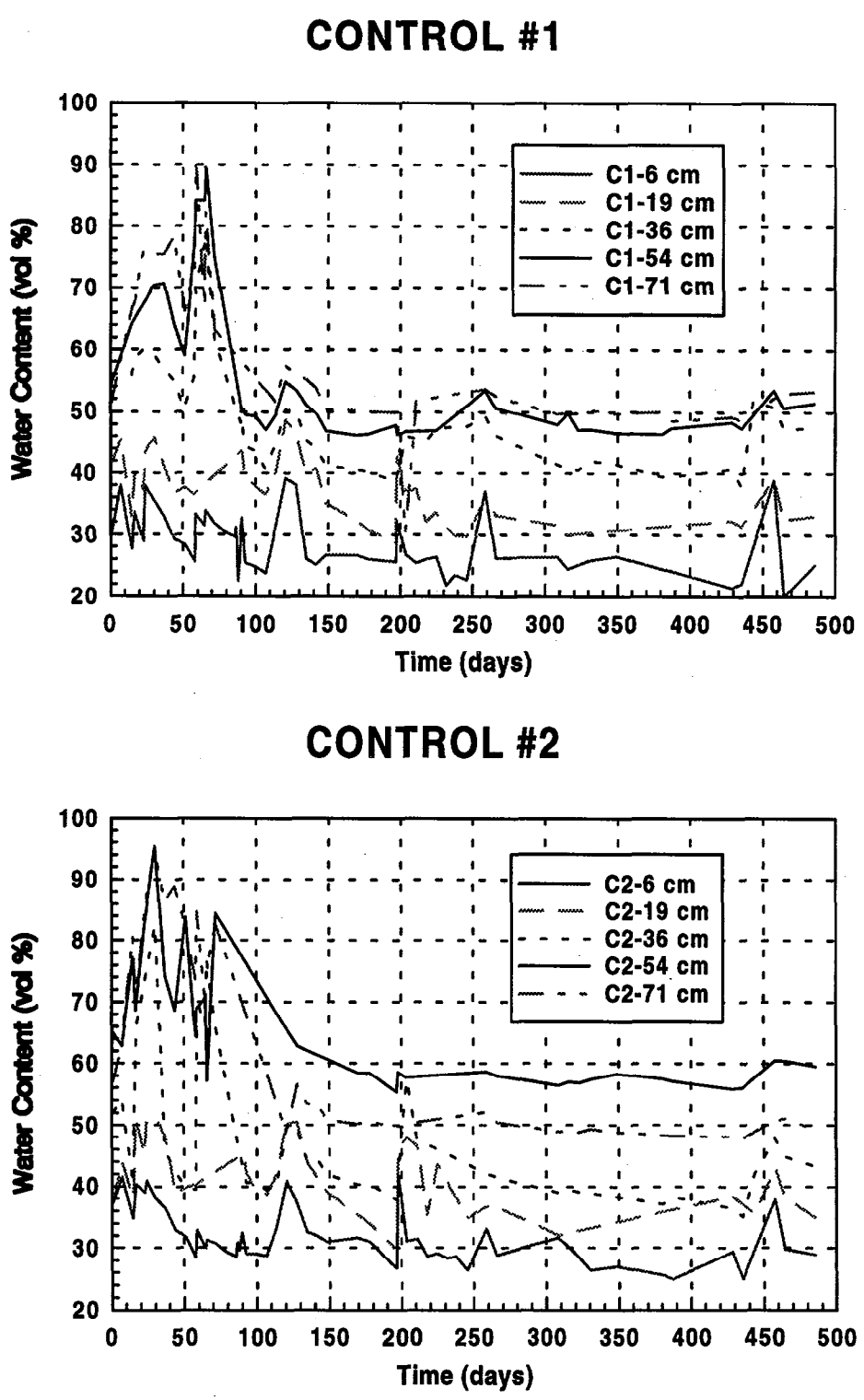

Figure 3.14: Water Contents Measured in Control Columns

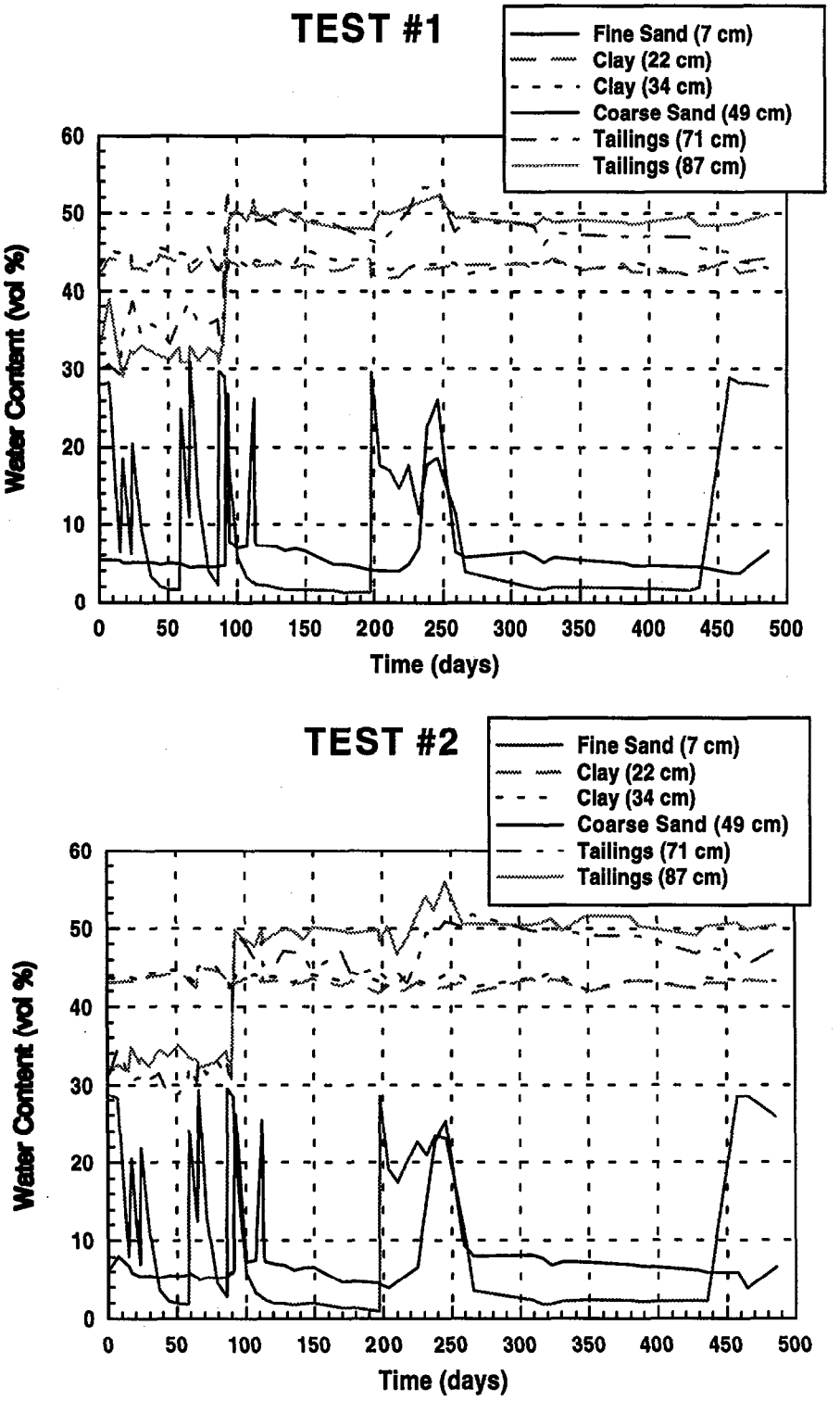

Figure 3.15: Water Contents Measured in Test Columns

The accuracy of the TDR data from Test Column #1 was verified by comparing to gravimetric measurements. After a prolonged dry period, water contents were measured by TDR. Holes were then drilled through the column to recover samples of cover materials and tailings for moisture content determination. This was done at 23 locations along the column including every 2 cm in the clay layer. Rain was then applied and the materials were immediately sampled for water content measurements, while the fine sand on top was still wet. Figure 3.16b compares the volumetric water contents (TDR) obtained at the two different times, as well as those obtained gravimetrically. As expected, the volumetric water content at each depth is higher than the corresponding gravimetric value. The volumetric and gravimetric water content measurements before and after rain are essentially the same. The small differences observed in the clay layer are within acceptable experimental error. These data do confirm that, even during prolonged dry periods, the clay did not lose a significant amount of moisture.

The average water contents in both the Control and the Test Columns are displayed in Figure 3.17a. The high water contents (above 50%) reported for the Control Columns were affected by the high ionic strength of the oxidized tailings pore water, as was previously discussed. The average water content for the Test Columns (Figure 3.17b) indicate excellent agreement between the columns. The Test Column water contents are considered to be accurate in the cover soils and probably only slightly high in the unoxidized covered tailings since the ionic strength of the pore water is low.

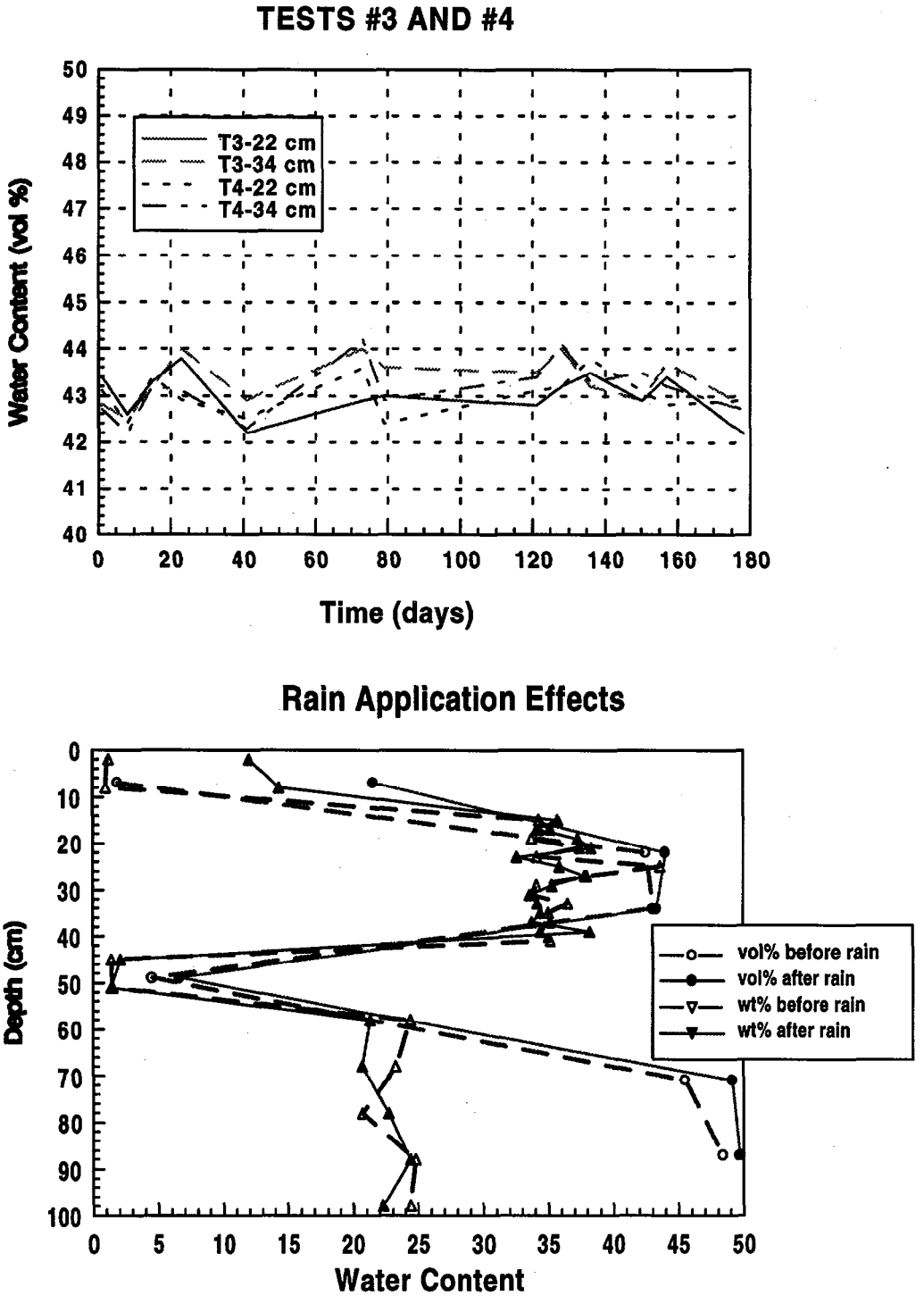

Figure 3.16: Water Contents Measured in Test Columns and Effects of Rain Application on Cover

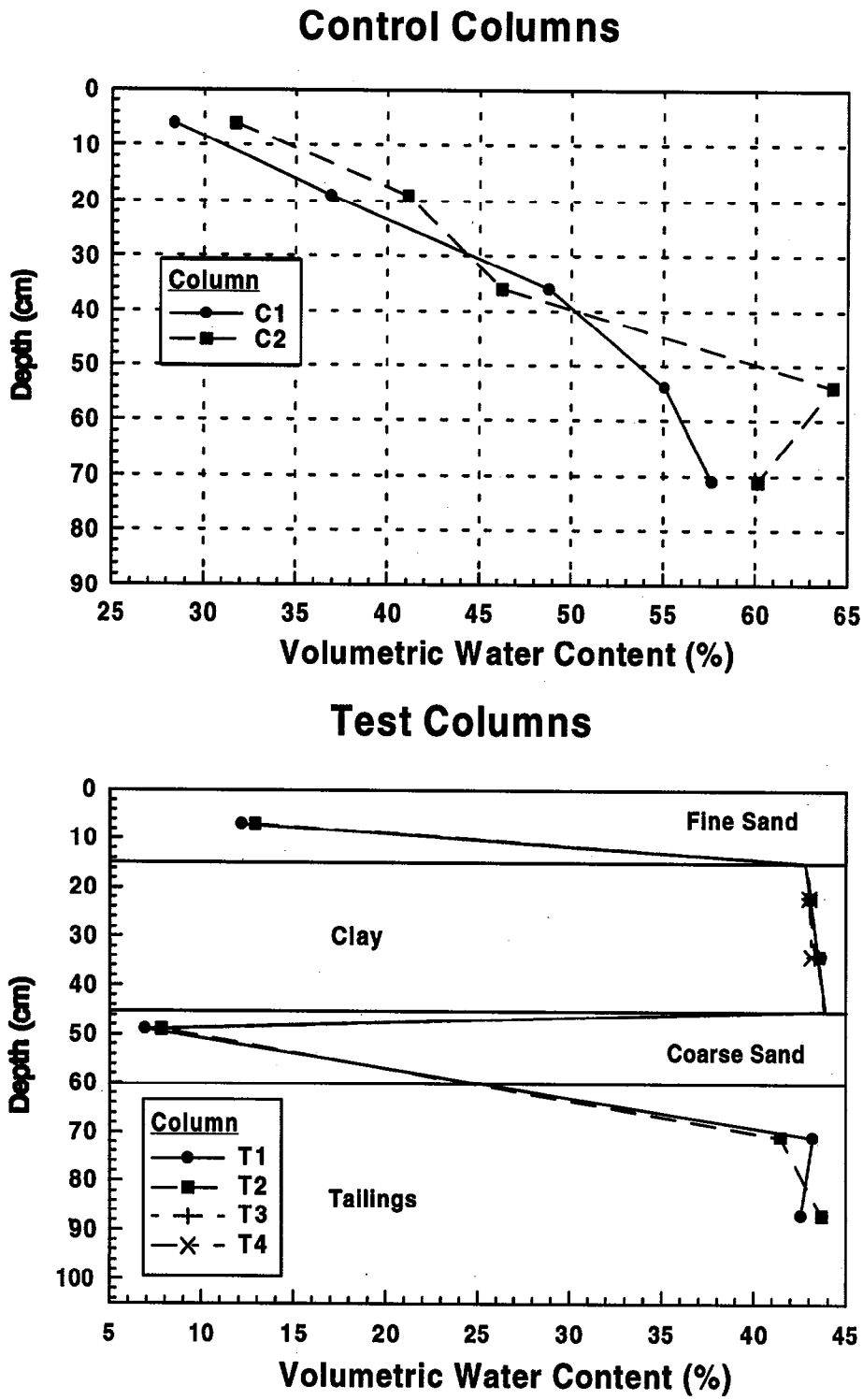

Figure 3.17: Average Water Contents

Drainage Water Quality

Iron and sulphate concentrations were measured regularly during the first year of the experiment. This was subsequently discontinued as it became evident that their concentrations follow the same trend as acidity. Total acidity measures the total concentration of species in solution capable of consuming alkaline materials. It is determined by titrating to pH 8.3 (Standard Methods, 1975). Total acidity was used as an indication of the water quality throughout the duration of the experiment.

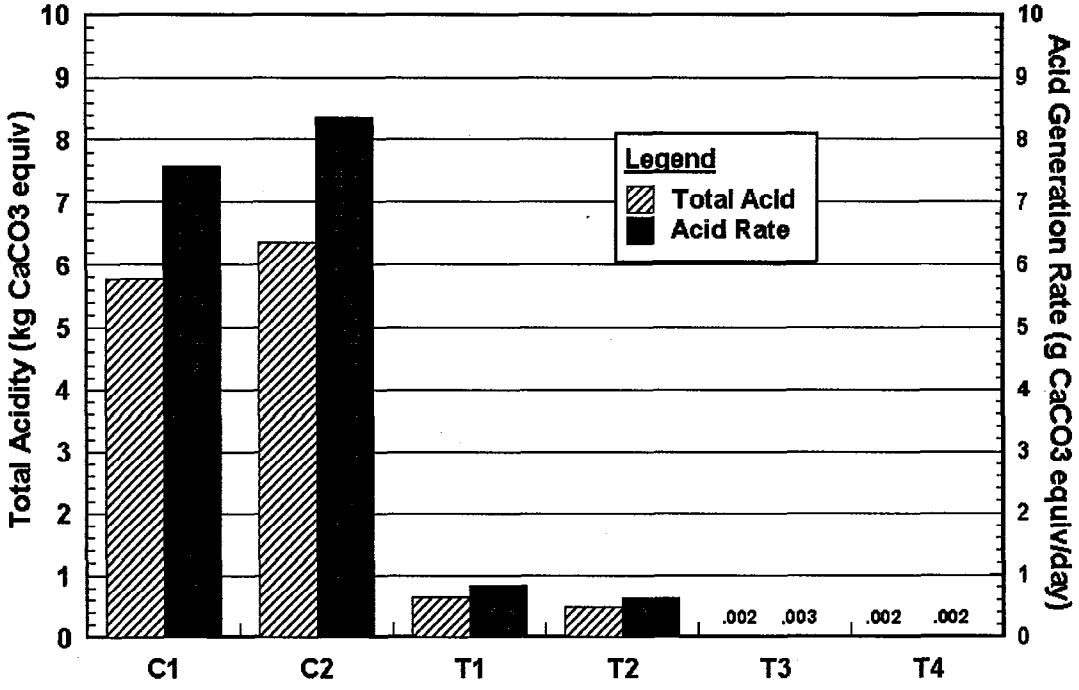

Figure 3.18: Total Acidity and Acid Production Rate in all Columns

The acidity produced by each column was quantified and the results are displayed in Figure 3.18. The total acidity was determined by measuring the g $CaCO_3$ equivalent/L of each volume of water that drained through the columns and multiplying that concentration by the respective volume. For the Control Columns, this includes both simulated rain and flush water. For the Test Columns, only flush water was measured since the simulated rain water did not permeate through the clay (what is predominantly reported as run-off). Test Columns #3 and #4 were flushed only twice and were started ~200 days after the other four columns had been operating. The total acidity produced (kg $CaCO_3$ equiv) in Tests #3 and #4 cannot, therefore, be compared with those produced in the other columns. The acid flux (g $CaCO_3$ equiv/day) is, however, comparable.

Close examination of Figure 3.18 reveals that a significant decrease in acid generation occurred in the covered tailings. The measured average decreases in acid flux were 90.87% for Tests #1 and #2 and ~99.9% for Tests #3 and #4. As expected, the reduction of the number of sampling ports and more stringent quality control methods adopted in Tests #3 and #4 minimized oxidation and acid production induced by test artifacts. This would account for the difference in the acidities between the two sets of Test Columns.

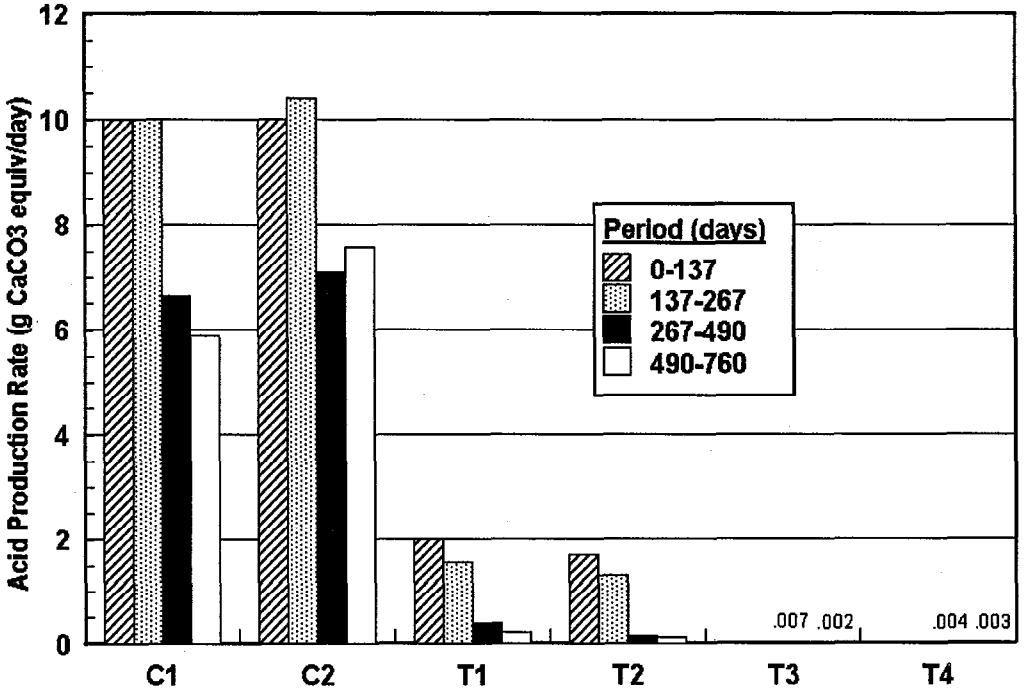

Figure 3.19: Acid Production Rate per Period

In Figure 3.19, the acid flux is presented for the four periods during which the columns were flushed. Such a representation permits examination of changes in acid generation over time. The acid flux was calculated by dividing the total acidity by the number of days the column was monitored per square centimeter. The acid flux data indicate that the rate of oxidation for the Control and Test Columns decreased with time. The average decrease was approximately 33% for the controls and 90% for the tests (Figure 3.20). This may be explained as follows. At time zero, there is a high oxygen availability (20.9%) for the surface tailings; these surface tailings will therefore oxidize quickly, and inert solid oxidation products will result. For the oxidation to continue in the deeper or surrounding tailings, the oxygen must diffuse through the inert solids on the surface. This process limits oxygen availability. This reasoning could apply either to surface tailings in contact with air in the Control Columns or to covered tailings in contact with air that leaked from the ports in the Test Columns.

The oxidation rate calculated for the uncovered tailings was around 10 mg of $CaCO_3$/day/cm^2. This oxidation rate cannot be related to field oxidation rates since the laboratory conditions were almost optimal for microbial activity (22°C). However, the laboratory results provide an estimate of the maximum acid flux generated by a tailings with similar mineralogy.

Another event which may have affected the rate of oxidation is the water content. The volumetric water content of the tailings in Test Columns #1 and #2 fluctuated from approximately 30% to 35% until the first flush when it increased to near saturation (50%). The increase in water content would decrease the flux of oxygen, and hence the rate of acid generation. This effect is not considered to be the primary cause of the decrease in oxidation rate, though, since the sharp increase in water content occurred near 90 days (Figure 3.15) whereas the significant decrease in the oxidation rate occurred after 267 days (Figure 3.19). It is interesting to note that the rate of oxidation remained relatively constant beyond 267 days. This suggests that the flux of oxygen through the sampling ports was decreasing very slowly at this point.

For Test Columns #3 and #4, no significant amount of acidity was produced. The flux that occurred in the 267-490 day period for these columns should be compared to that of the 0-137 day period for the other four columns. In this case, the three-layer composite soil covers show a nearly 100% efficiency. There was a small decrease in acid production in the second period. This could mean that, even though strict precautions were taken when packing the columns, some oxygen may have been trapped in the pores of the soils or the tailings prior to the commencement of the experiments.

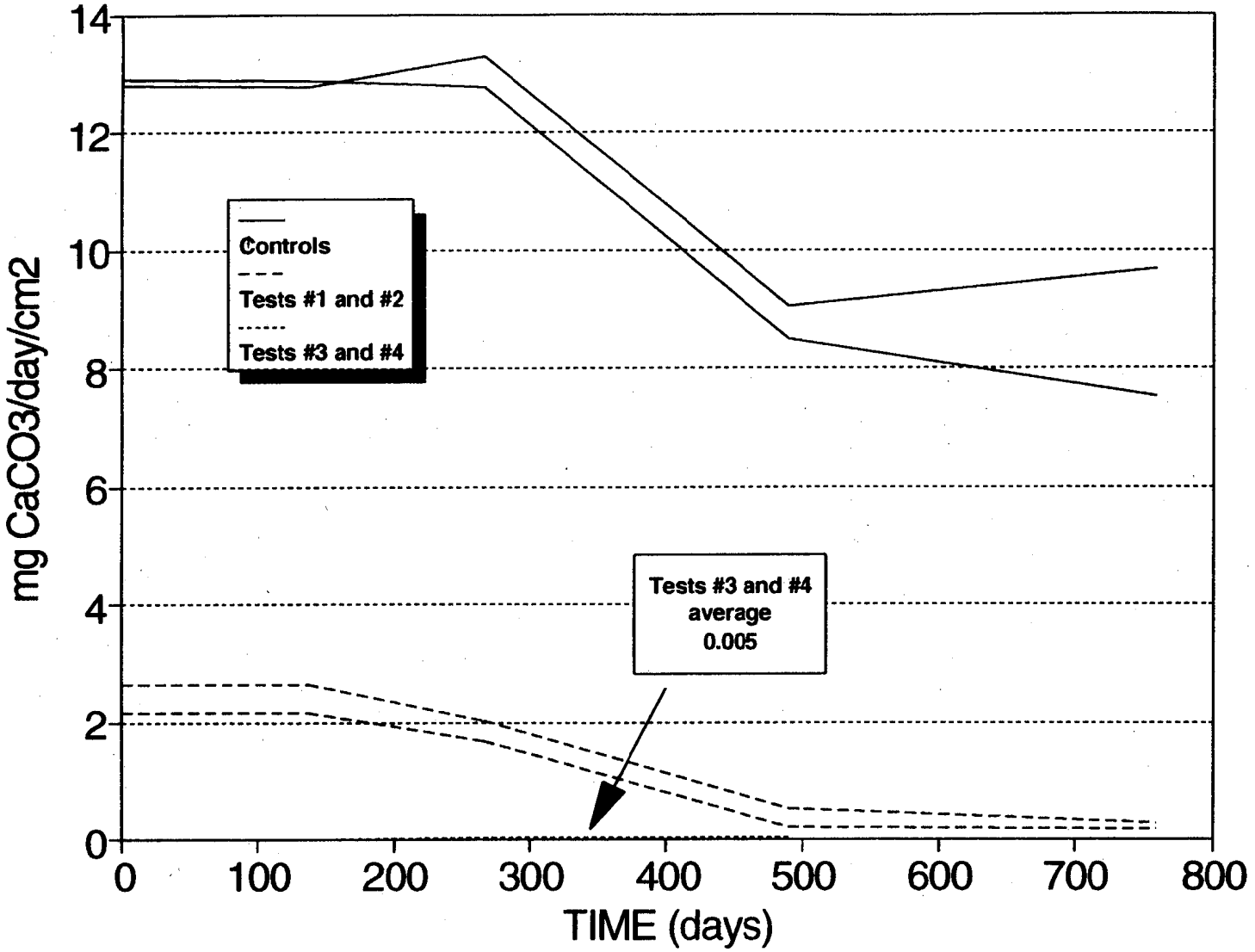

Figure 3.20: Variation of Acid Flux with Time in Control and Test Columns

3.2.3 Post-testing Geochemistry and Mineralogy

Tailings and Pore Water Examination

The laboratory simulation of the three-layer cover system was terminated after 760 days of monitoring. At the end of this period, Control Columns #1 and #2 and Test Columns #2 and #4 were dismantled. Tailings samples (approximately 2 kg) from Control Columns #1 and #2 were taken at depths of 5, 15, 25, 35, 50 and 75 cm and from Test Columns #2 and #4 at depths of 5, 15, 25 and 37 cm (depth below tailings surface). The tailings samples were stored at 7°C, sub-samples were then selected for density measurements, pore water analysis, water leach tests and bacteria count.

Oxygen

Figure 3.21 shows profiles of oxygen concentrations during each dry period, averaged for the two control columns. The data indicate that gaseous oxygen is penetrating the tailings deeper and deeper as oxidation, flushing and drying continued. This suggests that oxygen rapidly entered the tailings by diffusion, once the active sulphide minerals were depleted by oxidation. The oxygen concentration at 31 cm reached 2% after 600 days, suggesting that the surface tailings (above 30 cm) were probably completely oxidized by this time and were, therefore, not consuming any oxygen.

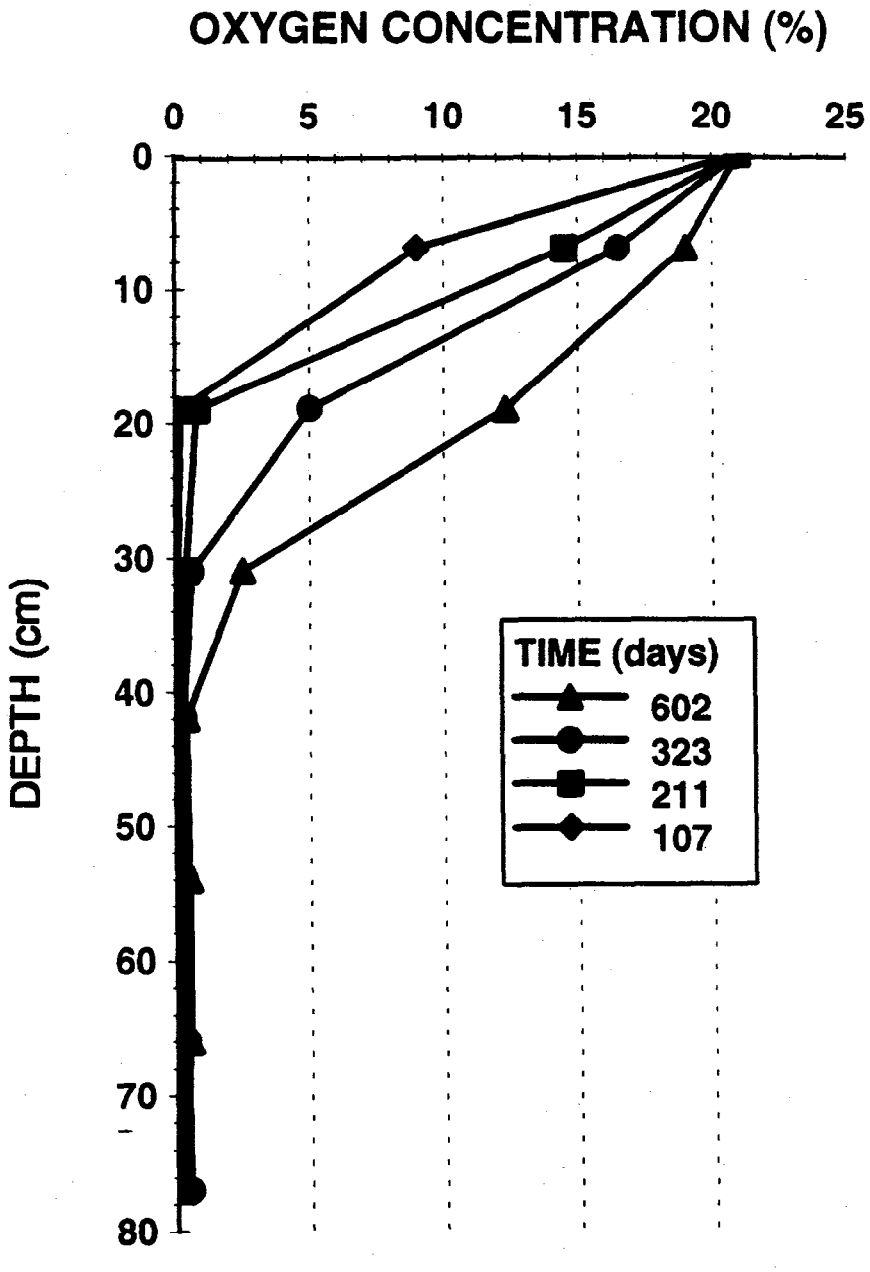

Figure 3.21: Gaseous Oxygen Profiles during Dry Periods

Density, Specific Gravity and Water Content

The density profiles are presented in Figure 3.22a. The data from Tests #2 and #4 are relatively constant, ranging between 2.0 and 2.2 Mg/m^3. These results indicate very little change in composition of the tailings and hence minimal oxidation, as shown by the acid production data. For the controls, the density of the tailings from surface to a depth of 25 cm was constant at 1.5 Mg/m^3, i.e. 25% lower than the original packed fresh tailings. From a depth of 25 cm, the density increased to 1.9 Mg/m^3 at 40 cm. Such a profile suggests depletion of sulphide minerals in the upper 25 cm due to oxidation. Leaching of the oxidation products will result in lower density. The density data are corroborated by the specific gravity profile also shown in Figure 3.22a.

The profiles in the uncovered tailings agree with the oxygen profiles discussed previously.

Volumetric (by TDR) and gravimetric water contents obtained from the Control Column (uncovered tailings) at the end of 760 days are presented in Figure 3.22b. The volumetric data suggest slight drying of the tailings in the upper 15 cm while the gravimetric data indicate the presence of slightly drier tailings in the bottom 50 cm. This apparent discrepancy can be explained by the density profile (Figure 3.22a). Assuming the density of water is 1.0 Mg/m^3 and air is weightless, the volumetric water content (θ_w) can be related to the gravimetric water content (w_n) and the total or bulk density (ρ_b) as follows:

$$\theta_w = [\frac{w_n}{1+w_n}]\rho_b \qquad [3.11]$$

This equation underscores the influence of density on the volumetric water content—higher densities observed in the bottom tailings would result in higher volumetric water content. The equation can be used to convert gravimetric water contents to volumetric values for comparison to TDR data.

The porosity profile has a similar shape to the gravimetric water content profile and indicates the presence of a slightly higher proportion of voids in the upper part of the tailings column (0-30 cm) where sulphide minerals are presumably depleted.

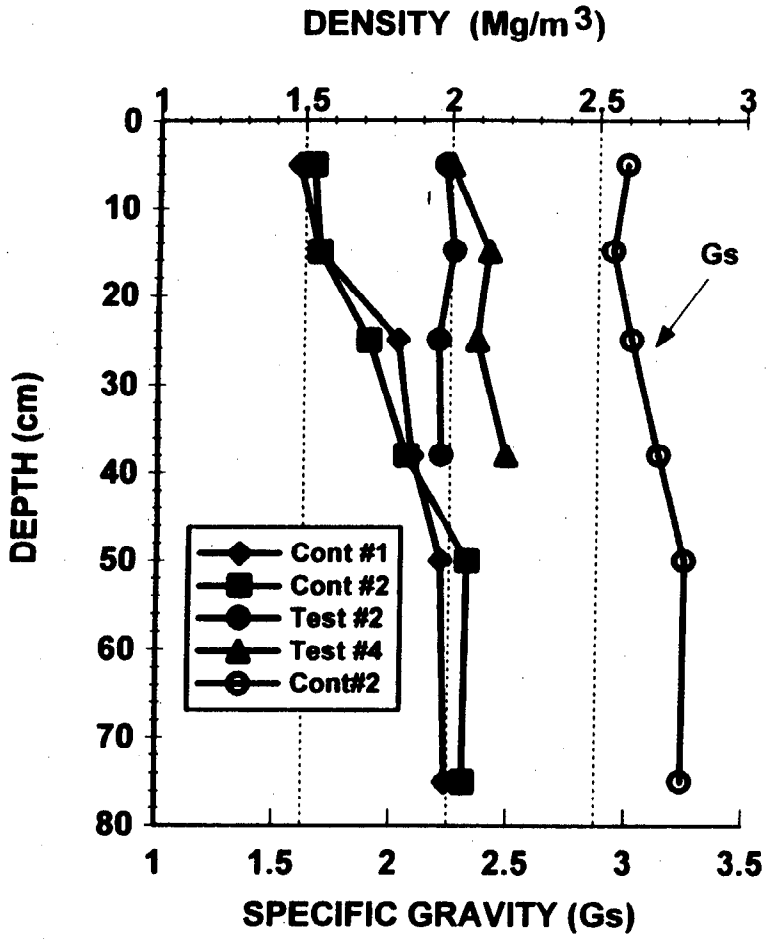

Figure 3.22a

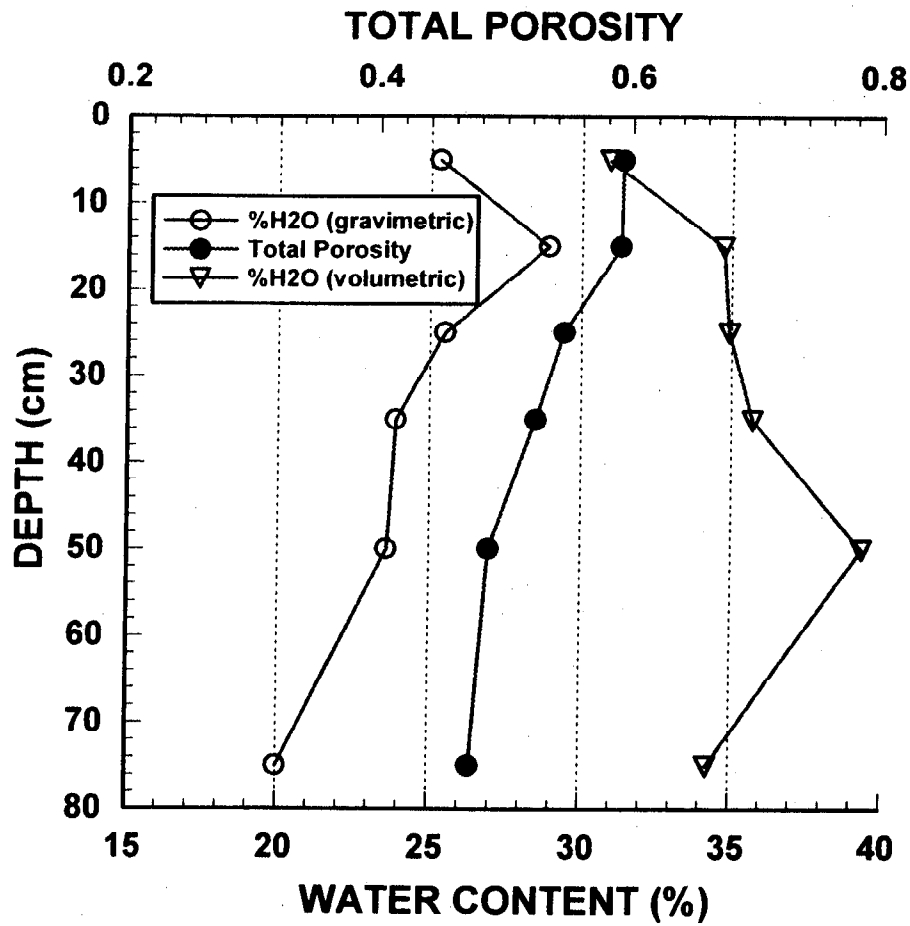

Figure 3.22b

Density, Specific Gravity, Porosity and Water Content Profiles after 760 Days

Pore Water Quality

Pore water samples were extracted (by squeezing) from approximately 200 g of tailings and analyzed for pH and for metals and sulphur by ICP method. Total dissolved iron concentration is presented in Figure 3.23. The results clearly show that iron concentrations in Controls #1 and #2 ranging between 1 and 15 g/L are more than 100 times higher than iron concentrations in Test #4, once again, confirming the efficiency of the soil covers. The oxidation front in the Control Columns is also well defined around 30 cm, with iron concentrations of 15 g/L compared to 5 g/L near the surface. The pore water iron concentration in Test #2 was around 1 g/L which is considerably higher than the concentration in Test #4. The increased iron concentration is due to the oxidation produced by test artifacts, as previously explained.

Water leach tests were also conducted on 50 g of tailings sub-samples to evaluate the presence of water soluble salts. The iron concentrations of pore water and wash water leach tests measured in the Control Columns are presented in Figure 11. There is similarity in the results between each method and both show parallel profiles of iron concentrations which means that there was no detectable quantity of water soluble iron-based oxidation products leached in this test.

The complete water quality data are presented in Tables 3-I through 3-IV. Two sets of data are presented for both squeezed and leach pore water. In general the pH is lower in the oxidized zone (0-30 cm) of the tailings profile than in the bottom layers. Sulphate, iron and other metal are all concentrated in the 25-35 cm zone where the oxygen profile suggests oxidation is active after 760 days. As expected, the pH is higher and metals and sulphate concentrations are lower in the covered tailings. Sulphate concentrations of ~2000 mg/L observed in the covered tailings were most likely derived from the original mill process water (Blowes and Jambor, 1990). The pH and sulphate data are also presented as profiles for both the uncovered (Control) and covered (Test) tailings in Figure 3.24. Metal profiles (Fe, Zn, Cu and Al), shown in Figure 3.25 indicate the same trend. These results support the oxygen and density data from which it was inferred that the zone of active oxidation is located at about 30 cm.

TABLE 3-I - ANALYTICAL RESULTS OF PORE WATER SAMPLES COLLECTED JANUARY 28, 1993

COLUMN CONT #1 28/01/93

DEPTH (cm)	pH	Fe mg/L	Fe+3 mg/L	Zn mg/L	Cu mg/L	Al mg/L	As mg/L	Cd mg/L	Pb mg/L	Se mg/L	Ca mg/L	K mg/L	Mg mg/L	Mn mg/L	Na mg/L	SO4 mg/L
5	1.55	5580	5880	12.7	69.39	1450	12.8	0.04	<0.25	1.36	365	<5.00	903	45.3	17.8	25920
15	1.7	5250	5480	18.5	148	1570	13.5	0.03	<0.25	1.22	520	<5.00	940	44.2	20.6	25800
25	1.8	16100	11350	150	308	3510	30	0.47	<0.25	3.25	521	<5.00	1800	72.1	12.3	57000
35	2.74	12600	5820	335	86.2	2000	19.1	1.27	<0.25	1.81	467	<5.00	708	35.6	16.9	34500
50	3.48	3320	3490	393	0.02	193	2.88	4.16	3.32	<0.50	479	23.3	62.4	6.91	18.9	8220
75	3.86	1070	201	73.6	0.02	18	0.56	0.08	2.06	<0.50	523	17.1	41.5	6.46	18.4	3450

COLUMN CONT #2 28/01/93

DEPTH (cm)	pH	Fe mg/L	Fe+3 mg/L	Zn mg/L	Cu mg/L	Al mg/L	As mg/L	Cd mg/L	Pb mg/L	Se mg/L	Ca mg/L	K mg/L	Mg mg/L	Mn mg/L	Na mg/L	SO4 mg/L
5	1.68	4500	4580	19.9	83.7	1600	13.3	0.63	<0.25	0.63	448	<5.00	956	47.76	17	24420
15	1.63	10400	7220	35.2	163	3000	25.1	0.12	<0.25	2.12	537	<5.00	1790	85.02	14.3	45900
25	3.77	2290	103	20.9	0.09	6740	1.14	0.28	0.48	0.65	535	28.7	44.9	5.55	24.1	6420
35	2.42	12700	5980	662	357	3990	32.4	4.02	<0.25	1.99	475	<5.00	1140	53.9	19	47100
50	3.6	1690	170	138	0.84	56.9	1.24	0.81	2.2	<0.50	503	17	57	5.68	22.8	4650
75	3.99	1580	4.67	32.6	<0.02	2.8	0.81	0.57	1.14	<0.50	545	28.3	39.9	5.85	23.7	4950

COLUMN TEST #2 28/01/93

DEPTH (cm)	pH	Fe mg/L	Fe+3 mg/L	Zn mg/L	Cu mg/L	Al mg/L	As mg/L	Cd mg/L	Pb mg/L	Se mg/L	Ca mg/L	K mg/L	Mg mg/L	Mn mg/L	Na mg/L	SO4 mg/L
5	3.94	1070	36.2	47.9	<0.02	16.9	0.61	<0.02	0.71	<0.50	102	19.4	27.3	7.92	13.6	2160
15	3.75	817	26.4	49.9	<0.02	14.6	0.44	0.04	0.83	<0.50	298	18.1	16.9	16.1	14.1	2190
25	3.81	670	19.2	46.2	<0.02	29	0.47	0.08	0.27	<0.50	569	18	10.3	4.65	13.2	2640
37	3.56	1030	32.7	186	<0.02	63.3	0.96	0.16	2.07	<0.50	546	22.9	20	24.6	13.9	3600

COLUMN TEST #4 28/01/93

DEPTH (cm)	pH	Fe mg/L	Fe+3 mg/L	Zn mg/L	Cu mg/L	Al mg/L	As mg/L	Cd mg/L	Pb mg/L	Se mg/L	Ca mg/L	K mg/L	Mg mg/L	Mn mg/L	Na mg/L	SO4 mg/L
5	5.3	18.4	2.66	5.84	<0.02	0.76	<0.25	<0.02	<0.25	<0.50	617	59.7	271	41	27.8	2670
15	5.61	19.2	5.8	18.8	0.75	4.5	<0.25	0.13	0.32	<0.50	626	96.8	589	104	63.8	4020
25	5.04	26.5	4.67	14.9	0.08	1.87	<0.25	0.04	<0.25	<0.50	581	62.4	273	45.5	26.8	2640
37	4.96	6.35	1.64	7.66	0.05	0.84	<0.25	<0.02	<0.25	<0.50	563	68	442	67.1	23.9	3240

TABLE 3-II - ANALYTICAL RESULTS OF PORE WATER SAMPLES COLLECTED FEBRUARY 8, 1993

COLUMN CONT #1 08/02/93

DEPTH (cm)	pH	Fe mg/L	Fe+3 mg/L	Zn mg/L	Cu mg/L	Al mg/L	As mg/L	Cd mg/L	Pb mg/L	Se mg/L	Ca mg/L	K mg/L	Mg mg/L	Mn mg/L	Na mg/L	SO4 mg/L
5	1.87	4970 i	3590	13.5	80.7	1300	11.2	0.04	<0.25	0.92	438	<5.00	830	42.9	18.1	22380
15	1.89	4150	4130	15.7	136	1300	10.7	0.03	<0.25	1.09	375	<5.00	770	37	22.4	21240
25	2.02	15800	14270	67.2	158	2700	24.4	0.23	<0.25	2.68	523	<5.00	1590	68.3	17	49500
35	2.87	11600	11680	184	52.2	2240	19.8	1.22	<0.25	1.97	466	<5.00	847	38.6	19.7	34500
50	3.31	9230	9320	432	15.9	1730	16	6.05	<0.25	1.63	458	<5.00	725	34.4	19	27690
75	4.06	1330	70	72.5	<0.02	5.3	0.65	0.09	1.52	<0.50	527	<5.00	43	5.93	20.2	3840

COLUMN CONT #2 08/02/93

DEPTH (cm)	pH	Fe mg/L	Fe+3 mg/L	Zn mg/L	Cu mg/L	Al mg/L	As mg/L	Cd mg/L	Pb mg/L	Se mg/L	Ca mg/L	K mg/L	Mg mg/L	Mn mg/L	Na mg/L	SO4 mg/L
5	1.95	4120	4050	11	55.4	1230	10.3	0.04	<0.25	0.75	531	<5.00	873	51	17.6	20160
15	1.8	6890	5680	12.9	84.2	1800	14.9	0.04	<0.25	1.54	491	<5.00	1070	52.2	17.9	30900
25	1.89	13700	9460	39.9	134	3000	25.7	0.15	<0.25	2.55	509	<5.00	1700	82.3	15.8	50100
35	2.24	20600	13760	252	210	3540	30.8	1.38	<0.25	2.74	461	<5.00	1580	72.3	15.3	58800
50	3.17	12500	12200	320	20.2	2720	24	1.65	<0.25	1.53	465	9.64	1110	51.7	20	39000
75	3.84	2300	169	43.8	<0.02	12.8	1.28	1.68	4.93	0.51	493	23.3	41.9	4.7	20.1	5220

COLUMN TEST #2 08/02/93

DEPTH (cm)	pH	Fe mg/L	Fe+3 mg/L	Zn mg/L	Cu mg/L	Al mg/L	As mg/L	Cd mg/L	Pb mg/L	Se mg/L	Ca mg/L	K mg/L	Mg mg/L	Mn mg/L	Na mg/L	SO4 mg/L
5	3.88	1110	40.9	42.5	<0.02	11.7	0.56	0.03	2.13	<0.50	231	23.1	21.7	6.81	17.3	2520
15	4.36	418	10.7	13.2	<0.02	3.04	<0.25	<0.02	0.67	<0.50	495	18.6	11.6	3.21	13.7	1920
25	4	413	10.1	94.8	<0.02	5	<0.25	0.06	0.67	<0.50	577	18.6	9.94	12.2	14.4	2220
37	4.12	337	15.1	23.8	<0.02	2.22	<0.25	<0.02	0.53	<0.50	585	19.8	8.62	7.98	13.8	1980

COLUMN TEST #4 08/02/93

DEPTH (cm)	pH	Fe mg/L	Fe+3 mg/L	Zn mg/L	Cu mg/L	Al mg/L	As mg/L	Cd mg/L	Pb mg/L	Se mg/L	Ca mg/L	K mg/L	Mg mg/L	Mn mg/L	Na mg/L	SO4 mg/L
5	4.12	5.31	2.31	11.6	0.1	1.87	<0.25	<0.02	<0.25	<0.50	726	59.4	192	36.3	22.2	2610
15	5.45	1.42	0.7	2.48	0.03	0.58	<0.25	<0.02	<0.25	<0.50	625	52.8	109	16.5	19.9	1950
25	5.41	7.58	0.7	8.31	<0.02	0.69	<0.25	<0.02	<0.25	<0.50	619	43.5	115	22.8	20.4	1980
37	5.29	0.9	1.75	12.4	<0.02	0.51	<0.25	<0.02	<0.25	<0.50	616	36	180	32.3	18.2	2250

TABLE 3-III - ANALYTICAL RESULTS OF LEACHATE FROM SAMPLES COLLECTED JANUARY 28, 1993

COLUMN CONT #1 28/01/93

DEPTH (cm)	pH	Fe mg/L	Fe+3 mg/L	Zn mg/L	Cu mg/L	Al mg/L	As mg/L	Cd mg/L	Pb mg/L	Se mg/L	Ca mg/L	K mg/L	Mg mg/L	Mn mg/L	Na mg/L	SO4 mg/L
5	2.37	1811	1567	33.8	59.6	873	7.12	1.12	<2.50	<5.00	332	<50.0	539	29.2	99.9	16452
15	2.39	3440	3020	21.6	118	1202	8.70	<0.20	<2.50	<5.00	861	<50.0	712	34.6	96.8	23247
25	2.50	13543	3464	121	274	2853	22.5	<0.20	<2.50	<5.00	1343	<50.0	1610	69.5	121	49955
35	3.26	9287	1932	353	641	2095	15.7	2.21	<2.50	<5.00	5947	<50.0	779	38.5	123	44342
50	4.28	2144	62	1050	0.69	181	<2.50	51.2	37.7	<5.00	6697	<50.0	68	7.61	120	22753
75	4.45	1972	28	873	<0.20	29.1	<2.50	9.86	23.8	<5.00	6666	<50.0	57.6	9.64	128	21512

COLUMN CONT #2 28/01/93

DEPTH (cm)	pH	Fe mg/L	Fe+3 mg/L	Zn mg/L	Cu mg/L	Al mg/L	As mg/L	Cd mg/L	Pb mg/L	Se mg/L	Ca mg/L	K mg/L	Mg mg/L	Mn mg/L	Na mg/L	SO4 mg/L
5	2.47	1366	1174	34.8	65.5	951	6.64	<0.20	<2.50	<5.00	394	<50.0	564	28.9	108	15845
15	2.37	6458	5469	31.8	153	2149	15.9	<0.20	<2.50	<5.00	871	<50.0	1282	64.9	118	39355
25	2.39	16483	5775	141	241	4161	31.4	<0.20	<2.50	<5.00	1498	<50.0	2386	121	141	69504
35	3.12	10858	2582	702	1210	3354	24.0	4.26	<2.50	<5.00	5729	<50.0	1108	54.6	135	57401
50	3.92	374	136	961	295	175	<2.50	43.3	44.8	<5.00	6808	107	73.5	9.16	137	20628
75	4.72	4166	32.3	430	2.73	16.0	4.63	15.4	<2.50	<5.00	7134	106	59.7	8.31	122	26422

COLUMN TEST #2 28/01/93

DEPTH (cm)	pH	Fe mg/L	Fe+3 mg/L	Zn mg/L	Cu mg/L	Al mg/L	As mg/L	Cd mg/L	Pb mg/L	Se mg/L	Ca mg/L	K mg/L	Mg mg/L	Mn mg/L	Na mg/L	SO4 mg/L
5	4.78	1622	138	1065	6.94	21.6	<2.50	0.49	<2.50	<5.00	209	95.5	40.9	11.3	91.1	5277
15	4.67	1356	11.3	1085	<0.20	4.38	<2.50	0.63	<2.50	<5.00	410	82.6	25.4	19.3	104	3255
25	5.00	1308	15.8	493	0.67	10.0	<2.50	<0.20	<2.50	<5.00	5738	127	23.6	5.25	100	1478
37	5.08	1141	2.70	847	0.40	6.21	<2.50	0.30	<2.50	<5.00	5905	140	24.5	26.0	101	2540

COLUMN TEST #4 28/01/93

DEPTH (cm)	pH	Fe mg/L	Fe+3 mg/L	Zn mg/L	Cu mg/L	Al mg/L	As mg/L	Cd mg/L	Pb mg/L	Se mg/L	Ca mg/L	K mg/L	Mg mg/L	Mn mg/L	Na mg/L	SO4 mg/L
5	5.55	127	<0.40	413	<0.20	<2.50	<2.50	0.46	<2.50	<5.00	7123	402	398	115	143	22027
15	5.50	91.0	2.9	646	0.60	<2.50	<2.50	1.44	<2.50	<5.00	7205	426	715	210	157	24530
25	5.57	93.6	<0.40	546	<0.20	5.63	<2.50	0.98	<2.50	<5.00	7525	471	494	139	154	24190
37	5.60	267	<0.40	334	14.1	15.3	13.7	16.4	21.3	20.4	7678	430	645	206	140	21958

TABLE 3-IV - ANALYTICAL RESULTS OF LEACHATE FROM SAMPLES COLLECTED FEBRUARY 28, 1993

COLUMN CONT #1 08/02/93

DEPTH (cm)	pH	Fe mg/L	Fe+3 mg/L	Zn mg/L	Cu mg/L	Al mg/L	As mg/L	Cd mg/L	Pb mg/L	Se mg/L	Ca mg/L	K mg/L	Mg mg/L	Mn mg/L	Na mg/L	SO4 mg/L
5	2.30	1917	1617	12.3	76.4	911	6.75	<0.20	<2.50	<5.00	439	<50.0	596	30.8	86.3	17316
15	2.32	2285	1962	21.5	125	1096	8.66	<0.20	<2.50	<5.00	391	<50.0	676	33.4	84.9	18562
25	2.25	11030	7582	59.1	145	2067	18.8	<0.20	<2.50	<5.00	1242	<50.0	1349	63.6	79.2	45298
35	3.00	8075	1742	432	1289	2126	18.0	3.17	<2.50	<5.00	3280	<50.0	896	42.0	82.3	37660
50	3.22	5180	1187	967	940	2533	18.4	22.6	<2.50	<5.00	5677	103	751	37.0	91.7	39356
75	4.62	2098	8.27	800	0.60	24.9	<2.50	6.11	22.2	<5.00	6858	68.6	50.5	8.03	85.1	21688

COLUMN CONT #2 08/02/93

DEPTH (cm)	pH	Fe mg/L	Fe+3 mg/L	Zn mg/L	Cu mg/L	Al mg/L	As mg/L	Cd mg/L	Pb mg/L	Se mg/L	Ca mg/L	K mg/L	Mg mg/L	Mn mg/L	Na mg/L	SO4 mg/L
5	2.34	1253	1083	12.8	54.5	961	6.90	<0.20	<2.50	<5.00	1773	<50.0	710	42.9	83.8	18757
15	2.19	4057	3303	12.4	79.2	1308	10.3	<0.20	<2.50	<5.00	470	<50.0	832	42.8	72.9	25519
25	2.20	9237	7271	42.4	126	2344	20.4	<0.20	<2.50	<5.00	1545	<50.0	1448	74.5	84.4	45701
35	2.66	17930	2838	328	744	2959	27.2	1.21	<2.50	<5.00	4763	<50.0	1551	75.5	80.6	60390
50	3.13	8278	1923	639	1165	3415	27.1	8.82	<2.50	<5.00	5395	97.3	1165	57.5	86.2	49874
75	4.71	3268	1.40	318	<0.20	8.30	<2.50	22.3	5.74	<5.00	7301	67.7	49.1	6.5	91.9	23589

COLUMN TEST #2 08/02/93

DEPTH (cm)	pH	Fe mg/L	Fe+3 mg/L	Zn mg/L	Cu mg/L	Al mg/L	As mg/L	Cd mg/L	Pb mg/L	Se mg/L	Ca mg/L	K mg/L	Mg mg/L	Mn mg/L	Na mg/L	SO4 mg/L
5	4.71	1469	<0.40	931	<0.20	2.81	<2.50	1.19	<2.50	<5.00	258	75.3	23.0	4.75	75.6	5089
15	4.95	1055	<0.40	631	<0.20	3.21	<2.50	<0.20	<2.50	<5.00	629	55.8	18.0	3.83	79.0	5556
25	5.09	872	473	287	<0.20	3.11	<2.50	<0.20	<2.50	<5.00	5068	74.1	15.1	4.66	58.6	15230
37	5.10	933	663	547	<0.20	<2.50	<2.50	<0.20	<2.50	<5.00	6197	123	15.5	7.59	72.3	20806

COLUMN TEST #4 08/02/93

DEPTH (cm)	pH	Fe mg/L	Fe+3 mg/L	Zn mg/L	Cu mg/L	Al mg/L	As mg/L	Cd mg/L	Pb mg/L	Se mg/L	Ca mg/L	K mg/L	Mg mg/L	Mn mg/L	Na mg/L	SO4 mg/L
5	5.35	103	<0.40	672	<0.20	6.60	<2.50	1.45	5.01	<5.00	8207	397	227	77.7	100.9	24899
15	5.43	75.1	<0.40	601	<0.20	6.00	<2.50	1.02	4.08	<5.00	7991	374	197	70.5	99.8	23551
25	5.30	14.8	<0.40	851	<0.20	6.06	<2.50	1.89	<2.50	<5.00	8019	386	184	62.1	89.8	23033
37	5.40	33.9	<0.40	894	<0.20	5.61	<2.50	2.00	8.14	7.87	8741	331	188	66.1	102.8	25143

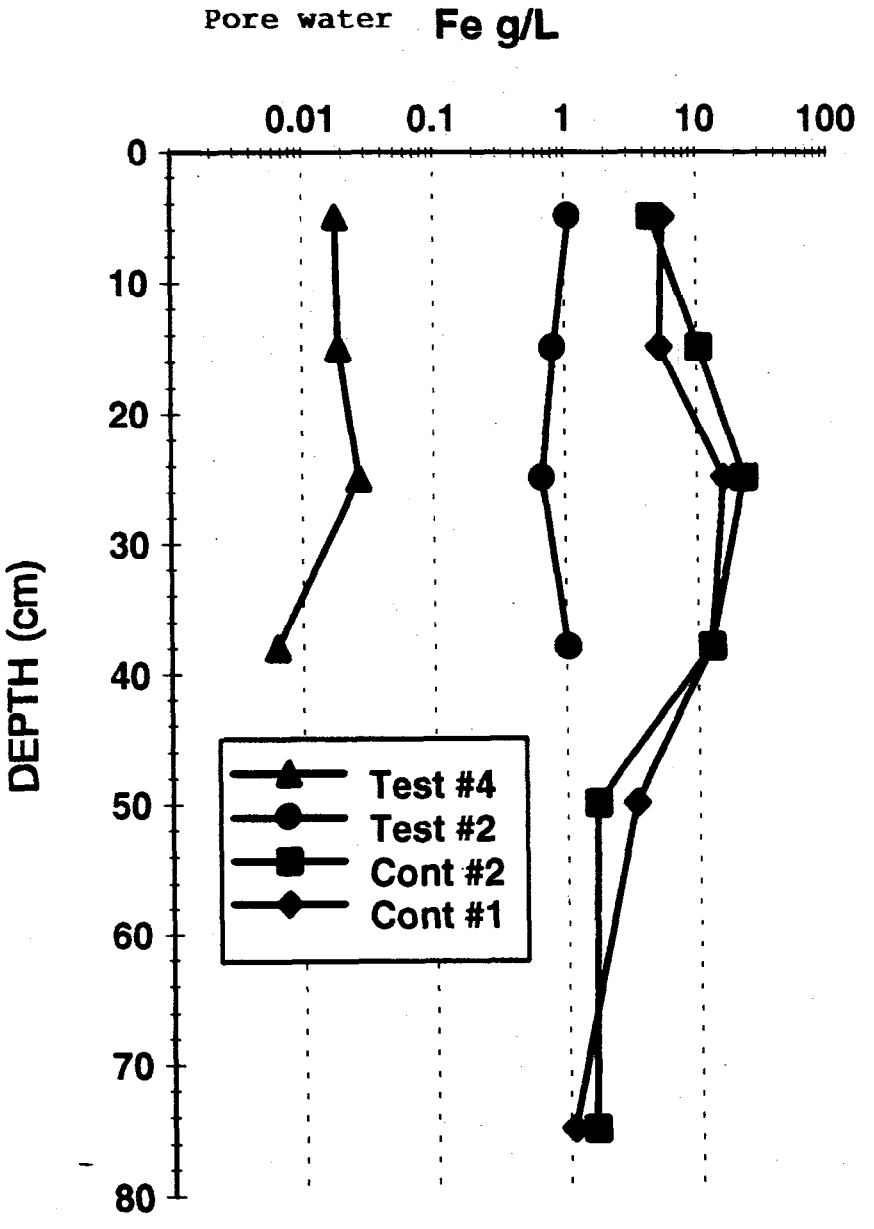

Figure 3.23: Iron Concentrations (g/L) of Pore Water from Control #1 and #2 and Test #2 and #4 versus Depth (cm)

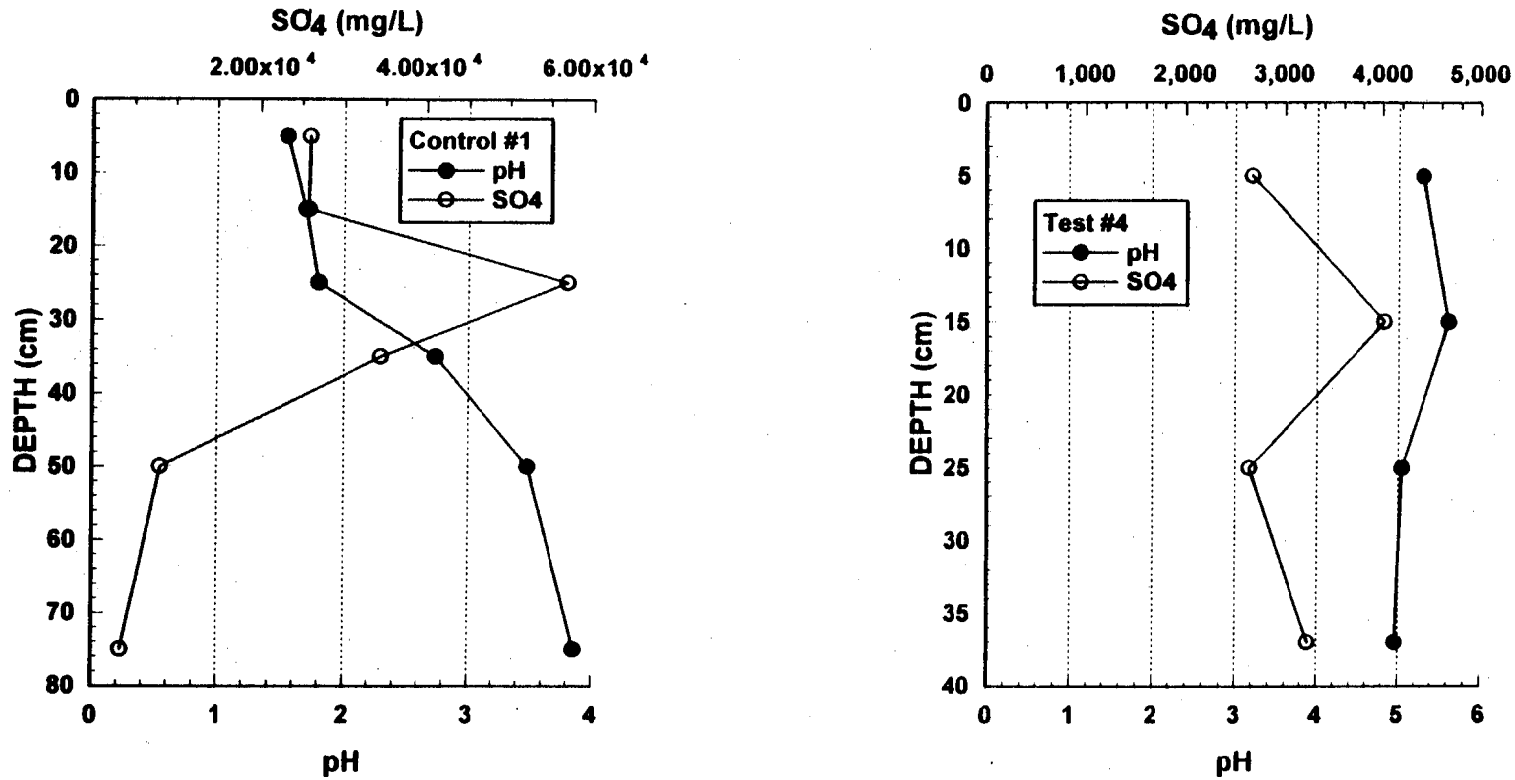

Figure 3.24: Sulphate and pH Profiles in Uncovered (Control) and Covered (Test) Tailings after 760 Days

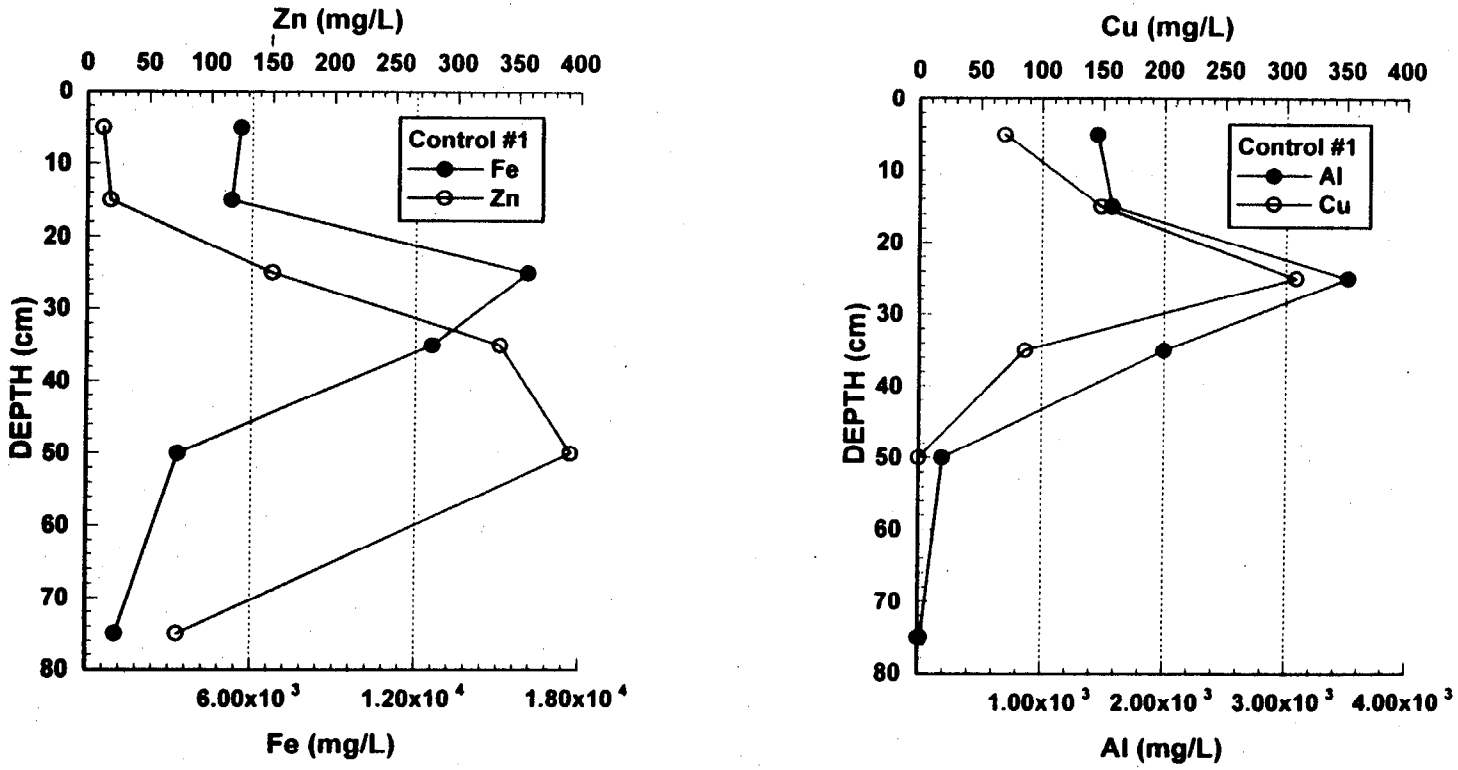

Figure 3.25: Pore Water Metal Profiles in Uncovered (Control) Laboratory Tailings after 760 Days

Aqueous equilibrium modelling, using MINTEQ, indicate supersaturation of the pore water with respect to gypsum and the aluminum sulphate mineral ($Al[OH]SO_4$] with the saturation indices being maximum around 30 cm depth (Figure 3.26). Figures 3.27 and 3.28 present profiles of saturation indices for the iron-bearing minerals ferrihydrite, goethite, melanterite and lepidocrocite. Again, sharp breaks in the profiles occur around 30 cm. Supersaturation with ferrihydrite does not occur until after 50 cm. Slight supersaturation of goethite occurs in the upper layers of the tailings. There is a transition zone around 30 cm below which high supersaturation with respect to goethite occurs.

At all depths in the two Control Columns, the tailings pore water is undersaturated with respect to malantorite. Lepidocrocite appears to be controlling the concentration of ferric iron in solution in the upper 30 cm where saturation occurs. High supersaturation with respect to lepidocrocite occurs in the lower 40 cm of the tailings. The shape of the pQ profiles (indication of the stability of ferric oxyhydroxide minerals) appears to be a mirror image of the saturation index profiles for ferrihydrite, goethite and lepidocroite (Figure 3.27). In general, values of pQ are about 41.0 in the upper 30 cm of the columns, which decrease to about 36.5 in the bottom. These data suggest the formation of freshly precipitating amorphous ferric hydroxide (ferrihydrite) in the bottom layer of the tailings. More crystalline ferric hydroxides (goethite and lepidocrocite) are most likely forming in the upper 30-35 cm of the column where considerable leaching is occurring.

Iron-oxidizing Bacteria

Bacteria count was also performed on tailings sub-samples to evaluate the population of iron-oxidizing microorganisms such as *Thiobacillus ferrooxidans*. Profiles of cell numbers are presented in Figure 3.29. The results indicate that Test Column #4 was sterile with respect to iron oxidizers because of the absence of oxygen which is required for the metabolism of these aerobic bacteria. Test Column #2 supported a population of approximately 1×10^5 cells, while Control Columns #1 and #2 showed a maximum number of cells of 1×10^7 near the oxidation front, at a depth of 30 cm.

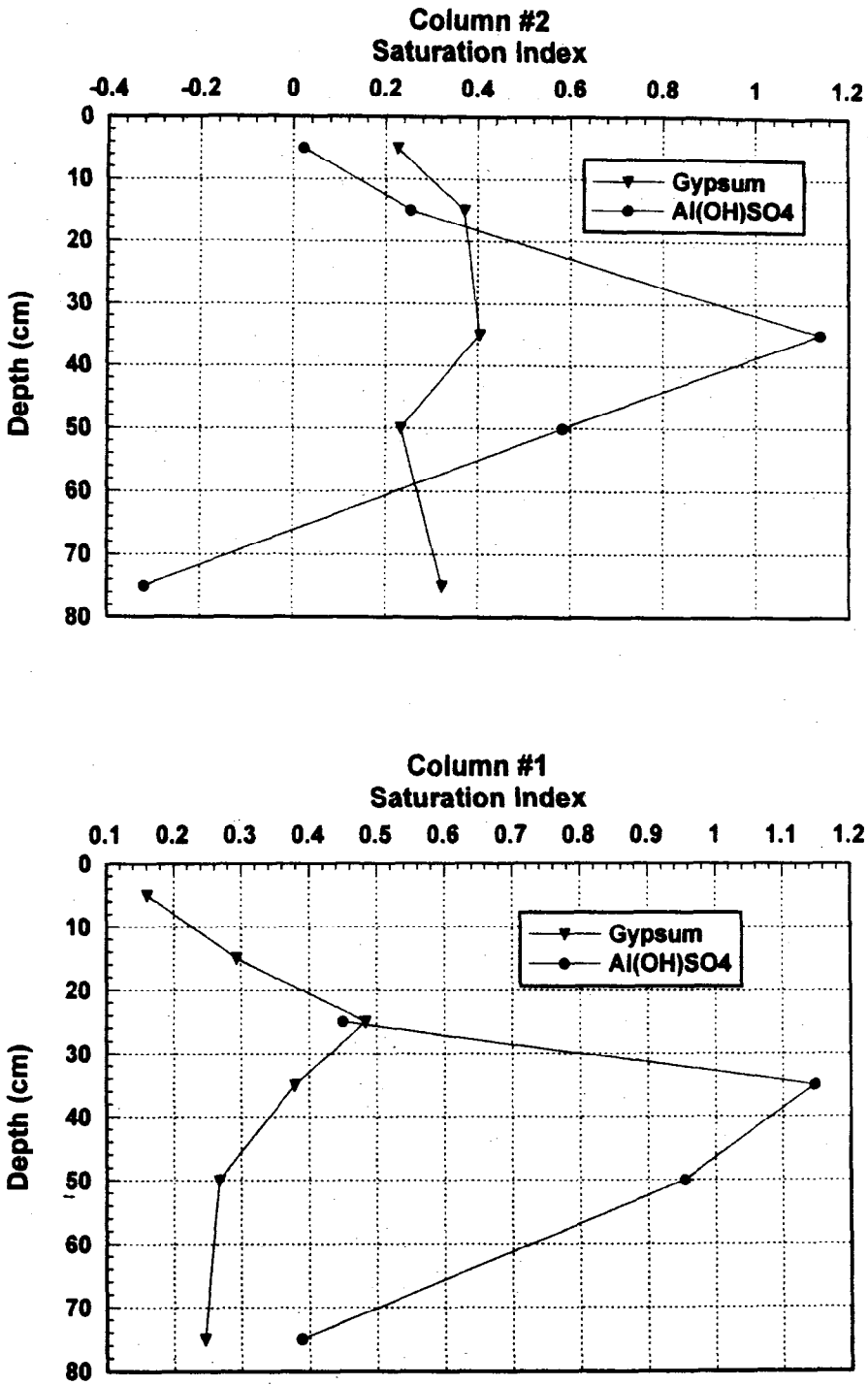

Figure 3.26: Profiles of Saturation Indices for Gypsum ($CaSO_4.H_2O$) and Aluminum Sulphate Mineral [$Al(OH)SO_4$] in Uncovered Tailings after 760 Days

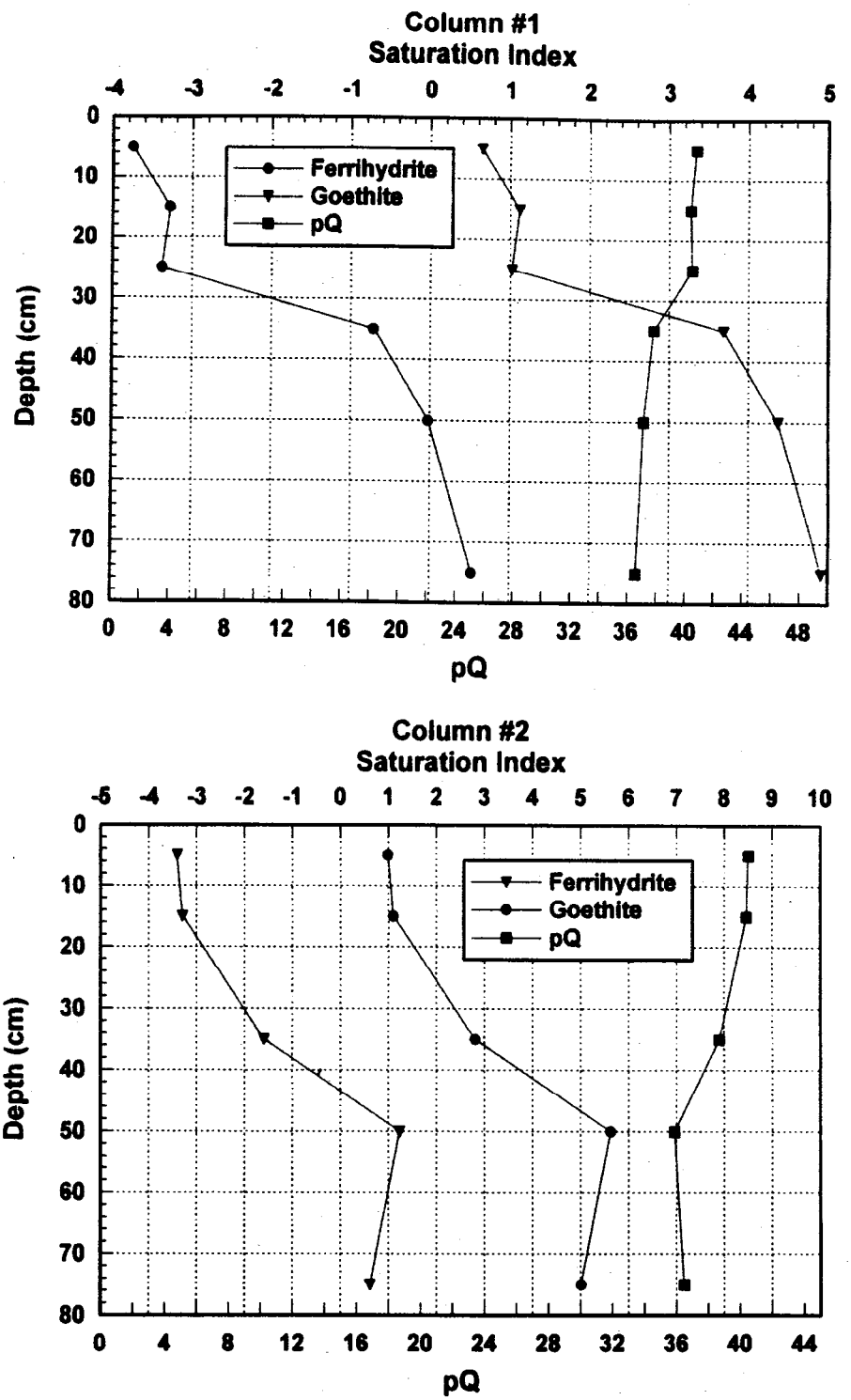

Figure 3.27: Profiles of Saturation Indices for Iron-bearing Minerals and Ferric Iron Hydroxide Activity Product, pQ

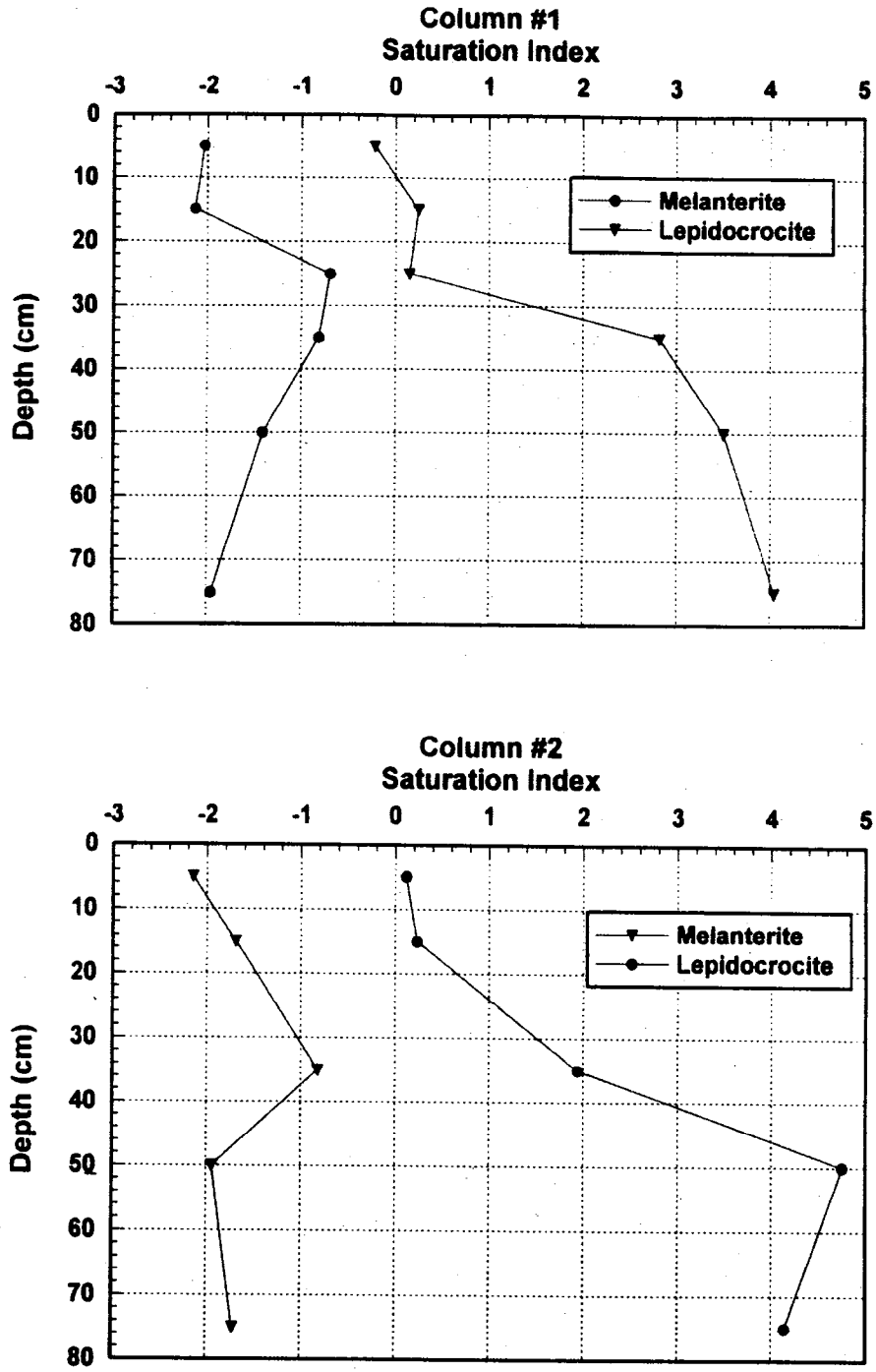

Figure 3.28: Profiles of Saturation Indices for Melanterite and Lepidocrocite

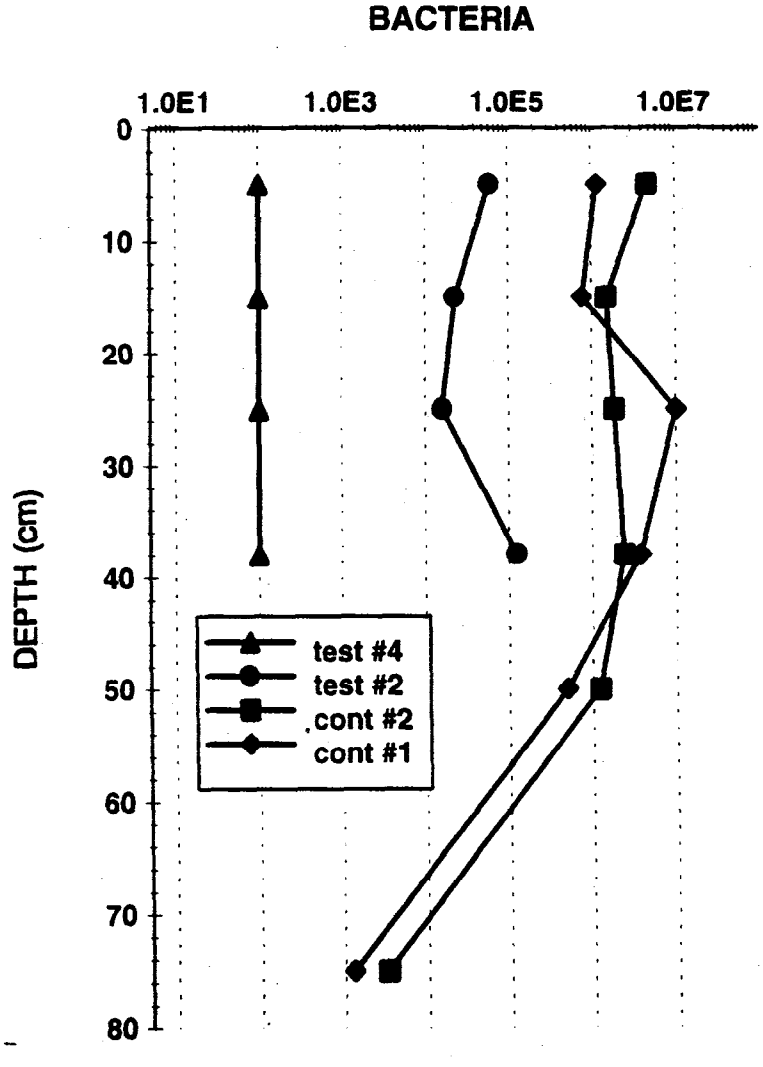

Figure 3.29: Profiles of Iron-oxidizing Bacteria Population in Uncovered (Control) and Covered (Test) Tailings

Grain Size Distribution

The porosity profile and the inferred distribution of amorphous iron oxydroxides (Figures 3.27 and 3.28) seemed to suggest a non-uniform particle size distribution in the tailings profile. Figure 3.30 presents the grain size distribution of the uncovered (Control) tailings at different depths at the end of the testing period (760 days). The data suggest no difference in particle size through the tailings profile. Thus the transformation of the sulphide minerals to iron oxyhydroxides did not result in changes in particle size. Consequently, the variation in porosity with depth presented in Figure 3.22 is due to volume changes resulting from oxidation.

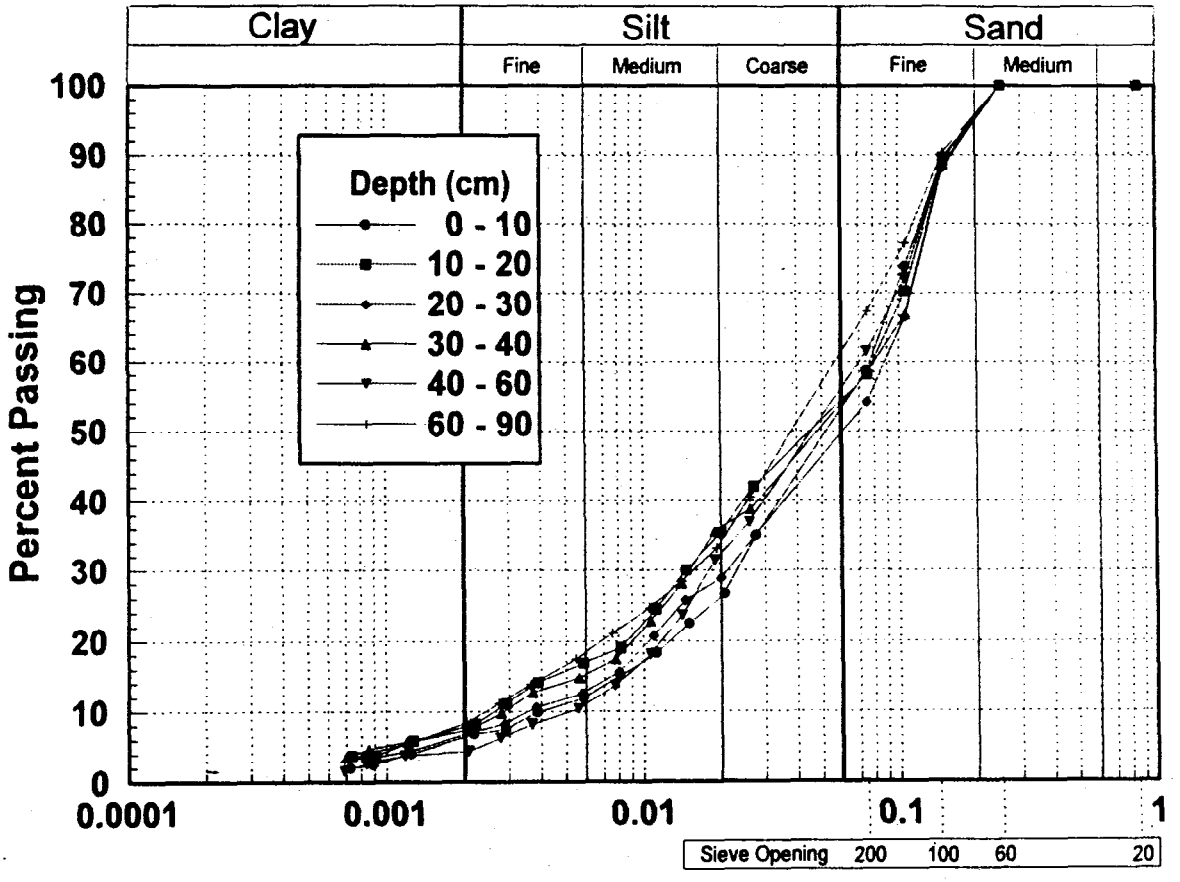

Figure 3:30: Grain Size Distributions of Uncovered (Control) Tailings at Various Depths after 760 Days

4.0 UNIVERSITY CONTRACTS

Four contracts awarded to universities to perform particular studies on the engineered soil covers are summarized below. Readers are refered to Volume 2 (University Contracts) for the complete university reports.

4.1 Chemical Interaction and Cyclic Freeze Thaw Effects on the Integrity of the Cover *(Mohamed et al., 1992)*

Two cases concerning water availability to the composite cover at the Waite Amulet site were investigated in the laboratory: the first adopted a positive water head to assess maximum water damage to the clay cover during freeze/thaw cycles; the second used a negative water head to simulate field condition in the autumn, also under freeze/thaw cycles. Physical and chemical analyses were performed and the results of which suggested that the integrity of the clay layer was reduced under positive head of water. This was attributed to: 1) aggregation of clay particles; 2) chemical interactions between the generated acidic solutions and heavy metals from the tailings, and the clay residence pore fluid, causing a reduction of the thickness of the double layer and an increase in the tendency of flocculation of the clay particles (hence, an increase in permeability); 3) reduction in the buffering capacity of the clay due to reduced pH values. In the second case, the integrity of the clay was only slightly reduced due to: 1) limited amount of water intake during freezing; 2) limited chemical interaction; however, the residence pore fluid cations in the clay were reduced as a result of further leaching,. The thickness of the double layer increases as does the tendency for clay dispersion, which in turn reduces the permeability of the clay cover to water. The negative water head used in this study, nevertheless, was much greater than the negative head at the air entry value of the clay obtained from soil suction experiments. Thus the clay was unsaturated. The results suggest that the case of a positive water head would be more applicable to field conditions. Thus physical structure of the clay layer would required monitoring.

4.2 Compatibility Assessments *(Mohamed et al., 1993)*

This study evaluated the compatibility of the 80 mil HDPE as a function of cyclic freeze/thaw and acidic leachate. The HDPE did not experience any changes in its physical and chemical properties within the experimental time frame. As well, the effect of cyclic freeze/thaw on the drainage characteristics of the clay cover were evaluated. The results indicated that the moisture drainage characteristics of the cover were greatly influenced by the leaching and cyclic freeze/thaw, due to aggregation and, hence, significant pore space readjustment. Finally, the effect of cyclic freeze/thaw on the oxygen diffusion in the soil cover was studied and it was found that the freeze-thaw influences both the air permeability and the oxygen content in the clay cover, which were reduced due to the increase in moisture content. When the soil samples were subjected to leaching, air permeability decreased by 1-2 orders of magnitude and oxygen concentration dropped to about zero. The difference in oxygen content, between samples saturated with distilled

4.3 Tailings Characterization and Flow Modelling *(Chapuis, 1992)*

The Geotechnical Group at École Polytechnique was awarded a research contract to measure the tailings hydraulic properties and conduct flow modelling. The results indicated vertical variation in gradation and hydraulic properties over short distances. In the central part of the tailings area, specific gravities ranged from 3.21 at a depth of 4.90 m to 3.55 at 5.60 m. The average particle size represented by D_{10} (the particle size at which 10% of the tailings are finer) is about 0.01 mm. The tailings in this area are sandy silts, with clay-size particles ranging from 2% to 10%.

Laboratory and field (piezometer) hydraulic conductivity tests indicated values in the range of 1.3-2.0 x 10^{-3} cm/s for tailings located in the test plot area. Flow modelling by finite element methods showed some anisotropy in hydraulic conductivity. An average anisotropy factor (K_H/K_V) of 80 was reported which was lower than the value of 100 obtained by Yanful and St-Arnaud (1992) for tailings located in the south-end section of the impoundment.

There was some discrepancy between the flow modelling results and field observations. The use of a hydraulic conductivity of 1 x 10^{-5} cm/s for the compacted clay layer in the flow model indicated considerable water percolation through the cover. This value of hydraulic conductivity was actually measured in the field on a compacted clay located outside the test plot. The clay was compacted and deliberately left without any protective layer (sand or gravel) to evaluate freeze/thaw effects. The initial hydraulic conductivity was determined to be ~$1.0x10^{-7}$ cm/s. The increase to $1.0x10^{-5}$ cm/s after a year could be attributed to structural changes resulting from freezing and thawing. The hydraulic conductivity of the clay in the actual composite cover did not change much from the initial value, even after two winter seasons. The use of a value of $1.0x10^{-7}$ cm/s in the flow model significantly reduced the vertical percolation through the cover. Another source of discrepancy in the modelling was the difference between the material properties (moisture retention and drainage curves) used and those measured. The curves used by École Polytechnique were not based on actual measurements.

Later flow modelling conducted by NTC (Section 2.3.4) incorporated the geomembrane lining on the cover slopes and measured material properties. The results indicated more realistic percolation rates that were similar to lysimeter data.

4.4 Evaluation of Gas Movements *(Alpers and Montgomery, 1992)*

The Department of Geological Sciences, McGill University, was given a contract to provide a geochemical evaluation of the movement of gases during sulphide oxidation. The evaluation was intended to improve understanding of the role of sulphur-bearing gases during oxidation of sulphidic tailings. The work was initiated in the fall of 1990 immediately following the construction of the test plots. It consisted of sampling of tailings pore gas for analysis of CO_2 and sulphur-bearing gases (COS, CS_2, H_2S and SO_2). It was postulated that the effectiveness of the covers in reducing sulphide oxidation could be evaluated by examining pore gas concentrations over time. One of the functions of the composite covers was to provide an impermeable barrier to meteoric waters and hence curb the production of acid waters. A quantitative analysis of pore gas was, therefore, considered a more comprehensive and sensitive indication of the extent and rates of sulphide oxidation and hence cover performance. In addition to the pore gas analysis, a limited evaluation of the geochemical evolution of water samples collected from covered and uncovered test plots was also conducted.

Results of pH measurements made on parallel instrumentation indicated agreement within 0.02 units. Initial CO_2 measurements (October 1990) were found to be high (apparently $\geq$ 20%) and negatively correlated with O_2 concentrations. Later CO_2 measurements made in November 1990 gave reasonable results with values ranging from 0.05% to 0.43%. A general trend of decreasing O_2 and increasing CO_2 concentrations with depth was observed for the covered test plots.

Stable isotope analysis for $\delta^{13}C$ and $\delta^{18}O$ in CO_2 intended to identify the source of CO_2 did not produce conclusive results. It was, however, inferred that sources of CO_2 could include (1) oxidation of organic matter, (2) dissolution of carbonate minerals in tailings, (3) dissolution of carbonate minerals in limestone added during revegetation, and (4) trapped air.

Analysis of sulphur-bearing gases did not yield any H_2S and SO_2. Taylor *et al.* (1982) evaluated the production of sulphur-bearing gases by the decomposition of sulphide minerals. They found that SO_2 was detectable only over completely dry sulphide minerals. Both H_2S and SO_2 have relatively high solubilities in water (Rose *et al.*, 1979). The McGill study concluded that, given the relatively humid conditions at Waite Amulet, it is likely that any H_2S or SO_2 produced by sulphide oxidation could be dissolved in water.

5.0 DISCUSSION

The results from laboratory, field and modelling studies all indicate that the composite soil cover is effective in reducing both water infiltration and oxygen diffusion into the underlying tailings. This cover consists of a compacted varved clay layer placed between two sand layers. The clay was placed in the field at a water saturation of about 90%. The effectiveness of the cover is governed by the hydraulic and physical properties of the cover such as moisture content, moisture-retention characteristics, hydraulic conductivity and grain size distribution. The effective diffusion coefficient of oxygen in the fine-grained layer, D_e, is critical to the effectiveness of the cover. Modelling results presented by Yanful (1993) indicate that the D_e of the compacted Waite Amulet clay used in construction of the cover is 9.9×10^{-9} m^2/s in the field and 3.9×10^{-9} m^2/s in the laboratory. These values of D_e are concentration independent diffusion coefficients which include the coefficient of diffusion of oxygen in air and a tortuosity factor characteristic of the soil. They do not include the air-filled porosity of the soil. This porosity was determined to be 0.021 which, if taken into account, would reduce the effective diffusion coefficient by two orders of magnitude.

In the short term (that is, during the three-year life of the project), no significant changes in the hydraulic and physical properties of the clay layer have been observed. Field and laboratory volumetric water contents were constant at ~43% during this period. The temperature and water content data indicated that the upper part of the clay layer is frozen during winter. An important consideration in this case is the effect of freezing and thawing on the integrity of the clay in the long term. This was investigated in the laboratory on 50 and 100 mm diameter samples by McGill University. The hydraulic conductivity, K, of the 50 mm clay samples increased by about an order of magnitude after three freeze-thaw cycles (that is from 7.0×10^{-9} cm/s to 1.7×10^{-7} cm/s). The effect of freeze-thaw on the 100 mm samples was more dramatic. K increased by 2.5 orders of magnitude after the first cycle and then decreased by about half an order of magnitude subsequently. Wong and Haug (1991) found that the hydraulic conductivity of a compacted clay soil and a till increased by about an order of magnitude during the first two freeze-thaw cycles and then remained nearly steady with subsequent cycles. Thus, it appears that most of the adverse effects of freeze-thaw occur in the first two cycles. The increase in K may be due to the formation of microcracks and clay aggregation during freezing (Mohamed *et al.*, 1992).

The hydraulic conductivity of the clay layer in the composite cover was measured in the field during 1991 and 1992 using an air entry permeameter similar to that described by Fernuik and Haug (1990). The results, presented in Table 5-I, indicate essentially no change in K with time. The K value of ~ 2.0×10^{-7} cm/s obtained in 1992 is similar to the initial design value.

TABLE 5-I - FIELD HYDRAULIC CONDUCTIVITY OF COMPACTED CLAY LAYER IN COMPOSITE COVER

TEST	PLOT #	SRI[1] (cm/s)	AEP[2] (cm/s)	YEAR
WA-R2-1	R2	2.44×10^{-7}	1.83×10^{-7}	1992
WA-R2-2	R2	6.05×10^{-7}	1.01×10^{-6}	1992
WA-R3-1	R3	1.92×10^{-7}	3.08×10^{-7}	1992
WA-R3-2	R3	1.58×10^{-8}	2.10×10^{-8}	1992
WAEP	R2	1.05×10^{-7}	1.11×10^{-7}	1991

[1] Single Ring Infiltrometer
[2] Air Entry Permeameter

The effects of freeze-thaw on the moisture retention characteristics of the clay were also investigated in the laboratory. The results indicated that the unfrozen clay exhibited high water potential with an air entry value of ~pF 3 (10 m of water). At constant values of soil water potential, clay samples subjected to increasing number freeze-thaw cycles exhibited lower amounts of water retention. As was the case with the hydraulic conductivity, the largest decrease in moisture retention was obtained after the first freeze-thaw cycle. Subsequent freeze-thaw cycles yielded relatively lower decreases in moisture retention (Mohamed *et al.*, 1993).

Modelling of field and laboratory oxygen concentration profiles showed that reductions in oxygen flux by the composite soil cover were in the range of 90 to 99% (Yanful, 1993). This is confirmed by drainage data obtained from laboratory columns installed to simulate covered and uncovered tailings. Water percolation through the cover was found to be only 4% of precipitation by hydrologic modelling. Field estimates using lysimeter data gave a percolation of ~ 6% of precipitation (Woyshner and Yanful, 1993). In a previous study, Yanful *et al.* (1990) found the infiltration into the uncovered tailings to be ~24.5%. Thus the cover has reduced the infiltration by 80% or from about 220 mm per year to 45 mm per year.

As expected, no water percolation was observed in the HDPE geomembrane. Its stability with respect to acid leach, tension stresses and freeze thaw was investigated in the laboratory and found to be of no concern. A tensile resistance of ~1.5 kN was obtained on both an unleached specimen and specimens exposed to acid (pH of 3) for varying times from 14 to 42 days at room temperature. After three freeze-thaw cycles, the tensile resistance was found to be about 1.56 Kn, suggesting that freezing conditions in the field would not likely affect the long term stability of the geomembrane cover. The main concerns would be mechanical shearing resulting from field equipment and traffic or the activities of burrow animals and long term exposure to sunlight.

6.0 CONCLUSIONS AND RECOMMENDATIONS

The design of a composite soil cover for reducing acid generation in reactive mine tailings involved the capillary barrier concept. The effectiveness of the cover was evaluated at the Waite Amulet tailings site using test plots and in the laboratory by means of columns. A coarse-grained soil underlying a compacted, nearly saturated clay soil drained to residual saturation (that is, minimum water content) and essentially prevented the clay from draining. Results of flow modelling and laboratory column verification indicated that a coarse-grained layer (fine sand) overlying the clay minimizes moisture losses (by evaporation) from the clay. In the field, this upper fine sand layer reduces run off, promotes storage and allows percolated water to reach the clay. The thicknesses of the various layers were 60 cm for the clay and 30 cm for both the coarse sand base and the upper fine sand cover. A 10 cm thick gravel crust blanketed the 1.2 m cover to minimize erosion. These thicknesses were reduced by half in the laboratory experiments.

A plastic or geomembrane cover (80 mil or 2 mm thick HDPE) was also evaluated and found to be an effective water barrier. An oxygen concentration of 6% observed in the sand base underlying the geomembrane which was believed to be a result of horizontal transport of oxygen from the edges of the cover.

Based on the results, the following general conclusions can be made:

- Acid production rates observed in uncovered tailings in the laboratory ranged from 7.5 to 12.9 mg of $CaCO_3$/day/cm^2.
- The acid production rates decrease with time.
- Profiles of oxygen concentrations, density, iron concentrations in pore water, iron concentrations in water leach tests and bacteria population clearly indicate an active front of oxidation at a depth of 30 cm after 760 days.
- Acid production rates in soil-covered tailings averaged 0.005 mg of $CaCO_3$/day/cm^2, indicating a reduction of 99.9% over the Control (uncovered tailings) tests.
- The profiles of oxygen concentrations, density, iron concentration in pore water, bacteria population and cumulative acidity confirm the effectiveness of the three-layer soil cover as a barrier to oxygen diffusion.
- Water percolation into the tailings was determined to be 4% of precipitation by hydrologic modelling and 6% of precipitation from field lysimeter data. These results indicate the infiltration into the tailings is reduced by 80%.

- The effective diffusion coefficient of oxygen in the clay in the composite soil cover was determined to be 3.9 x 10^{-9} m^2/s in the laboratory and 9.9 x 10^{-9} m^2/s in the field.

- The field hydraulic conductivity of the clay was found to be about 1.0 x 10^{-7} cm/s during 1991 and 1992. From the results of laboratory studies, it is not conceivable that the hydraulic conductivity would be increased by freeze-thaw.

It is recommended that the tailings in each test plot lysimeter be sampled and examined for signs and extent of oxidation. This would involve detailed pore water analysis and mineralogical investigation. The water balance of the two soil-covered test plots should be confirmed by further field monitoring through the fall of 1993. The results presented and discussed in this report and those of the recommended additional monitoring should be integrated into a set of design and construction protocols for soil covers for use by mining companies and consultants. A new project should be initiated to investigate the effects of root penetration on the soil covers.

7.0 REFERENCES

BALL, J.W., E.A. JENNE, and D.K. NORDSTROM, "WATEQ2-A computerized chemical model for trace and major element speciation and mineral equilibria of natural waters", in *Chemical Modeling in Aqueous Systems: Speciation, Sorption and Kinetics* (ed. E.A. Jenne), Am. Chem. Soc. Symposium Series 93, Washington D.C., 1979, pp. 815-835.

BENSON, C. and D. DANIEL, "Influence of clods on hydraulic conductivity of compacted clay", *Journal of Geotechnical Engineering*, ASCE, Vol. 116, No. 8, 1990, pp. 1231-1248.

BLOWES, D.W. and J.L. JAMBOR, "The pore water geochemistry and the mineralogy of the vadose zone of sulphide tailings, Waite Amulet, Quebec", *Applied Geochemistry*, Vol. 5, 1990.

CHAPUIS, R.P., "Participation à l'évaluation sur le terrain de recouvrements géologiques", Rapport Final, préparé pour Centre de recherches minérales, mars, 1992, Le Centre de développement technologique de l'École Polytechnique, Montréal, Canada , Projet C.D.T. P1538.

COLLIN, M., "Mathematical Modelling of Water and Oxygen Transport in Layered Soil Covers for Deposits of Pyritic Mine Tailings", Licentiate Treatise. Department of Chem. Ecg., Royal Institute of Technology, Stockholm, 1987.

DANIEL, D.E., D.C. ANDERSON and S.S. BOYNTON, "Fixed-wall versus flexible-wall permeameters", in Hydraulic Barriers in Soil and Rock, ASTM Special Technical Publication 874, 1985, pp. 107-122.

DAVE, N.K., T.P. LIM, R.S. SIWIK and R. BLACKPORT, "Geophysical and biohydrogeochemical investigations of an active sulfide tailings basin, Noranda, Quebec, Canada", in *1986 National Symposium on Mining, Hydrology, Sedimentology and Reclamation*, University of Kentucky, Lexington, Kentucky, 8-11 December 1986, pp. 13-19.

DAVIS, J.L. and W.J. CHUDOBIAK, "*In situ* meter for measuring relative permittivity of soils", Geological Survey of Canada Paper 75-1A, 1975, pp.75-79.

ELSBURY, B.R., D.E. DANIEL, G.A. SRADERS and D.C. ANDERSON, "Lessons learned from a compacted clay liner", *Journal of Geotechnical Engineering*, ASCE, Vol.116, No. 11, 1990, pp. 1641-1660.

FELMY, A.R., D.C. GIRVIN and E.A. JENNE, "MINTEQ—A computer program for calculating aqueous geochemical equilibria", U.S.E.P.A., Athens, GA, EPA-600/3-84-032, 1984.

FERNUIK, N. and M. HAUG, "Evaluation of in situ permeability methods". *Journal of Geotechnical Engineering,* ASCE, Vol. 116, No. 2, 1990, pp. 297-311.

FILION, M.P. and K. FERGUSON, "Acid mine drainage research in Canada", Proceedings of the International Symposium on Tailings and Effluent Management, Halifax, 1989, pp. 61-72.

LAMBE, T.W., "The engineering behavior of compacted clay", *Journal of the Soil Mechanics Foundations Division*, ASCE, Vol. 84, No. SM2, 1958, pp. 1655-1 to 1655-35.

LANGMUIR, D. and D.O. WHITTEMORE, "Variations in the stability of precipitated ferric oxyhydroxides", in Nonequilibrium Systems in Natural Water Chemistry, ed. J.D. Hem, *ACS Advances in Chemistry Series*, No. 106, American Chemical Society, Washington, DC, 1971.

MOHAMED, A.M.O., R.N. YONG, and F. CAPORUSCIO, "Chemical interaction and cyclic freeze thaw effects on the integrity of the proposed soil cover system", Final Report submitted to Gouvernement du Québec, March 1992, CRM 7125-G-001, Geotechnical Research Centre, McGill University, Montreal, Canada,

MOHAMED, A.M.O., R.N. YONG, and F. CAPORUSCIO, "Field Evaluation of the effectiveness of engineered soil covers for reactive tailings: Compatibility evaluation, Final Report submitted to Gouvernement du Québec, March 1993, CRM 7125-G-001 PPV1, Geotechnical Research Centre, McGill University, Montreal, Canada,

MONTGOMERY, S., and C.N. ALPERS, "Waite Amulet Gas Sampling Study", Final Report Prepared Centre de recherches minérales, Fiscal Year 1991-1992, Department of Geological Sciences McGill University, Montreal, Canada.

MILLINGTON, R.J. and R.C. SHEARER, "Diffusion in aggregated porous media", *Soil Sci.*, Vol. 111, 1971, pp. 372-378.

NICHOLSON, R.V., R.W. GILLHAM, J.A. CHERRY and E.J. REARDON, "Reduction of acid generation in mine tailings through the use of moisture-retaining cover layers as oxygen barriers", *Canadian Geotechnical Journal*, **26(1)**, 1989, pp. 1-8.

NORDSTROM, D.K., "Aqueous pyrite oxidation and the consequent formation of iron minerals", in Acid Sulphate Weathering, *Soil Sci. Soc. Amer.*, Spec. Publ. 10, 1982, pp. 37-56.

PATTERSON, D.E. and M.W. SMITH, "Unfrozen water content in saline soils: Results using time domain reflectometry", *Canadian Geotechnical Journal*, **22**, 1985, pp. 95-101.

RAHARDJO, H., J. LOI and D.G. FREDLUND, "Typical matric suction measurements in the laboratory and the field using thermal conductivity sensors", Proceedings of the Indian Geotechnical Conference - '89, Vasakhapatnam, India, 1989.

RAMUSON, A. and J.C. ERIKSSON, "Capillary barriers in covers for mine tailings dumps", National Swedish Environmental Protection Board Report 3307, 1986.

ROSE, A.W., H.E. HAWKES and J.S. WEBB, Geochemistry in Mineral Exploration, 2nd ed., Academic Press Ltd., 1979, 657 pp.

ROWE, R.K. and J.R. BOOKER, "POLLUTE v.5.0 1-D Pollutant migration through a non-homogeneous soil—User manual", Geotechnical Research Centre, Faculty of Engineering Science, University of Western Ontario, Report No. GEOP 90-1, 1990

SATTLER, P. and D.G. FREDLUND, "Use of thermal conductivity sensors to measure matric suction in the laboratory", *Canadian Geotechnical Journal*, Vol. 26, No. 3, 1989, pp. 491-498.

SCHROEDER, P.R., J.M. MORGAN, T.M. WALSKI and A.C. GIBSON, "The Hydrologic Evaluation of Landfill Performance (HELP) Model", U.S. Environmental Protection Agency, Office of Solid Waste and Emergency Response, Washington, DC, 1984.

SCHROEDER, P.R. and R.L. PEYTON, "Verification of the Hydrologic Evaluation of Landfill Performance (HELP) Model Using Field Data", U.S. Environmental Protection Agency, Hazardous Waste Engineering Research Laboratory, Office of Research and Development, Cincinnati, OH, 1987.

STANDARD METHODS, Standard Methods for the Examination of Water and Wastewater, 14th Edition., 1975, APHA-AWWA-WPCF.

ST-ARNAUD, L.C., E.K. YANFUL, R. PRAIRIE and N.K. DAVE, "Evolution of acidic pore water at the Waite Amulet tailings site, Noranda, Quebec", Proceedings of the International Symposium on Tailings and Effluent Management, Halifax, CIM, Vol. 14, 1989, pp. 93-102.

TAYLOR, C.H., S.E. KESLER and P.L. CLOKE, "Sulphur gases produced by the decomposition of sulphide minerals: Application to geochemical exploration", *Journal of Geochemical Exploration*, Vol. 17, 1982, pp. 185-185.

TOPP, G.C., J.L. DAVIS and A.P. ANNAN, "Electromagnetic determination of soil water content: Measurement in coaxial transmission lines", *Water Resources Research*, Vol. 6, No. 3, 1980, pp. 574-582.

TOPP, G.C. and J.L. DAVIS, "Time domain reflectometry (TDR) and its application to irrigation scheduling", in Advances in Irrigation, Vol. 3, Academic Press Inc., 1985.

WHEELAND, K.G. and G. FEASBY, "Innovative decommission technologies via Canada's MEND program", Conf. Hazardous Materials Control '91, Washington, DC, 1991.

WONG, L.C. and M.D. HAUG, "Cyclical closed-system freeze-thaw permeability testing of soil liner and cover materials", *Canadian Geotechnical Journal,* Vol. 28, No.6, 1991, pp. 784-793.

WOYSHNER, M.R. and E.K. YANFUL, "Hydrologic analysis and prediction in a composite soil cover", Joint CSCE-ASCE National Conference on Environmental Engineering, Montreal Canada, 12-14 July, 1993.

YANFUL, E.K., L.C. ST-ARNAUD and R. PRAIRIE, "Generation and evolution of acidic pore waters at the Waite Amulet tailings site", Rapport final. Centre de technologie Noranda, 1990.

YANFUL, E.K. and L.C. ST-ARNAUD, "The hydrogeochemistry and geotechnique of the Waite Amulet tailings site near Rouyn-Noranda, Quebec, Canada", Proceedings of the First Canadian Conference on Environmental Geotechnics, sponsored by the Canadian Geotechnical Society, 1991.

YANFUL, E.K., "Engineered soil covers for reactive tailings: Theoretical concepts and laboratory development", Proceedings of the 2nd Intl. Conf. on the Abatement of Acidic Drainage, Montreal, Canada, 16-18 September, 1991, Vol. 1, pp. 487-504.

YANFUL, E.K. and L.C. ST-ARNAUD, "Migration of acidic pore waters at the Waite Amulet tailings site near Rouyn-Noranda, Quebec, Canada, *Canadian Geotechnical Journal*, Vol. 29, 1992, pp. 466-476.

YANFUL, E.K, "Oxygen diffusion through saturated soil covers on sulphidic mine tailings", *ASCE Journal of Geotechnical Engineering*, in press, 1993.

YONG, R.N., A.M.O. Mohamed and F. Caporuscio, "Field Evaluation of the effectiveness of engineered soil covers for reactive tailings", Final Report submitted to Gouvernement du Québec, March 1991, Dossier 89TE17, Geotechnical Research Centre, McGill University, Montreal, Canada.

ZEGELIN, S.J. and I. WHITE, "Improved field probes for soil water content and electrical conductivity measurement using time-domain reflectometry", *Water Resources Research*, Vol. 25, No. 11, 1989, pp. 2367-2376.

APPENDIX A

METEOROLOGICAL DATA AT AMOS AND DUPARQUET, QUÉBEC

Meteorological Information at Amos, Quebec.													Amos (7090120)
Lat. 48 34, Long. 78 08	Alt. 310 m	Jan	Feb	Mar	Apr	May	Jun	Jul	Aug	Sep	Oct	Nov	Dec	Annual
Rainfall (mm)	1991	0.0	0.0	20.1	28.2	80.8	70.6	127.2	86.0	110.4	87.2	31.6	11.6	653.7
	1992	8.4	0.0	8.0	65.3	84.5	53.4	80.9	125.7	98.0	61.0	64.0	4.0	653.2
	Normal (1961-90)	3.1	2.8	12.4	35.2	74.7	104.6	107.5	113.2	110.9	76.1	30.6	7.0	678.1
Snowfall (cm)	1991	65.2	23.2	47.6	26.6	0.0	0.0	0.0	0.0	9.0	5.8	35.3	42.8	255.5
	1992	47.6	36.4	46.0	3.8	3.0	0.0	0.0	0.0	1.0	8.4	26.2	56.4	228.8
	Normal (1961-90)	48.6	36.2	36.3	18.9	1.4	0.0	0.0	0.0	0.1	8.5	39.1	53.1	243.6
Total Precipitation (mm)	1991	65.2	23.2	67.7	54.8	80.8	70.6	127.2	86.0	119.4	93.0	66.9	54.4	909.2
	1992	56.0	36.4	54.0	69.1	87.5	53.4	80.9	125.7	99.0	69.4	90.2	60.4	882.0
	Normal (1961-90)	51.3	38.9	48.8	54.1	76.0	104.7	107.5	113.2	111.0	84.5	69.4	59.4	920.3
Snow Pack, month end (cm)	1991	55.0	57.0	54.0	0.0	0.0	0.0	0.0	0.0	0.0	0.0	7.0	27.0	-
	1992	54.0	62.0	56.0	2.0	0.0	0.0	0.0	0.0	0.0	0.0	na	na	-
	Normal (1961-90)	70.3	78.4	52.3	3.1	0.0	0.0	0.0	0.0	0.0	0.5	16.0	44.6	-
Pan Evaporation (mm)	1991	-	-	-	-	163	213	196	146	89	52	-	-	859
	1992	-	-	-	-	207	174	141	127	87	-	-	-	736
	Normal (1968-92)	-	-	-	-	148	161	172	134	79	51	-	-	745
Lake Evaporation (mm) a/	Normal (1951-80)	-	-	-	-	108	119	128	102	58	-	-	-	516
	% of Pan Evaporation	-	-	-	-	72.5	74.1	74.5	76.3	73.8	-	-	-	-
Potential ET (mm) b/	Normal (1961-90)	0	0	0	8	67	103	122	102	62	26	0	0	489
	% of Pan Evaporation	-	-	-	-	45.1	64.0	71.1	75.7	78.4	50.6	-	-	-
Temperature, Average (C)	1991	-18.9	-11.7	-7.9	3.4	10.9	15.9	17.4	16.6	9.3	4.4	-2.6	-13.5	1.9
	1992	-17.1	-16.1	-11.6	-0.4	9.3	12.4	14.5	14.4	10.8	2.2	-6.7	-11.1	0.1
	Normal (1961-90)	-17.3	-15.4	-8.3	0.9	8.8	14.1	17.0	15.2	10.4	4.3	-3.6	-13.7	1.1
Temperature, Maximum (C)	1991	-12.2	-5.6	-1.1	9.0	17.5	22.6	23.5	22.3	14.4	8.5	1.0	-8.4	7.6
	1992	-12.3	-9.9	-11.6	5.1	16.6	19.0	20.4	19.7	15.8	5.9	-1.4	-6.5	5.1
	Normal (1961-90)	-11.8	-9.5	-2.2	6.4	15.0	20.0	23.1	20.9	15.2	8.3	-0.3	-8.9	6.4
Temperature, Minimum (C)	1991	-25.5	-17.8	-14.6	-2.2	4.2	9.2	11.2	10.9	4.2	0.2	-6.1	-18.6	-3.7
	1992	-21.8	-22.2	-18.2	-5.9	2.0	5.7	8.6	9.0	5.8	-1.5	-7.9	-15.7	-5.2
	Normal (1961-90)	-22.9	-21.4	-14.4	-4.6	2.6	7.7	11.0	9.7	5.5	0.4	-6.9	-18.4	-4.2

a/ Lake evaporation calculations are based on work by Kohler, Nordenson, and Fox, U.S. Weather Bureau Res. Paper No. 38.
b/ Potential Evapotranspiration calculated with the Thornthwaite method (1948), Geol. Rev. 38 (1): 55-94.
na = not available

Meteorological Information for Duparquet, Quebec.													Duparquet (709BBDH)
Lat. 48 31, Long. 79 16	Alt. 290 m	Jan	Feb	Mar	Apr	May	Jun	Jul	Aug	Sep	Oct	Nov	Dec	Annual
Rainfall (mm)	1991	5.0	0.0	5.0	20.0	67.9	48.7	64.0	119.1	87.7	100.3	48.1	5.6	571.4
	1992	0.0	0.0	2.0	81.6	66.5	64.5	89.9	128.6	154.8	57.8	70.9	4.0	720.6
	Normal (1981:05-1980:12)	1.6	4.4	14.6	36.6	88.1	95.2	105.0	100.9	112.7	85.9	31.2	5.5	639.8
Snowfall (cm)	1991	65.0	31.3	54.0	32.0	3.0	0.0	0.0	0.0	12.0	14.0	37.0	37.2	285.5
	1992	84.0	46.1	42.5	6.2	8.0	0.0	0.0	0.0	4.0	10.6	37.0	82.0	320.4
	Normal (1981:05-1980:12)	68.3	51.0	49.1	16.2	3.5	0.5	0.0	0.0	1.0	11.8	39.2	75.3	317.1
Total Precipitation (mm)	1991	70.0	31.3	59.0	52.0	70.9	48.7	64.0	119.1	99.7	114.3	85.1	42.8	856.9
	1992	84.0	46.1	44.5	87.8	74.5	64.5	89.9	128.6	158.8	68.4	107.9	86.0	*******
	Normal (1981:05-1980:12)	69.9	55.3	63.5	55.5	91.6	95.7	105.0	100.9	113.7	97.7	70.4	80.9	936.7
Snow Pack, month end (cm)	1991	40.0	50.0	35.0	0.0	0.0	0.0	0.0	0.0	0.0	0.0	0.0	12.0	-
	1992	47.0	52.0	43.0	0.0	0.0	0.0	0.0	0.0	0.0	0.0	na	na	-
	Normal (1981:05-1980:12)	49.6	50.3	41.3	0.2	0.0	0.0	0.0	0.0	0.0	0.9	4.0	23.0	-
Potential ET (mm) a/	Normal (1981:05-1980:12)	-	-	-	12.7	68.2	100.1	124.1	102.9	63.7	26.1	-	-	497.8
Temperature, Average (C)	1991	-18.6	-12.0	-7.7	3.3	10.6	16.0	17.1	16.4	9.3	4.3	-2.6	-13.2	1.9
	1992	-17.0	-16.7	-11.8	-0.5	9.5	12.0	14.5	13.9	10.9	2.4	-4.9	-11.5	0.1
	Normal (1981:05-1980:12)	-16.9	-14.5	-8.3	1.6	9.2	13.8	17.4	15.6	10.8	4.5	-3.5	-13.3	1.3
Temperature, Maximum (C)	1991	-12.0	-5.7	-0.2	9.6	17.5	23.5	24.2	23.1	14.4	8.5	1.3	-7.7	8.0
	1992	-11.0	-9.9	-4.3	5.5	16.8	18.7	20.6	19.8	15.7	6.2	-1.1	-6.0	5.9
	Normal (1981:05-1980:12)	-10.6	-8.0	-1.8	7.5	15.8	20.1	23.7	21.2	15.6	8.9	-0.0	-8.1	6.9
Temperature, Minimum (C)	1991	-25.2	-18.2	-7.7	-3.0	3.6	8.4	10.0	9.7	4.2	0.0	-6.5	-18.7	-3.6
	1992	-22.9	-23.4	-19.2	-6.4	2.2	5.2	8.4	8.0	6.0	-1.5	-8.6	-17.0	-5.8
	Normal (1981:05-1980:12)	-23.1	-21.0	-14.7	-4.3	2.5	7.5	11.1	9.9	6.0	0.1	-7.0	-18.4	-4.3

a/ Potential Evapotranspiration calculated with the Thornthwaite method (1948), Geol. Rev. 38 (1): 55-94.
na = not available

APPENDIX B

HYDRAULIC HEADS DATA AT WAITE AMULET COVERS SITE

October 1990

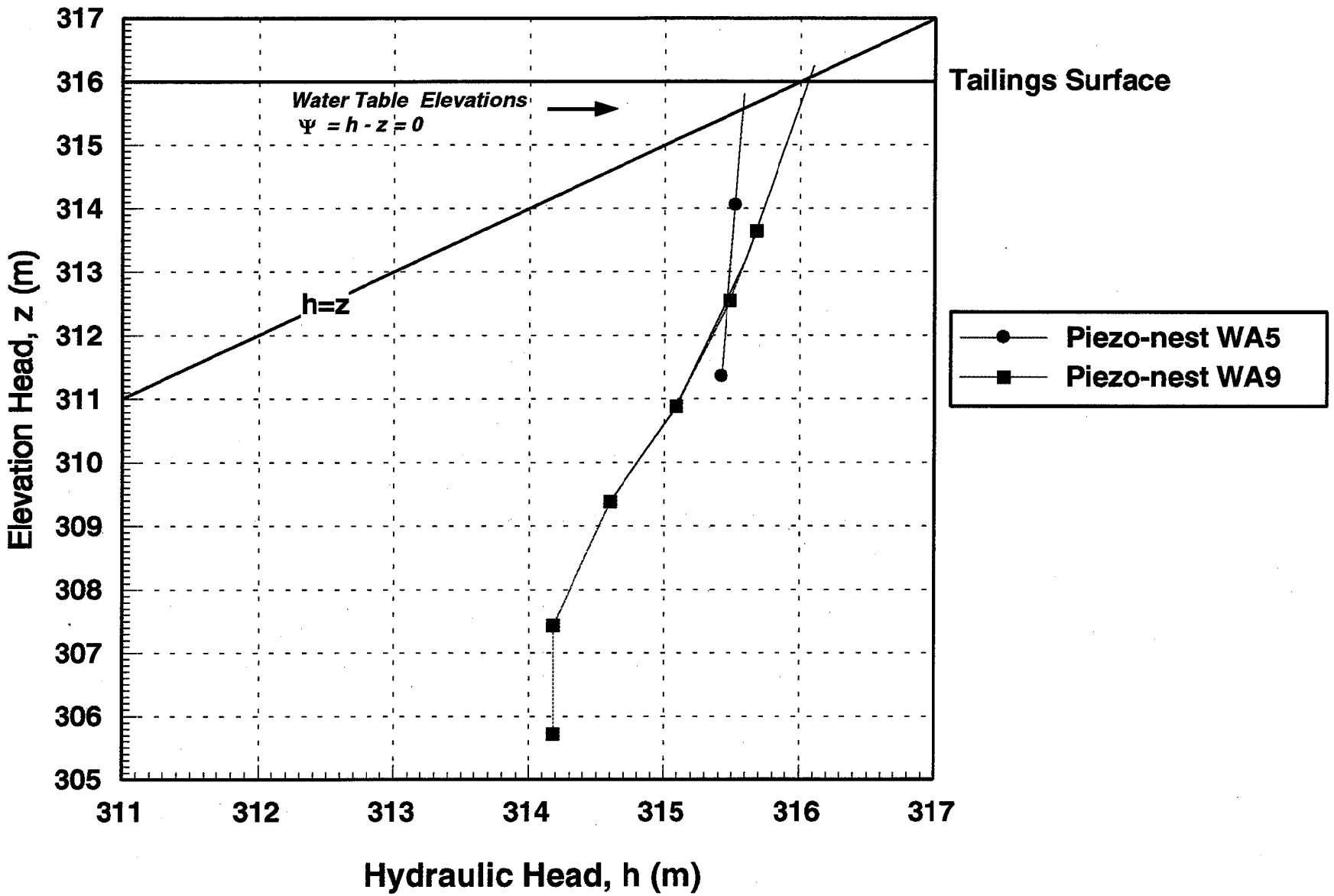

Table 1. Hydraulic Heads at the Waite Amulet Experimental Covers Site.

Piezometer Number	Piezometer Elevations			Water Level Elevations (Hydraulic Heads)									
	Top (m)	Ground (m)	Screen (m)	Oct 90 (m)	Nov 90 (m)	Feb 91 (m)	May 91 (m)	Jul 91 (m)	Oct 91 (m)	Mar 92 (m)	May 92 (m)	Oct 92 (m)	Nov 92 (m)
R1-1	317.34	316.24	312.29	316.00	316.06	314.58	315.89	314.89	315.77	-	315.88	315.64	315.71
R1-2	317.42	316.35	314.28	316.07	316.09	ICE	316.02	314.85	315.84	-	315.82	315.65	315.66
R2-1	317.56	317.58	312.17	315.69	315.96	314.42	316.05	315.02	315.72	-	315.91	315.80	315.66
R2-2	317.58	317.58	314.16	315.87	315.80	314.55	315.77	314.84	315.59	-	315.73	315.58	315.95
R3-1	317.67	317.47	312.22	315.73	315.77	314.53	315.80	314.92	315.56	-	315.71	315.60	315.69
R3-2	317.56	317.41	314.11	315.75	315.80	314.46	315.82	315.03	315.68	-	315.77	315.70	315.87
R4-1	317.01	316.64	312.16	315.73	315.47	314.51	315.76	314.91	315.54	-	315.67	315.59	315.62
R4-2	317.11	316.85	314.26	316.00	315.97	314.60	316.04	315.24	315.91	-	316.15	315.93	316.06
WA5-1	317.10	315.75	311.35	315.42	-	314.15	315.46	314.51	315.35	313.63	315.45	-	-
WA5-2	317.11	315.77	314.05	315.52	-	314.10	315.54	314.51	315.51	DRY	315.57	-	-
WA9-1	317.13	316.05	309.38	314.60	-	313.48	314.61	313.76	314.36	313.00	314.40	-	314.55
WA9-2	317.12	316.07	314.44	315.33	-	ICE	315.65	DRY	315.89	-	315.72	-	-
WA9-3	317.13	316.07	310.88	315.09	-	313.71	315.01	313.96	314.76	313.18	314.79	-	314.88
WA9-4	317.09	316.07	312.55	315.48	-	313.95	315.41	314.26	315.25	313.43	315.29	-	315.35
WA9-5	317.13	316.04	313.64	315.68	-	314.03	315.57	314.28	315.50	313.63	315.48	-	315.47
WA9-6	317.28	316.04	307.43	314.18	-	313.14	314.21	313.34	313.96	312.61	314.01	-	314.16
WA9-7	317.14	316.10	305.71	314.18	-	313.07	314.17	313.31	314.00	-	-	-	-
WA10-1	317.12	316.42	309.12	-	-	-	315.54	314.71	314.92	-	315.19	-	315.39
WA10-2	317.16	316.40	314.82	-	-	-	315.65	315.01	314.92	-	315.07	-	315.45

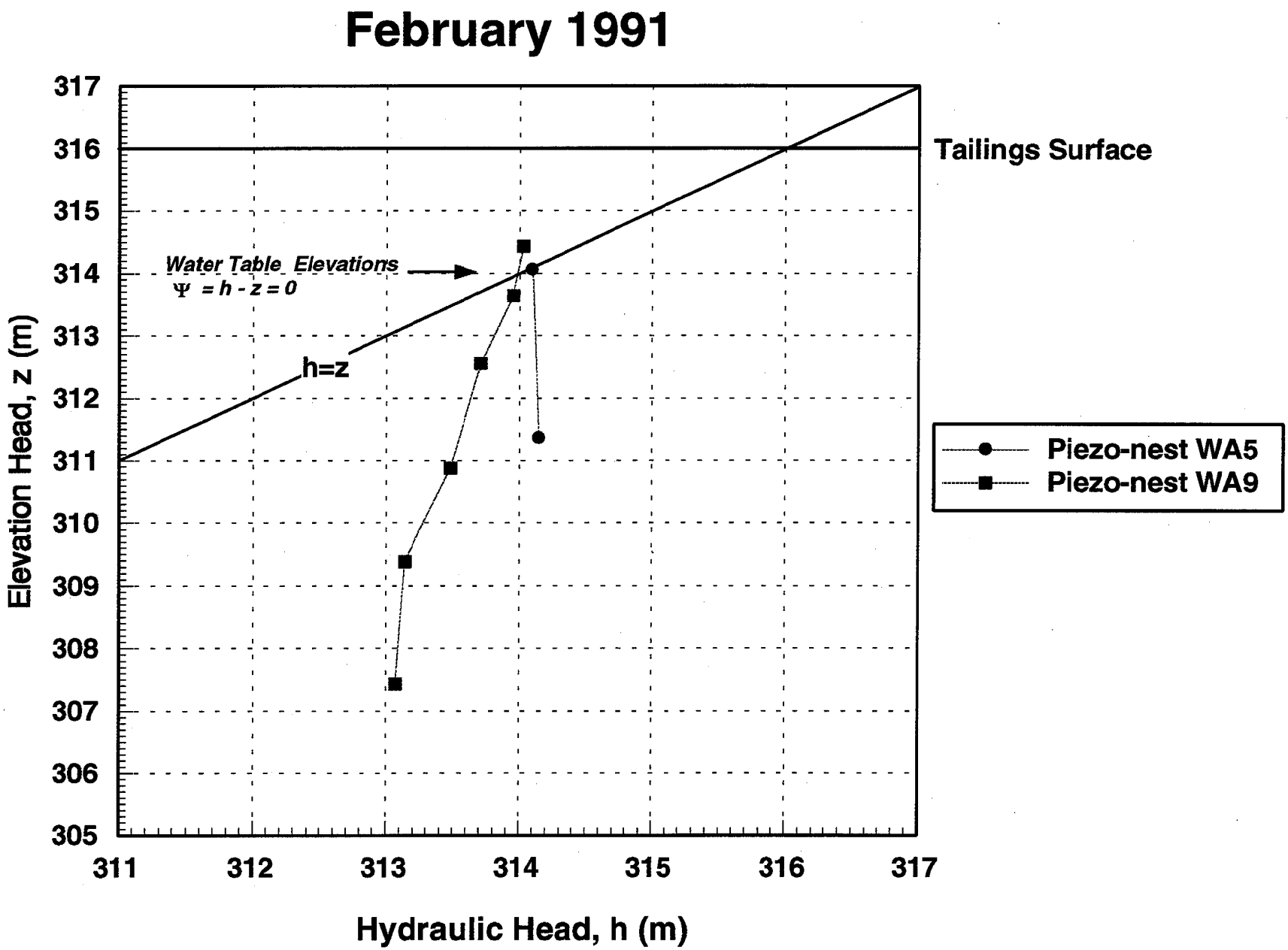
February 1991
317
316
315
314
313
312
311
310
309
308
307
306
305
Elevation Head, z (m)
Water Table Elevations
Ψ = h - z = 0
h=z
Tailings Surface
Piezo-nest WA5
Piezo-nest WA9
311
312
313
314
315
316
317
Hydraulic Head, h (m)

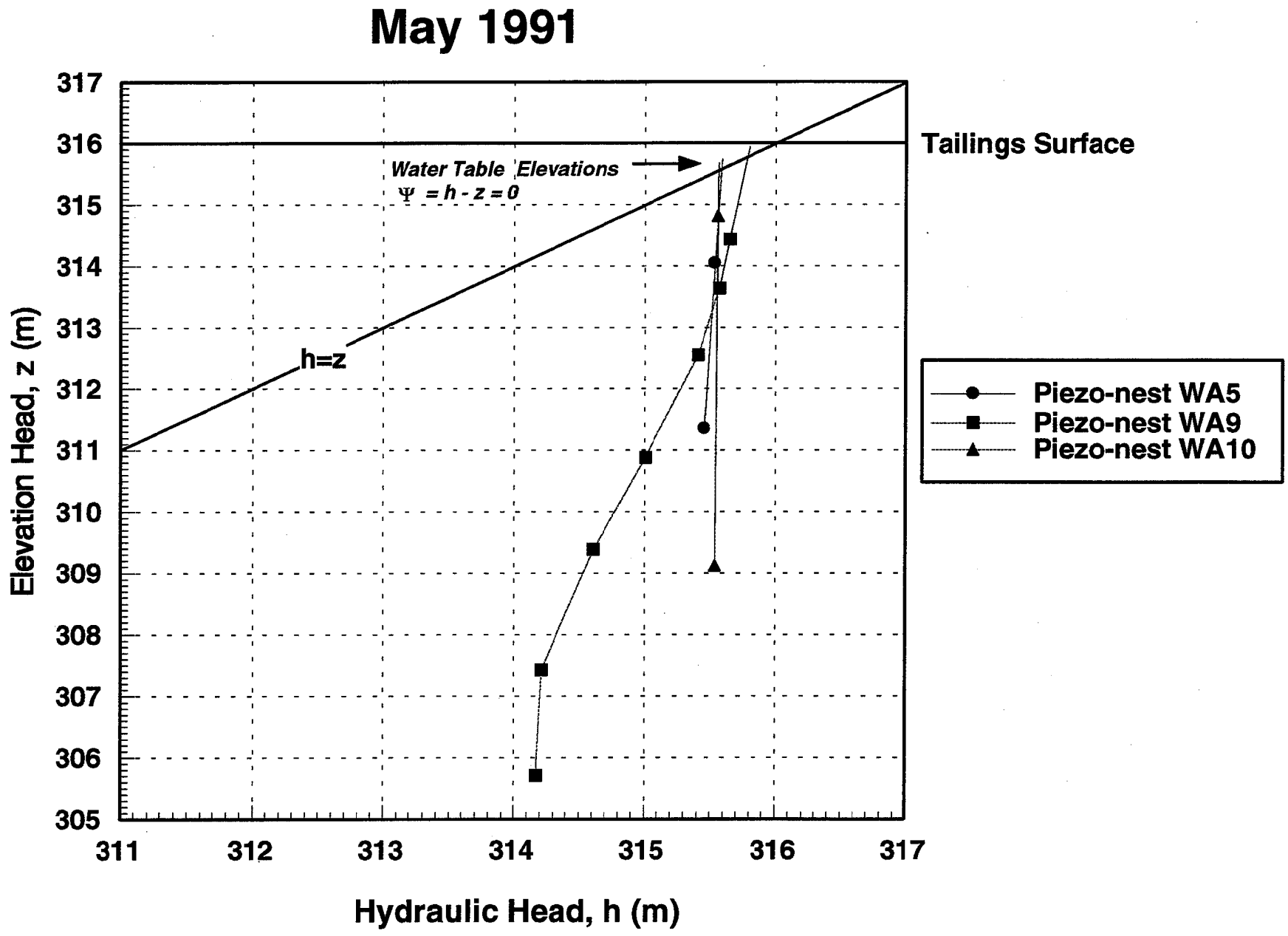
May 1991
Tailings Surface
Water Table Elevations
Ψ = h - z = 0
h=z
Piezo-nest WA5
Piezo-nest WA9
Piezo-nest WA10
Elevation Head, z (m)
Hydraulic Head, h (m)
317
316
315
314
313
312
311
310
309
308
307
306
305
311
312
313
314
315
316
317

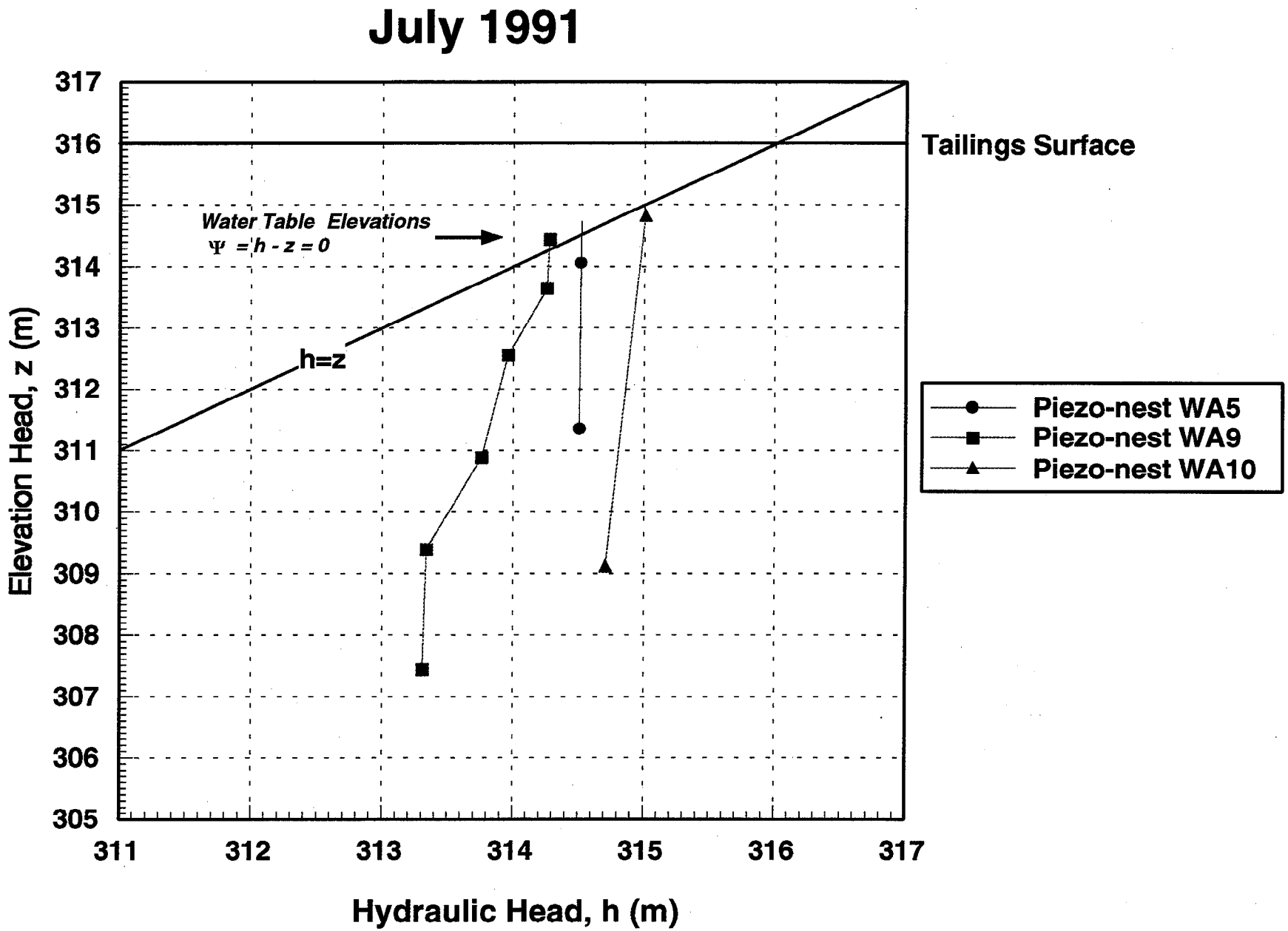
July 1991
317
316
315
314
313
312
311
310
309
308
307
306
305
Elevation Head, z (m)
311
312
313
314
315
316
317
Hydraulic Head, h (m)
Water Table Elevations
Ψ = h - z = 0
h=z
Tailings Surface
Piezo-nest WA5
Piezo-nest WA9
Piezo-nest WA10

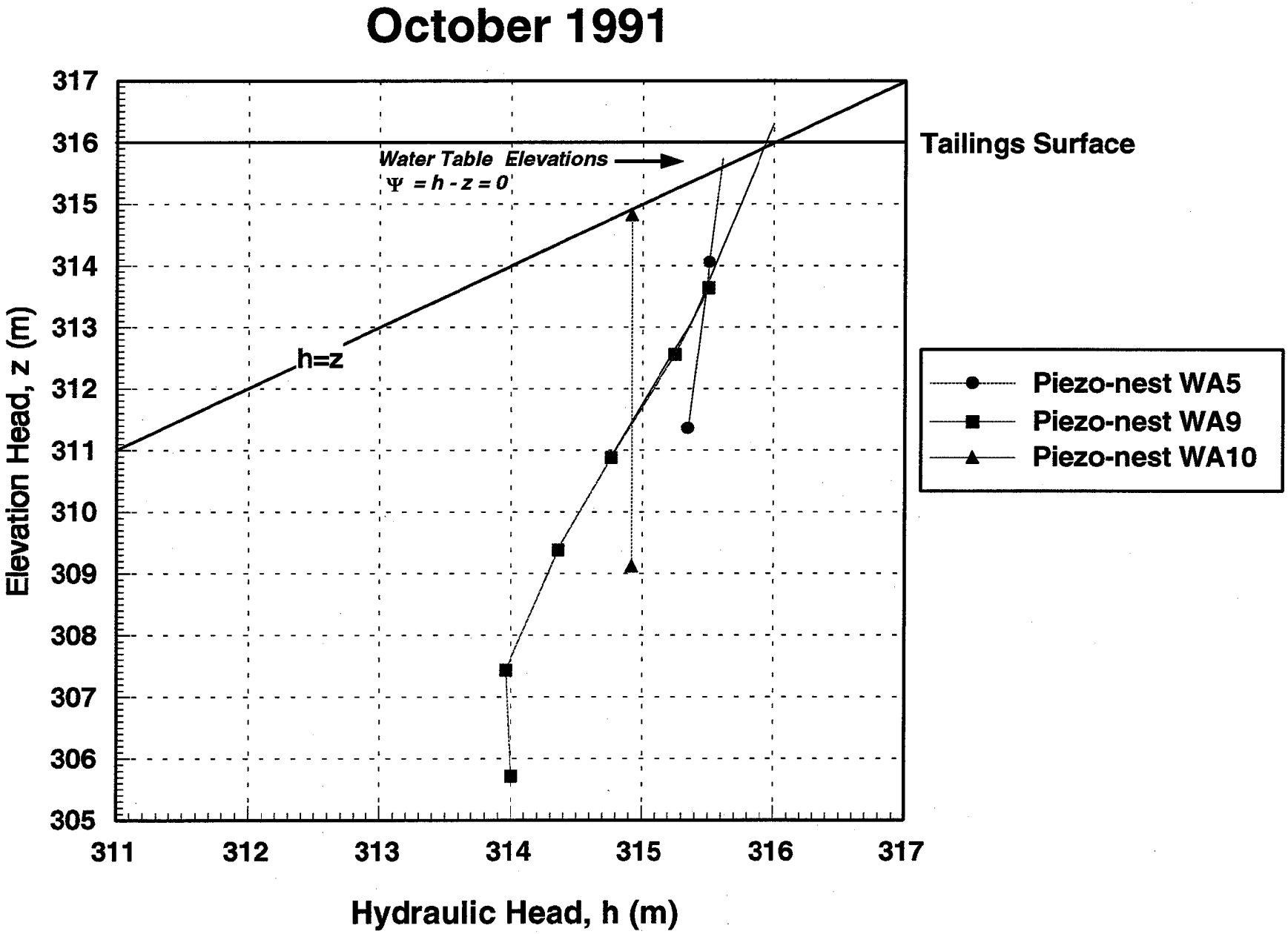
October 1991
Tailings Surface
Water Table Elevations
Ψ = h - z = 0
h=z
Piezo-nest WA5
Piezo-nest WA9
Piezo-nest WA10
Elevation Head, z (m)
Hydraulic Head, h (m)
317
316
315
314
313
312
311
310
309
308
307
306
305
311
312
313
314
315
316
317

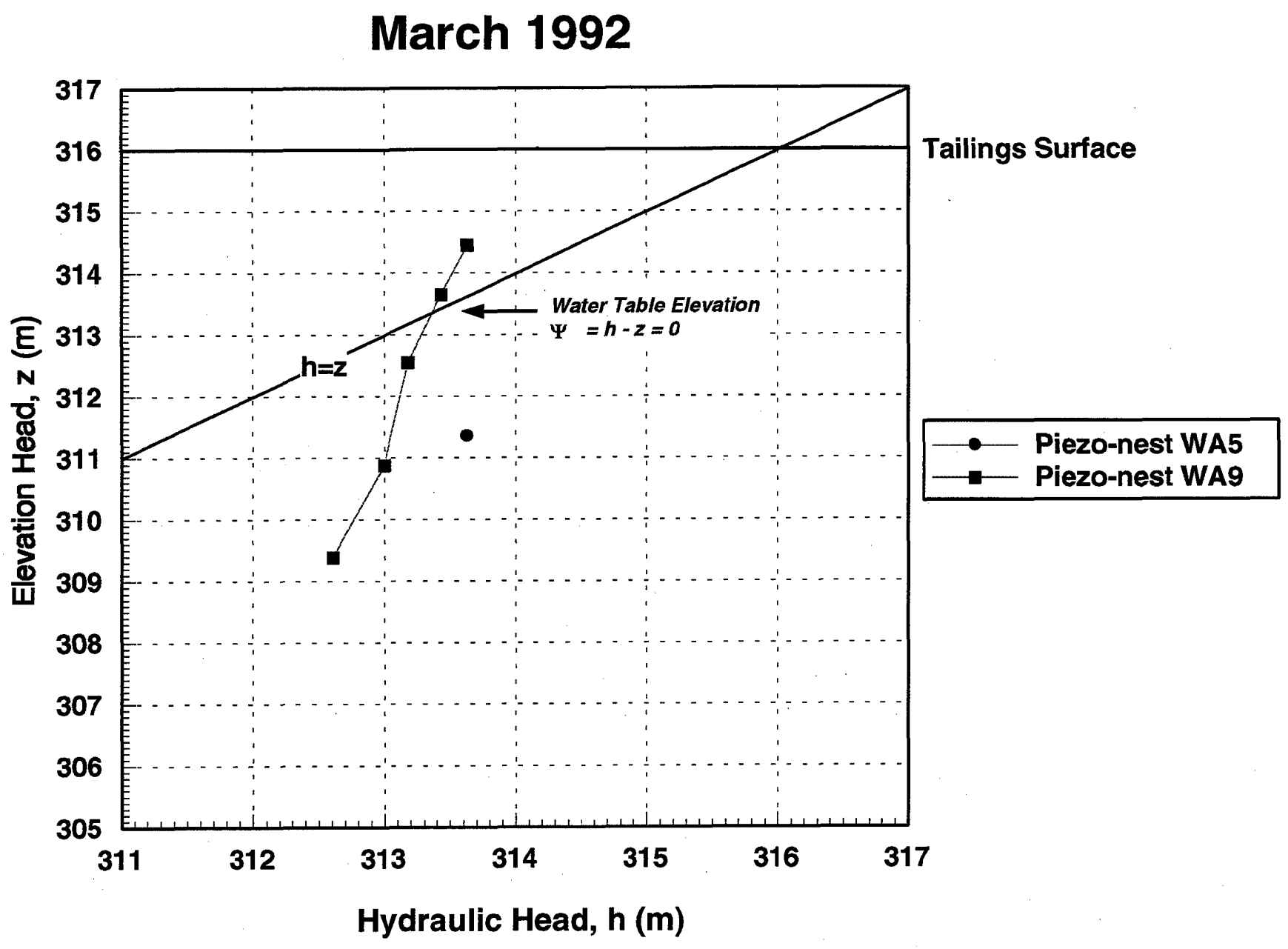
March 1992
317
316
315
314
313
312
311
310
309
308
307
306
305
Elevation Head, z (m)
311
312
313
314
315
316
317
Hydraulic Head, h (m)
Tailings Surface
Water Table Elevation
Ψ = h - z = 0
h=z
Piezo-nest WA5
Piezo-nest WA9

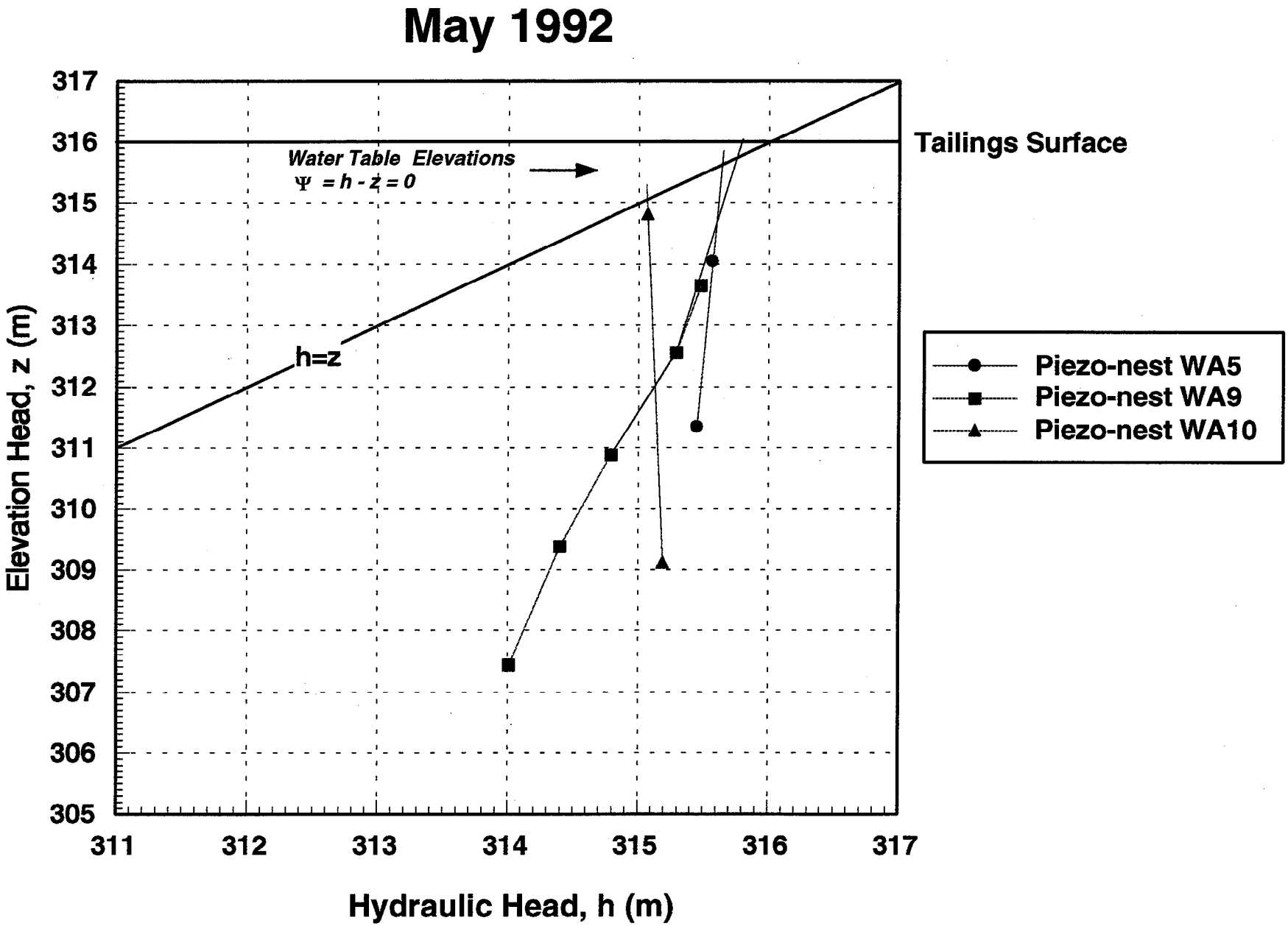
May 1992
Tailings Surface
Water Table Elevations
Ψ = h - z = 0
h=z
Piezo-nest WA5
Piezo-nest WA9
Piezo-nest WA10
Elevation Head, z (m)
Hydraulic Head, h (m)
317
316
315
314
313
312
311
310
309
308
307
306
305
311
312
313
314
315
316
317

November 1992

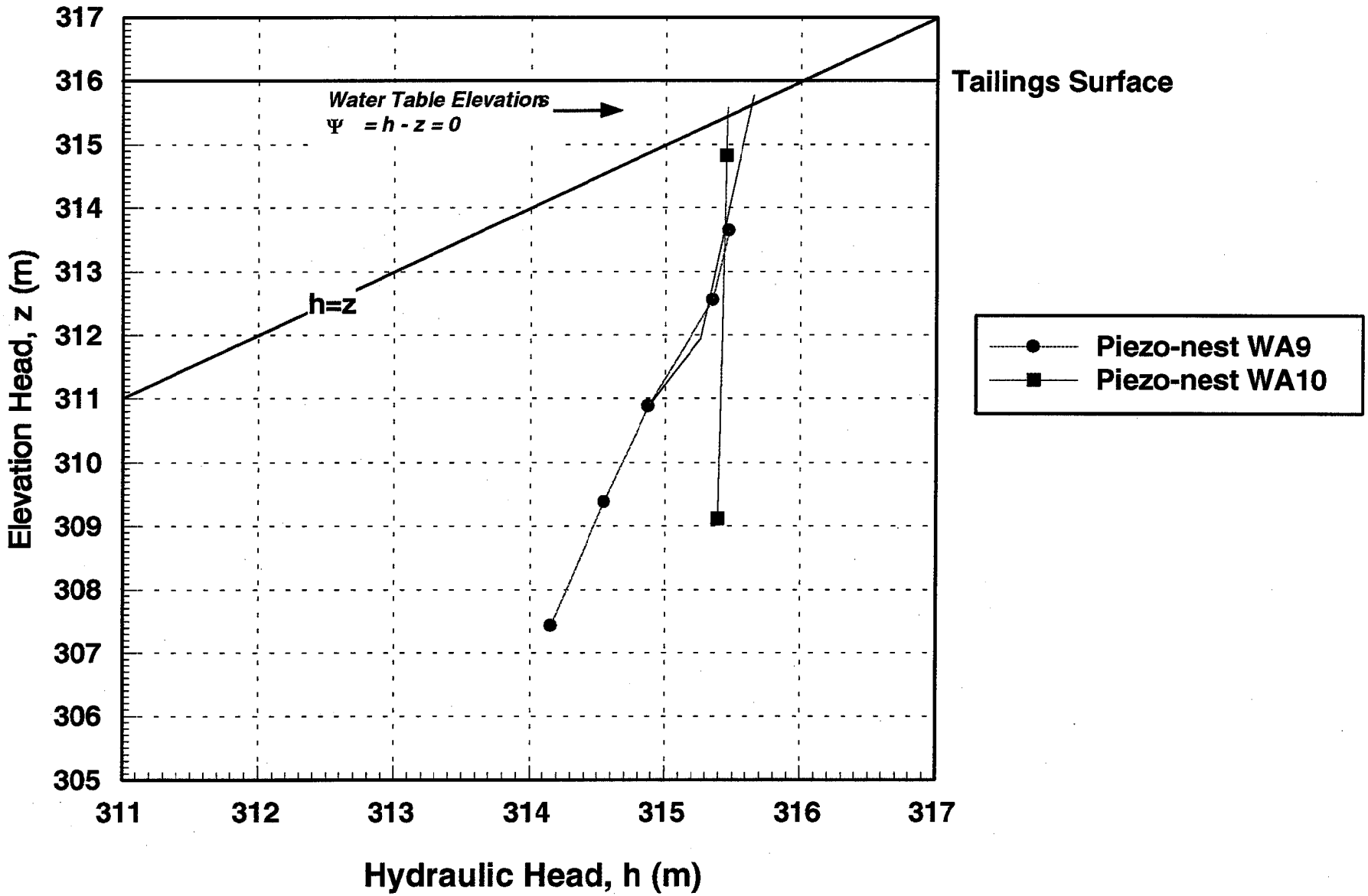

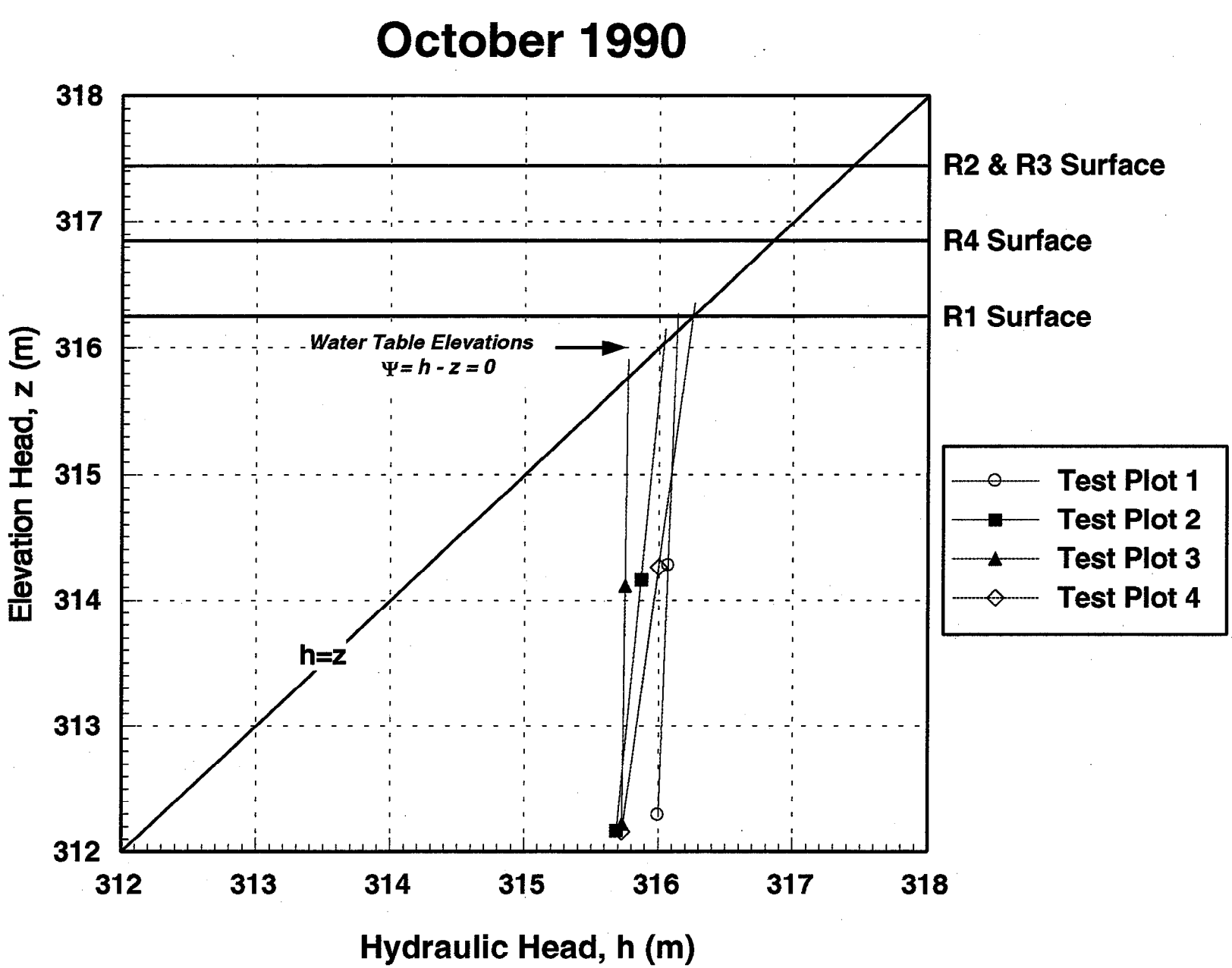
October 1990
318
317
316
315
314
313
312
312
313
314
315
316
317
318
Elevation Head, z (m)
Hydraulic Head, h (m)
R2 & R3 Surface
R4 Surface
R1 Surface
Water Table Elevations
Ψ = h - z = 0
h=z
Test Plot 1
Test Plot 2
Test Plot 3
Test Plot 4

November 1990

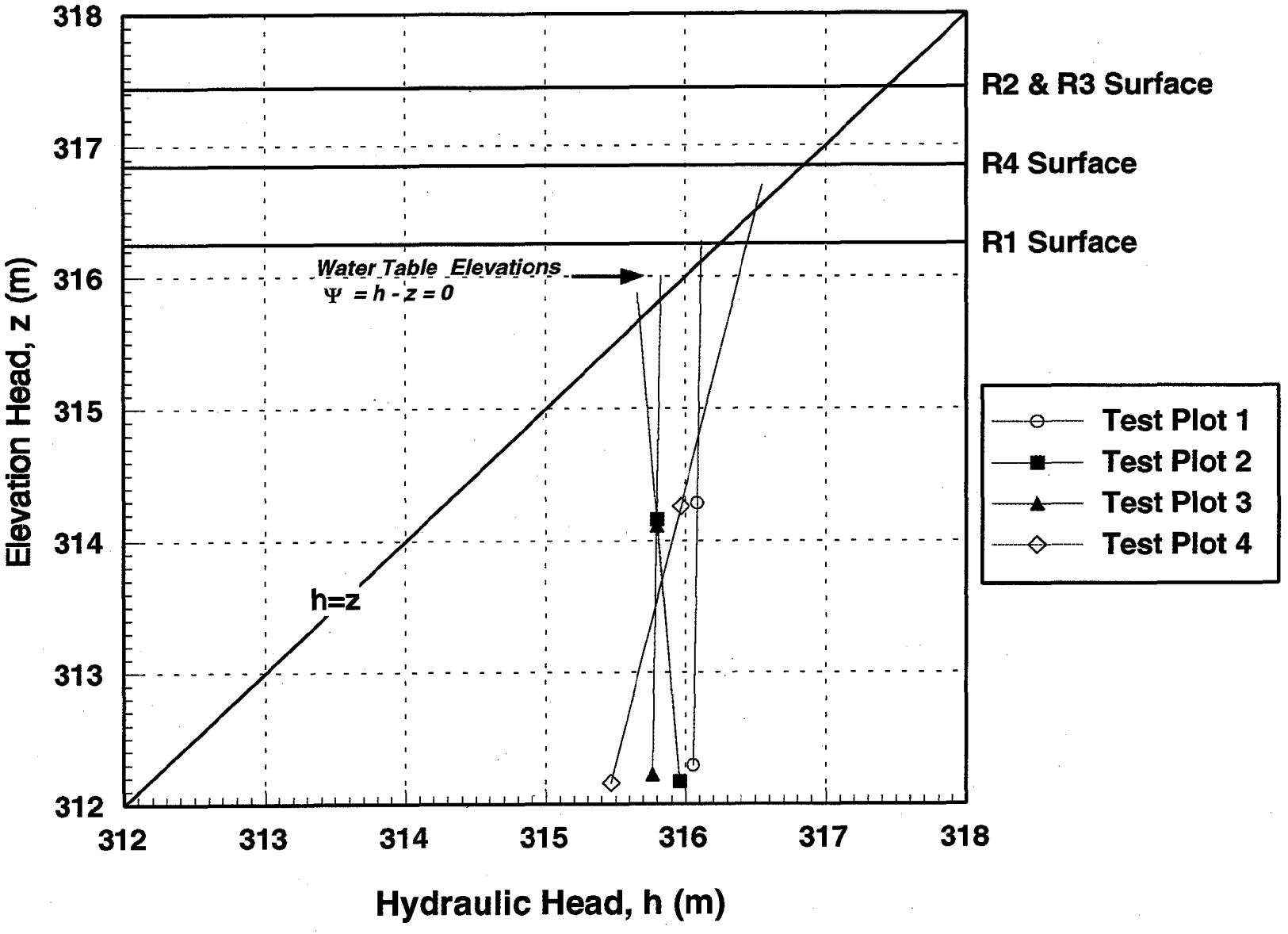

February 1991

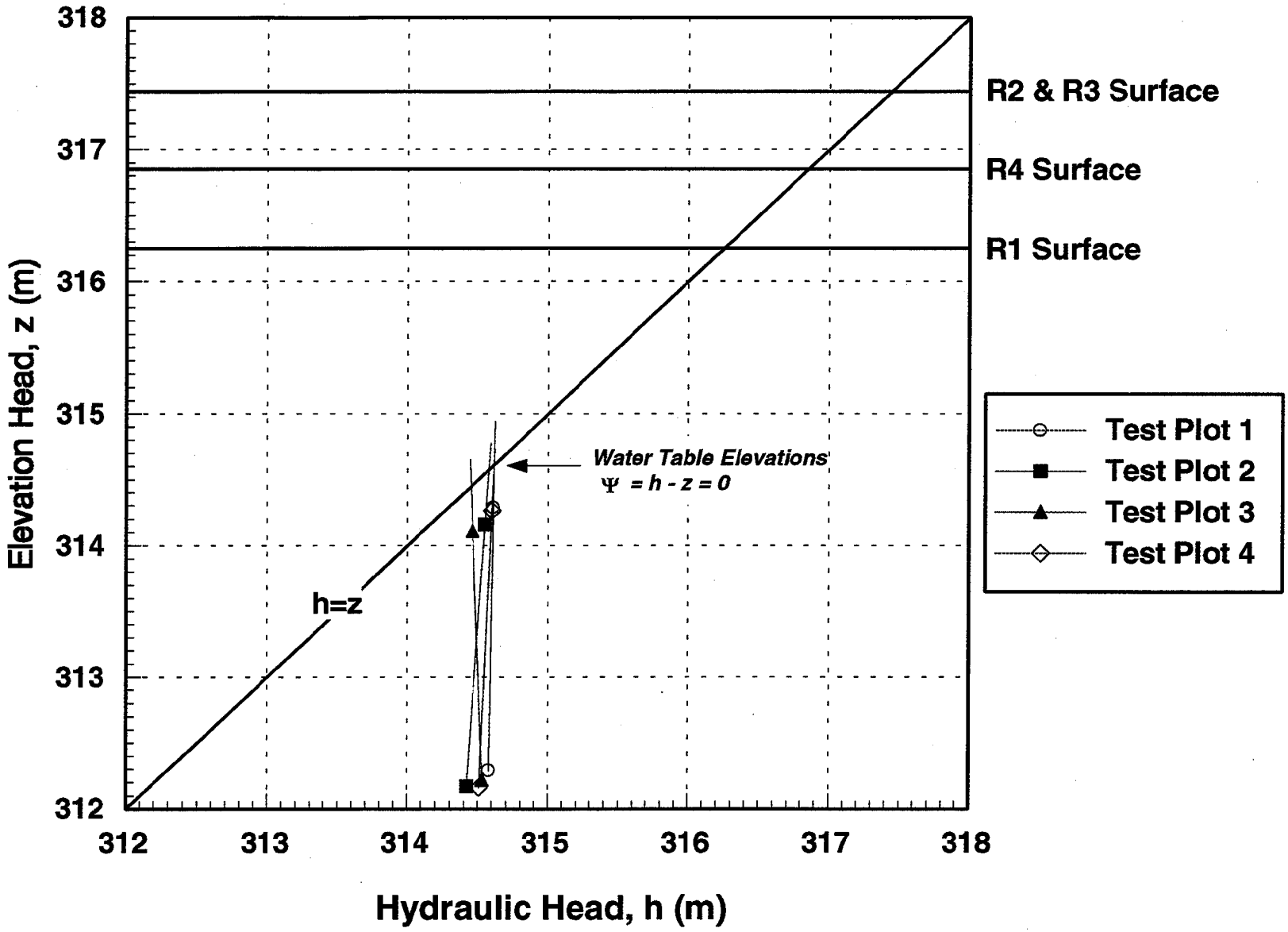

May 1991

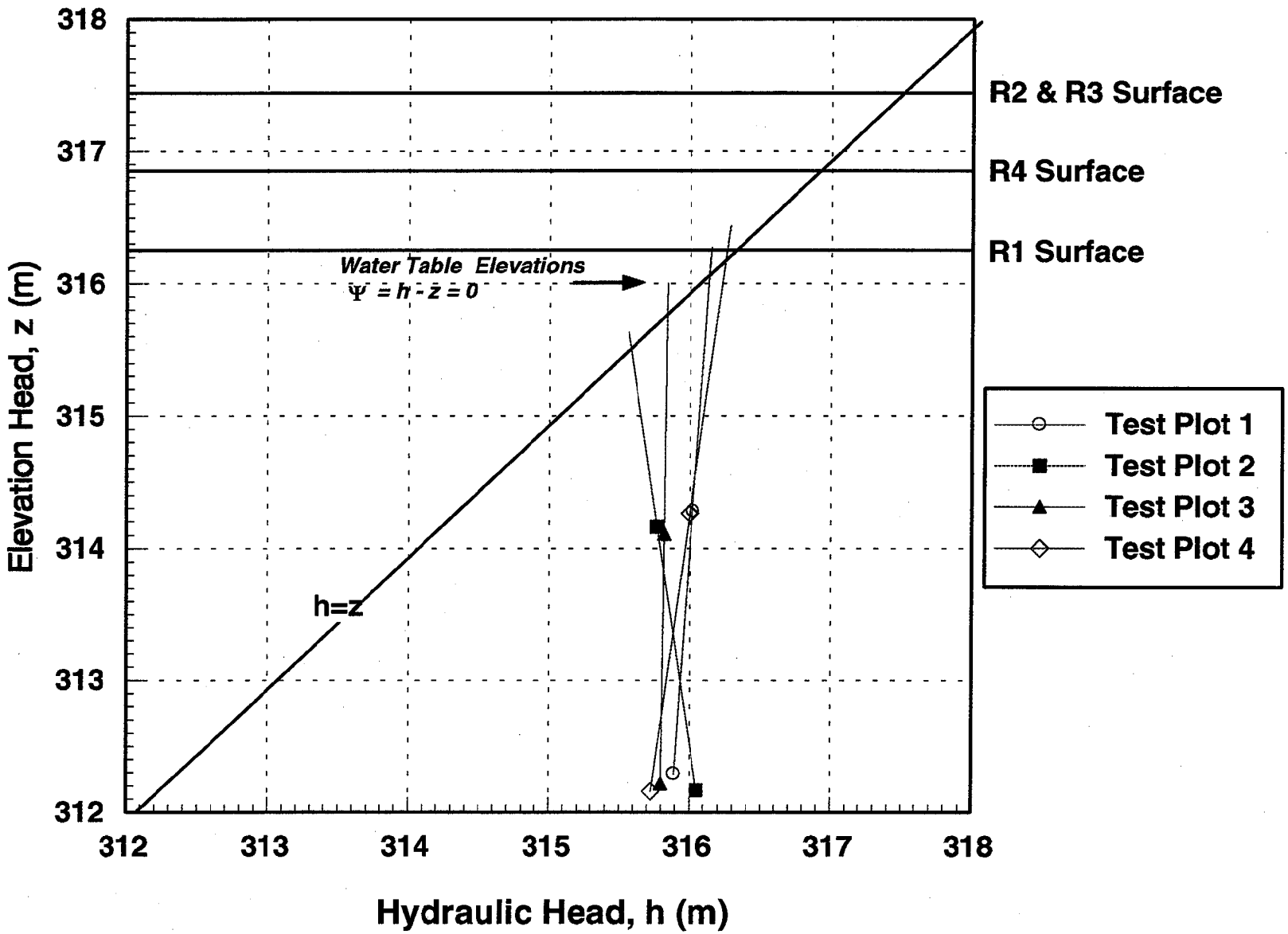
318
317
316
315
314
313
312
312
313
314
315
316
317
318
Elevation Head, z (m)
Hydraulic Head, h (m)
R2 & R3 Surface
R4 Surface
R1 Surface
Water Table Elevations
Ψ = h - z = 0
h=z
Test Plot 1
Test Plot 2
Test Plot 3
Test Plot 4

July 1991

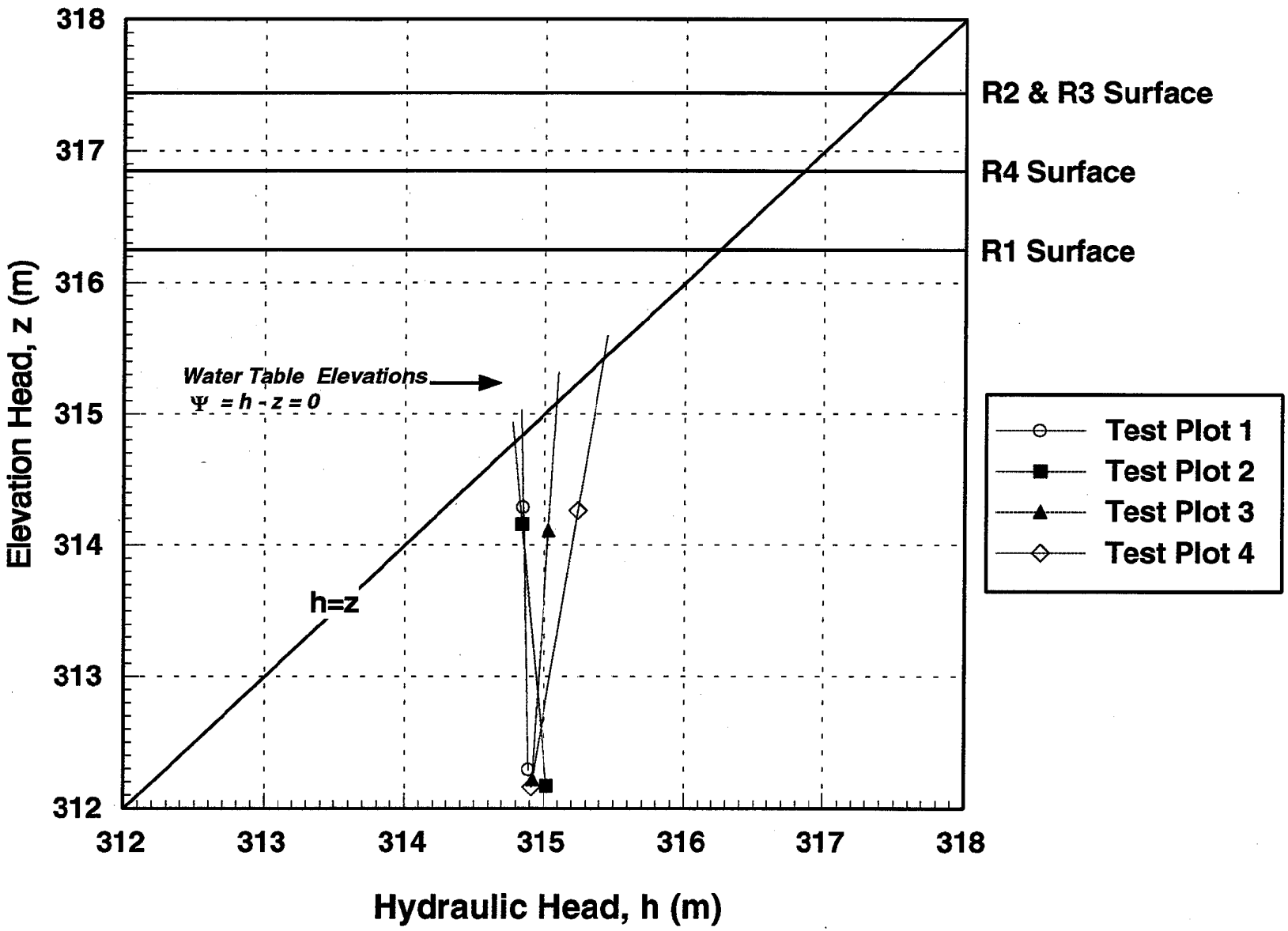
318
317
316
315
314
313
312
312
313
314
315
316
317
318
Elevation Head, z (m)
Hydraulic Head, h (m)
R2 & R3 Surface
R4 Surface
R1 Surface
Water Table Elevations
Ψ = h - z = 0
h=z
Test Plot 1
Test Plot 2
Test Plot 3
Test Plot 4

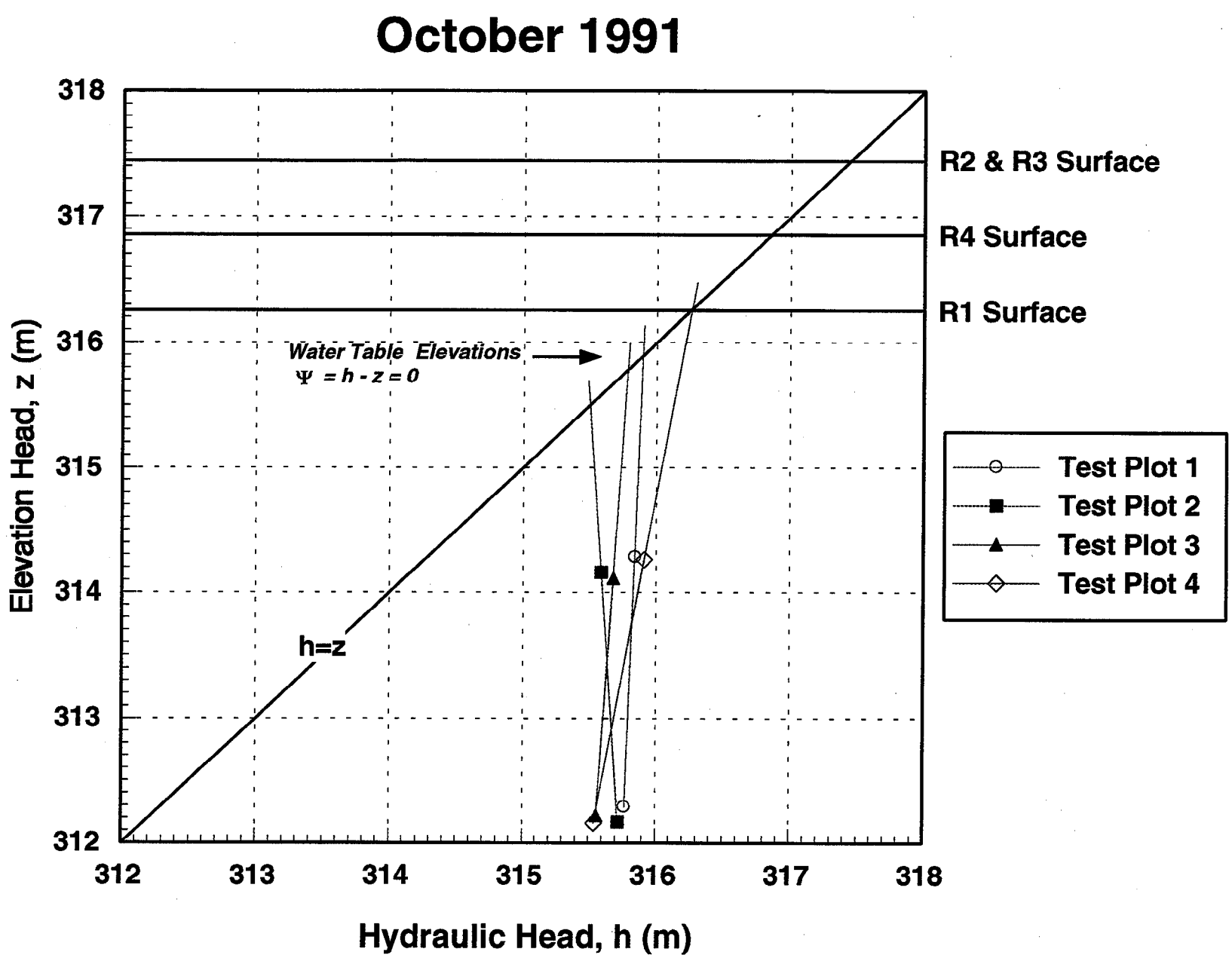
October 1991
318
317
316
315
314
313
312
312
313
314
315
316
317
318
Elevation Head, z (m)
Hydraulic Head, h (m)
R2 & R3 Surface
R4 Surface
R1 Surface
Water Table Elevations
Ψ = h - z = 0
h=z
Test Plot 1
Test Plot 2
Test Plot 3
Test Plot 4

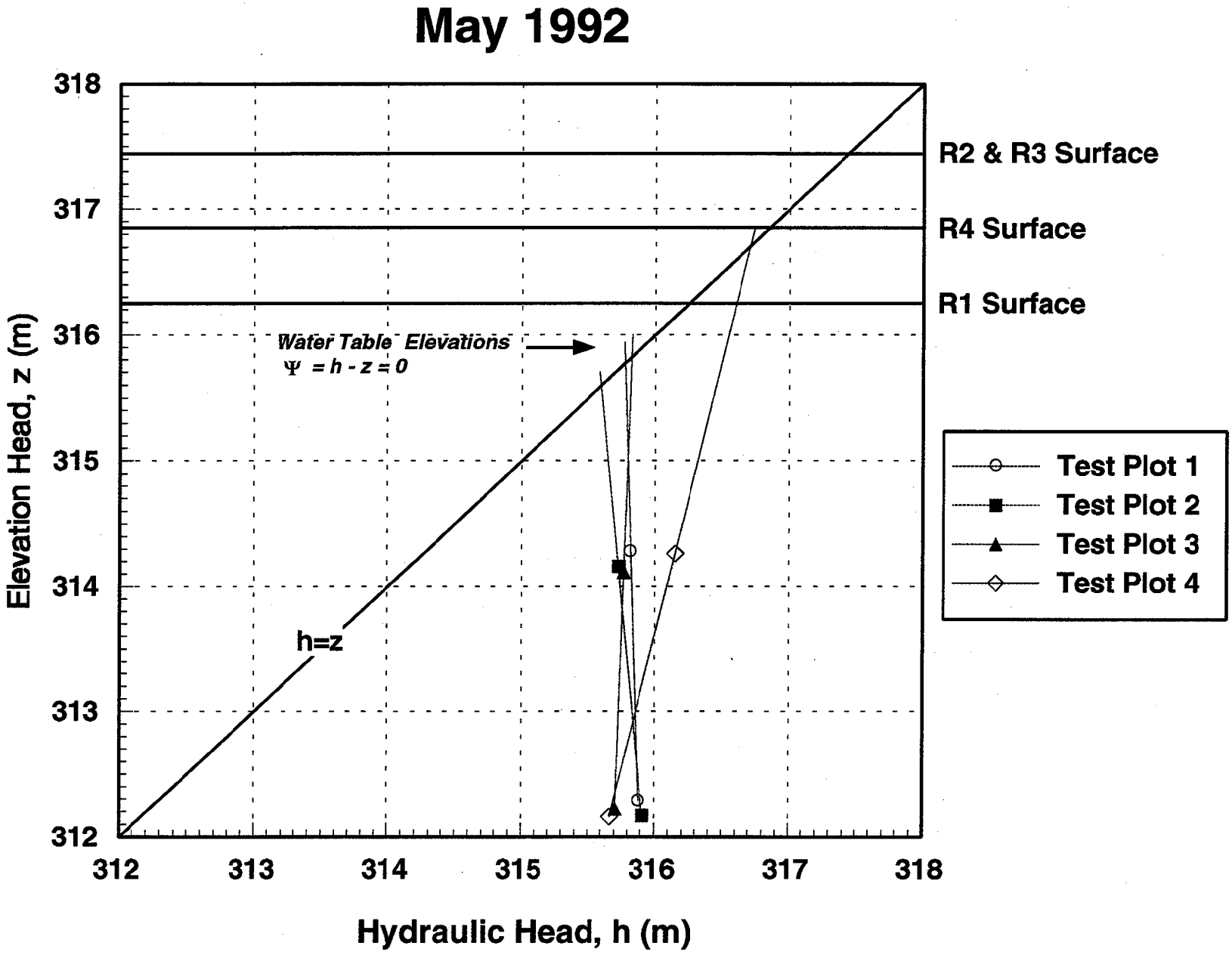
May 1992
318
317
316
315
314
313
312
312
313
314
315
316
317
318
Elevation Head, z (m)
Hydraulic Head, h (m)
R2 & R3 Surface
R4 Surface
R1 Surface
Water Table Elevations
Ψ = h - z = 0
h=z
Test Plot 1
Test Plot 2
Test Plot 3
Test Plot 4

November 1992

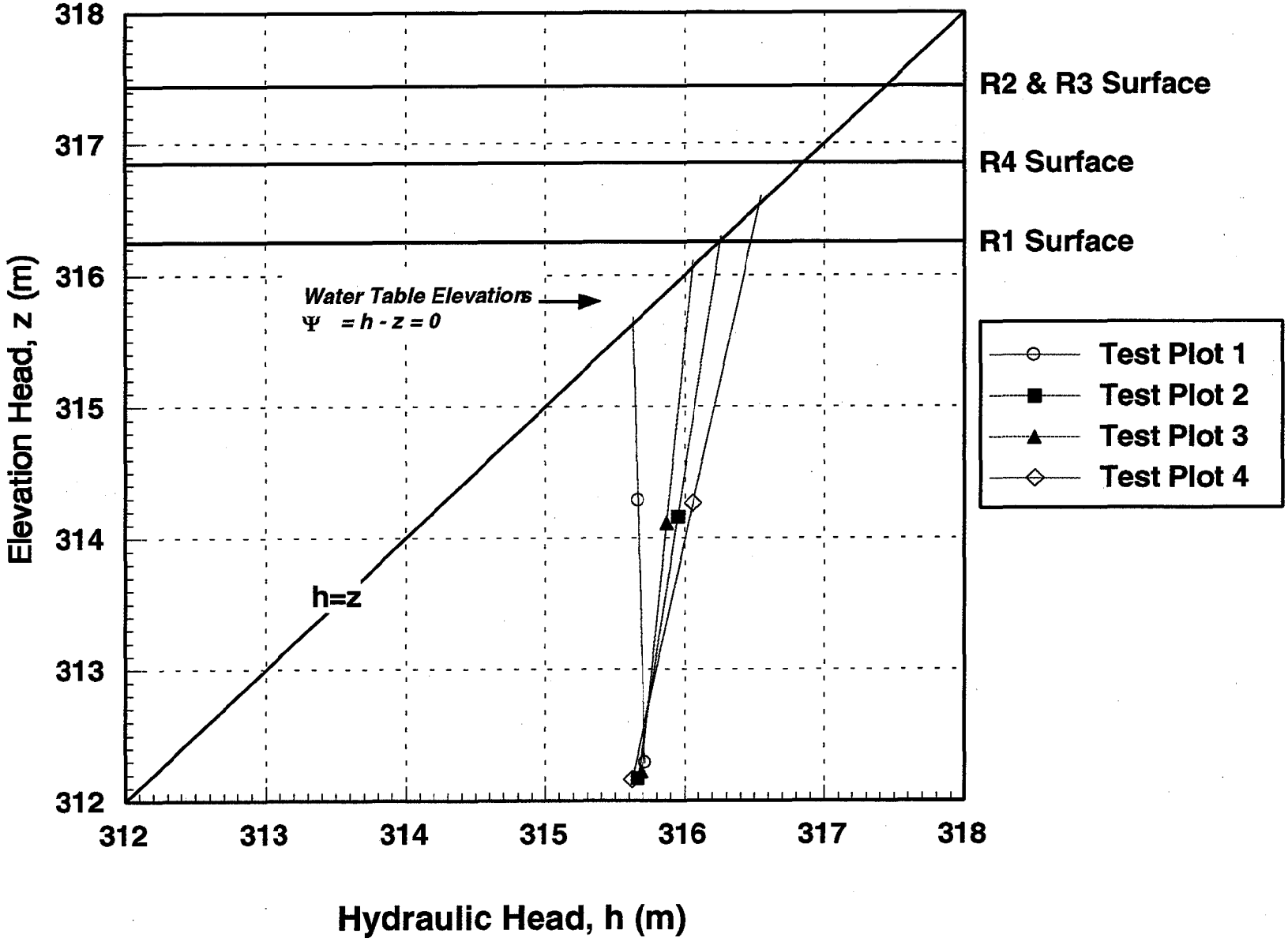

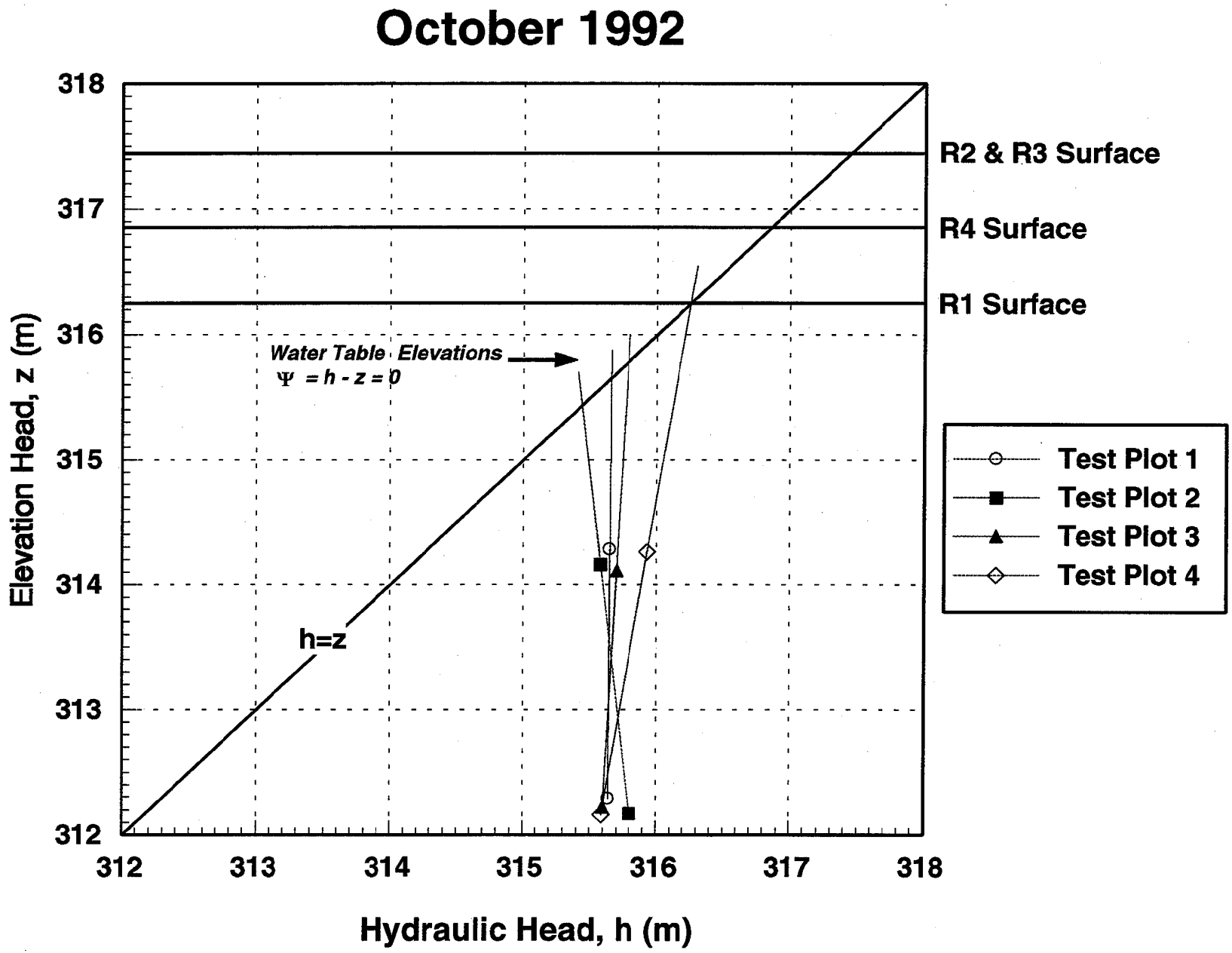
October 1992
318
317
316
315
314
313
312
312
313
314
315
316
317
318
Elevation Head, z (m)
Hydraulic Head, h (m)
R2 & R3 Surface
R4 Surface
R1 Surface
Water Table Elevations
Ψ = h - z = 0
h=z
Test Plot 1
Test Plot 2
Test Plot 3
Test Plot 4

APPENDIX C

FIELD MONITORING DURING 1993

APPENDIX C: FIELD MONITORING DURING 1993

Field Activities

During 1993, precipitation and pan evaporation were measured with a data logger from June to September and site visits were conducted in May, June, August and September. Discharge volumes from the lysimeters and water levels in the piezometers were measured. Water samples of the lysimeter outflow and of the tailings saturated-zone were collected and analyzed for major metal and ion concentrations by ICP method. The clay covers (R2 and R3) and the control (R1) were augered and soil samples recovered. Porewater samples from the clay and tailings were extracted by squeezing and samples of the sand base were washed. The collected water samples were analyzed for major metal and ion concentrations. Samples of the lysimeter tailings solids were analyzed for total sulphur as an indication of alteration by oxidation. Pore gas oxygen content was measured *in situ* as and indication of the rate of oxidation. Water content of all soil samples were measured by gravimetry, and at the site, water content was measured by time-domain reflectometry (TDR). Saturated hydraulic conductivity of the clay was measured *in situ* with an air-entry permeameter to verify any changes due to freeze/thaw.

Findings

In the latter part of 1992, when the lysimeters beneath the covers began to report water, the lysimeter discharge valves were closed and only opened to measure and sample the discharge volume. During 1993, when the valve at R3 was opened, an initial volume of accumulated water was released, followed by a continuous trickle of approximately 1 L/min. This suggests that the discharge pipe leading between the lysimeter and the manhole is cracked, allowing water from the saturated tailings mass to enter the pipe. Water quality data (presented later) also support this hypothesis. The crack may have originated close the manhole, above the shut-off valve, where accumulated water in the pipe could have frozen during winter. The lysimeter at R3 was therefore declared non-functional and the data discarded. The lysimeter at R2, however, appeared quite functional and outflow volumes were measured. Table 3 shows the observed percolation through the clay cover which drained from the lysimeter at R2. Percolation was observed to be 4% of precipitation which is consistent with the results from the HELP model. As expected, the lysimeter at R4 (geomembrane cover) did not report water in 1993.

The HELP modelling exercise can also be corroborated with the evaporation measurements. In 1993, pan evaporation was measured from June 11 to September 22 and was observed to be 431 mm. Precipitation during the same period was observed to be 361 mm. The HELP model predicted evaporation from the cover to be 69% of precipitation from June through September. 69% of the measured precipitation is 249 mm, or 58% of the measured pan evaporation. Therefore, the actual evaporation is 58% of pan evaporation, which is reasonable for a well drained non-vegetated soil in the Abitibi region. For example, evaporation from non-vegetated tailings at the Kidd Creek thickened tailings cone near Timmins, Ontario was observed to be 55% of pan evaporation.

Likewise, for a small reservoir where the lack of water does not limit evaporation, 70% is common. Therefore, field observations of evaporation confirm the results of the HELP modelling exercise.

TDR measurements during 1993 (Table 4) show no change in saturation and therefore indicate that the capillary barrier continued to function in 1993. These results are supported by gravimetric water content measurements (Fig. 1). Figure 1 also shows a higher degree of saturation of the tailings mass as compared to that of the lysimeter tailings. In the lysimeter, the tailings are isolated from the tailings mass and drain to residual saturation, which appears to be about 17% by weight. In the tailings mass, water extends above the water table, due to surface tension, manifesting in a zone of higher saturation called the "capillary fringe". The tailings in the lysimeter at R1 are not at residual saturation because they are exposed to influx of water by precipitation.

Water levels in the piezometers were measured in May, August and September (Table 5). Figure 2 features the water table elevations which were calculated from these measurements. No significant changes were observed in 1993.

The hydraulic conductivity (K) of the clay at R2 and R3 were measured in 1993, as they were in 1991 and 1992. Laboratory experiments (Mohamed *et al.* 1992) showed that K increases approximately two orders of magnitude after the first freeze-thaw cycle and changes little with subsequent freeze-thaw cycles. At the field test site, an increase of K from the initial measurement of 1×10^{-7} cm/s was not observed. Therefore, future degradation of K due to freezing and thawing is not anticipated.

Samples of the lysimeter discharge and the saturated-zone tailings porewater were analyzed for major metal and ion concentrations; the water quality results appear in Tables 6 and 7, respectively. Table 8 summarizes the results with regard to pH, acidity, SO_4, Fe(T) and Zn. The lysimeter discharge at R3 appears to be a mix of lysimeter water and groundwater from the tailings mass, which supports the hypothesis that the lysimeter discharge pipe is cracked. At R2, there appears to be a slight improvement in the quality of water reporting from the lysimeter, while at R1, the uncovered (control) plot, the water quality has degraded. Likewise, the shallow saturated-zone of the tailings below the covers shows a similar trend. In general, though, the chemical data supports the inference presented in the body of the report that, in the short term, stored acidity in the tailings precludes any confirmed observable improvements of pore water quality. This is expected since a maximum of 50 mm of infiltration has flushed the tailings in lysimeter R2, which is only about 1/6 of a pore volume. In the lab, the cover simulation column experiments have shown that approximately 1 pore volume of water was needed before significant improvements in water quality were observed.

The clay covers and lysimeters were augered and soil samples collected. Porewaters were extracted and analyzed for major metal and ion concentrations (Table 9). Figure 3 compares the results from R1, R2 and R3 with regard to SO_4, Fe(T) and Zn. Sulphate levels in the lysimeter tailings ranged between 15,000 mg/L and 65,000 mg/L at the

control (R1) and between 4,000 mg/L and 14,000 mg/L at the covered plots R2 and R3. Total iron ranged between 4,000 mg/L and 20,000 mg/L at R1 and between 1,000 mg/L and 6,000 mg/L at the covered plots. The highest levels in the tailings were measured at the bottom of the lysimeters, which generally compare to those levels in the discharge water. The lowest levels in the tailings were measured from the upper part of the lysimeters which presumably have been flushed by infiltration. In general, the constituent concentrations in the uncovered tailings are 3 to 4 times higher that those in tailings which were covered. However, if a comparison is made between samples of the covered tailings which have been flushed by infiltration and those in the control with the highest values, then a 93% reduction is achieved. In this comparison, the covered tailings values (4,300 mg/L SO_4 and 1,300 mg/L Fe(T)) are an indication of the expected levels achieved under the clay cover and the highest values in the control (63,000 mg/L SO_4 and 20,000 mg/L Fe(T)) are reasonable levels for exposed tailings. These values are comparable to the porewater data from the laboratory column experiments.

The tailings samples were dried and the gravimetric content of sulphur measured. Figure 4 shows the results with regard to sulphate and sulphide. No conclusive trends are depicted, which suggests that extensive oxidation has not occurred. This is supported by field observations of the tailings colour; they are black and do not show hues of red or orange.

Figure 5 illustrates the gaseous oxygen concentrations measured during 1993. These data do not significantly deviate from measurements conducted in 1991 and 1992, and therefore support the diffusion coefficients and oxygen fluxes presented in the body of the report.

Conclusions

The findings of the monitoring during 1993 further support those presented in the body of the report. In particular, the water balance which was developed with the HELP modelling is confirmed. Based on chemical analysis of the tailings porewater in the lysimeters, significant reduction in tailings oxidation (93%) appears feasible under a composite soil cover that is similar in design to those presented in this report. In addition, outflow from the lysimeter under the clay cover at R2 shows improvement in water quality which, with future analysis, may confirm the reduction of tailings oxidation.

Table 1: Rainfall at Waite Amulet, 1993

Day	May (mm)	Jun (mm)	Jul (mm)	Aug (mm)	Sep (mm)
1	--	1.3	0.0	3.0	0.0
2	--	2.8	10.5	4.5	0.0
3	--	0.5	0.3	15.0	0.3
4	12.4	0.3	0.0	17.8	1.8
5	11.7	0.0	10.0	0.0	0.0
6	0.3	0.0	0.3	0.0	2.3
7	0.0	0.3	0.0	0.0	0.0
8	0.0	0.0	2.8	0.0	0.5
9	0.0	9.1	17.5	0.0	11.8
10	0.0	2.3	0.0	23.3	3.8
11	0.0	0.0	1.8	20.0	1.8
12	0.8	0.0	3.3	0.0	0.0
13	0.3	0.0	0.0	0.0	2.8
14	9.1	12.3	0.8	0.0	38.3
15	10.7	1.0	0.0	0.0	3.5
16	9.4	0.0	0.0	17.8	0.0
17	1.5	17.3	0.0	2.8	0.0
18	0.0	0.0	0.5	0.0	0.8
19	1.0	0.0	1.3	0.0	0.0
20	0.3	1.0	9.5	0.0	0.0
21	0.5	0.5	0.0	0.0	0.0
22	0.0	2.5	0.5	0.0	--
23	0.0	0.0	0.0	2.8	--
24	19.6	0.0	0.0	7.8	--
25	2.5	0.0	0.0	0.0	--
26	2.0	4.0	14.5	0.0	--
27	0.0	0.3	0.3	3.3	--
28	4.6	17.8	1.3	0.8	--
29	0.3	0.3	20.5	0.0	--
30	0.0	0.0	0.5	14.8	--
31	33.0	--	0.0	8.3	--
Total	119.9	73.3	95.8	141.5	--

Table 2: Pan evaporation at Waite Amulet, 1993.

Day	Jun (mm)	Jul (mm)	Aug (mm)	Sep (mm)
1	--	6	4	2
2	--	4	5	4
3	--	2	8	0
4	--	5	4	5
5	--	6	1	1
6	--	8	3	4
7	--	5	4	1
8	--	4	5	2
9	--	6	4	10
10	--	5	10	3
11	3	7	5	-1
12	5	5	2	-2
13	9	1	3	2
14	12	2	4	19
15	3	3	4	-5
16	5	4	8	-0
17	7	3	3	-0
18	2	2	4	3
19	6	2	4	1
20	6	10	2	3
21	1	0	5	4
22	7	0	4	--
23	5	3	4	--
24	9	6	4	--
25	8	7	2	--
26	6	11	5	--
27	3	0	5	--
28	6	3	1	--
29	2	8	2	--
30	5	1	11	--
31	--	5	2	--
Total	164	134	132	--

Table 3: Observed percolation through the clay cover at test plot R2.

Period:	Oct 26 - Nov 20, 1992	Nov 20, 1992 - May 21, 1993	May 21 - Jun 11, 1993	Jun 11 - Aug 19, 1993	Aug 19 - Sep 22, 1993	Oct 26, 1992 - Sep 22, 1993
Season:	Fall	Winter - Early spring	Spring	Summer	Late summer - Fall	Annual
Precipitation (mm):	75	440	82	257	105	958
Lysimeter discharge, R2 (L):	10	0	30	20	22	82
Lysimeter discharge, R2 (mm):	5	0	14	9	10	37
Lysimeter discharge, R2 (% of precipitation):	6%	0	17%	4%	10%	4%

Note: Precipitation from Nov 1992 to May 1993 was measured at Duparquet, Quebec.

Table 4: Volumetric water content by TDR method at Waite Amulet studied site.

Test Plot	Material	Depth (cm)	Date (1993):	May 21	June 11	August 19
R2	Clay	30-60		43	43	42
	Clay	60-90		46	45	46
	Sand Base	90-120		9	9	9
	Tailings	120-150		50	50	49
	Tailngs	150-180		60	60	56
R3	Clay	30-60		45	45	44
	Clay	60-90		44	45	43
	Sand Base	90-120		8	9	8
	Tailings	120-150		52	52	52
	Tailngs	150-180		57	57	54
R4	Sand Base	30-60		9	9	--
	Tailings	60-90		53	53	--

Table 5: Water Level Elevations in the Piezometers at the Waite Amulet Experimental Covers Site.

Piezometer Number	Piezometer Elevations Top (m)	Ground (m)	Screen (m)	Water Level Elevations Oct 90 (m)	Nov 90 (m)	Feb 91 (m)	May 91 (m)	Jul 91 (m)	Oct 91 (m)	Mar 92 (m)	May 92 (m)	Oct 92 (m)	Nov 92 (m)	May 93 (m)	Aug 93 (m)	Sep 93 (m)
R1-1	317.34	316.24	312.29	316.00	316.06	314.58	315.89	314.89	315.77	-	315.88	315.64	315.71	315.72	315.34	315.14
R1-2	317.42	316.35	314.28	316.07	316.09	ICE	316.02	314.85	315.84	-	315.82	315.65	315.66	315.72	315.12	315.21
R2-1	317.56	317.58	312.17	315.69	315.96	314.42	316.05	315.02	315.72	-	315.91	315.80	315.66	315.70	315.43	315.27
R2-2	317.58	317.58	314.16	315.87	315.80	314.55	315.77	314.84	315.59	-	315.73	315.58	315.95	315.88	315.66	315.48
R3-1	317.67	317.47	312.22	315.73	315.77	314.53	315.80	314.92	315.56	-	315.71	315.60	315.69	315.72	315.49	315.33
R3-2	317.56	317.41	314.11	315.75	315.80	314.46	315.82	315.03	315.68	-	315.77	315.70	315.87	315.79	315.66	315.54
R4-1	317.01	316.64	312.16	315.73	315.47	314.51	315.76	314.91	315.54	-	315.67	315.59	315.62	315.63	315.48	315.35
R4-2	317.11	316.85	314.26	316.00	315.97	314.60	316.04	315.24	315.91	-	316.15	315.93	316.06	316.08	315.91	315.78
WA5-1	317.10	315.75	311.35	315.42	-	314.15	315.46	314.51	315.35	313.63	315.45	-	-	315.46	315.16	315.04
WA5-2	317.11	315.77	314.05	315.52	-	314.10	315.54	314.51	315.51	DRY	315.57	-	-	315.52	315.34	315.27
WA9-1	317.13	316.05	309.38	314.60	-	313.48	314.61	313.76	314.36	313.00	314.40	-	314.55	314.49	314.06	313.96
WA9-2	317.12	316.07	314.44	315.33	-	ICE	315.65	DRY	315.89	-	315.72	-	-	316.03	315.31	315.17
WA9-3	317.13	316.07	310.88	315.09	-	313.71	315.01	313.96	314.76	313.18	314.79	-	314.88	314.83	314.44	314.40
WA9-4	317.09	316.07	312.55	315.48	-	313.95	315.41	314.26	315.25	313.43	315.29	-	315.35	315.32	314.91	314.83
WA9-5	317.13	316.04	313.64	315.68	-	314.03	315.57	314.28	315.50	313.63	315.48	-	315.47	315.47	315.02	314.93
WA9-6	317.28	316.04	307.43	314.18	-	313.14	314.21	313.34	313.96	312.61	314.01	-	314.16	314.06	313.76	313.67
WA9-7	317.14	316.10	305.71	314.18	-	313.07	314.17	313.31	314.00	-	-	-	-	-	-	-
WA10-1	317.12	316.42	309.12	-	-	-	315.54	314.71	314.92	-	315.19	-	315.39	315.27	314.95	314.78
WA10-2	317.16	316.40	314.82	-	-	-	315.65	315.01	314.92	-	315.07	-	315.45	314.97	315.02	314.88

Table 6: Major metal and ion concentrations in lysimeter discharge water at Waite Amulet test plots.

Test Plot	Discharge	Temp °C	Cond. µmol.	Redox mV	pH	Acidity mg/L CaCO3	Al mg/L	As mg/L	Ca mg/L	Cd mg/L	Cu mg/L	Fe(T) mg/L	K mg/L	Mg mg/L	Mn mg/L	Na mg/L	Pb mg/L	SO4 mg/L	Se mg/L	Zn mg/L	Fe(+2) mg/L	Fe(+3) mg/L
May 17,1993																						
R1	30 L	15.40	27000.00	375.00	2.49	45700.00	3930.00	36.99	412.31	2.28	302.54	20000.00	5.90	937.12	30.79	15.03	< 0.25	61170.00	4.22	619.62	--	2640.00
R3-1	~ 1 L/m	13.10	4390.00	12.00	4.09	1680.00	9.01	0.89	447.81	< 0.025	0.24	1400.00	118.81	205.05	15.81	41.05	< 0.25	4260.00	< 0.50	3.19	--	9.50
R3-2	~ 1 L/m	10.70	4380.00	-2.00	5.67	1500.00	4.73	0.90	457.60	< 0.025	< 0.025	1170.00	119.64	201.58	13.51	40.64	< 0.25	3960.00	< 0.50	0.88	--	7.33
R3-3	~ 1 L/m	10.90	4140.00	-15.00	5.78	1400.00	3.97	0.76	474.04	< 0.025	< 0.025	1080.00	118.81	202.18	12.13	39.80	< 0.25	3840.00	< 0.50	0.29	--	6.75
June 11, 1993																						
R2	30 L	--	--	--	--	--	47.00	8.43	376.00	< 0.030	< 0.030	11900.00	49.20	409.00	175.00	17.90	< 0.25	22800.00	0.59	54.00	10750.00	--
R3	~ 1 L/m	--	--	--	--	--	9.50	1.46	431.00	< 0.030	< 0.030	2110.00	84.00	158.00	19.60	37.30	< 0.25	5490.00	< 0.50	14.90	2090.00	--
August 19, 1993																						
R1	5 L	--	--	--	--	--	4570.00	40.30	456.00	2.35	368.00	24700.00	< 5.00	1550.00	52.90	13.40	< 0.25	79200.00	2.39	652.00	--	15200.00
R2	20 L	--	--	--	--	--	78.70	6.76	390.00	< 0.025	< 0.025	11600.00	46.50	389.00	168.00	19.00	< 0.25	21930.00	0.98	91.30	--	710.00
R3	~ 1 L/m	--	--	--	--	--	3.47	1.50	480.00	< 0.025	< 0.025	2560.00	80.50	121.00	16.90	43.60	< 0.25	5730.00	< 0.50	2.59	--	160.00

Table 7: Major metal and ion concentrations in sampled water from piezometers at Waite Amulet studied site.

Piezometer	Temp °C	Cond. µmol.	Redox mV	pH	Acidity mg/L CaCO3	Al mg/L	As mg/L	Ca mg/L	Cd mg/L	Cu mg/L	Fe mg/L	K mg/L	Mg mg/L	Mn mg/L	Na mg/L	Pb mg/L	SO4 mg/L	Se mg/L	Zn mg/L	Fe(+3) mg/L
May 17, 1993																				
R1-1	8.8	2360	99	6.02	270	4.04	< 0.25	378.23	< 0.025	< 0.025	130.77	7.35	122.70	19.05	40.63	< 0.25	1647.24	< 0.50	0.48	1.89
R1-2	9.2	5300	365	2.81	2800	181.21	2.03	445.83	0.13	8.32	992.18	< 5.00	294.18	31.70	24.25	< 0.25	5190.00	< 0.50	141.17	161.00
R2-1	8.9	4160	31	7.41	50	4.57	< 0.25	387.00	< 0.025	< 0.025	68.64	49.69	592.43	1.20	31.91	< 0.25	3150.00	< 0.50	0.05	4.63
R2-2	8.7	1930	202	5.99	260	7.85	< 0.25	401.74	0.03	0.76	84.68	5.21	51.41	3.46	30.36	< 0.25	1306.08	< 0.50	17.99	12.00
R3-1	8.9	8880	-5	7.83	30	3.23	< 0.25	306.95	< 0.025	< 0.025	12.91	103.92	1210.00	1.31	844.02	< 0.25	6840.00	< 0.50	< 0.02	1.64
R3-2	8.6	3290	255	3.59	870	18.04	0.53	483.03	< 0.025	0.57	521.38	13.31	123.26	12.33	31.54	< 0.25	2494.33	< 0.50	21.10	35.50
R4-1	8.2	9470	-30	7.76	30	6.43	< 0.25	356.64	< 0.025	< 0.025	7.52	109.66	1640.00	1.75	573.35	< 0.25	8850.00	< 0.50	< 0.02	0.32
R4-2	8.4	2050	90	7.81	70	4.92	< 0.25	486.15	< 0.025	< 0.025	46.72	6.87	59.45	1.69	26.93	< 0.25	1287.05	< 0.50	3.64	3.68
WA5-1	12.1	4540	-10	6.78	170	2.98	< 0.25	443.11	< 0.025	< 0.025	125.83	32.39	437.12	10.19	235.40	< 0.25	2758.16	< 0.50	< 0.02	2.22
WA5-2	9.9	9520	-8	7.45	30	2.27	< 0.25	406.97	< 0.025	< 0.025	7.32	74.71	2250.00	2.16	53.33	< 0.25	10590.00	< 0.50	0.24	2.90
WA9-1	16.2	3370	-54	7.54	40	2.34	< 0.25	113.45	< 0.025	< 0.025	15.82	42.34	75.71	0.77	644.83	< 0.25	1392.49	< 0.50	< 0.02	0.94
WA9-2	16.4	2790	275	3.29	500	14.54	0.34	441.06	< 0.025	0.51	284.45	30.82	128.79	5.48	21.73	< 0.25	2072.33	< 0.50	1.16	20.50
WA9-3	16.2	7710	-12	7.72	20	2.56	< 0.25	499.45	< 0.025	< 0.025	2.12	118.03	710.92	1.35	923.56	< 0.25	5940.00	< 0.50	< 0.02	0.19
WA9-4	15.7	5170	-58	7.64	20	2.32	< 0.25	312.90	< 0.025	< 0.025	9.27	65.08	880.31	1.18	87.17	< 0.25	4290.00	< 0.50	< 0.02	0.57
WA9-5	15.1	2790	-33	7.87	20	2.40	< 0.25	572.96	< 0.025	< 0.025	28.01	47.49	177.45	1.62	24.65	< 0.25	2065.40	< 0.50	< 0.02	0.55
WA9-6	15.2	4810	-16	7.32	50	2.83	< 0.25	205.70	< 0.025	< 0.025	15.88	51.94	291.30	9.59	732.46	< 0.25	2930.97	< 0.50	< 0.02	1.16
WA10-1	17.6	1760	12	7.68	40	2.54	< 0.25	70.33	< 0.025	< 0.025	9.11	22.26	43.23	0.58	339.78	< 0.25	124.35	< 0.50	< 0.02	0.66
Blanks																				
WA2-1	--	--	--	--	--	3.23	< 0.25	0.90	< 0.025	< 0.025	< 0.02	< 5.00	0.54	< 0.01	9.15	< 0.25	< 0.75	< 0.50	< 0.02	< 0.03
WA2-2	--	--	--	--	--	2.77	< 0.25	0.70	< 0.025	< 0.025	< 0.02	< 5.00	< 0.50	< 0.01	9.49	< 0.25	< 0.75	< 0.50	< 0.02	< 0.03
WA2-3	--	--	--	--	--	3.35	< 0.25	0.59	< 0.025	< 0.025	< 0.02	< 5.00	< 0.50	< 0.01	9.87	< 0.25	< 0.75	< 0.50	< 0.02	< 0.03
Spikes																				
WA11-1	--	--	--	--	--	2.26	2.21	3.13	2.31	2.15	2.26	< 5.00	< 0.50	2.18	9.57	2.44	6.76	2.23	2.43	2.09
WA11-2	--	--	--	--	--	2.22	2.19	3.13	2.30	2.15	2.28	< 5.00	< 0.50	2.17	9.43	2.43	6.93	2.23	2.45	2.06
WA11-3	--	--	--	--	--	2.59	2.24	2.96	2.31	2.16	2.29	< 5.00	< 0.50	2.17	9.33	2.43	9.33	2.29	2.42	1.86

Note: Spikes contain 2 mg/L of: As, Ca,Cd, Cu, Fe, K, Mn, Pb, Se, Zn, Na.

Table 8: Water quality summary of the lysimeter dicharge and tailings porewater.

Station	Date	pH	Acidity (mg/L CaCO3)	SO4 (mg/L)	Fe(T) (mg/L)	Zn (mg/L)
Lysimeter discharge:						
R1	Oct 1990	3.8	52600	51300	2010	840
	Dec 1990	--	--	43100	1590	8570
	May 1991	--	--	98400	385	1190
	Jul 1991	3.2	22500	22710	1950	2430
	May 1992	--	--	9500	1910	445
	Nov 1992	--	--	79890	21650	1400
	May 1993	2.5	45700	61170	20000	620
	Aug 1993	2.3	69070	79200	24700	652
	Sep 1993	2.4	42070	--	--	--
R2	Nov 1992	--	--	30990	16520	261
	Jun 1993	3.6	17990	22800	11900	54
	Aug 1993	2.7	16124	21930	11600	91
	Sep 1993	3.2	15950	--	--	--
R3	Nov 1992	--	--	15540	7790	203
	May 1993	5.1	1527	4020	1217	1.5
	Jun 1993	6.3	3410	5490	2110	15
	Aug 1993	2.9	3324	5730	2560	2.6
Saturated zone tailings porewater:						
2 m below tailings surface:						
R1	May 1991	--	--	--	--	--
	May 1992	--	--	3580	591	73
	May 1993	2.8	2800	5190	992	141
R2	May 1991	--	--	4380	74	1.5
	May 1992	--	--	3700	80	0.03
	May 1993	6.0	260	1306	85	18
R3	May 1991	--	--	3510	872	25
	May 1992	--	--	2970	412	6.1
	May 1993	3.6	870	2494	521	21
R4	May 1991	--	--	2529	423	27
	May 1992	--	--	1620	141	40
	May 1993	7.8	70	1287	47	3.6
4 m below tailings surface:						
R1	May 1991	--	--	2475	205	3.1
	May 1992	--	--	1440	168	0.7
	May 1993	6.0	270	1647	131	0.05
R2	May 1991	--	--	700	7.3	0.42
	May 1992	--	--	1190	22.3	21
	May 1993	7.4	50	3150	69	0.05
R3	May 1991	--	--	6630	21	0.39
	May 1992	--	--	3790	6.8	< 0.025
	May 1993	7.8	30	6840	13	< 0.025
R4	May 1991	--	--	7020	12	< 0.025
	May 1992	--	--	7320	6.9	< 0.025
	May 1993	7.8	30	885	7.5	< 0.025

Table 9: Major metal and ion concentrations in pore water from the Waite Amulet test plots.

Test Plot	Material	Depth (cm)	W (%)	pH	Al mg/L	As mg/L	Ca mg/L	Cd mg/L	Cu mg/L	Fe(T) mg/L	K mg/L	Mg mg/L	Mn mg/L	Na mg/L	Pb mg/L	SO4 mg/L	Se mg/L	Zn mg/L	Fe(+3) mg/L
R1	Lysimeter Tailings	0 -10	27.81	--	1150.00	10.69	475.11	0.21	15.77	5190.00 <	5.00	335.54	12.23	16.23 <	0.25	19299.00	0.77	68.31	1140.00
		10 - 25	27.37	--	881.42	8.57	473.32	0.43	60.05	4130.00 <	5.00	321.38	11.31	17.75 <	0.25	15750.00	0.79	148.37	1510.00
		25 - 40	28.43	--	1310.00	12.39	482.75	0.88	141.62	5880.00 <	5.00	387.88	14.70	17.59 <	0.25	21300.00	0.97	289.33	3690.00
		40 - 55	30.30	--	3240.00	28.09	472.70	3.83	154.64	14700.00 <	5.00	784.79	27.26	15.62 <	0.25	45900.00	2.78	675.26	4190.00
		55 - 60	30.40	--	4790.00	39.22	470.58	5.54	198.90	20000.00	5.45	1020.00	35.04	19.48 <	0.25	63300.00	3.41	951.76	3380.00
R2	Clay	40 - 50	32.66	--	9.64 <	0.25	37.33 <	0.025	0.34	31.04 <	5.00	17.85	0.16	72.55 <	0.25	340.82 <	0.50	2.30	1.62
		50 - 55	32.98	--	2.50 <	0.25	54.16 <	0.025 <	0.025	1.26 <	5.00	21.00	0.22	74.59 <	0.25	295.76 <	0.50	0.16	0.32
		55 - 65	31.59	--	1.98 <	0.25	40.28 <	0.025	0.03	0.41 <	5.00	15.92	1.77	58.95 <	0.25	213.94 <	0.50	0.05	0.67
		65 - 75	35.87	--	5.87 <	0.25	55.14 <	0.025	0.03	4.36 <	5.00	17.09	0.63	50.31 <	0.25	144.09 <	0.50	0.05	4.45
		75 - 85	35.97	--	3.05 <	0.25	91.56 <	0.025	0.06	1.68 <	5.00	19.12	0.55	53.50 <	0.25	200.76 <	0.50	0.08	1.00
	Sand	85-95	3.29	--	284.78 <	0.25	1016.09 <	0.020 <	0.020	411.90 <	5.00	213.80	6.06	903.91 <	0.25	5308.97 <	0.50	3.86	93.08
		95-105	9.21	--	81.14 <	0.25	270.09 <	0.020 <	0.020	64.13 <	5.00	62.10	1.82	305.98 <	0.25	1152.05 <	0.50 <	0.03	38.77
		105-115	4.15	--	136.89 <	0.25	728.62 <	0.020 <	0.020	150.19 <	5.00	148.45	4.07	635.18 <	0.25	2392.07 <	0.50 <	0.03	111.34
		115-120	3.54	--	74.72 <	0.25	792.06 <	0.020 <	0.020	45.79 <	5.00	125.97	2.33	727.79 <	0.25	3318.38 <	0.50 <	0.03	17.86
		120-130	4.19	--	96.95 <	0.25	579.88 <	0.020 <	0.020	128.97 <	5.00	103.79	4.92	614.16 <	0.25	2439.74 <	0.50	3.75	38.68
	Lysimeter Tailings	130-145	17.56	4.55	5.70	0.59	552.46	0.07 <	0.025	1318.00	54.69	133.45	84.55	46.55	1.41	4257.00 <	0.50	97.42	23.30
		145-160	18.32	4.86	2.69	1.23	537.89 <	0.025 <	0.025	3012.00	53.01	265.07	186.97	40.71	0.57	7893.00	0.63	102.69	357.00
		160-175	17.15	4.36	3.78	2.38	513.85 <	0.025 <	0.025	5236.00	56.05	341.97	261.31	33.81	0.83	11964.00	1.01	276.84	138.00
		175-190	18.89	4.50	13.46	2.75	518.65 <	0.025 <	0.025	6053.00	71.74	412.72	354.11	32.00	3.95	13944.00	1.30	443.83	199.00
R3	Clay	35 - 50	37.52	--	3.59 <	0.25	140.81 <	0.025 <	0.025	2.06 <	5.00	38.26	0.22	63.16 <	0.25	452.31 <	0.50	0.07	1.72
		50 - 65	37.07	--	1.85 <	0.25	174.36 <	0.025 <	0.025	0.18 <	5.00	53.79	0.36	76.14 <	0.25	620.43 <	0.50 <	0.03	0.05
		65 - 75	40.01	--	1.75 <	0.25	280.52 <	0.025 <	0.025	0.24 <	5.00	50.70	2.03	75.93 <	0.25	820.92 <	0.50 <	0.03	0.07
		75 - 85	44.37	--	1.96 <	0.25	294.84 <	0.025 <	0.025	0.57 <	5.00	49.12	2.41	75.93 <	0.25	903.03 <	0.50	0.04	0.17
		85 - 95	43.82	--	1.82 <	0.25	345.05 <	0.025 <	0.025	0.32 <	5.00	53.11	0.27	76.74 <	0.25	1036.08 <	0.50	0.03	0.18
	Sand	95-105	2.75	--	88.27	24.37	1221.65	2.03 <	0.020	80.18 <	5.00	156.82	5.25	893.94 <	0.25	5032.69 <	0.50	5.82	48.51
		105-115	5.46	--															97.14
		115-125	6.57	--	21.23 <	0.25	788.17 <	0.020 <	0.020	20.79 <	5.00	84.50	1.26	403.36 <	0.25	5138.56 <	0.50 <	0.03	12.79
	Lysimeter Tailings	125-140	14.29	3.97	64.06	0.81	701.37	2.83 <	0.020	1075.75	34.01	237.40	146.68	78.12	4.79	5761.12 <	0.50	657.78	
		140-155	17.00	4.14	15.87	0.50	622.85	0.27 <	0.020	1192.54	40.12	201.65	138.33	70.01	3.08	5383.47 <	0.50	571.66	15.55
		155-170	18.59	4.27	8.73	0.53	665.83	0.10 <	0.020	1438.89	33.24	173.61	119.15	63.71	1.42	5356.91 <	0.50	298.03	19.36
		170-185	17.68	4.48	2.79	0.47	637.79 <	0.020 <	0.020	1520.20	28.07	146.25	105.34	56.11	0.73	5040.66 <	0.50	175.65	21.54
		185-200	17.78	4.35	7.89	0.49	663.61 <	0.020 <	0.020	1490.81	32.48	152.59	132.01	62.37	2.32	5208.40	0.96	171.95	18.20

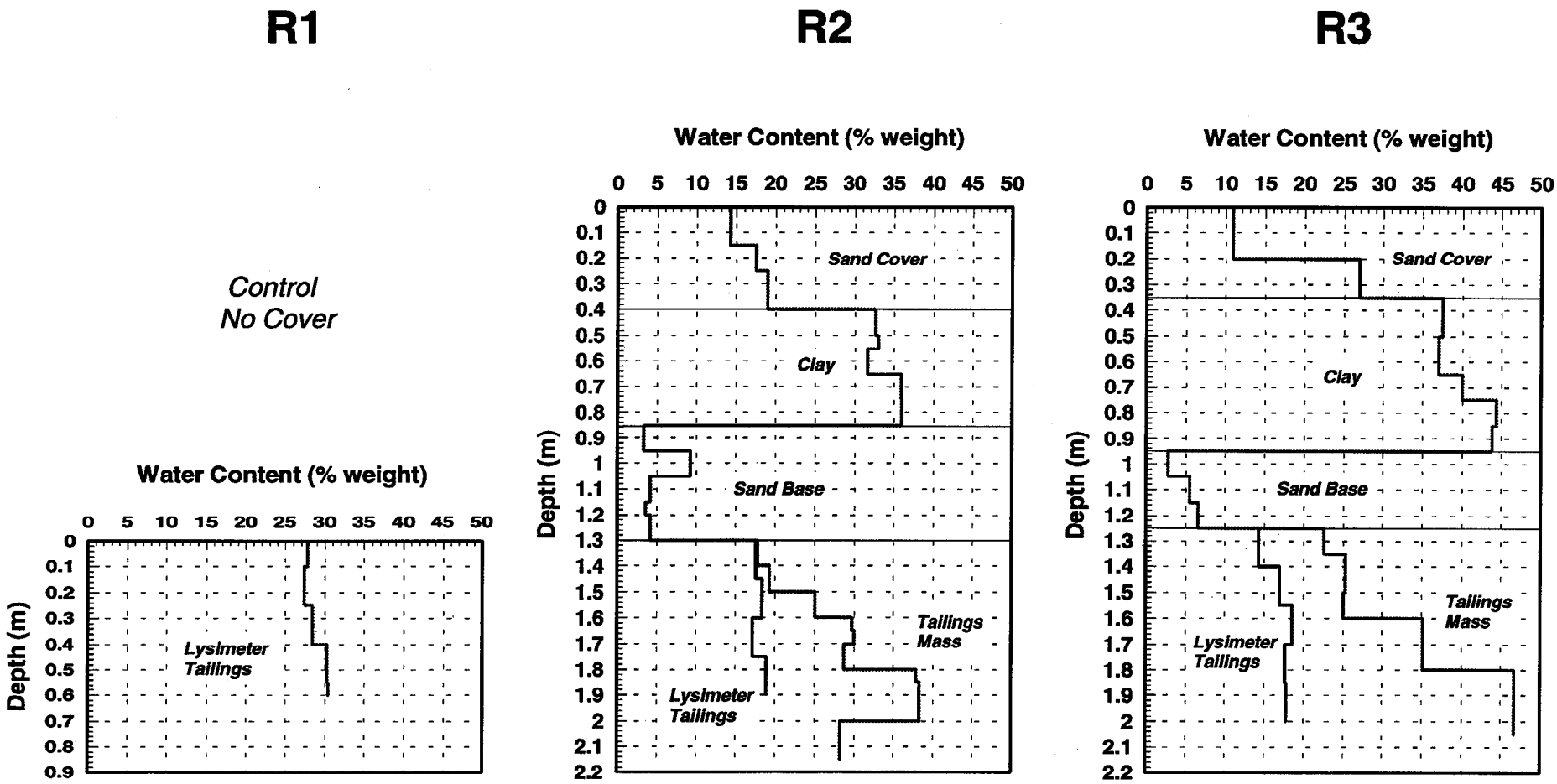

Figure 1: Gravimetric water content measurements in June 1993.

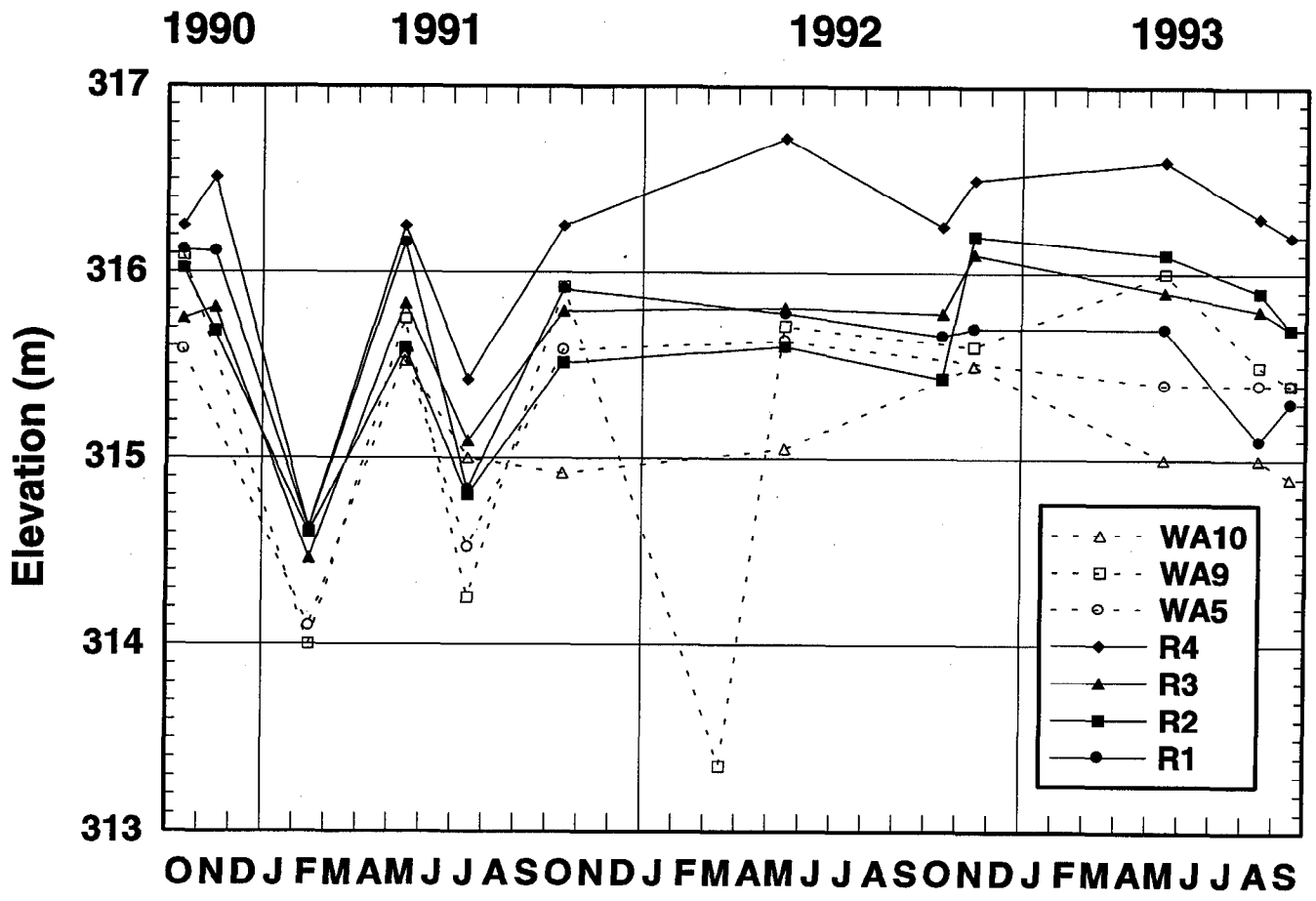

Figure 2: Water table elevations at piezometer nests.

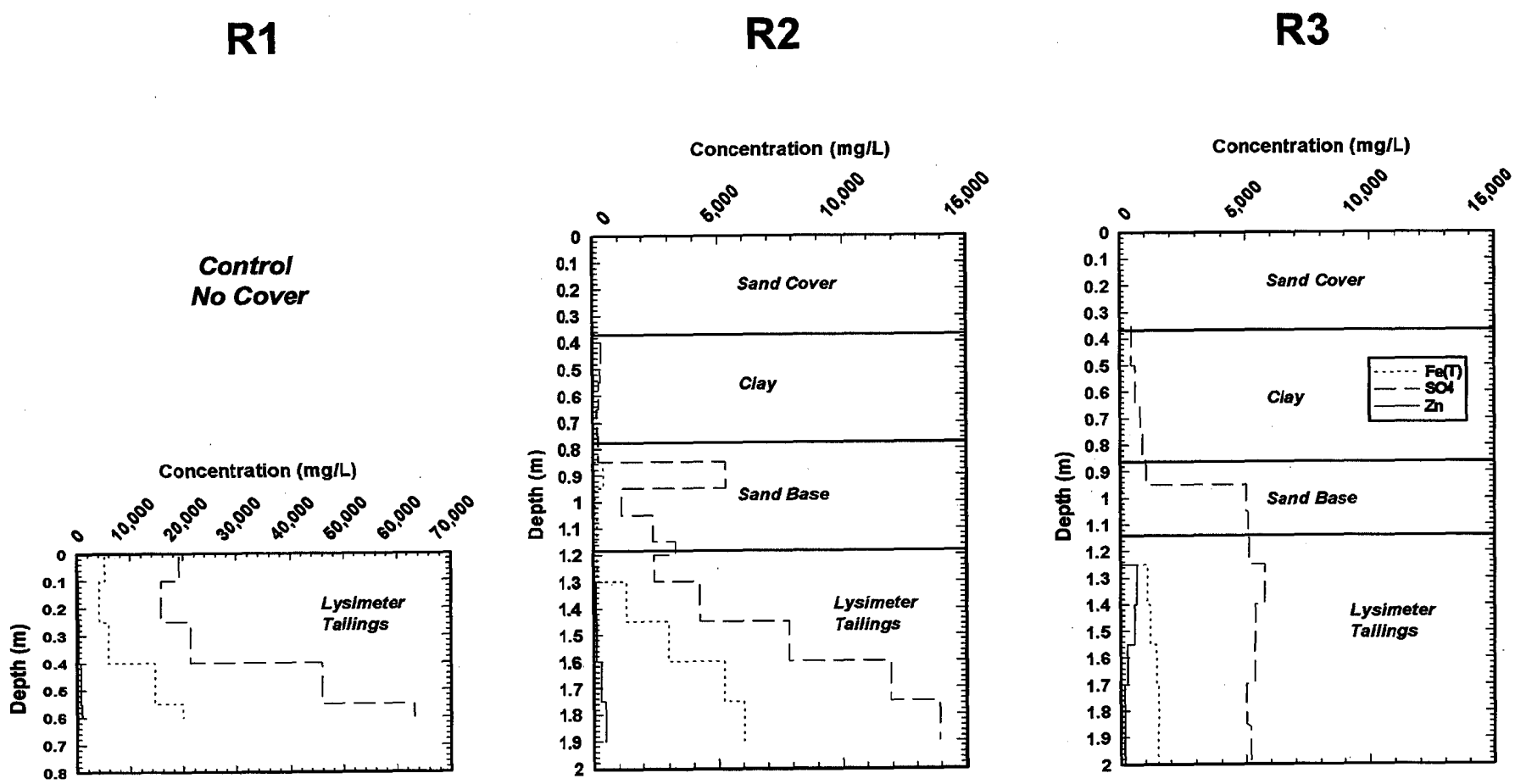

Figure 3: Constituent concentrations in porewater during June 1993.

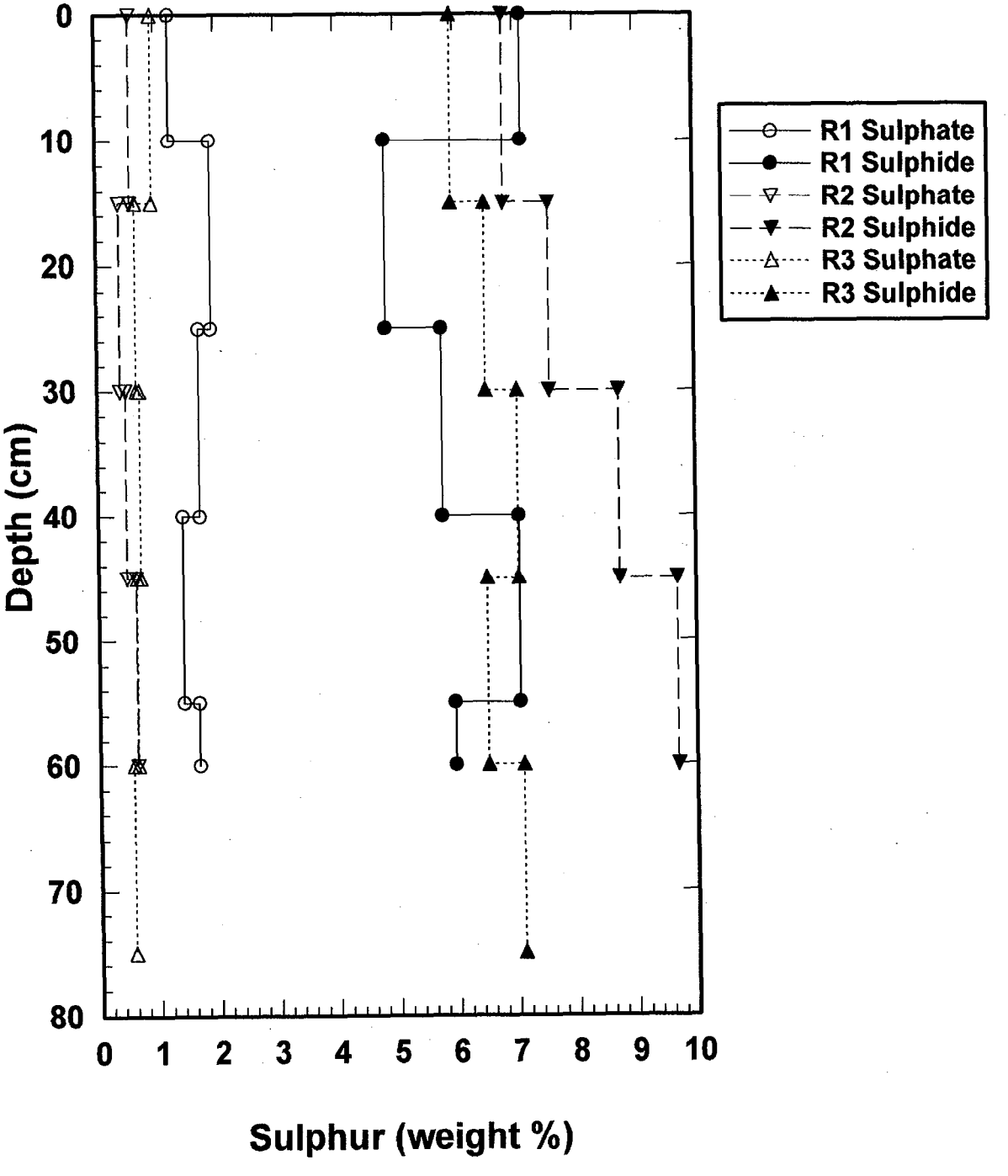

Figure 4: Lysimeter tailings sulphur content.

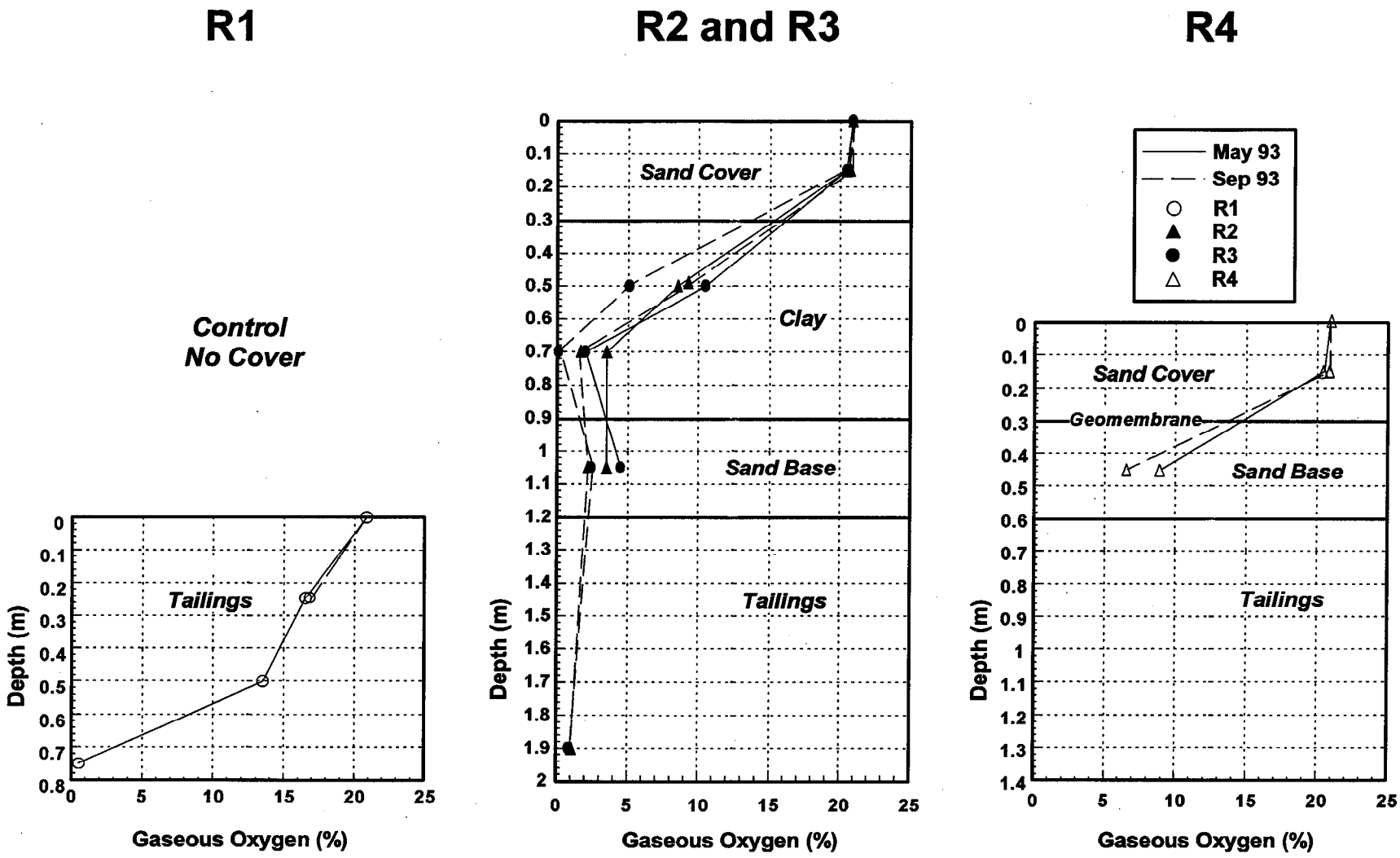

Figure 5: Gaseous oxygen concentrations.